Development of Biomolecular Tools for Studying Host-Virus Interactions of the Hepatitis C Virus

Neda Nasheri Ardekan

Thesis submitted to the
Faculty of Graduate and Postdoctoral Studies
In partial fulfillment of the requirements for the
PhD degree in Microbiology & Immunology

Department of Biochemistry, Microbiology & Immunology
Faculty of Medicine
University of Ottawa

Abstract

Hepatitis C virus (HCV) is a growing health concern in Canada and around the world, as it currently infects 3% of the global population. While there is no vaccine available against this virus, novel and effective treatment regimens have improved prospects for the cure of HCV. Complications caused by HCV can lead to severe liver disease and even death. The limited viral proteome forces HCV to rely heavily on various host factors for its replication. Additionally HCV modulates the host physiology to facilitate its pathogenesis; consequently, the in dept study of essential host-virus interactions expands our understandingof how the virus and related species commandere host cell machinery. This understanding can help create new therapeutic strategies, which may have applications towards HCV and other related RNA viruses.

While numerous studies have demonstrated that HCV modulates the abundance of various host proteins, the systematic study of the virus's effect on the enzymatic activity has been relatively unexplored. For this reason, activity-based protein profiling (ABPP) was applied to study the changes in the activity of host enzymes during HCV replication. ABPP is a functional proteomics technique that employs active site-directed probe (ABP) to report on the activity of enzymes within complex proteomes, such as living cells. Herein, directed and non-directed ABPs were employed for specific as well as global profiling of the alterations in the activity of cellular enzymes during HCV replication. As a result, essential host enzymes that are differentially active during HCV infection were identified. Furthermore, I have developed a quantitative ABPP method for relative quantification of the cellular enzymes activity during HCV infection. These results contribute to the discovery of disease-associated biomarkers, with diagnostic significance, and aid in the identification of potential targets for therapeutic interventions.

In addition to developing protein-based tools to study host-virus interactions, I employed a novel technique to investigate the interactions of micro-RNA 122 (miR-122), an essential HCV host factor, with the viral RNA genome. This *in vitro* screening approach, interrogates the folding of HCV RNA using viral RNA-coated magnetic bead (VRB) to determine target site accessibility for RNA silencing. This method predicts the relative affinity of small RNAs towards HCV genomic RNA that are not easily predicted by informatic means, and led to discovery of potent miR-122 interaction site within the large, highly-structured HCV RNA genome. For that reason, VRB assay may represent an attractive tool for the examination of target site accessibility for RNA silencing.

Acknowledgements

First and foremost I offer my sincerest gratitude to my supervisor, Dr. John Pezacki, who has been a tremendous mentor for me. I would like to thank him for encouraging my research and allowing me to grow as a scientist in his laboratory. John has provided me with an abundance of opportunities to flourish intellectually through conducting interesting and challenging research projects, participating in collaborations with diverse, well-known research groups, preparing scientific manuscripts and conference presentations, as well as demanding a high standard of quality in all my endeavours. His advice on both research as well as on my career has been invaluable. Thank you for pushing me further than I thought I could go. I would also like to thank my committee members Dr. Daniel Figeys and Dr. Marc-André Langlois for their brilliant comments and suggestions.

Very special thanks goes out to Yanouchka Rouleau, Allison Sherratt, and Shifawn O'Hara who provided me with direction, technical support and became more of friends, than colleagues. I would also like to thank my friends in the chemistry and biochemistry labs, particularly Ragunath Singaravelu, for our scientific debates, exchanges of knowledge, skills, and venting of frustration during my graduate program, which helped enrich the experience.

I would also like to thank my parents, two elder sisters, and elder brother. They were always supporting me and encouraging me with their best wishes. At the end, I would like to express special appreciation and thanks to my beloved husband, Naeim, for his love, patience and understanding. He was always there cheering me up and stood by me through the good times and bad.

Table of Contents

List of Abbreviations

2D-GE	2D-Gel Electrophoresis
ABP	Activity-Based Probe
ABPP	Activity-Based Protein Profiling
ACC	Acetyl-CoA Carboxylase
ACP	Acyl Carrier Domain
ADH7	Alcohol Dehydrogenase
AHCY	Denosylhomocysteinase
Alb-uPA	Plasminogen Activator Transgene controlled by Albumin Promoter
ALDH1A	Aldehyde Dehydrogenase
ALDOA	Aldolase A
AmpN	Ampicillin
BP	Benzophenone
CDK	Cyclin-Dependent Kinase 2
CERT	Ceramide Transfer Protein
CoA	Coenzyme A
Cy3	Cyanine-3
DENV	Dengue Virus
DH	Dehydrase
DMEM	Dulbecco's Modified Eagle Medium
DML	Dimethyl Labeling
dsRNA	Double-Stranded RNA
DTT	Dithiothreitol
ECMV	Encephalomyocarditis Virus
EIA	Enzyme Immunoassay
emPAI	Exponentially Modified Protein Abundance Index
ENO1	Alpha-Enolase
ER	Endoplastic Reticulum
FAPP	Four-Phosphate Adaptor Protein
FASN	Fatty Acid Synthase
FBS	Fetal Bovine Serum
FDA	Food and Drug Administration
FGR	Full-Genomic HCV Replicon
FP	Fluorophosphonate
Golph3	Golgi phosphoprotein 3
GORS	Genome-Scale Ordered RNA Structures
HCC	Hepatocellular Carcinoma

HCV	Hepatitis C Virus
HEK-293	Human Embryonic Kidney cells
HIV-1	Human Immunodeficiency Virus-1
HLTF	Helicase-Like transcription Factor
HMGCS	Hydroxymethylglutaryl-CoA Synthase
HS-Huh7.5	Human Serum Differentiated Huh7.5 Cells
Huh-7	Human Hepatoma Cell Line
IDH1	Isocitrate Dehydrogenase 1
IFN	Interferon
IOD	Integrated Optical Density
IRES	Internal Ribosome Entry Site
IVT	*In Vitro* Transcription
kDa	Kilodalton
KR	β-ketoacyl Reductase
KS	β-ketoacyl Synthase
LC-MS/MS	Liquid Chromatography-Tandem Mass Spectrometry
LD	Lipid Droplet
LDL	Low Density Lipoprotein
LNA	Locked Nucleic Acid
Luc	Luciferase
LXR	Liver X Receptor
MAT	Malonyl/Acetyl Transferase
METAP1	Methionyl Aminopeptidase 1
miRNA	MicroRNA
MRE	Micro-RNA Recognition Element
MRSA	Multi-Resistant *Staphylococcus aureus*
MS	Mass Spectrometry
MW	Membranous Web
NADH	Nicotinamide adenine dinucleotide
Neo	Neomycin
NS	Non-Structural
nt	Nucleotide
OBD	On-Bead Digestion
OGG1	8-Oxoguanine Glycosylase
ORF	Open Reading Frame
OSBP	Oxysterol Binding Protein
p19	19 kDa Protein
PAGE	Polyacrylamide Gel Electrophoresis
PAT	Palmitoyltransferase
PBP	Penicillin Binding Protein
PBS	Phosphate Buffered Saline

PGD	6-Phosphogluconate
PH	Pleckstrin Homology
PI	Phosphoinositide
PI3K	Phosophoinositide-3 Kinase
PI4K	Phosphoinositide 4 Kinase
PI4P	Phosphatidylinositol 4-Phosphate
PIK	Phosphoinositide Kinase
PKD	Protein Kinase D
PPAR	Peroxisome Proliferator Activated Receptor
PPM1B	Protein Phosphatase 1B
PPT	PhosphoPantetheine Transferase
PTM	Post-Translational Modification
RC	Replication Complex
RdRp	RNA-dependent RNA Polymerase
RhN3	Rhodamine azide
RISC	RNA-Induced Silencing Complex
RNAi	RNA Interference
RNase	Ribonuclease
RT-qPCR	Real-time quantitative PCR
RXR	Retinoid X Receptor
SARS	Severe acute respiratory syndrome
SCD	Stearoyl CoA Desaturase
SCID	Severe Combined Immunodeficiency
SD	Standard Deviation
SDS	Sodium Dodecyl Sulfate
SE	Standard Error
SGR	Subgenomic HCV Replicon
SHAPE	Selective 2'-Hydroxyl Acylation Analysed by Primer Extension
siRNA	Short-interfering RNA
SL	Stem Loop
SNP	Single Nucleotide Polymorphism
SRE	Sterol Response Element Gene
SREBP	Steroid Responsive Element Binding Protein
ST3GAL5	ST3 Beta-Galactoside Alpha-2,3-Sialyltransferase 5
SVR	Sustained Virological Response
TCEP	Tris(2-carboxyethyl)phosphine
TE	Thioesterase
THL	Tetrahydrolipstatin
TOFA	5-(Tetradecyloxy)-2-Furoic Acid
USUV	Usutu virus
UTR	Untranslated Region

VLDL	Very Low Density Lipoprotein
VR	Variable Region
VRB	Viral RNA Coated Magnetic Bead
WNV	West Nile Virus
YFV	Yellow Fever Virus

List of Figures

List of Tables

Chapter 1: Introduction

1.1 Hepatitis C Virus (HCV)

1.1.1 HCV Infection

Hepatitis C infection is a global concern that affects approximately 3% of the world population (213). Acute infection with hepatitis C is usually asymptomatic, but sometimes it can be manifested with typical symptoms of acute viral hepatitis, such as malaise, fatigue, anorexia, nausea, abdominal pain, jaundice, and dark urine (250). Acute viremia can resolve spontaneously, however, seventy to ninety percent of the infected individuals will develop chronic infection, which can lead to fibrosis, steatosis, and hepatocellular carcinoma (HCC)(128). Hepatitis C virus (HCV) can be transmitted by exposure to contaminated blood, and by sexual intercourse (230). Importantly, upon liver transplantation, HCV infection of the graft is inevitable without treatment (180).

Unfortunately, there is no vaccine available against HCV that is approved for clinical use as a preventive strategy (153). Former regimens for treating HCV infection include pegylated type I interferon, plus ribavirin for a period of 24-48 weeks (292, 455), which was not fully effective in most patients, and hard to tolerate due to significant side effects (292, 455). However, the rapid progress in the development of direct acting antivirals (DAAs), is improving the prospect of anti-HCV therapy and achievement of sustained virological response (SVR) (31). Current interferon-free treatment regimens combine two or three DAAs against HCV NS3, NS5A and NS5B (31). Despite the recent breakthrough in HCV treatment, there are still some challenges left to be addressed; such as the high pricing of DAAs, possible emergence of drug resistance or naturally occurring polymorphism in HCV sequences which can influence the efficacy of HCV treatment response (123, 201, 210, 287). Consequently, although exciting new therapies exist against HCV, it still remains to be a major global health concern and it is essential to understand the

fundamental aspects of its life cycle to develop novel treatment options and antivirals to combat this and related infections.

1.1.2 HCV Genome and Encoded Proteins

HCV is a member of the genus *Hepacivirus* within the *Flavivirdae* family (230). Its genome is comprised of an approximately 9.6 kb long, single-stranded RNA with positive polarity that carries a long open reading frame flanked by the 5′- and 3′- untranslated regions (5'UTRs) (230). The HCV genome encodes an approximately 3,000 amino acid polyprotein that is cleaved by viral and cellular proteases into three structural proteins (core, E1 and E2), which form the mature virion, as well as seven non-structural proteins (p7, NS2, NS3, NS4A, NS4B, NS5A, and NS5B) that are involved in viral replication (17).

Genetic diversity is a major feature of the HCV genome that renders the virus the ability to evade the host immune response and therefore complicates the process of vaccine and therapeutic development. Based on the sequence variance in the 5'UTR and in the regions encoding the core, E1 and NS5B proteins, HCV is classified into 7 phylogenetically and geographically distinct genotypes (369, 370, 376). Within genotypes, distinct clusters may be found that are called subtypes. In terms of virulence, HCV genotypes and subtypes are similar; however, they vary in susceptibility to direct-acting antiviral agents (DDAs) and interferons (genotypes 1 and 4 are less responsive) (192, 365). Also, it is worth mentioning that even within each infected individual, HCV exists as a spectrum of quasispecies (103).

1.1.3 HCV Lifecycle

Serum-derived HCV particles associate with lipoprotein components, therefore it has been suggested that HCV forms lipoviral particles (LVPs) (16, 289), which can facilitate virus entry

into hepatocytes and protect the virus from antibody neutralization. HCV exclusively replicates in hepatocytes and this tissue tropism is determined by many host factors that are involved with different aspects of the HCV life cycle. HCV entry occurs through initial interaction of the viral envelope proteins (E1 and E2) or virion-associated lipoproteins with low-density lipoprotein receptor (LDL-R), which leads to the binding of the envelope proteins with several cell-surface molecules including CD81, scavenger receptor BI (SR-BI), as well as tight junction proteins claudin-1 (CLDN-1) and occludin (OCLN) (231). HCV particles are internalized via clathrin-dependent endocytosis (143). pH-dependent fusion of the viral envelope with endosomes releases the genome, which is subsequently translated through its internal ribosome entry site (IRES) into a long polyprotein (232). The host signalase and signal peptide peptidase enzymes cleave the HCV polyprotein within the structural proteins (312). Next the NS2–NS3 junction is autocleaved by NS2-NS3 cysteine protease, and the remaining protein junctions are separated by the NS3-NS4A serine protease (146, 147). Following their synthesis, all the HCV non-structural proteins are recruited to the endoplastic reticulum (ER) membrane (90). NS4B that has a hydrophobic structure, rearranges the ER membranes to form the membranous web (MW) (67) consisting of double membrane vesicles (93, 94). Membranous web is the primary site of the viral replication (94, 124), where the viral RNA-dependent RNA polymerase (RdRp), NS5B, synthesizes the anti-genomic minus-strand and the subsequent genomic plus-strand RNA (164). Next, the Core protein which becomes associated with lipid droplets (LDs) following translation and processing (150, 260), is recruited to the replication complex through the interaction with NS5A and NS2 to encapsidate the genomic RNA and form the premature viral particle (69, 231, 400). The emerging virion is then recruited to the Golgi network by interactions with several essential host factors residing at the trans-Golgi network (13, 14), where it is coated with

glycosylated E1 and E2 proteins (417). Virion maturation and release occur through association with VLDL via the Golgi secretory pathway (106), and eventually the mature viral particles egress by budding from the plasma membrane (229, 231). The details of molecular mechanisms involved in the HCV particle assembly and secretion are still under investigation.

1.1.4 HCV Study Models

1.1.4.1 Model Systems In Vitro

For nearly a decade after the discovery of HCV in 1989, there was no *in vitro* model to study viral replication and protein function (238). In 1999, Lohman and co-workers established the first non-infectious subgenomic replicons of HCV from genotype 1b. In this replicon system, the open reading frame (ORF) encoding for Core to NS2 was replaced with a reporter gene (firefly luciferase) or a selection marker (neomycin phosphotransferase, which provides resistance to G418). Expression of the HCV replicase proteins (NS3-NS5B) is driven by the ephalomyocarditis virus (EMCV) IRES element, while the HCV IRES serves for the synthesis of the reporter or the selection marker (Figure 1-1A, B) (204, 239, 240). Consequently, after transfection into the permissive human hepatoma cell line (Huh7), only the cells supporting efficient HCV replication express sufficient amounts of the reporter or the selection marker and thus can be selected to establish cell lines that stably express HCV replicon RNA. Later on, bi- and tri-cistronic replicon systems have been developed that contain the entire HCV genome and are called full-genomic replicons (Figure 1-1C) (131, 160, 318).

In 2005, Wakita and co-workers reported the first, and so far the only infectious isolate of HCV derived from genotype 2a, designated JFH-1, and was cloned from the serum of a Japanese patient with fulminant hepatitis (424). Since then, various chimeras between JFH-1 and other

genotypes, as well as JFH-1 isolates with adaptive mutations that allow for more efficient replication in cell culture, have been developed (80, 280, 317, 345). This infectious model has provided an excellent system for the study of the HCV life cycle, virus-host interactions and evaluation of antiviral agents.

1.1.4.2 Model Systems In Vivo

For many years the only available *in vivo* model for HCV was chimpanzees. This model was instrumental to the understanding of the clinical course of HCV infection, transmission, immune response, and tissue tropism (211). However due to the limited availability, the cost for acquiring and maintaining chimpanzees, along with ethical considerations, the use of this animal model is now banned in Europe and by the NIH, and very restricted in other countries (135, 251).

Therefore the development of a small animal model that allows for robust HCV infection was crucial for the HCV studies.

Since rodent hepatocytes do not support the HCV entry and replication (321), a chimeric mouse model was developed by Dr. Kneteman and colleagues that allows for the HCV infection to physiologically relevant titers. In this model, primary human hepatocytes are transplanted into immunodeficient (SCID) mice carrying a plasminogen activator transgene driven by the albumin promoter (Alb-uPA). Since the expression of Alb-uPA transgene is lethal to hepatocytes, only mice with livers that are nearly completely repopulated by the transplanted human hepatocytes can survive (399). Such human liver chimeric mice then become susceptible to HCV infection and can support HCV infection in the absence of adaptive immune response (266). In this chimeric mouse-model, not only HCV replication occurs at biologically relevant levels, but also infectious viral particles are produced and released (266, 425). The uPA-SCID mouse model has

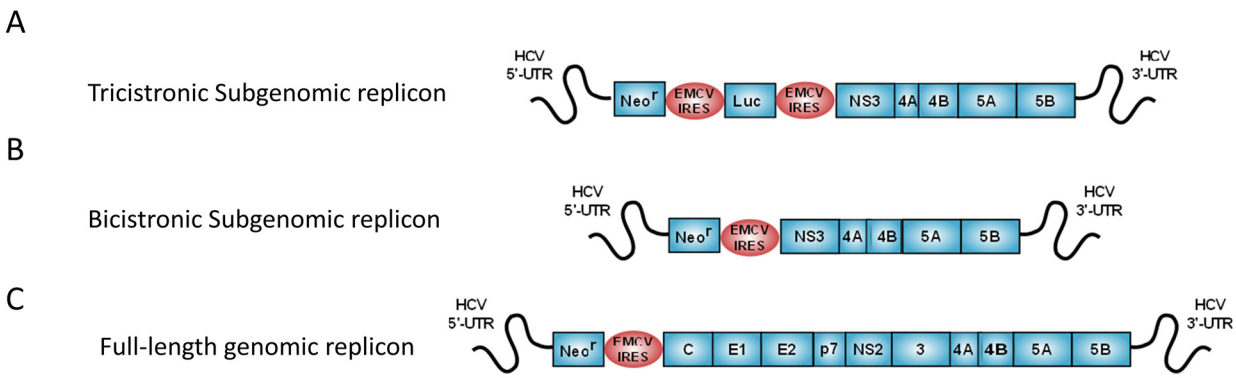

Figure 1-1. Schematic representations of the HCV replicon systems. Expression of the HCV proteins is driven by the ephalomyocarditis virus (EMCV) IRES element, and the HCV IRES serves for the synthesis of the Luciferase (Luc) or Neomycin. (A) and (B) Subgenomic HCV replicons. (C) full-length genomic HCV replicon. All replicon systems demonstrated are derived from genotype 1b.

been efficiently used to study the host-virus interactions, as well as to assess the efficacy of anti-HCV agents (251).

In spite of its usefulness, the uPA-SCID mouse model has several limitations, including the absence of the adaptive immune response. For this reason, genetically humanized mice were generated that carry some of the known human restriction factors for the HCV entry such as CD81, SR-BI, CLDN-1, and OCLN (89). This immune-competent "humanized" murine model supports HCV entry but not the replication (422), therefore recently a novel transgenic mouse has been developed that allows for the complete HCV life cycle. In addition to expressing the human entry factors for HCV, these mice are STAT1 or IFNαβ receptor deficient and thus are drastically impaired in type I and III IFN signaling (involved in innate immune response) (88). The humanized mouse model can be specifically employed to examine the efficacy of the HCV entry inhibitors, and vaccine candidates.

1.1.5 Host Factors Essential for HCV Replication

The limited viral proteome forces HCV to rely heavily on cellular factors for every step of its life cycle: For example, HCV entry occurs through the interaction of the viral envelope proteins with the host receptors (89, 231). Viral polypeptide is synthesized by the host cell protein synthesis machinery and its subsequent processing into ten viral proteins depends on cellular proteases. Host-mediated post-translational modifications of the viral proteins, such as glycosylation of E1 and E2 (122), and phosphorylation of NS5A (333), as well as direct interactions with cellular factors such as F-box and leucine rich repeat protein2 (FBL2) (426) and liver-specific microRNA miR-122 (177, 178, 426), are also deemed essential viral protein maturation and replication. Furthermore, viral particle assembly and release require the cellular pathways for

lipid metabolism as well as very low density lipoprotein (VLDL)/low density lipoprotein (LDL) assembly and secretion (267, 416).

Because the major problem with direct-acting antivirals is the emergence of resistant mutants, targeting the essential host factors for the HCV life cycle represents a strategy for antiviral design, as escape mutations are less likely to occur (190).

1.1.5.1 HCV & microRNA-122

MicroRNAs (miRNAs) are a class of endogenous non-coding small RNAs that regulate virtually every biological process including cell cycle, differentiation, metabolism, and apoptosis (30, 105). miRNAs originate from the nucleus as pri-miRNAs and undergo subsequent cleavages by cellular ribonucleases (RNases), to create approximately 22-nucleotide (nt) mature miRNAs (195, 439). Mature miRNAs function as a component of miRNA-induced silencing complex (miRISC) and exert their regulatory effects by Watson-Crick base pairing between 7-8 consecutive bases in the 5' end of miRNAs (referred to as the 'seed' sequence) and the 3'UTR of the target mRNA (59). As part of the RNA silencing pathway, miRISC binding generally induces either mRNA destabilization or translational repression (59).

MicroRNA-122 (miR-122) is a highly abundant, liver-specific miRNA that is involved in cholesterol metabolism and suppression of hepatocellular carcinoma (218). Aldolase A (AldoA) and N-myc downstream regulated gene 3 (Ndrg3) are two known cellular targets of miR-122, which regulate cell metabolism and growth, respectively (97, 100). miR-122 is also involved in maintaining iron homeostasis by repressing hemochromatosis (Hfe) and hemojuvelin (Hjv) mRNAs, which function as activators of hepcidin that regulates iron availability (176). Moreover, several proto-oncogens such as cyclin G1 and the insulin-like growth factor 1 (IGF-1)

receptor are among the direct targets of miR-122, implicating the regulatory role of miR-122 in tumorgenesis (22, 108).

Interestingly, miR-122 also positively modulates HCV transcription, translation, and genome stabilization (144, 169, 177, 178). Within the UTRs of the HCV genomic RNA, three highly conserved miR-122 recognition elements (MREs) exist: two in the 5'UTR and one in the 3'UTR (144, 177, 178). The interaction of miR-122 with the seeds sites in the 5'UTR of the HCV genome is vital for the viral life cycle (437).

Due to the crucial role of miR-122 in HCV replication cycle, locked nucleic acid (LNA)-modified phosphorothioate oligonucleotide that binds to and sequesters microRNA-122 (miravirsen) is in phase II clinical trial and has demonstrated promising results (119, 170). It is noteworthy that miR-122 is also a tumor suppressor; therefore it has been recommended that treatment with miR-122 antagonists should be carried out with caution and in short duration (437).

1.1.5.2 HCV & Host Lipid Metabolism

HCV depends on the host cell lipid biosynthesis and secretion as well as altered membrane structures in order to replicate (183, 271, 316, 348). For this reason, HCV hijacks elements of the cellular lipid metabolism and VLDL/LDL assembly pathways. Numerous genome-wide RNAi screens have also revealed that host genes involved in lipid metabolism, membrane biogenesis, and trafficking are crucial for HCV replication (40, 41, 209, 222, 394). HCV components, including those responsible for viral particle assembly, closely associate with lipid droplets (LD) (50, 245). Consequently, HCV employs various mechanisms to increase the cellular lipid content, including induction of lipid biosynthesis, impeding β-oxidation of fatty acids, and

hindering secretion of VLDL/LDL (32, 270, 315, 363, 391). This disturbance of lipid homeostasis leads to the development of liver disease and steatosis in HCV infected patients (414). In fact, steatosis is the main feature of chronic HCV infection, with a reported prevalence of 40%-80% (5).

There are several known molecular mechanisms that contribute to HCV-induced steatosis, such as activation of the steroid responsive element binding proteins (SREBP 1c and 2), which control the expression of enzymes involved in fatty acid and cholesterol metabolism, along with inducing *de novo* lipogenesis (388). Moreover, HCV inhibits the transcription of peroxisome proliferator activated receptors (PPAR α and γ) that control the transcription of enzymes responsible for fatty acid oxidation (77), such as the carnitine palmitoyltransferase-1 (CPT-1), the rate-limiting enzyme of mitochondrial β-oxidation (66). Finally, it has been shown that HCV core protein interferes with VLDL assembly by reducing the activity of microsomal triglyceride transfer protein (MTTP) and thus impairs the process of lipid secretion (270). All these processes contribute to the development of steatosis by HCV.

Several studies have reported that hepatic steatosis is negatively correlated with achievement of sustained virological response (SVR) after peg-interferon and ribavirin treatment (338, 343, 361, 445). Moreover, it has been demonstrated that steatosis is a risk factor for the development of HCC (209, 297, 310). Therefore, a better understanding of the molecular basis of the HCV-induced steatosis, will likely result in a more successful handling of the disease as well as improved antiviral success rates.

1.1.5.3 Induction of Internal Membrane Biogenesis during HCV Replication

Hepatitis C virus, like other plus-strand RNA viruses, promotes the rearrangement of intracellular membranes to form viral replication complexes. It also induces the enrichment of phosphatidylinositol 4-phosphate (PI4P) pools near its replication and assembly sites, by activating phosphoinositide 4 kinases (PI4Ks) in endoplastic reticulum (ER) and the Golgi (34, 40, 334, 364). Moreover, genome wide siRNA screens have identified the PI4P pathway to be critical for HCV replication (34, 40, 334, 364).

Phosphatidylinositol (PI) is an essential phospholipid component of the eukaryotic cell membrane that can be phosphorylated at positions 3, 4, and 5 of the inositol ring to generate phosphoinositdes (PIPs). There are seven known PIPs in eukaryotic cells, which have distinct biological role. A number of phosphoinositide kinases and phosphatases control the production and conversion of phosphoinositide species. Thus far, 19 phosphoinositide kinases (PIKs) and 28 phosphoinositide phosphatases have been identified in mammalian cells (354). The localization of PIPs provides codes that define the identity of different cellular membranes and associated organelles. PI4P, the most abundant cellular PIP, is mainly produced by the monophosphorylation of PI at the D-4 position of the inositol ring by one of the four different phosphoinositide 4 kinases (PI4Ks). PI4Ks have been categorized into two types; type II are sensitive to adenosine while type III demonstrate sensitivity to Wortmannin (23). Based on the domain structure, there are two isoforms of each type of PI4Ks; PI4KIIα and PI4KIIβ; PI4KIIIα and PI4KIIIβ (also known as PI4Kβ).

Due to the recruitment and activation of PI4KIIIα, HCV-induced membranous web is enriched with PI4P (34, 335). However, the significance of the Golgi-localized PI4KIIIβ (126) in the life cycle of HCV remains controversial. siRNA knockdown studies have revealed that PI4KIIIβ

silencing has a stronger effect on reducing the replication of HCV genotype 1b compared to genotype 2a (35, 154, 335, 395). Also, there is growing evidence that PI4P and its binding proteins at the Golgi play a key role in viral secretion. Therefore, it has been suggested that PI4KIIIβ is involved in the HCV secretion (40, 68).

Another significant PIK in HCV infection is PI3K. Several studies have indicated the activation of the PI3K/Akt pathway during HCV infection. PI3K is the kinase responsible for the production of PI(3,4)P2 as well as PI(3,4,5) P3, which in turn act as secondary messengers for several signalling pathways. HCV NS4B and NS5A have been shown to increase PI3K activity (306, 386, 387). Moreover, the PI3K/Akt pathway is also implicated in promoting *de novo* lipogenesis by activating SREBPs in response to insulin (223). These findings suggest multiple roles of PI3K in HCV replication cycle.

Since the above mentioned lipid kinases play important roles in the life cycle of many viruses from various viral families, such as Rous sarcoma virus (an alpharetrovirus), Epstein–Barr virus (a DNA Herpesvirus), HIV-1 (a Retrovirus), SARS (a Coronavirus), multiple Picornaviruses and Coxackivirus (27, 79, 303, 356, 447), they can be excellent targets for developing panviral therapeutics. For example AL-9, a member of the 4-anilino quinazoline class of compounds, which inhibits PI4KIIIα and prevents membranous web formation, has been shown to have anti-HCV effect (38).

1.2 RNA Silencing

RNA silencing or RNA interference (RNAi), is the major regulator of gene expression in eukaryotes (262). RNA silencing is mediated by double-stranded RNA (dsRNA), which is cleaved into small RNA duplexes of 21-30 nucleotides (nt) by cellular ribonucleases. These

small RNA duplexes mediate gene suppression by targeting complementary RNAs and lead to a combination of translational repression, transcript destabilization and degradation, as well as transcriptional suppression (130, 134, 461). There are two major classes of small noncoding RNAs; the short interfering RNAs (siRNAs) associated with RNA silencing and endogenous micro-RNAs (miRNAs) implicated in the regulation of gene expression. Due to its efficiency, RNAi is being considered as an important tool not only for functional genomics, but also for specific therapeutic strategies that directly target the viral RNAs or mRNAs of disease-related genes (7).

1.2.1 Antiviral Effect of RNA Silencing

Besides developmental regulation of gene expression in eukaryotes, RNA interference is involved in adaptive protection against viruses, and defense against transposable elements (134, 320, 429). Viral dsRNA molecules are produced in cells that are infected with diverse types of viruses (76, 185). Also, ample studies have demonstrated that viral replication triggers antiviral RNA silencing immunity in plants and invertebrates, through processing of viral dsRNA into siRNAs, and therefore conferring the antiviral state in these organisms (76, 185, 326, 392). In mammals, while viral dsRNAs are the activator of the innate immune response that limit viral spread by impacting on cellular translation and cytokine production, as well as promoting cell death (115), viral genomes have complex interactions with the host miRNA pathway (374, 401). Several mammalian viruses, including members of the *Herpesvirus* family and human immunodeficiency virus 1 (HIV-1), have been demonstrated to encode viral miRNAs that regulate host or viral gene expression (367, 390, 397). Importantly, endogenous cellular miRNAs have also been shown to specifically interact with mammalian viruses to limit their replication (214, 309, 349, 401). In contrast, a highly abundant, liver-specific, miR-122 facilitates the

replication of HCV (discussed in more detail in *Chapter 3*). These findings implicate small RNAs and the RNA silencing pathway as important regulators of viral infection, invasion and persistence in mammalian cells.

1.2.2 RNA Silencing Pathway

Precursor miRNAs are transcribed by the RNA polymerase II or III and processed by the cellular ribonucleases such as Dicer and Drosha into mature miRNAs (30, 130, 446). siRNAs and miRNAs guide a multi-subunit ribonuclease, containing an Argonaute (AGO) protein, referred to as RNA-induced silencing complex (RISC) (95). Once the small dsRNAs are assembled into RISC, the AGO protein unwinds the duplex and one strand of the small RNA is used as a guide (the guide strand) to target homologous RNA, and the other strand (the passenger strand) is degraded immediately by the cellular exonucleases (Figure 1-2) (258, 330). The thermodynamic stability at the ends of the small RNA duplex determines which strand is incorporated into RISC; in fact the 5′ end of the guide strand is less stable than the 5′ end of the passenger strand (157, 329). Upon hybridization of the guide strand with its target RNA, the AGO protein mediates cleavage of a single phosphodiester bond in the target RNA, between nt 10 and 11(95). The cleavage products are subsequently degraded by the cellular 3’ and 5’ exonucleases, as the resultant RNA cleavage products do not have the 5’ cap and poly(A) tail (298). The RISC complex can then be recycled to mediate multiple rounds of cleavage in an ATP-dependent manner (158). Therefore, this process leads to a highly efficient and sequence-specific knockdown of a particular gene.

1.2.3 Factors Affecting the Efficiency of RNA Silencing

Many factors contribute to the overall efficiency of RNA silencing. Numerous studies have led

to the establishment of parameters that, when incorporated into a rational siRNA design algorithm, increase the probability of selecting an effective siRNA (i.e. one capable of silencing gene expression by >50%) (96, 148, 339). Firstly, siRNAs should have a G+C content between 30-52% (96, 148, 339). High G+C content can inhibit duplex unwinding, whereas low G+C content is associated with decreased functionality, likely due to a lower target affinity and specificity (39, 339). The G+C content also typically correlates with accessibility (96, 191, 339); however, relying on G+C content alone may result in a large number of predicted false negatives (139). Designed siRNAs should have a low internal stability at the 3' terminus of the sense (passenger) strand since this will determine which strand of the duplex will be incorporated into RISC (191, 339, 357). In addition, siRNAs should lack inverted repeat sequences since palindromes can cause internal secondary structures that result in poor RISC loading (339). Lastly, several sense (passenger) strand base preferences have been described which correlate with increased siRNA efficacy, including an A base at position 3, a U base at position 10, the absence of a G base at position 13 and the presence of an A/U base at position 19 (339). The preference for a U at position 10 likely reflects the RISC endonuclease' preference to cleave the 3' end of U>A,G>C (96, 339) and the A/U at position 19 is likely a reflection of strand selection (191, 339, 357).

Despite a rational approach to siRNA design, only a fraction of siRNAs are effective at reducing the expression of their RNA targets, also the efficiency of different siRNAs directed against the same target often varies significantly (148, 293, 347). Additional parameters must therefore algorithms, despite the fact that target site accessibility is known to hamper efficient knockdown (46, 54, 203, 415, 444).

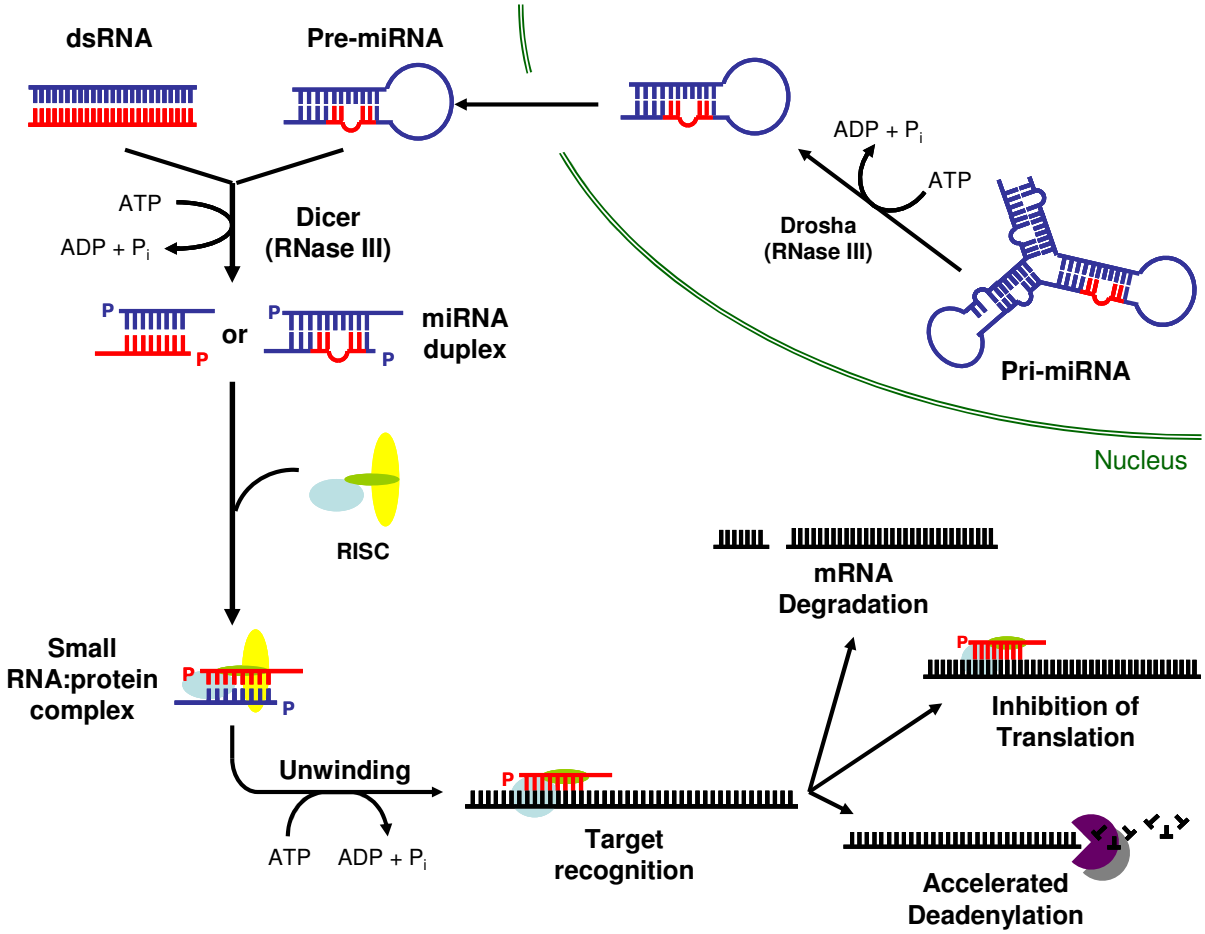

Figure 1-2. The RNA silencing pathway. The basic mechanism for RNA silencing is the cleavage of dsRNAs in the cytoplasm into small RNA duplexes (siRNAs and miRNAs). The cleavage of dsRNAs, which can have endogenous or exogenous origins, occurs by Dicer and the resultant 21–23nt dsRNA duplexes with symmetric 2–3nt 3' overhangs and 5'-phosphate and 3'-hydroxyl groups, are then incorporated into the RISC that unwinds the small RNA duplex and uses the guide strand to target the complementary RNAs for degradation, translational inhibition, or accelerated deadenylation. (Adapted from Sagan, SM. 2009. *Development of Protein- and RNA-based Tools for Studying Small RNAs Using Tombusvirus p19 and Native Target RNA Microarrays.* Ph.D. thesis, University of Ottawa. Canada)

affect the efficiency of siRNAs, such as target site accessibility or the presence of RNA binding proteins. These parameters are not taken into account by many currently available siRNA design

Applications of RNA Silencing

Through conserved pathways in eukaryotes from yeast to humans, small noncoding RNAs direct molecular machinery to silence gene expression (162). More recently, RNA interference has become a standard tool in molecular biology for understanding gene function and is being pursued extensively for therapeutic purposes. Since RNA silencing causes effective down-regulation of gene expression, it provides a simple alternative to creating knock-out cell lines or transgenic animals for gene investigations (26). Moreover, RNAi has been successfully used against many infectious agents such as viruses (118, 173, 331), although viruses are often able to escape RNAi-mediated silencing by accumulating point mutations within their genomes (149, 421, 436). Nevertheless, RNAi has been widely used as an experimental tool that has recently become the focus of drug development efforts to treat a variety of diseases and disorders.

The endogenous mammalian RNAi system, miRNAs, regulate almost every cellular process, thus their aberrant expressions have been associated with a wide variety of pathological conditions, such as those associated with cancer, autoimmune diseases, viral infections, and stem cell development (15, 28, 81, 159, 308, 313, 419). This revelation makes them attractive targets for molecular-based therapies. The premise is that the improvement of a disease symptoms or even cure is possible if we can employ reliable techniques to alter miRNA levels in specific cells and tissues. There are two main strategies that can be employed to achieve this goal: The first is the use of synthetic miRNA mimics to restore the expression level of a particular miRNA back to normal levels (242), and the second strategy is the use of miRNA “sponges” to block the action of over-expressed miRNAs (242). However, these strategies present with serious challenges as

most miRNAs are pleiotropic thus altering levels of any given miRNA may result in unintended consequences (308). Nevertheless, miRNAs have a promising future to be used as diagnostic and prognostic markers for many diseases as well as becoming therapeutic targets. Consequently RNAi technology is being perused as a novel therapeutic strategy to modulate gene expression, combat infections, as well as metabolic and developmental diseases.

1.3 Proteomics

It has been estimated that the human genome encodes for about 20,300 proteins (136). In a single cell, approximately 10,000 proteins are expressed (33, 340). However, non-synonymous single nucleotide polymorphisms (nsSNPs), alternative splicing, and post-translational modifications (PTMs), have made the human proteome extensively complex (1, 2, 466). Moreover, while the mRNA levels can highly correlate with the protein levels; transcriptomics does not take into account protein degradation rates, PTMs, protein localizations and concentrations inside the cellular compartments (340, 466). Therefore, proteomics data correlate better with the biological phenotypes than mRNA data (340, 466).

It has been more than three decades that liquid chromatography-tandem mass spectrometry (LC-MS/MS) has become the main method for protein analysis. In this method, which is also called shotgun or bottom-up proteomics, proteins are extracted, denatured, enzymatically digested, and chromatographically separated prior to mass spectrometry (MS) analysis. Tandem MS first measures the mass-to-charge ratio of the eluting ionized peptide, and then selects the peptide ions individually to obtain sequence information (441).

In order to comprehensively analyze the human proteome, the shotgun method has been improved at each and every step. For example, digestion with multiple enzymes, extensive

protein and peptide fractionation, as well as long operation and processing MS times, allowed for deep coverage of proteome in several cell lines and tissues (120, 195, 273, 281, 433). Furthermore, the technological advances in high throughput and high-resolution MS methods have generated the scale of data comparable to genomic and transcriptomic technologies (340). This poses a computational challenge that requires robust informatics tools that allow for comparative and quantitative analyses.

The advances in proteomics have led to a shift in the focus of the research community to functional mapping of physiologically and pathologically relevant proteomes (48). Today, extensive research is dedicated to map the spatiotemporal fluctuations of proteomes responsible for various cellular activities in response to stimuli or perturbations, to better understand the molecular basis for human diseases and develop potential therapeutic interventions. Moreover, proteomics holds great potential to characterize clinically useful biomarkers for diagnostic and prognostic purposes (48, 340). As such, proteomics, together with other "omics", will greatly advance the developing field of molecular medicine (65, 278).

1.4 Functional Proteomics

Recent advances in genomic and proteomic technologies have created a wealth of knowledge regarding the proteins encoded by the eukaryotic and prokaryotic genomes, as well as alterations in their expressions during various physiological states. However, determining the function of these proteins and relevance of these expression changes in complex biochemical pathways remained challenging. Moreover, protein activities are affected by complex molecular interactions and post-translational modifications. Therefore, effective methods were required to decipher the myriad functions of proteome and their modes of regulation.

1.4.1 Activity-Based Protein Profiling (ABPP)

Activity-based protein profiling (ABPP) is a groundbreaking functional proteomic strategy that allows examining the catalytic states of enzyme classes in native biological systems, assigns function to proteins with unknown functions, and provides insight into enzymes mechanisms (28, 70). In this strategy, small molecule inhibitors, which are conjugated to reporter or affinity tags, are exploited to target the catalytic active sites of different enzyme classes (28, 70, 257) (Figure 1-3). Labeled proteins are then purified and subsequently identified by mass spectrometry. These active-site directed probes, which are also referred to as activity-based probes (ABPs) are designed with the intention of exploiting conserved mechanistic features of their targeted enzyme family (70, 101, 172, 381). The reaction between the ABP and its active protein targets usually results in an irreversible covalent bond, which facilitates subsequent analysis through the reporter or affinity tag. As such, ABPP enables us to identify differentially active proteins in complex cellular micro-environments; this is particularly important as enzyme activity does not necessarily correlate with its abundance (70, 364). ABPP thus has the potential to make important contributions to understanding human physiology and pathology, by advancing the fields of biomarker discovery, *in vivo* imaging, and drug target discovery.

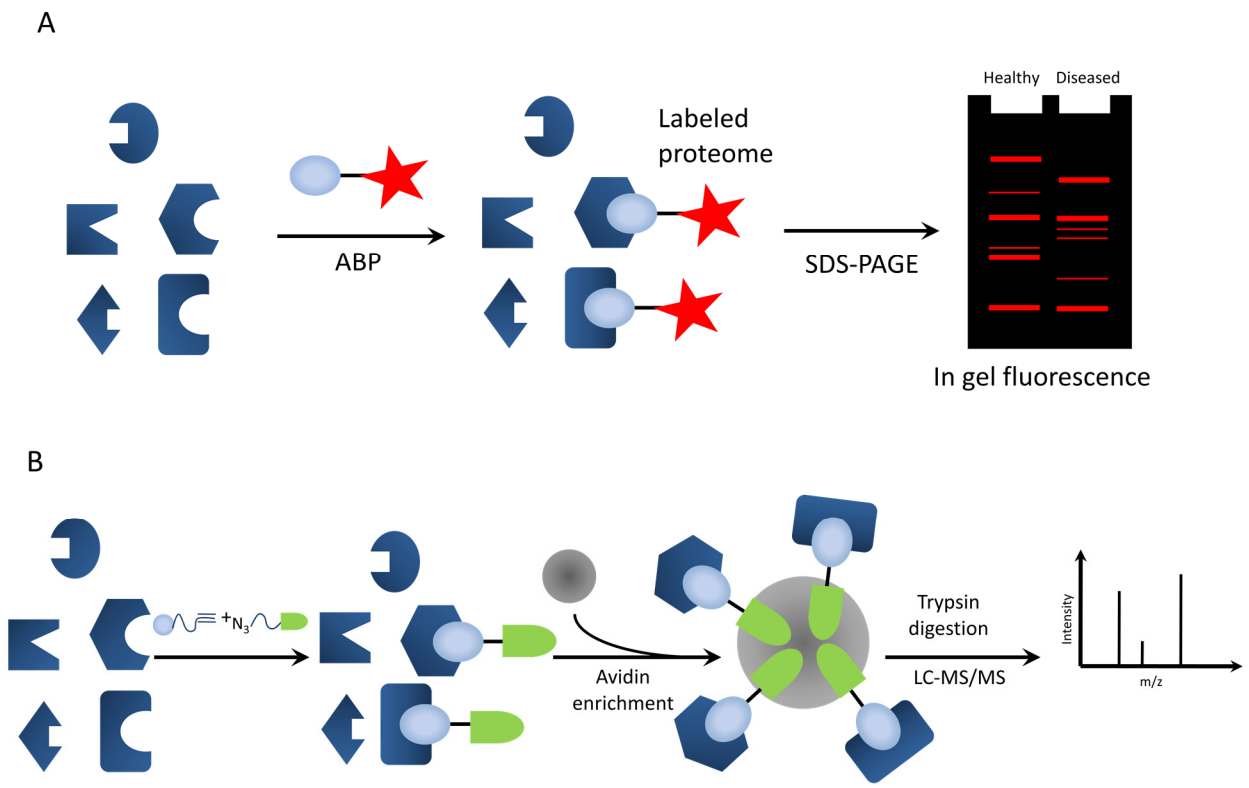

Figure 1-3. Activity based protein profiling. Activity-based probes consist of small molecules that are able to make covalent bond to the active site of a specific enzyme or an enzyme family. These probes are conjugated to either a fluorescent (A), or biotin (B) tag, so that their targets can be identified by in-gel fluorescence, or mass spectrometry respectively.

ABPP studies have been applied in virology to identify the alterations in the host enzymatic functions, assign catalytic functions to previously uncharacterized viral proteins, visualize altered cellular proteome, develop new antiviral therapeutics and viral diagnostics (41, 42, 301, 344, 372). Thereby ABPP can be employed to interrogate the catalytic state of the host enzymes involved in HCV infection, leading to the identification of novel host factors with clinical importance in HCV pathogenesis and persistence. Moreover, ABPP allows for the screening of small molecules with inhibitory potential that can subsequently be used as drugs (290).

1.4.1.1 Activity-Based Probes (ABPs)

Based on the nature of the reactive warhead, ABPs can be categorized into at least three different classes: directed or mechanism-based ABPs, substrate-based ABPs and non-directed ABPs (42, 70). Directed ABPs have an electrophile inhibitor as the reactive group that binds to the catalytic amino acid residue of the target enzyme via a nucleophilic attack (Figure 1-2). Examples of class-wide mechanism-based ABPP probes include electrophilic phosphonate esters, modified fluoroglycosides, and natural products like wortmannin and microcystin that target serine hydrolase, glycosidase, kinase and threonine phosphatase families, respectively (235, 236, 368, 418, 454).

Although mechanism-based ABPs are effective in targeting enzyme families with known covalent inhibitors, many enzyme classes do not use conserved active-site nucleophiles or electrophiles to catalyze their enzymatic reactions and thus cannot form covalent adducts with mechanism-based suicide inhibitors. To expand the number of enzyme classes addressable by ABPP, non-directed ABPs that contain mild reactive electrophiles were developed (3, 4). For example, non-directed sulfonate ester (3, 372), α-chloroacetamide (29), and spiroepoxide (36) probes successfully labeled different enzyme families with various cellular roles.

1.4.1.1.1 *In Situ/In Vivo* Activity-Based Probes

Initially ABPs were applied with bulky reporter groups (i.e. fluorophore or biotin), which limited their uptake and distribution in cells and tissues. Consequently, early ABPP experiments were only carried out *in vitro,* on homogenized cells or tissues. Since physical disruption of cellular membranes and organelles may alter the concentrations of endogenous protein activators/inhibitors, *in vitro* labeling can only approximate the functional state of the targeted enzymes (380, 381). In response to these limitations, and in order to provide a more physiologically relevant enzymatic profile, a "tag-free" version of ABPP was developed. In this approach, ABPs that bear a small bio-orthogonal functional group, such as a terminal alkyne (≡) or azide (N_3), were designed , so that can react via Huisgen's 1,3-dipolar cycloaddition (click chemistry) to form a stable triazole products (202). Therefore to visualize or isolate the enzymes bound to the *in situ* ABPs, the labeling is followed by a "click" reaction between the probed proteins and the "clickable" fluorescent or affinity tags (Figure 1-4C) (381). The small size of these bio-orthogonal groups greatly improved the ABP cell permeability for *in situ* and *in vivo* proteome labeling (42, 291).

1.4.1.2 Comparative ABPP

Comparative ABPP is the most common application of ABPP in biology that could lead to target discovery. In this approach, two or more different proteomes are comparatively analyzed in parallel to identify distinct biological properties (e.g. healthy versus disease, or normal versus abnormal) (Figure 1-4A). Then the altered enzyme activities identified by ABPP can be hypothesized to regulate a certain phenotype (291, 381). Further experiments are then required to test such hypotheses.

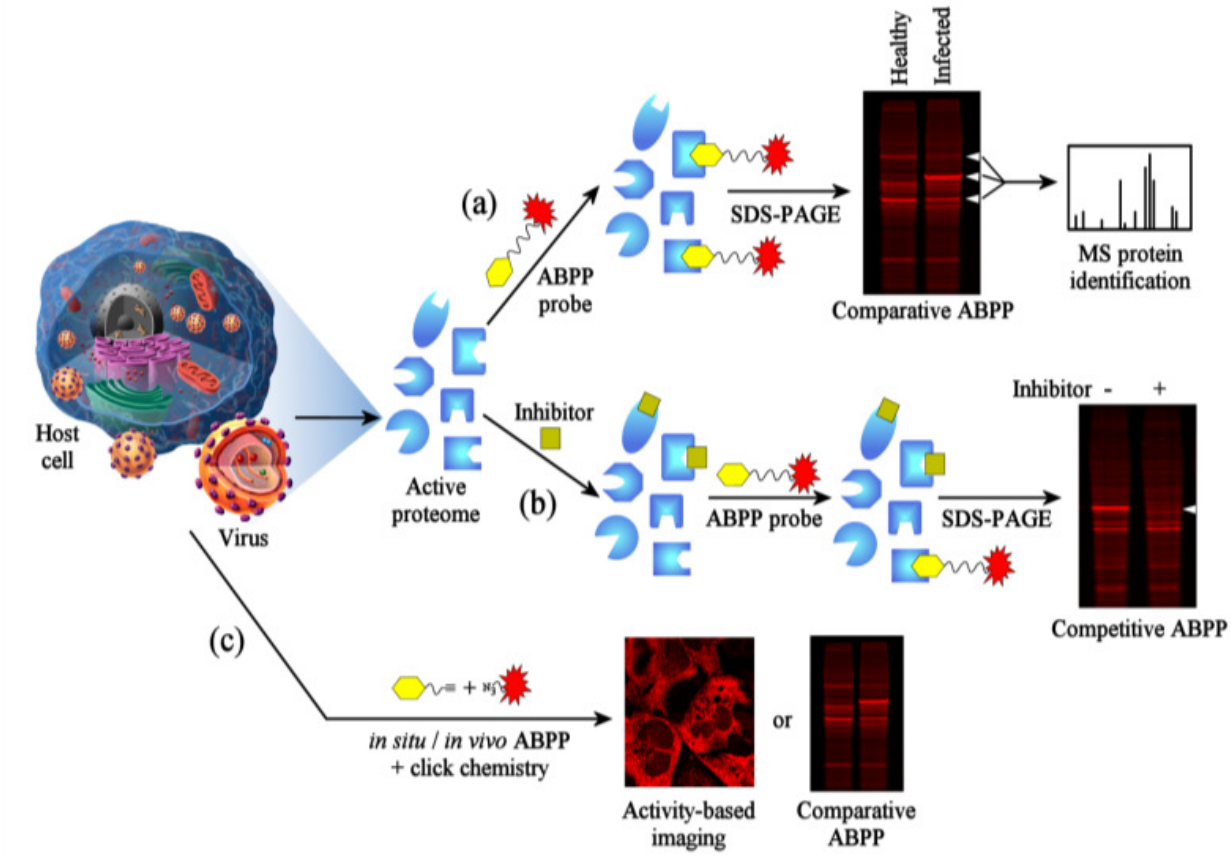

Figure 1-4. Applications of ABPP to study viral replication and infection. (a) Comparative ABPP has been extensively used to screen for differentially active enzymes during viral propagation with the potential to become therapeutic and diagnostic candidates. (b) Competitive ABPP is being used to screen inhibitor libraries and determine the specificity and sensitivity of potential therapeutics against both host and viral enzymes involved in the viral life cycle. (c) Comparative and imaging ABP probes have been used in situ by using the bioorthogonal click chemistry to monitor the variability of subcellular enzymatic activity induced by viral pathogenesis and the general experimental flow is depicted (adapted from (42)).

Comparative ABPP has been applied in virology to compare the differential activity between healthy and virus infected host proteomes (Figure 1-4A). Viral proteins and their altered host proteomes are good candidates for comparative ABPP analyses, since viruses usually have a manageable number of proteins, and coordinated host-virus interactions are indispensible for every step of the viral replication. Essential host enzymes that show differential activity during viral infection have the potential to be considered as antiviral targets (41, 42, 301, 372).

1.4.1.3 Competitive ABPP

Another important application of ABPP is the discovery of enzyme inhibitors. In this approach, inhibitors are screened and identified by their ability to compete with ABPs for the enzyme active sites, therefore potent inhibitors are able to outcompete and thus block probe labeling of their specific targets (Figure 1-4B) (28, 70). Since ABPP allows for performing inhibitor assays on enzymes in their native conformation, there is no need to for recombinant expression and purification of enzymes. Moreover, high throughput screening for inhibitor potency and selectivity is possible with competitive ABPP, as a library of compounds can be tested against many enzymes in parallel (21).

While conventional antiviral drugs focus on targeting viral proteins to minimize side effects, the limited number of viral targets and the rapid emergence of drug-resistant viral mutations urged the exploring the host cell targets as alternatives for antiviral therapeutics. For that reason, competitive ABPP has recently been applied for screening and testing antiviral drugs against SARS Coronavirus and the Ebola pseudotype virus (12, 42, 360). Modern virology and antiviral drug discovery are thus expected to be benefited by ABPP. The high-throughput characterization of newly identified antiviral targets, as well as inhibitor discovery, may lead to the development of novel viral diagnostics and antiviral therapeutics.

In conclusion, ABPP is a valuable technique for providing unique information on the enzymatically-active proteome, which complements other large-scale profiling methods, such as abundance-based proteomics, SILAC, microarray, and systems biology approaches. The future challenges for the application of ABPP in virology will be to determine which of the myriad of host enzymes are essential for virus infection. These newly identified ABPP candidates will represent novel targets for the development of viral diagnostics and antiviral therapeutics.

In this thesis, I report the application of several known and novel, directed as well as non-directed ABPs, in investigation of alterations in the host enzymatic activities during HCV replication. Herein, the results of these specific and global profiling assays, which led to the discovery of a number of novel host factors for HCV, are presented and discussed.

Chapter 2: Materials & Methods

2.1 Introduction

The methodology described in this chapter is designed to investigate the interactions of HCV with the essential host factors during its replication, with an intention to provide insight into the unexplored aspects of the HCV life cycle. For this purpose, I have employed RNA-based, as well as protein-based techniques to analyze the effect of several different host factors on HCV replication cycle. As such, this chapter provides details of the two complementary approaches used: miRNA seed-site accessibility assays and activity-based protein profiling assays.

2.2 HCV Replicons and Viruses

HCV subgenomic replicons (genotype 1b, Con1, Genbank Accession Number: AJ242654), pFKI389neo/NS3-3'/5.1 and pFKI389luc/NS3-3'/5.1 plasmids, were kindly provided by Ralf Bartenschlager (Institute of Hygiene, University of Heidelberg, Heidelberg, Germany). The replicons harbour either neomycin resistance (neoR; pFK-I389neo/NS3-3'/5.1) or the firefly luciferase (luc; pFKI389luc/NS3-3'/5.1) gene at the 5' end, driven by the HCV IRES, but otherwise are identical and express the HCV non-structural proteins (NS3 to NS5B) from the encephalomyocarditis virus (EMCV) IRES and are described previously (240). Insertion of SL V and VI of the core ORF into the pFK-I389luc/NS3-3'/5.1 replicon was done using SL-NruI/AscI oligonucleotide (Table 2-1) (Sigma-Aldrich, Oakville, ON). The fragment was excised with NruI and AscI and inserted into pFK-I389luc/NS3-3'/5.1 replicon. Mutagenesis of the pFK-I389luc/NS3-3'/5.1 replicon was performed using QuikChange Lighting kit (Stratagene, La Jolla, CA), and primers are listed in Table 2-1 according to the manufacturer's protocol. $JFH1_T$ harbors 3 amino acid changes that enhance infectious virus production and was derived from the cell culture-adapted JFH1 strain JFH-AM1, as previously described (345).

Table 2-1. Sequence of oligonucleotides.

Oligo name	Position†	Sequence
Mutagenic Primers		
MRE 1 Forward	9-45	5'-ccgattgggggcgacacagcaccatagatcactcccc-3'
MRE 1 Reverse	9-45	5'-ggggagtgatctatggtgctgtgtcgcccccaatcgg-3'
MRE 2 Forward	21-62	5'-gacactccaccatagatcacagccctgtgaggaactactgtc-3'
MRE 2 Reverse	21-62	5'-gacagtagttcctcacagggctgtgatctatggtggagtgtc-3'
MRE 3 Forward	9373-9409	5'-gaacggggagctaaacacagcaggccaataggccatc-3'
MRE 3 Reverse	9373-9409	5'-gatggcctattggcctgctgtgtttagctccccgttc-3'
MRE 4 Forward	8789-8826	5'-ggagacagctagacacacagcagtcaattcctggctag-3'
MRE 4 Reverse	8789-8826	5'-ctagccaggaattgactgctgtgtgtctagctgtctcc-3'
MRE 4nc Forward	8781-8819	5'-gctgcgtgggagacagctagacatacgccagtcaattcc-3'
MRE 4nc Reverse	8781-8819	5'-ggaattgactggcgtatgtctagctgtctcccacgcagc-3'
Stem Loop Sequence Insert		
SL-Nru1/Asc1	272-549	5'-gcgaaaggccttgtggtactgcctgatagggtgcttgcgatgc cccgggaggtctcgtagaccgtgcaccatgagcacgaatcctaaacctcaaag aaaaaccaaacgtaacaccaaccgccgcccacaggacgtcaagttcccgggc ggtggtcagatcgttggtggagtttacctgttgccgcgcaggggccccaggttg ggtgtgcgcgcgactaggaagacttccgagcggtc ggcgcgcc-3'

† - positions in reference to full length HCV genotype 1b isolate Con1 genome (Genbank accession #: AJ238799.1)

2.3 Cell Culture

All cells were maintained at 37°C, 5% CO_2 in a humidified incubator. Huh7 and Huh7.5 cells were grown at 37 ºC, with 5 % CO_2 in Dulbecco's Modified Eagle Medium, 10 % fetal bovine serum (FBS) (NorthBio), 50 units/mL penicillin and 50 µg/mL streptomycin. HeLa cells were maintained in Minimum Essential Medium (MEM; Invitrogen, Burlington, ON, Canada) containing 10% FBS, 50 U/mL penicillin, 50 mg/mL streptomycin and sodium pyruvate. Additionally, Huh-7 media was supplemented with 1X minimal essential medium (MEM) non-essential amino acids. Huh7.5 cells stably expressing the HCV subgenomic and full-length replicons (genotype 1b, Con1 Genbank Accession Number: AJ238799)(318) were kind gifts from Dr. Charles Rice (Rockefeller University, USA), and were cultured in Huh7 media supplemented with 250 µg/ml G418 Geneticin (GIBCO-BRL, Burlington, ON).

2.4 Statistical Analyses

Individual experiments in this thesis were performed no less than triplicates in order to confirm the reproducibility of the results. Statistical differences were assessed using different methods including standard error, standard deviation, and the student t-test in GraphPad Prism v4.01 software package (GraphPad Software Inc., La Jolla, CA). The specific details of statistical analyses are described further in each chapter.

2.5 Methods for Examining Target-Site Accessibility (TSA) Using Viral RNA-Coated Magnetic Beads (VRB)

2.5.1 *In Vitro* Transcription (IVT)

In vitro transcripts were generated using the MEGAscript™ T7 kit (Ambion, Austin, TX) according to the manufacturer's protocol. Briefly, the template DNA was linearized with the

restriction enzyme *ScaI* (New England Biolabs, Pickering, ON), precipitated for less than 30 min, and resuspended in RNase-free water to a final concentration of 0.5 μg/μL. The IVT reaction was set up in a final volume of 20 μL and incubated at 37 ºC for 4 h. In order to degrade the template DNA, 1 μL of *DNase I* was added and the reaction was incubated for an additional 15 min at 37 ºC. The *in vitro* transcripts were then cleaned up using the MEGAclear™ kit (Ambion, Austin, TX) according to the manufacturer's protocol. A 20 μL reaction typically produced ~100 μg of RNA. The concentration was determined by measurement of the absorbance at 260 nm with an ND-1000 spectrophotometer (NanoDrop Technologies, Rockland, DE), and RNA integrity was verified by electrophoresis on a 0.8% agarose gel in TBE.

2.5.2 5' and 3' End Biotinylation of the HCV Transcripts

For the VRB TSA assay, HCV subgenomic replicon RNA transcripts were biotinylated at the 3'-end using the 3'-EndTag Nucleic Acid Labeling system (Vector Laboratories, Burlingame, CA) according to the manufacturer's protocol. Also 5'-end biotinylation was performed using the 5'-EndTag Nucleic Acid Labeling system (Vector Laboratories, Burlingame, CA) according to the manufacturer's protocol. The EZ-Link Maleimide-PEG11-Biotin label (Thermo Fisher Scientific, Ottawa, ON, 20 mM) was dissolved in RNase-free DMSO (Sigma-Aldrich, Saint Louis, MO) and the final reaction volume was 20 μL. Labeled HCV subgenomic replicon RNA was then purified using the MEGAclear kit (Ambion, Austin, TX) and the RNA integrity was verified by agarose gel electrophoresis and quantified by measurement of the absorbance at 260 nm with an ND-1000 spectrophotometer (NanoDrop Technologies, Rockland, DE).

2.5.3 *In Vitro* Hybridization

One microgram of biotinylated HCV subgenomic replicon RNA was diluted in 1X Hybridization buffer (20 mM HEPES, pH 7.8, 50 mM KCl, 10 mM $MgCl_2$,1 mM DTT) supplemented with 0.2

U/µl SUPER-In RNase Inhibitor (Ambion, Austin, TX) in a total volume of 20 µL. The Cy3-labeled miR-122 was diluted to final concentrations ranging from 10nM to 500nM. Hybridizations were then carried out at 37°C for 30 min.

2.5.4 Magnetic Microbead Preparation and Immobilization of RNA

Approximately $5X10^6$ streptavidin-coated Dynabeads M-280 (Invitrogen, Burlington, ON) were used per sample. After resuspension, beads were washed 1X with 1X B&W buffer (2X B&W buffer: 10 mM Tris-HCl, pH 7.5 + 2M NaCl) and then washed 2X with solution A (0.1M NaOH + 0.05M NaCl) at room temperature in order to make them RNase free. Finally, the beads were washed 2X with Hybridization buffer at room temperature prior to incubation with the hybridization reactions. The *in vitro* hybridization reactions in solution were then added to the streptavidin-coated Dynabeads and they were then incubated at 37°C for 30 min to capture the biotinylated HCV subgenomic replicon RNAs. After immobilization, the VRBs were washed 4X with the hybridization buffer and resuspended in 12 µL of RNase free PBS. The beads were visualized by fluorescence using Olympus 1x81 inverted confocal microscope (Olympus Optical Co LTD, Japan).

2.5.5 VRB Image and Data analyses

The quantification of signal intensities from the VRBs was performed using Image-Pro® Plus 4.5 software (Media Cybernetics, Inc, Silver Spring, MD) by calculating the integrated optical density (IOD) from individual beads. Net signal intensities were obtained by local-ring background subtraction (net = raw – background). The net signal intensity for each bead was then normalized to the area of the bead (net IOD/area) and averaged for approximately 100 beads per image.

For normalization purposes, the net IODs from the control hybridization reactions were carried out in the absence of HCV subgenomic replicon RNA and the results were subtracted from the net IODs. Hybridizations were carried out at final miR-122 concentrations ranging from 10nM to 500 nM. From these hybridizations, standard curves for native HCV RNA were generated from linear least squares fitting of the net IODs *vs.* miR-122 concentrations. Target site accessibility was assessed by the the slope of the miR-122 hybridization to native HCV RNA.

2.5.6 RNA Isolation and Quantitative RT-PCR

For quantitative RT-PCR (q RT-PCR) analyses total RNA was isolated from HCV subgenomic replicon-transfected Huh7.5 cells at 72 and 120 h post-transfection using the RNeasy extraction kit (Qiagen, Mississauga, ON). RNA extracts were then subjected to *DNase I* (Ambion, Austin, TX) digestion. Total RNA was then purified with the DNA-free kit (Ambion, Austin, TX). The concentration was determined by measurement of the absorbance at 260 nm with an ND-1000 spectrophotometer (NanoDrop Technologies, Rockland, DE). Approximately 0.5 µg/well of total RNA was loaded onto a 0.8% agarose gel to determine the integrity. One microgram of total RNA was used for cDNA synthesis using the Superscript II kit (Invitrogen, Burlington, ON) according to the manufacturer's protocol. Quantitative PCR (qPCR) was performed on an iCycler (Bio-Rad, Hercules, CA) using iQ SYBR Green Supermix (Bio-Rad, Hercules, CA), and primers directed against the HCV IRES region (Forward 5'-GTC TGC GGA ACC GGT GAG TA-3' and Reverse 5'-GCC CAA ATC TCC AGG CAT T-3'), and the 18S rRNA (Forward 5'-GCG ATG CGG CGG CGT TAT TC-3' and Reverse 5'-CAA TCT GTC AAT CCT GTC CGT GTC C-3'). A 20 µL reaction was assembled according to the manufacturer's protocol. For data analysis, the $2^{-\Delta\Delta Ct}$ method was used (237) and mean fold changes relative to unmutated HCV

subgenomic replicon-transfected cells were calculated. Each qPCR experiment was carried out in triplicates and repeated three times.

2.5.7 Northern Blot analysis

Approximately 2 μg/well of total RNA was loaded onto a 1% agarose gel. Biotinylated negative-sense probes complementary to the HCV genome NS5B region nts 6648-7770 (Genbank accession #AJ242654) and the β-actin gene (Genbank accession #X00351) were synthesized using the MEGAscript™ T7 kit (Ambion, Austin, TX). *In vitro* transcriptions were performed as described above with the inclusion of biotin-11-UTP and biotin-11-CTP (Perkin Elmer, Boston, MA) at molar ratio of 1:3 with unlabeled UTP and unlabeled CTP, respectively. The biotinylated negative-sense probes were used at a final concentration of 2.2 ng/uL and 0.133 ng/uL for the HCV and β-actin probes, respectively. Northern blotting and hybridization were carried out using the NorthernMAX kit (Ambion, Austin, TX) and Hybond XL nylon membranes (GE Healthcare, Piscataway, NJ). The bound riboprobes were detected using the Chemiluminescent Nucleic Acid Detection Module (Pierce, Rockford, IL) according to the manufacturer's protocol.

2.5.8 Luciferase Assays

Cells transfected with unmutated or MRE-mutated HCV RNA replicon were harvested 24 or 72 h post-infection and the luciferase activity was determined by using the luciferase reporter assay (Promega, Madison, WI). Luminescence was measured with an Lmax luminometer (Molecular Devices Corporation, Sunnyvale, CA). Values were normalized against total protein content using the Bio-Rad DC Protein Assay (Bio-Rad, Mississauga, ON) according to the manufacturer's protocol.

2.5.9 Alignment of HCV sequences

miR-122 seed match conservation for MRE4 was performed using the Quickalign tool provided by the Los Alamos HCV database (http://hcv.lanl.gov/cgi-bin/QUICK_ALIGN/QuickAlign.cgi) (208). The location of MRE 4 was found in the H77 reference sequence and used for alignment against the 465 HCV sequences in the database. Sequences were assigned to a specific genotype and subtype and only those classified are shown in Table 3-2.

2.6 Methods for Activity-Based Protein Profiling

2.6.1 Activity Based Protein Profiling Using Orlistat-Based Probe

2.6.1.1 Expression of the HCV Proteins

For the expression of the individual HCV proteins, Huh7 cells were seeded at a confluency of 60-70% and then transfected with E1/E2, Core, NS2, NS4B, NS5A and NS5B expression plasmids suspended in transfection media comprised of DMEM without FBS, along with lipofectamine 2000 (Invitrogen Canada Inc., Burlington, ON). After 4 h, DMEM in 20% FBS was added in equal volume to the transfection media.

2.6.1.2 Inhibitor Treatments

Huh7 cells that stably expressing HCV replicon were seeded in a 6-well plate. After 24h, at a confluency of 80%, cells were treated with Orlistat, Cerulenin, C75, and TOFA all purchased from Cayman Chemicals (Michigan, USA) at 10 μM final concentration for 48 h at 37˚C. At this time point, cells were washed once with PBS and lysed with cell culture lysis buffer (Promega, Madison, WI). Luciferase Assay substrate was added and the luminescence was measured with an Lmax luminometer (Molecular Devices Corporation, Sunnyvale, CA). Values were

normalized against total protein content using the Bio-Rad DC Protein Assay (Bio-Rad, Mississauga, ON) according to the manufacturer's protocol.

2.6.1.3 Active Proteome Extraction for Labeling

Subconfluent cells were washed with ice-cold PBS pH 7. The chimeric liver tissues were subjected to Dounce homogenization at 50% power (T8 Ika-Werke Homogenizer, GMBH (Staufen, Germany). The lysates were then sonicated (10 pulses, 50% duty cycle; Sonifier 250, Branson Ultrasonic (Danbury, CT) in ice-cold PBS supplemented with 1% Triton X-100. The protein extract was quantified with the DC protein assay (BioRad), and diluted with PBS to a final protein concentration of 1 mg/ml.

2.6.1.4 In Vitro and In Situ Proteome Labeling and Analysis

For *in vitro* proteome labeling, probes were added to cell lysates (50 μg) in 50 μL of PBS at a final concentration of 10 μM in the presence or absence of excess Orlistat, C75, or Cerulenin competitor (a final concentration of 100 μM). Unless indicated otherwise, samples were incubated for 1 h at room temperature. For heat-denatured samples, the proteome was heated for 10 minutes at 95 °C, prior to adding the probes. After incubation, 100 μL of the freshly premixed click chemistry reaction cocktail in PBS [rhodamine-azide (200 μM, 100 mM stock solution in DMSO), tris(2-carboxyethyl)phosphine hydrochloride (TCEP) (2 mM, 50 mM freshly prepared stock solution in deionized water), tris[(1-benzyl-1H-1,2,3-triazol-4-yl)methyl] amine (TBTA) (200 μM, 50 mM stock solution in DMSO) and $CuSO_4$ (2 mM, 50 mM freshly prepared stock solution in deionized water)] was added and vortexed, then incubated for 2 h at room temperature with gentle mixing. The reactions were terminated by the addition of prechilled acetone (1 mL), placed at −80 °C for 15 min and centrifuged at 14000 rpm for 15 min at 4 °C to precipitate proteins. The protein pellets were allowed to air-dry for 10 min, resuspended in 25 μL

1 × standard reducing SDS-loading buffer, heated for 10 min at 95 °C; and separated by 10% SDS-PAGE, then visualized by in-gel fluorescence scanning using the *FMBIO Fluorescence Scanner (Hitachi).*

For *in situ* labeling, Huh7 cells were grown to 80–90% confluence in 6-well plates under the conditions described above. The medium was removed, and then cells were treated with 0.5 mL of medium-containing probe (20 μM), with or without Orlistat, C75, TOFA, or Cerulenin (200 μM). Probes were applied from DMSO stocks, while DMSO never exceeded 1% in the final solution. The same volume of DMSO was used as a negative control. After 2 h of incubation at 37 °C/5% CO_2, the medium was aspirated, and cells were washed with PBS to remove the excessive probe, and lysed with 200μl of ice-cold PBS containing 1% Triton. The lysate was then homogenized by sonication, and diluted to 1 mg/mL with PBS. Probe targets were detected by click chemistry with rhodamine-azide, SDS-PAGE analysis, followed by in-gel fluorescence scanning.

2.6.1.5 Western Immunobloting

Subsequent to in-gel fluorescence scanning, the proteome is transferred onto Hybond-P PVDF membrane (Amersham Biosciences). Thereafter, the membrane was blocked for 1 h in 3% dried skim milk in Tris-buffered saline (TBS) with 0.05% Tween-20. Human FASN and protein tyrosine phosphatase 1D (PTP-1D, as the loading control), HCV core, E1/E2, NS2, NS4B, and NS5A, were targeted with: a mouse monoclonal anti-FASN (2000-fold dilution; Santa Cruz Biotechnology), a mouse monoclonal anti-PTP-1D (10,000-fold dilution; BD Laboratories), a mouse monoclonal anti-HCV core (2000-fold dilutions Abcam), a goat monoclonal anti-HCV E1 (1:2000, Virostat), a mouse monoclonal anti-FLAG (2000-fold dilutions, SIGMA), a mouse monoclonal anti-HCV NS4B (2000-fold dilutions, Abcam), and a mouse monoclonal anti-NS5A

(2000-fold dilution; ViroStat), respectively. Bound primary antibody was detected with HRP-conjugated anti-mouse antibody, and the blots were developed using chemoluminescent detection system (ECL prime, Amersham).

2.6.1.6 Measurement of Cellular Triglyceride Levels

At 48h post-transfection, lipids were extracted from 10^6 trypsinized cells. Triglyceride levels were analyzed directly by spectrophotometric analyses, using the triglyceride quantification kit (BioVision, Mountain View, CA), according to the manufacturer's instructions. Total protein levels were quantified with DC protein assay (BioRad). Triglyceride levels were expressed per mg of protein.

2.6.1.7 Fluorescence Microscopy

Huh7 cells at 60-70% confluency were fixed for 15 min with 4% paraformaldehyde and 4% sucrose in PBS. After two PBS washes, cells were permeabilized with 0.25% Triton X-100 (Sigma) in PBS for 5 min and blocked with 10% bovine serum albumin (BSA) in PBS for 30 min at 37°C. Immunofluorescence staining was performed by incubation with the following primary antibodies in 3% BSA/PBS: mouse monoclonal anti-NS5A (1:1000; Chemicon International, Billerica, MA), rabbit monoclonal anti-FASN (1:50, Santa Cruz Biotechnology), mouse monoclonal anti-dsRNA (1:3000; Scicons, cat.no. 10010200). Consequently, the samples were washed 3x with PBS for 5 min and incubated for 1 hour at 37°C in 3% BSA/PBS containing the respective secondary antibody: Rhodamine Red-X donkey anti-rabbit (1:1000); or Cy2 donkey anti-mouse (1:1000) (Jackson ImmunoResearch). The samples were then washed by 1 % Tween-20 and 0.5 mM of EDTA in PBS (3×5 min). Fluorescence images were collected using an Axiovert 200M inverted microscope (Carl Zeiss, Thornwood, NY) equipped with the

Axiovision 3.1 software. The cells were then photographed with an AxioCam connected to the inverted microscope.

For ABPP imaging, the cells were incubated with Orlistat probe (30 μM) for 4 h in growth medium at 37˚C and 5 % CO_2. Medium containing 1 % DMSO was used as a negative control. The cells were then washed twice with PBS, and fixed with 4 % paraformaldehyde in PBS for 15 min at room temperature, washed with PBS (2×5 min with gentle agitation), and permeabilized with 0.1 % Triton-X 100 in PBS for 15 min at room temperature, and washed with PBS (2×5 min with gentle agitation). The cells were blocked with 3 % BSA in PBS for 30 min at room temperature, and washed with PBS (2×5 min with gentle agitation). The cells were then treated with a freshly pre-mixed click chemistry reaction solution of rhodamine–azide (10 μM final concentration from a 10 mM stock solution in DMSO), TCEP (1 mM final concentration from a 50 mM freshly prepared stock solution in deionized water), TBTA (100 μM final concentration from a 10 mM stock solution in DMSO), and $CuSO_4$ (1 mM final concentration from a 100 mM freshly prepared stock solution in deionized water), in PBS for 1 h at room temperature. The cells were washed with PBS (1×5 min with gentle agitation), and cold methanol (1×5 min with gentle agitation), followed by 1 % Tween-20 and 0.5 mM of EDTA in PBS (3×2 min with gentle agitation), and with PBS (2×5 min with gentle agitation). For co-localization of FASN and HCV replication complex, indirect immunofluorescent cytochemical staining was carried out with either anti-NS5A or anti-dsRNA as described above.

Colocalization analyses were performed using colocalization analysis plug-in of ImageJ (National Institude of Health, NIH) and the Mander's and Pearson's coefficient were calculated by Mander's calculator, and the results are shown as the mean of 5 different image sets per sample, subsequent to background correction and exclusion of zero-zero pixels.

2.6.2 Activity Based Protein Profiling Using β-Lactam Probes

2.6.2.1 In Vitro and In Situ Proteome Labeling

For *in vitro* proteome labeling, probes were added to cell lysates (50 μg) in 50 μL of PBS at a final concentration of 10 μM. For heat-denatured samples, the proteome was heated for 10 minutes at 95 °C, prior to adding the probes. Samples were incubated for 1 h at room temperature, followed by adding 100 μL of the freshly premixed click chemistry reaction cocktail in PBS [rhodamine-azide (200 μM, 100 mM stock solution in DMSO), tris(2-carboxyethyl)phosphine hydrochloride (TCEP) (2 mM, 50 mM freshly prepared stock solution in deionized water), tris[(1-benzyl-1H-1,2,3-triazol-4-yl)methyl] amine (TBTA) (200 μM, 50 mM stock solution in DMSO) and $CuSO_4$ (2 mM, 50 mM freshly prepared stock solution in deionized water)] and incubation for 2 h at room temperature with gentle mixing. The reactions were terminated by the addition of prechilled acetone (1 mL), placed at −80 °C for 15 min and centrifuged at 14000 rpm for 15 min at 4 °C to precipitate proteins. The protein pellets were allowed to air-dry for 5 min, resuspended in 30 μL 1 × standard reducing SDS-loading buffer, heated for 10 min at 95 °C; and separated by 10% SDS-PAGE, then visualized by in-gel fluorescence scanning using the *FMBIO* fluorescence scanner (Hitachi).

For *in situ* labeling subconfluent cells were treated with media containing *10* μM of the probes for 4h at 37˚C. The media was then aspirated and the cells were washed 2x with PBS and lysed in ice-cold PBS supplemented with 1% Triton X-100. Subsequent to quantification, the proteome was prepared for click chemistry as described above.

2.6.2.2 Two-Dimensional Analysis of Labeled Proteomes

Precipitated protein pellets (250 μg) were resuspended in 125 μl of isoelectric focusing (IEF) buffer (7 M Urea, 2 M thiourea, 4% CHAPS, 1% DTT) containing 0.2% Ampholytes pH 3-10 (biolytes, Bio-Rad, Hercules, CA). IPG strips pH 3-10 NL, 7 cm, or pH 4-7NL, 7cm (Bio-Rad) were passively rehydrated with the resuspended proteomes for 16 h. The rehydrated protein IPG strips were then submitted to isoelectric focusing using the Protean IEF Cell (Bio-Rad) with the following conditions: 200 V rapid ramp for 30 min, 500 V rapid ramp for 30 min, 2 h linear ramp to 6,500 V, and 2 h focusing (rapid ramp) at 6,500 V. The accumulated voltage-hour (VH) fell between a ranges of 14,000 - 17,500 VH.

Prior to SDS-PAGE separation, proteins immobilized on the IPG strips were reduced (1% DTT) and alkylated (4% iodoacetamide) in SDS equilibration buffer (6 M urea, 30% glycerol, 2% SDS, 50 mM tris-HCl, pH 8.8). The SDS-PAGE separation was performed on a 10% gel (1.5 mm thickness) at constant 150 V per gel. The gels were then scanned for fluorescence and were subsequently incubated overnight in fixing solution (50% v/v Ethanol, 5% v/v acetic acid). Finally, gels were stained with silver nitrate and scanned using the Fluor-S imager (Bio-Rad) in order to visualize the entire cellular proteome.

2.6.2.3 Identification of Labeled Protein Candidates

The fluorescent gel images were aligned with the silver stained gel images to locate the labeled protein spots. Protein candidates displaying heat-sensitive activity were selected as specific targets, while candidates showing heat-insensitive reactivity were considered as non-specific targets. The selected spots were manually excised under a laminar flow hood. Gel spots were destained with potassium ferricyanide solution (15 mM potassium ferricyanide, 50 mM sodium thiosulfate), rinsed three times with water, and then shrunk with acetonitrile. The gel pieces were

reswelled with 20 µl of trypsin solution (0.01 µg/µl in 50 mM ammonium bicarbonate) and incubated overnight at 37°C.

2.6.2.4 Enrichment and Mass Spectrometry

Biotin-azide click chemistry and streptavidin-enrichment of probe-labeled proteomes was performed as previously described (380), with an additional acetone precipitation step included after the click reaction to maximize protein recovery. After enrichment, streptavidin-agarose beads (Peirce) were washed as described, and bound proteins were processed as follows for mass spectroscopy. For on-bead trypsin digestion, the streptavidin beads were washed 5 more times with 50 mM ammonium bicarbonate (ABC), reduced with 10 mM DTT in 50 mM ABC (65 ^{o}C for 15 min) and alkylated by addition of 25 mM iodoacetamide (room temperature for 30 min). The beads were washed twice in 50 mM ABC then bound proteins were digested with 10 ng/µL sequencing grade modified trypsin (Promega) overnight at 37^{o}C. As the negative control, a no probe experiment was carried out, in which the naïve proteome was clicked with biotin azide, followed by streptavidin enrichment and on-bead digestion. Few hits that were obtained from this negative control are considered to be from the non-specific interactions of some abundant proteins with streptavidin and were excluded from the list of the hits obtained from the labeled samples.

Ten microliter of each digest was analyzed by nano LC–MS/MS using an LTQ XL linear ion trap MS (Thermo Fisher Scientific, Ottawa, ON, Canada) coupled to a nanoAcuity ultrahigh-pressure liquid chromatography system (Waters, Milford, MA). With a flow rate of 0.4 uL/min, peptides were eluted from a 100 mm i.d. 6100 mm nanoAcquity UPLC 1.7 mm C18 column (Waters, Mississauga, Ontario) with the following gradient: 1% B for 1 minute, 1%–45% B over 18 minutes, 45%–85% B over 3 minutes, 85%–1% B over 1 minute. The column was

reequilibrated with 1% B for an additional 8 minutes. Solvent A is 0.1% formic acid in Optima LCMS water (Fisher Scientific Canada, Whitby, Ontario). Solvent B is 0.1% formic acid in acetonitrile.MS/MS spectra were acquired automatically on doubly, triply, and quadruply charged ions. The peaklist files of MS2 spectra of the excised protein spots were searched against IPI Human database or the NCBI using MASCOT™ (Matrix Science, London, UK) for protein identification. The following parameters for mass spectral identification were used: peptide tolerance of 1.5 Da, MS/MS tolerance of 1.5 Da, and possible 1 missed cleavage site. The cut-off ions score was 30, above which ion scores indicate identity.

2.6.3 Activity Based Protein Profiling Using PIK-BPyne Probes

2.6.3.1 Viral Infection

$JFH1_T$ infection of Huh7.5 was performed in 100 mm dishes. For this purpose, 24 hours after seeding, cells were either infected with $JFH1_T$ (MOI = 0.1) or mock infected. 24h post-infection (or mock infection), medium was removed and replaced with fresh medium (the normal DMEM + 10 % FBS). Infected and mock infected cells were subjected to *in situ* labeling with PIK-BPyne probe 96h post-infection.

2.6.3.2 In Situ Active Proteome Labeling For Streptavidin Enrichment

For *in situ* probe labeling, confluent cells were incubated with the indicated concentration of probe in complete media for 1h to allow the probe to enter the cell. Cells were washed with PBS, followed by exposure to UV light (365 nm) in PBS at 37^{o}C for 30mins. Cells were lysed by sonication in 1% Triton-X 100 in PBS.

Whole proteome diluted in lysis buffer (1 mg/ml) was pre-incubated with 100 μM PIK-BPyne probe for 30 min in the presence or absence of competitive inhibitor (200 μM), followed by

exposure to UV light (365 nm) for 45mins in a 96-well plate on ice. For *in situ* probe labeling, confluent cells were incubated with 50 μM of probe in complete media for 1h to allow the probe to enter the cell. Cells were washed with PBS, followed by exposure to UV light (365 nm) in PBS at 37°C for 30mins. Cells were then lysed by sonication in 1% Triton-X 100 in PBS.

Biotin-azide click chemistry and streptavidin-enrichment of probe-labeled proteomes was performed as previously described (381), with an additional acetone precipitation step included after the click reaction to maximize protein recovery. Twenty microgram of each proteome sample was isolated prior to enrichment for relative abundance ("Input") and activity ("Streptavidin-enriched"). After enrichment, streptavidin-agarose beads (Peirce) were washed as described (380), and bound proteins were either removed by boiling in Laemmli buffer for western blot analysis, or processed for mass spectroscopy as described above.

2.6.3.3 Western Immunoblotting

Protein samples were separated by 8% SDS PAGE followed by transfer to PVDF membrane (Amersham Biosciences). Membranes were incubated overnight at 4°C with polyclonal anti-PI3Kα (1 in 500), anti-PI4KIIIβ (1in1000) (Millipore), or anti-PI4KIIα (1in1000) (Santa Cruz Biotechnology Inc) diluted in 2.5% BSA in TBST or anti-PI4KIIIα (1 in 500) (Cell signalling) diluted in 5% BSA in TBST. Donkey anti-rabbit conjugated HRP, or goat anti-mouse conjugated HRP secondary antibody were diluted in 3% milk in TBST and incubated with membranes for 1h at room temperature (Jackson ImmunoResearch Labs). Proteins were visualized by film using ECL prime substrate (Amersham).

Chapter 3: Investigation of Target-Site Accessibility of HCV RNA Genome to MicroRNA-122

Statement of Contributions

The content of this chapter has been published in the journal of Virology (285) and permissions have been obtained for reusing the materials and figures in this thesis.

I have helped to design all of the experimental approaches. I also performed the majority of experiments with contributions fron the other authors being mainly related to the preparations of materials and technical support. I analyzed the data along with my supervisor, and wrote the drafts of the manuscript.

3.1 Introduction

MicroRNA-122 (miR-122) is a highly abundant, liver-specific miRNA that positively modulates HCV replication, translation, and virion production (144, 168, 169, 177, 178, 438). Three miR-122 recognition elements (MREs) have already been characterized in the HCV genome with two in the 5'UTR and one in the 3'UTR (144, 177, 178). The HCV 3'UTR site is located in the variable region (VR) stem loop of the HCV 3'UTR (MRE 3) while the two HCV 5'UTR sites are closely spaced between stem loops (SL) I and II (MREs 1 and 2) (Figure 3-1B). Although the 3'UTR site appears to have no role in the stimulation of viral replication or translation (144), the relative contribution of the two 5'UTR binding sites for miR-122 to these processes is still a subject of debate (434). A study by Jangra *et al.* suggests that efficient HCV replication is more dependent on miR-122 binding to the 5' site in proximity to SL I (MRE 1) while translation is equally stimulated by miR-122 binding to both MREs 1 and 2 (169, 438). Many of these works, however, have been limited to analysis of the outcome of exogenous addition or sequestration of miR-122 and of mutation analyses of these three MREs (144, 169, 177,

178). Importantly, it was recently shown that miR-122 binding to MREs1 and 2 stabilizes the HCV genome and protects it from degradation by cellular RNA exonucleases (225, 226, 277, 366).

Even though miR-122 antagonists exhibit great anti-HCV promise by effectively reducing HCV titers in both chimpanzees and humans (170, 212), several studies demonstrate that miR-122 is not essential for HCV replication, and low levels of replication have been observed in the absence of miR-122 (9, 74, 186). Moreover, low doses of the miR-122 sequestration treatment in previously mentioned studies still allowed for viral replication, suggesting even low levels of miR-122 are still able to facilitate HCV replication (212). Thus, in the presence of limiting miR-122, such as during miR-122 sequestration-based treatment, it is important to know which of the HCV MREs maintain their roles as *bona fide* miRNA binding sites.

Notably, there is evidence that miR-122 binding modifies the secondary structure of the HCV genomic RNA (84, 277, 437); however, the kinetics of miR-122 interactions with these MREs have yet to be examined in depth. Therefore, in this chapter, the importance of target site accessibility in miR-122 binding to HCV MREs and the physiological relevance of these interactions will be addressed. Herein, HCV RNA coated magnetic beads (VRB) assay was employed to characterize the hybridization kinetics of miR-122 to its MREs on the HCV genome under native conditions. Importantly, the methodology described here could be extended to other systems, including the examination of small RNA interactions with highly structured genomes of other RNA viruses.

3.1.1 HCV RNA Genome Structure and Organization

The positive-sense HCV RNA genome serves as a template for translation, negative-strand synthesis, and for packaging into virions. A number of well-defined *cis*-acting RNA elements have been identified that mediate these processes during the HCV life cycle. For example, the 5' UTR of HCV contains the IRES element that is responsible for cap-independent translation of the HCV polyprotein (299). Also there is a stem-loop upstream of the IRES (SL1) that has been suggested to play a role in viral replication (110, 196). Furthermore, the 3' UTR of the genome contains three distinct structural domains important for viral replication: a variable region, a poly (U/UC) tract, and a highly conserved 98-nt sequence known as the 3' X tail (109, 456, 459). Additionally, there are a number of well-defined conserved stemloop structures throughout the coding regions, as well as extensive uncharacterized long-range RNA-RNA interactions that seem to be essential for viral replication (75, 87, 216, 261, 371, 408).

Davis *et al*. utilized highly advanced RNA structure prediction algorithms to show that evolutionarily conserved, genome-scale ordered RNA structures (GORS) are quite prevalent in HCV (75). In fact, examination of aligned viral genome indicated the existence of extensive RNA structures throughout the HCV genome, while, there was no evidence of GORS upon examination of closely related *Pestivirus* and *Flavivirus* genera (75, 371). Interestingly, it has been hypothesized that GORS may play a role in protecting RNA viruses from Dicer-mediated small RNA regulation, and thus allow the virus to persist in its natural hosts (75, 371). This suggests that target site accessibility may be an important factor when designing therapeutics that directly target these highly-structured

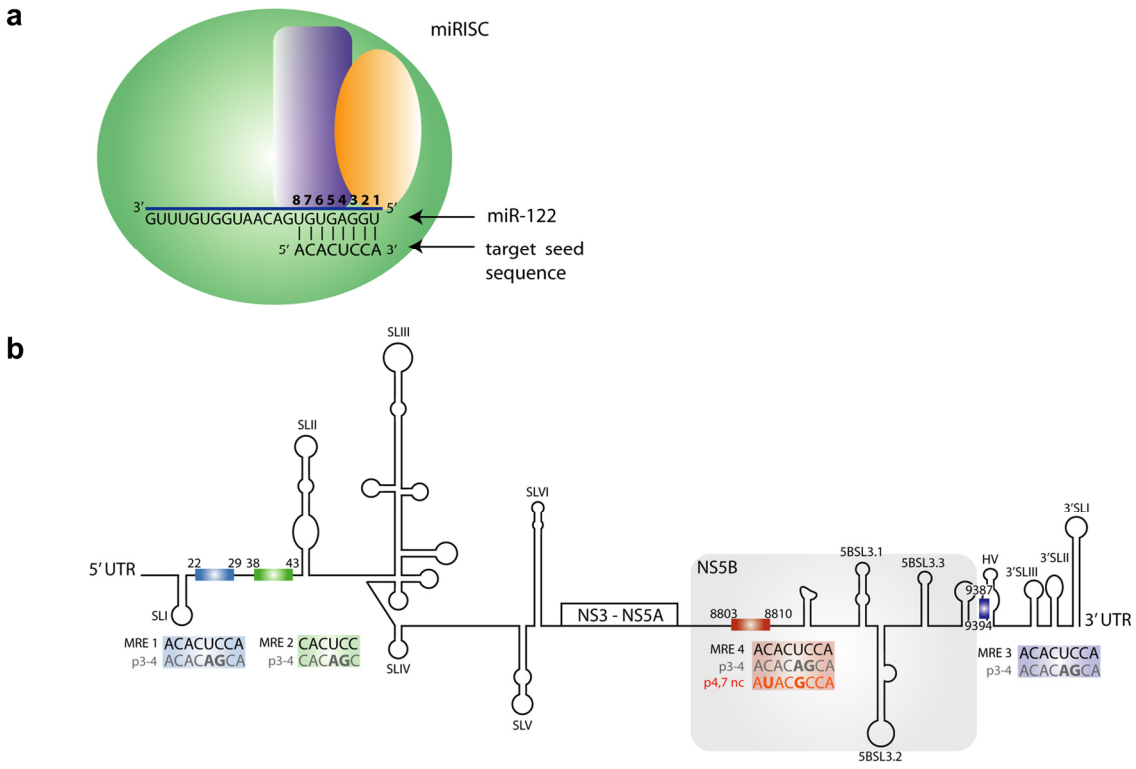

Figure 3-1. Secondary structure and miR-122 binding sites of interest in the 5′ and the 3′ ends of the HCV genome. (a) Binding of miR-122 guide strand as part of RNA induced silencing complex (miRISC) to MREs with seed sequence (nucleotides 2–8 at the 5′ end) highlighted. (b) The secondary structure is shown for the 5′UTR and domains V and VI in the core coding sequence along with the 3′UTR and a portion of the NS5B coding sequence. Numbers refer to the nucleotide positions of the full-length HCV genotype 1b isolate Con1. Highlighted are the four microRNA response elements (MREs) of interest and the respective mutations used in this study. For all four sites, a double mutation was performed at seed positions 3 and 4 (p3–4) while for only MRE 4, an additional non-coding (nc) double mutation was performed at seed positions 4 and 7 (p4,7).

viral genomes, including small RNA species such as short-interfering RNAs (siRNAs). HCV is a particularly attractive target for siRNA-based antiviral therapy, as its entire replication cycle occurs in the cytoplasm, and its single-stranded RNA genome functions as both an mRNA and the template for viral replication.

3.1.2 Importance of Target-site Accessibility in Efficiency of RNA Silencing

The impact of target site accessibility on the efficiency of RNA silencing has been extensively studied and it was found that the folded state of the target RNA can considerably hamper the effectiveness of siRNAs (45, 46, 54, 148, 294, 347, 393, 415). Moreover, the effect of secondary structure of target RNA on miRNA potency has also been well-established (187, 188, 241, 294, 342). Generally, areas of higher structure are less susceptible to miRNA modification, due to limited accessibility. In comparison to mRNAs, RNA-based viral genomes, such as HCV, tend to be longer and adopt a greater degree of secondary and higher-ordered RNA structures, which will have further impact on miRNA seed site accessibility.

An innovative method called RNA*xs* was developed in an attempt to address the issue of target site accessibility in mRNAs (393); however, this method cannot account for GORS in RNAs as long as the genome of RNA viruses. Another novel method employing high-throughput selective 2'-hydroxyl acylation analysed by primer extension (SHAPE) was applied to characterize secondary structure elements within the entire genome of HIV-1(431). SHAPE allowed for identification of the evolutionarily conserved structural elements within HIV-1 genome and it was demonstrated that the folding of the genomic RNA assists with the viral protein folding during translation (431). This approach, while highly innovative, is not designed for the interrogation of target site accessibility of small

RNAs. Furthermore, the HCV genomic RNA contains a larger amount of structured RNA or GORS than HIV-1 (75, 371). As such, this approach cannot be used for the interrogation of target site accessibility of miR-122 MREs on the HCV genome.

3.2 Rationale

Existing computational methods fail to assess target site accessibility of complex large RNA targets such as HCV genomic RNA. Therefore a novel assay is required for interrogation of target site accessibility of miR-122 MREs on the HCV genomic RNA.

3.3 Hypothesis

Viral RNA coated magnetic bead (VRB) assay may represent an effective method to examine miR-122 interactions with the HCV genome.

3.4 Results

3.4.1 VRB-Based Comparison of miR-122 Target Sites' Hybridization

Our group has previously reported a novel method of utilizing HCV RNA coated magnetic beads (VRBs) to measure siRNA target site accessibility in various regions of the HCV genome (347). This technique allowed us to observe that under native conditions in aqueous solution, HCV RNA genome retains a complex, highly ordered RNA structure representative of its *in vivo* conformation (347). Herein, I have extended the VRB assay to measure the hybridization kinetics of miR-122 with the folded state of the HCV genomic RNA. Specifically, I sought to determine the relative target site accessibility of the three well known MREs of miR-122 in the HCV genome (Figure 3-1B). All VRB target site accessibility analyses were performed on the HCV genotype 1b

subgenomic replicon containing stem loops (SL) V and VI of the core coding sequence (Figures 3-1B and 3-4A), since these domains have been implicated in interactions with the IRES (SL II-IV) (197). The inclusion of these domains allows for a more representative model of the higher order RNA interactions that occur in the HCV genome.

As in our previous target site accessibility study, the HCV replicon RNA (Figure 1-1B) was end labeled with maleimide-PEG11-biotin (347). In order to distinguish the relative accessibility of the MREs, DNA probes were designed covering each of the MREs independently (Tables 2-1 and 3-1).

Hybridization of the probes to the replicon was performed to block miR-122 from binding to specific individual MREs; then the replicon RNA was hybridized to fluorophore-conjugated miR-122 guide strand under native conditions. Subsequently, the miRNA-hybridized HCV replicon RNA was captured on streptavidin-coated magnetic microbeads and visualized using fluorescence microscopy to assess seed site accessibility (Figures 3-2 and 3-4B). To account for non-specific interactions of the miRNAs to the beads, control reactions were performed in the absence of HCV replicon RNA. Background levels of fluorescence produced by these images were used for normalization of net integrated optical density (IOD) values. The observed fluorescence in the presence of miR-122 and HCV RNA is representative of the hybridization kinetics of the unblocked sites. This parameter depends solely on the target site accessibility when complementarity and thermodynamics (i.e. GC content) are roughly the same for the different seed sites.

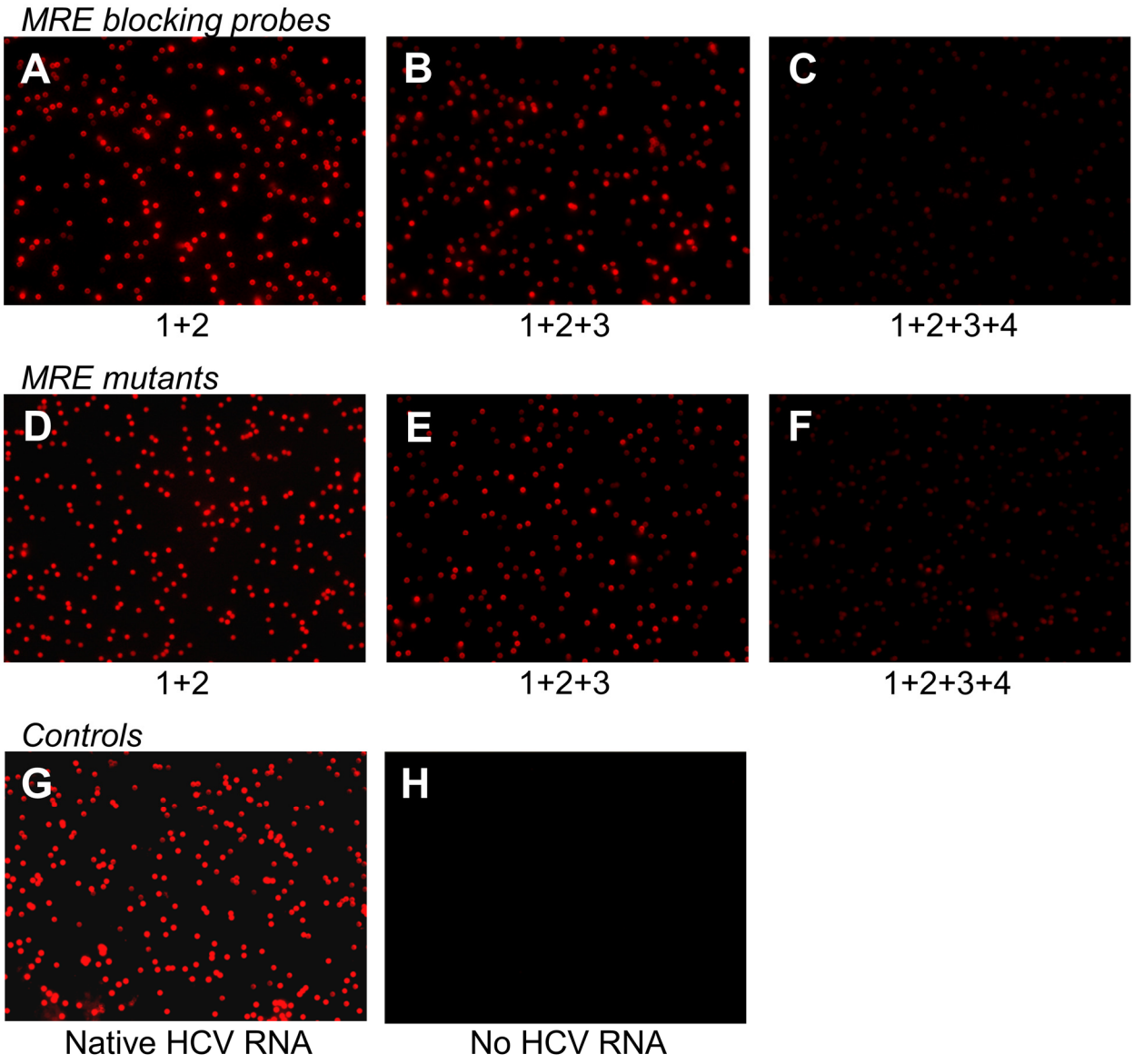

Figure 3-2. Representative fluorescence images of VRBs after hybridization with 50 nM Cy3-labeled miR-122 in the presence of probes blocking MRE sites of interest (A-C) and mutated HCV replicon conjugated to the microbeads (D-F). Also shown are native HCV RNA VRBs in the absence of mutations and probes (G) along with a representative image of the hybridization reactions carried out in the absence of HCV replicon RNA to assess non-specific binding of the miR-122 to the beads (H).

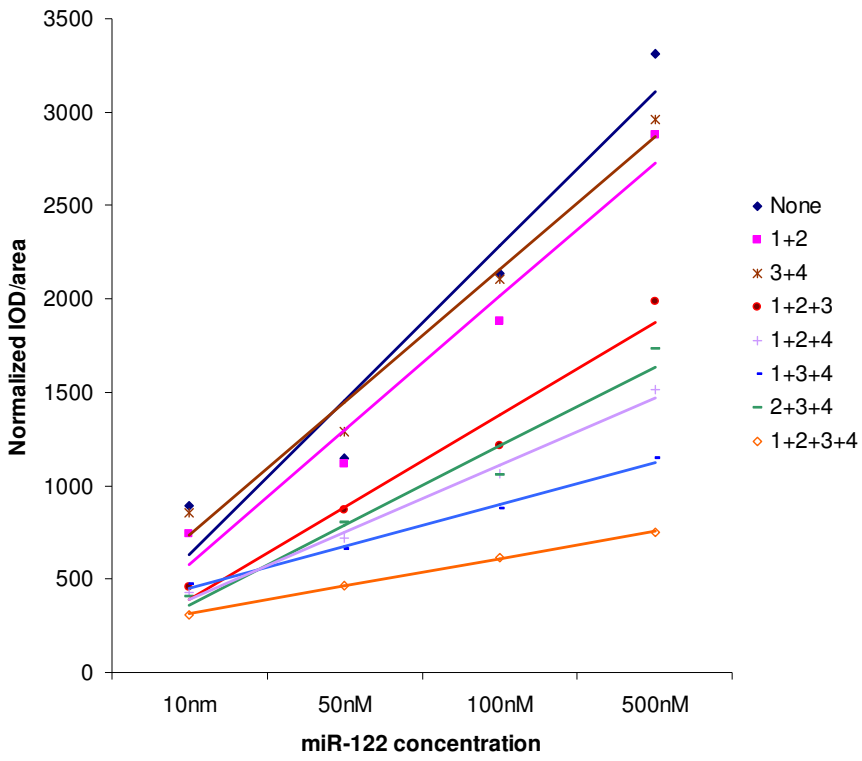

Figure 3-3. Sample scatter plot displaying hybridization kinetics by quantification of net IODs from individual beads (n=100) from images of increasing miR-122 concentrations hybridization to VRBs in the presence of probes blocking combination of MREs (1 -4). Line of best fits are plotted for data corresponding to Figure 3-4C.

Multiple combinations of the probes were used in order to assess the accessibility of each independent MRE. Representative images of the miR-122 hybridizations on the VRBs are shown in Figure 3-2A-C. Quantification of signal intensities from individual beads per image (n = 100) in the presence of increasing concentrations of miR-122 (10nM to 500nM) was used to generate line graphs for miR-122 binding under each set of conditions (Figure 3-3). Similar to our previous study (347), the slope was used as a measure of target site accessibility or, in this case, miR-122 seed site accessibility. As a positive control, a highly potent siRNA, NS5B-7256 siRNA, directed against the NS5B region was used (435). We have previously shown this siRNA targets a highly accessible portion of the HCV replicon RNA (347) and, predictably, generates a considerably high amount of signal in the VRB assay (Figure 3-4C). Moreover, the signal generated by the NS5B-7256 siRNA was considerably higher than that of any of the miR-122 hybridizations; however, this was expected since the siRNAs exhibit perfect complementarity with their target sites in the replicon as compared to the restricted complementarity of miR-122 to its seed sequence region. As a negative control, GL3 siRNA was used since it possesses no sequence complementary to HCV replicon RNA and produces no difference in signal (Figure 3-4C) when compared to the background, as previously shown (347). Together, these controls demonstrate the specificity and sensitivity of the VRB-based technique.

3.4.2 Identification of a High Affinity Fourth miR-122 Binding Site in HCV RNA

In the presence of probes blocking MREs 1, 2 and 3, results from VRB assays showed that there was still a significantly high signal level compared to the background (Figure 3-4C). This observation suggested that there might be additional miR-122 binding sites in

the genome. Thus we consulted ViTa, an online database for predicted miRNA binding sites in viral genomes to look for additional sites in the replicon (155). The additional predicted sites represented a combination of potential miR-122 binding sites based on either seed site interactions or marginal sites with partial or no complementarity to the seed sequence but with compensatory binding to the 3' end of the miR-122 (Table 3.1).

The *in vitro* VRB assay allows for a preliminary analysis of relative microRNA affinity for binding sites; however, it is not entirely representative of RISC-bound miRNAs and other factors that influence accessibility *in vivo*. For example, other RNA binding proteins are known to modulate RNA accessibility for small RNAs (187, 188, 241, 294). However, this study gives a baseline for binding as RISC-bound RNA would be expected to have similar or perhaps lower target-site accessibility.

Since seed sites represent the dominant miRNA binding site characteristic (30), our primary interest was identifying all potential sites displaying maximum complementarity to the miRNA seed sequence. Interestingly, the HCV replicon RNA sequence displayed an additional potential 8 nucleotide seed site for miR-122 (MRE 4) found in the coding region of NS5B, the HCV-encoded RNA dependent polymerase, (nts 8803-8810, Figure 3-1B); miR-122 interactions with this site could potentially explain the remaining signal observed. We focused on this seed site as it displayed the highest complementarity (with potential for supplementary binding with HCV at the 3' end of the miR-122) and the highest predicted minimum free energy of binding (Table 3-1). While seed pairing is an important predictor of true microRNA binding sites (52, 53, 219, 220), seed sites are neither necessary nor sufficient for miRNA-mediated regulation as seed sites have been shown to be inactive when tested in reporter constructs (85, 269). Thus, the extension of

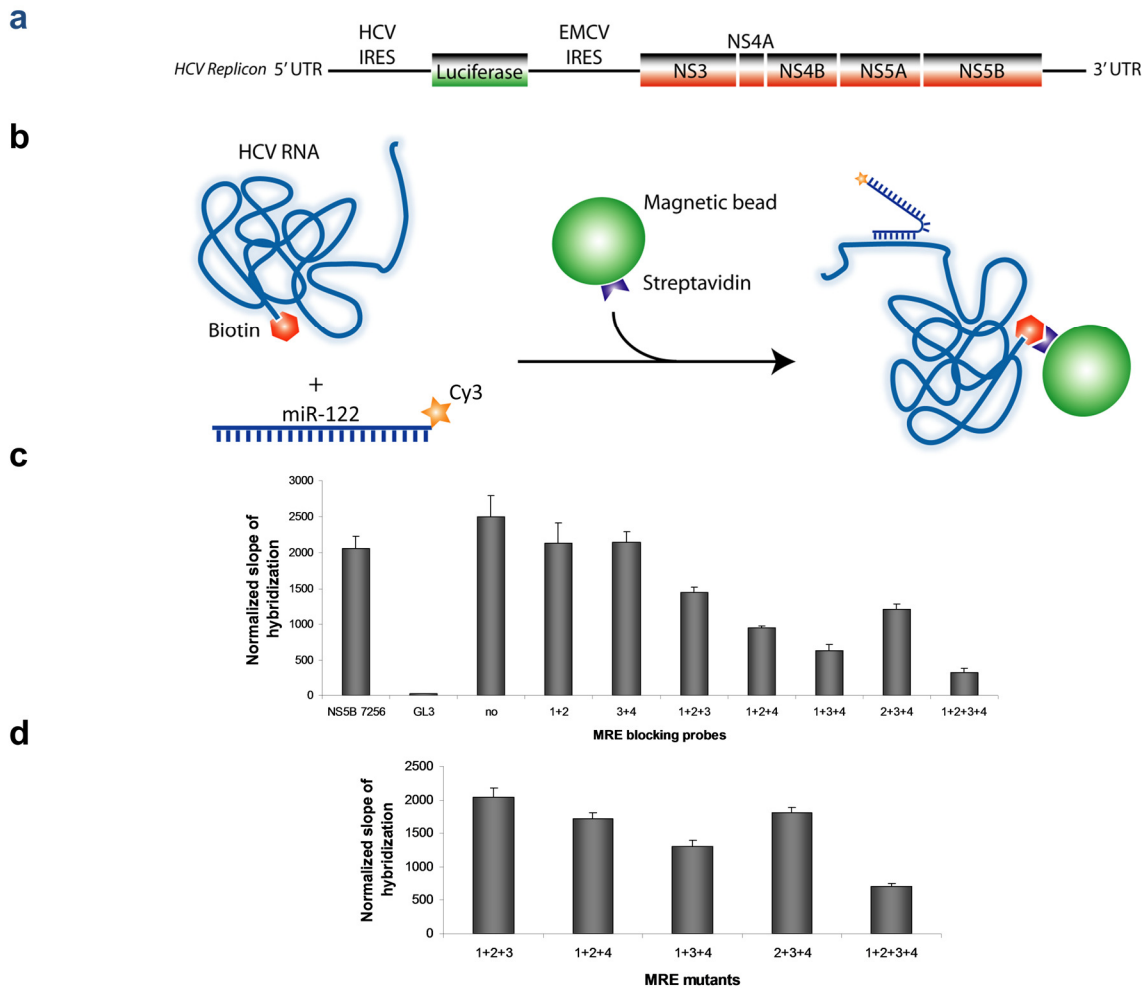

Figure 3-4. miR-122 affinity for HCV RNA seed sites. (a) Schematic diagram of HCV subgenomic replicon RNA. (b) Biotin-labeled replicons were mutated or blocked with probes to prevent miR-122 binding, incubated under native or denaturing conditions with Cy3-conjugated miR-122. The hybridized miRNAs-HCV RNA complex is then captured on magnetic streptavidin-conjugated microbeads. The beads were washed and imaged by fluorescence microscopy. (c,d) Hybridization of increasing concentrations of miR-122 (10nM–500nM) to the VRBs in the presence or absence of probes (c) blocking miR-122 binding sites of interest (MREs 1–4). (d) The experiment was repeated using a decreased miR-122 concentration gradient (5 nm–100 nm) with mutations instead of probes to disrupt binding. All MREs were mutated at positions 3 and 4 of the seed site as shown in Figure 3-1 b. Slopes from native hybridization of control siRNAs, NS5B 7256 (positive control directed against highly accessible portion of HCV) and GL3 (negative control with no target site in HCV replicon) are also shown. The data represent the mean of three images from three independent hybridizations. For each image, net IODs were calculated from individual beads (n = 100) over the concentration gradients and were used to produce slopes. Error bars represent s.d. of three independent hybridizations. Student's *t*-test values for pairwise comparisons of samples with three MREs blocked or mutated are shown in Table 3-3.

Table 3-1. ViTa predicted miR-122 binding sites in the HCV genotype 1b isolate Con1 used for TSA analysis.[**]

HCV target location (nts)	miRanda score[***]	Hypothesized hybridization of nucleotides[*]	MRE Annotation[†]
9372-9394	148	UGUUUGUGGUAACAGUGUGAGGU |||||||| TGAACGGGGAGCUAA**ACACUCCA**	MRE 3
2-29	163	UGUUUGUGG-UAA---CAG-UGUGAGGU ||: | || ||| | | ||||||| CCAGCCCCCGAUUGGGGGCG**ACACUCCA**	MRE 1
8789-8810	171	UGUUUGUGGUAACAGUGUGAGGU |:||| | | | |||||||| GGAGACAGC-TAGAC**ACACUCCA**	MRE 4
9013-9035	154	UGUUUGUGGUAACAGUGUGAGGU || |||| ||:|| ||||| UUUCACUCCAUAGUU**ACU**C**UCCA**	N/A
6796-6823	141	UGUUUGUGG--UAA--CAGUGU-GAGGU |: ||:||| :|| ||||| |||| AUCAAUACCUGGUUGGGUC**ACA**G**CUCC**C	N/A

[†] - as referenced in this study

*- shows proposed method of Watson-Crick binding (|) and non-Watson crick pairing of MRE (top strand) nucleotides (:) with miRNA seed sequence (bottom strand) nucleotides in bold

[**]- ViTa prediction methods described in (155)

***- Score based on target complementarity and free energy of formation (37)

Table 3-2. Conservational analysis of miR-122 binding site (MRE 4) in NS5B coding region.

Subtypes	Polymorphisms relative to MRE 4 in H77 reference sequence							
H77 (nt 8806-8813)	**A**	**C**	**A**	**C**	**T**	**C**	**C**	**A**
G1a								4 X G
(n=142)								1 X C
G1b							2 X T	
(n=229)	6 X G			1 X A		1X T	2 X G	
G1c								
(n=3)								
G2a								13 X T
(n=14)			14 X T	2 X T	14 X C			1 X C
G2b								12 X T
(n=13)			13 X T		13 X C			1 X C
G2c								
(n=1)			1 X T		1 X C			1 X T
G2k								
(n=1)			1 X T		1 X C			1 X T
G3a								
(n=4)								
G3b								
(n=2)								
G3k								
(n=1)								
G4a								
(n=9)		1 X T						3 X G
G4d								
(n=2)								
G5a								
(n=3)			3 X T		3 X C			1 X G
G6a								
(n=15)								
G6b								
(n=1)		1 X T			1 X C			1 X T
G6c								
(n=1)								
G6d								
(n=1)								1 X C
G6e					1 X Y			1 X G

(n=1)		
G6f		
(n=2)		
G6g		
(n=2)		1 X C
G6h		
(n=1)		1 X T
G6i		
(n=2)		
G6j		
(n=2)		
G6k		
(n=3)		1 X T
G6l		
(n=1)		
G6m		
(n=4)	3 X T	
G6n		
(n=2)		
G6o		
(n=1)		
G6p		
(n=1)		
G6q		
(n=1)	1 X T	

the VRB assay to include the fourth site, serves an additional purpose in validating miR-122's interaction *in vitro* with MRE 4.

A fourth probe was designed to cover the newly discovered seed site and, as expected, in the presence of all four probes against MREs 1-4, the signal was reduced significantly (Figure 3-2A-C). However, blocking of this fourth site in addition to the three other MREs still resulted in a signal level above the background. This remaining signal is likely attributed to non-specific miR-122 binding to the HCV RNA, as well as weak binding to the aforementioned marginal sites. In fact, recently it has been proposed that HCV RNA acts like a sponge for miR-122 (107). Fluorescence analysis of miR-122 hybridization to the VRBs was extended to include the fourth site (Figure 3-4C). By analyzing the slopes of hybridization produced by using three probes simultaneously (thereby leaving one MRE available to miR-122 for binding), it is possible to compare the accessibility of each individual site). The probe based VRB assay suggests that the hierarchy of miR-122 affinity to the seed sites is as follows: MRE 4>1>3>2 (Figure 3-4C). Therefore, it is surprising to find that the site in the coding region appears to be the most accessible.

3.4.3 Site-Directed Mutagenesis of miR-122 Seed Sites in HCV Replicons

The use of probes may cause changes in the secondary structure of the RNA, so we repeated our analysis using double substitution mutations in the MREs corresponding to the sites 3 and 4 in the seed sequence of miR-122 (p3-4) (Figure 3-1A, B) to disrupt miR-122's interactions with each individual MRE, as previously done (177, 178). Furthermore, to better represent limited kinetic conditions, the miR-122 concentration range was decreased for the analysis of the triple mutants to 5nm-100nM. The results of

the mutation-based VRB target site accessibility analysis under these conditions (Figure 3-4D) mirrored that

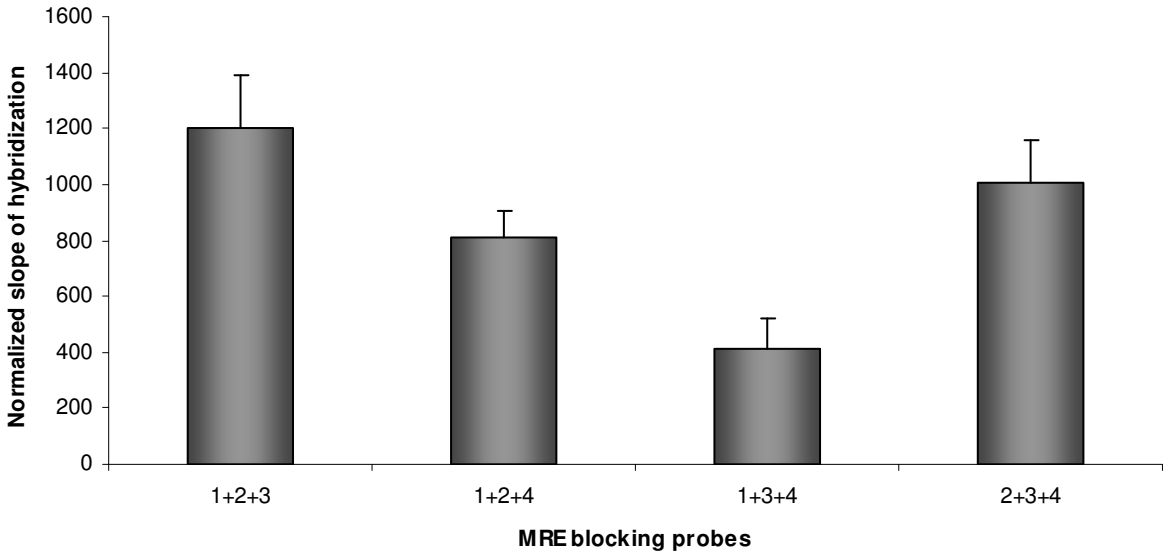

Figure 3-5. Slopes from native hybridization of increasing concentrations of miR-122 (5nM-100nM) to the VRBs, in the presence of probes blocking 3 of 4 miR-122 binding sites of interest (MREs 1-4). The data represent the average of three images from three independent hybridizations, and net IODs calculated from individual beads (n=100) from each image analyses over the concentration gradients were used to produce slopes. Error bars represent SD of three independent hybridizations. Student t-test values are shown in Table 3-3.

of the initial probe-based study. Also, the probe-based analysis was repeated using the decreased concentration range and also followed the same trend (Figure 3-5).

3.4.4 Cooperativity of miR-122 Binding In Vitro in HCV 5'UTR

By far, MRE 2 displayed the lowest accessibility according to the probe-based VRB target site accessibility results ($p<0.004$) (Figures 3-5C, D, 3-6 and Table 3-1). It is interesting to note that while MREs 1, 3, and 4 are predicted by the ViTa, the MRE 2 is not even predicted by this database (Table 3-1). This is due in part to the reduced level of complementarity of MRE 2 to the miR-122 seed sequence compared to the other three MREs of interest (6 nts compared to 8nts) (Figure 3-1B). However, Jopling *et al.* found that binding to both MRE 1 and 2 sites was required to ensure viral RNA amplification. Also, another study showed that miR-122 binding to both 5′ sites independently has a relatively equal positive stimulation on HCV translation (168), suggesting that MRE 2 displays high efficacy and retains some seed site accessibility *in vivo*. *In vitro,* however, this may potentially be attributed to the fact that MRE 2 is a more efficient miR-122 binding site due to its cooperativity with MRE 1 (177). Indeed, since our study was published, it was found that there is a non-conventional binding mode for miR-122 at MREs 1 and 2 (107).

Previous studies have suggested that closely spaced miRNA binding sites act synergistically, perhaps since one bound RISC complex may recruit cofactors for additional repression (127, 346). Consequently a potential explanation for our observations is that binding at MRE 1 may decrease secondary structure in the adjacent area, thereby increasing accessibility to MRE 2. A previous *in vitro* study, in which miR-122 binding at MRE 1 induced an opening in the conformation of the IRES by disrupting

a long-range annealing motif (84), supports this hypothesis. A closer examination of the probe-based VRB target site accessibility assay results sheds some light on this cooperativity. The signal produced by the HCV RNA with only both 5'UTR MREs unblocked (probes 3 + 4 in Figure 3-4B) is $(1.8 \pm 0.2) \times 10^2$ while the sum of the signals produced when each individual site is accessible (probes 1+3+4 and 2+3+4 in Figure 3-4B) is $(1.2 \pm 0.2) \times 10^2$. The increase ($p<0.03$) over the sum implies that there is cooperativity exhibited between the two sites (i.e. binding to one of the two sites increases binding to the other).

3.4.5 Inhibitory Role of Forth miR-122 Binding Site in HCV

The VRB assay results also highlight the binding efficacy of miR-122 to MRE 4 *in vitro* (Figure 3-4C, D, and Figure 3-5). However, the functional role of MRE 4 during HCV replication is not known. Most ORF sites, in fact, have been shown to be generally less effective (127). In order to assess the biological relevance of MRE 4 and compare it to that of the three other sites, the HCV subgenomic replicon containing p3–4 mutated MREs was introduced into Huh-7.5 human hepatoma cells. The combined effects of the mutations on the rates of translation and replication of the replicon were assessed. A replicon lacking the stem loops in the core coding sequence was used for this portion of the study as we found, along with others (197), that they decrease HCV IRES-dependent translation.

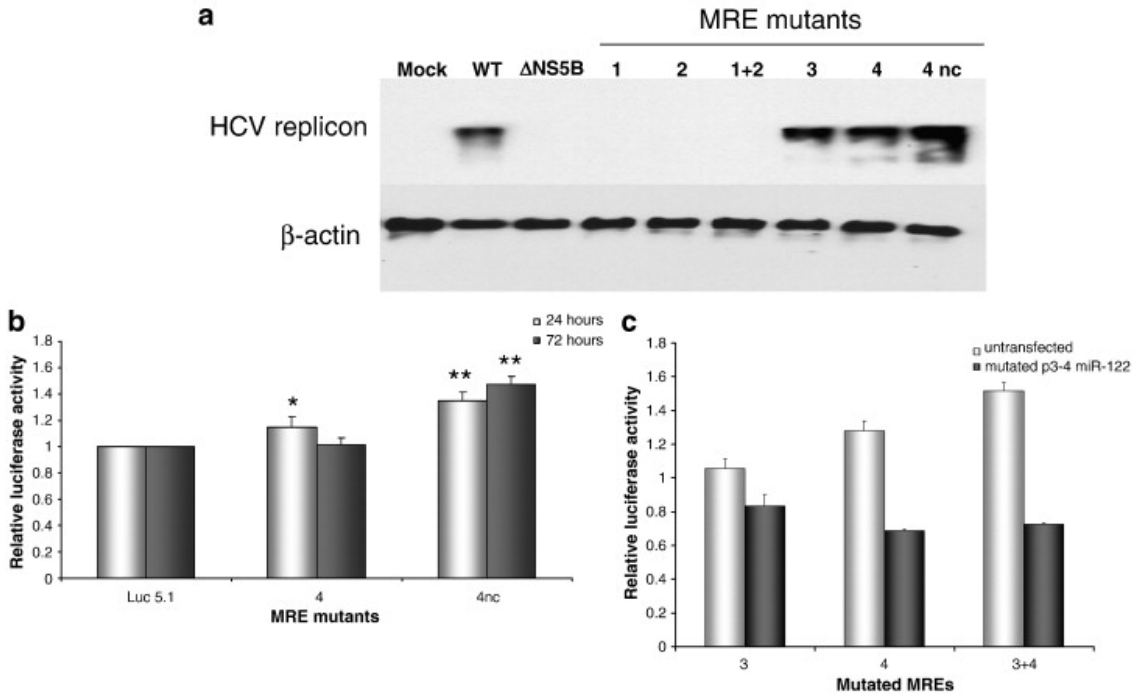

Figure 3-6. Mutational analysis of miR-122 seed sites' roles in HCV translation and replication. Bicistronic HCV subgenomic replicon with HCV IRES-driven luciferase reporter and mutated miR-122 seed sites was transfected in Huh-7.5 cells. All MREs were mutated at positions 3 and 4 of the seed site; also, MRE 4 was mutated such that a non-coding mutation (4nc) would occur as shown in Figure 3-1b. (a) Northern blot analysis of HCV replicon expression in total RNA extracted from Huh-7.5 cells 72 h post-transfection. Naïve HCV replicons (WT) and mock transfections are also shown. Expression of β-actin was used as a loading control. Representative blot is shown (n = 3). A replicon containing a deletion in the NS5B gene is also included to discern background levels. (b) Firefly luciferase activity relative to wildtype (Luc 5.1) after 24 (n = 3) and 72 (n = 2) hours post transfection for MRE 4 mutant harboring cells. *P < 0.05 relative to Luc 5.1 expressing cells. **P < 0.008 relative to Luc 5.1 expressing cells. (c) Firefly luciferase activity of cells expressing mutants relative to wildtype (Luc 5.1) after 24 (n = 3) hours post transfection and cells also transfected with mutant miR-122 (n=3) bearing compensatory mutations to the mutated MREs (mutated p3–4 miR-122). Values in (b) and (c) were normalized by protein content, and error bars represent s.d. of independent experiments.

Analysis of HCV RNA levels 72 h post-transfection by Northern blot (Figure 3-6A) revealed that mutations of MREs 1 and 2 resulted in decreased viral titres as previously reported (144, 168, 177, 178, 212). Meanwhile, disruption of MRE 3 resulted in no significant changes in viral replication, also in accordance with previous studies (144, 177). Conversely, mutations of the MRE 4 resulted in an overall increase in HCV RNA levels. These results were similarly reproduced with quantitative RT-PCR at 72 and 120 h post-transfection (Figure 3-7). Furthermore, HCV IRES-driven expression of the luciferase reporter was enhanced by mutations to MRE 4 (Figure 3-6B).

With regards to the newly discovered MRE 4, no functional role for this seed site has yet been established. In an effort to illuminate its role, we had performed the same p3–4 mutations in MRE 4; however, in the instance of MRE 4, this resulted in a substitution mutation in the NS5B gene. Therefore, we also performed an alternate p4,7 double silent mutation (4nc) (Figure 3-1B) in order to ensure the results we were observing were not as a result of changes in the RNA polymerase activity of NS5B, but strictly due to disruption of miR-122 binding at this site. An increase in both viral RNA titres (Figure 3-6A and 3-7) along with a stimulation of HCV-IRES driven translation of the luciferase reporter was seen (Figure 3-6B) upon silent mutation of MRE 4. While it is well established that miRNA binding sites in the 3′UTR have been known to efficiently impede translation and induce mRNA destabilization, seed sites in the ORF have generally been found to be less effective (127). However, our mutational analysis and VRB assay results suggest that the ORF site (MRE 4) displays the highest affinity for miR-122 *in vitro* ($p < 0.0003$) (Figures 3-4D, 3-5, and Table 3-3) and is quite functional in an inhibitory role in translation and replication of the virus. Lastly, we have found that

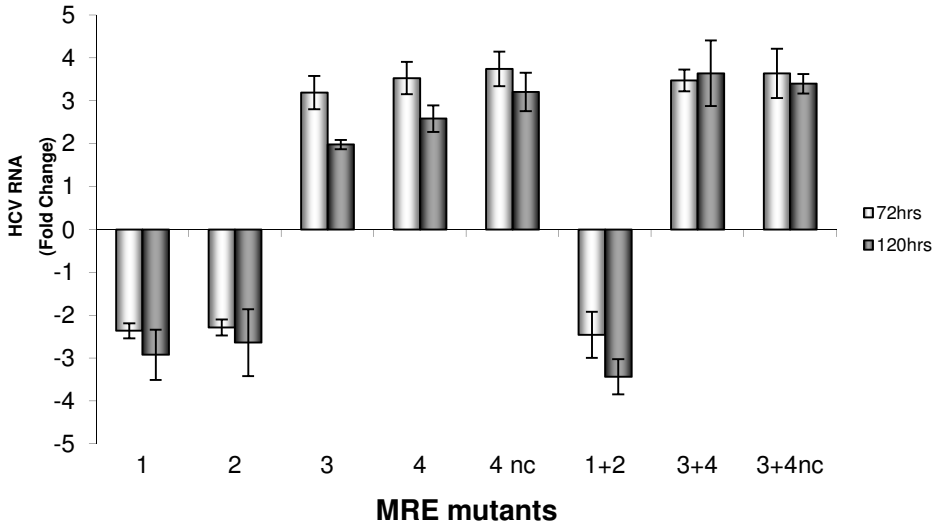

Figure 3-7. Functional analyses of mutations in the miR-122 seed sites determined by qRT-PCR of HCV RNA. Bicistronic HCV subgenomic replicon with HCV IRES driven luciferase reporter and mutated miR-122 seed sites was transfected in Huh-7.5 cells. All MREs were mutated at positions 3 and 4 of the seed site; also, MRE 4 was mutated such that a non-coding mutation (4nc) would occur as shown in Figure 3-1b. Quantitative RT-PCR analysis of HCV replicon expression in total RNA extracted from Huh-7.5 cells 72 (n=3) and 120 (n=3) hrs posttransfection. Results are shown as mean fold changes compared to naïve HCV replicons transfected cells. *P<0.003 relative to Luc 5.1 expressing cells. **P<0.0003 relative to Luc 5.1 expressing cells.

Table 3-3. **Student t-test values for Figures 3-4C, D, and 3-5.**

Figure 3-4C - p values			
Sites blocked	1 + 2 + 4	1 + 3 + 4	2 + 3 + 4
1 + 2 + 3	0.03	0.001	0.06
1 + 2 + 4	N/A	0.005	0.3
2 + 3 + 4	0.3	0.002	N/A
Figure 3-4D - p values			
Sites mutated	1 + 2 + 4	1 + 3 + 4	2 + 3 + 4
1 + 2 + 3	0.03	0.003	0.2
1 + 2 + 4	N/A	0.01	0.8
2 + 3 + 4	0.8	0.005	N/A
Figure 3-5 – p values			
Sites blocked	1 + 2 + 4	1 + 3 + 4	2 + 3 + 4
1 + 2 + 3	0.0004	0.0003	0.02
1 + 2 + 4	N/A	0.004	0.005
2 + 3 + 4	0.005	0.001	N/A

transfection of miR-122 bearing compensatory mutations to restore the miRNA interaction at MRE 4 resulted in decreased ($p < 0.001$) HCV-IRES driven translation of luciferase reporter thereby further validating MRE 4 as an inhibitory miR-122 binding sites in HCV (Figure 3-6C).

3. 5 Discussion

Collectively, this study demonstrates the importance of the newly characterized fourth miR-122 binding site in HCV RNA in its viral lifecycle. The target site affinity analysis reveals that MRE 4 displays the highest *in vitro* hybridization rate to miR-122 in HCV RNA compared to the previously characterized sites. While prior studies have proposed that miRNA targets sites in the coding region are less frequent and effective (30, 127), genome-wide analyses have identified a significant amount of ORF targeting (30). One study has demonstrated that active translation impedes miRISC association with mRNAs in the ORF (129). However, we report that MRE 4, found in the NS5B gene, has a potent inhibitory role on HCV replication. This curious result may be explained by the decreased local structure in NS5B leading to increased miR-122 accessibility, which compensates for the ability of ribosomes to clear the miRISC association with MRE 4. Additionally, it has been previously suggested that structural elements within HCV RNA cause pausing of active translation by the ribosome (444). Then it is possible that the surrounding local secondary structure (Figure 3-1B) impedes the ribosome, thereby stabilizing the miRISC association with MRE 4, leading to reduced translation and replication.

It should be noted that the *in vitro* VRB assay does not take into account the other factors that influence accessibility *in vivo*. These factors include the influence of RISC or other RNA binding proteins, which play a significant role in modulating RNA accessibility for small RNAs (167, 187, 188, 241, 294). It is possible that such additional host factors may be responsible for the

increased efficacy of an ORF site like MRE 4. Alternatively, the increased complementarity displayed by MRE 4 to miR-122, through its supplementary binding at the 3′ end in addition to its seed sequence complementarity (Table 3-1), may enable the miRNA to effectively withstand and block active translation.

Analysis of the degree of conservation of the sequence for the MRE 4 in the HCV RNA ORF, demonstrates that the site is well-conserved in genotypes 1, 3, 4, and 6, yet poorly conserved among genotypes 2 and 5 (Table 3-2). Interestingly, this site is conserved in 91.3% of HCV genotype 1b isolates, which represent a subtype of HCV that is known to be more aggressive and more likely to proceed from acute to chronic infection (104, 462). I hypothesize that one potential evolutionary role for miRNA sites in the ORF (MRE 4) is to suppress viral titres as a means of immune evasion, as previously suggested by Mahajan and others (249). While the miR-122 mediated positive modulation through interactions in the 5′UTR has been deemed essential, the MRE 4 site negatively counterbalances the effects of MRE 1 and 2. The existence of both stimulatory and inhibitory miR-122 recognition elements within HCV RNA may help to maintain optimal levels of HCV during infection.

In a recent study, Luna and colleagues investigated the miR-122 interactions with HCV genome *in situ* using cross-linking and immunoprecipitation of RNA bound to Argonaute protein (Ago-CLIP) and demonsterated that binding of miR-122 to MRE 4 is very strong, specific, and sensitive to miR-122 sequestration (243). Therefore this study further validates our findings and also shows that the interaction of miR-122 to MRE 4 *in situ* occurs in an ago-dependent manner. Moreover, the same study confirms the sponge effect of HCV RNA with regards to miR-122 sequestration (243).

While the existence of MREs 1, 2, and 3 was previously established (144, 177, 178), the role of other ORF sites (e.g. MRE 4) has yet to be explained in the context of the HCV lifecycle. Despite the recent promise of antisense oligonucleotides targeting miR-122 suggests that these potentially repressive sites have a limited significance on HCV compared to the positive modulatory sites in the 5′UTR (MREs 1 and 2), our results herein propose that recruitment of miR-122 to the ORF site (MRE 4) results in a decrease of HCV levels that is likely resulting from negative effects on translation, stability, and replication of HCV RNA. Further studies are required to distinguish at which regulatory level (translational repression or mRNA destabilization) MRE 4 plays a role. Since a slightly lower increase on luciferase activity (i.e. decreased regulation by MRE 4) at 72 h is seen compared to 24 h, I am inclined to believe the effect is mainly on translational repression since the luciferase activity at 24 h will be more representative of translation. However, I cannot exclude the potential role of mRNA destabilization, which a recent study suggests, is a predominant mechanism by which mammalian miRNAs mediate their repression (130). For future studies, it will also be of interest to monitor the relative biological relevance of these types of MREs in other infectious HCV models and comparing the relative contributions of each site on replication, translation, and virion production, as previously done for MREs 1 and 2 (144, 168, 177, 178).

Jopling *et al*. previously demonstrated cooperativity between MRE 1 and MRE 2 in mediating miR-122's positive modulation of HCV through mutational analysis of a luciferase reporter with a HCV 5′UTR (177). The VRB-based target site analysis also demonstrates cooperativity in binding between both sites in the 5′UTR. A previous *in vitro* study, in which miR-122 binding at MRE 1 induced an opening in the conformation of the IRES by disrupting a long-range

annealing motif, supports this hypothesis (84). It seems likely that miR-122's binding to MRE 1 is crucial to enable miR-122's access to MRE 2, at least *in vitro*.

While miRNA binding sites in the ORF are generally weaker, the results herein are the first characterization of a fourth miR-122 recognition element in the NS5B gene of HCV RNA. This site plays a significant inhibitory role at both the translational and replication levels. The newly characterized miR-122 seed site appears to be highly accessible, and its inhibition of HCV may contribute to the HCV's immune evasion and progression to chronic infection.

Overall, these results highlight the competing roles in HCV replication and translation of the miR-122 binding sites in the 5′UTR (stimulatory) compared to those in the ORF (inhibitory) (Figure 3-8). This study highlights the capacity of the VRB assay to validate computationally predicted miRNA target sites and evaluate the cooperativity of miRNA binding to closely spaced target sites. The target site accessibility results revealed the increased accessibility of MRE 1 compared to MRE 2 and the cooperativity in binding displayed between these two sites in the 5′UTR.

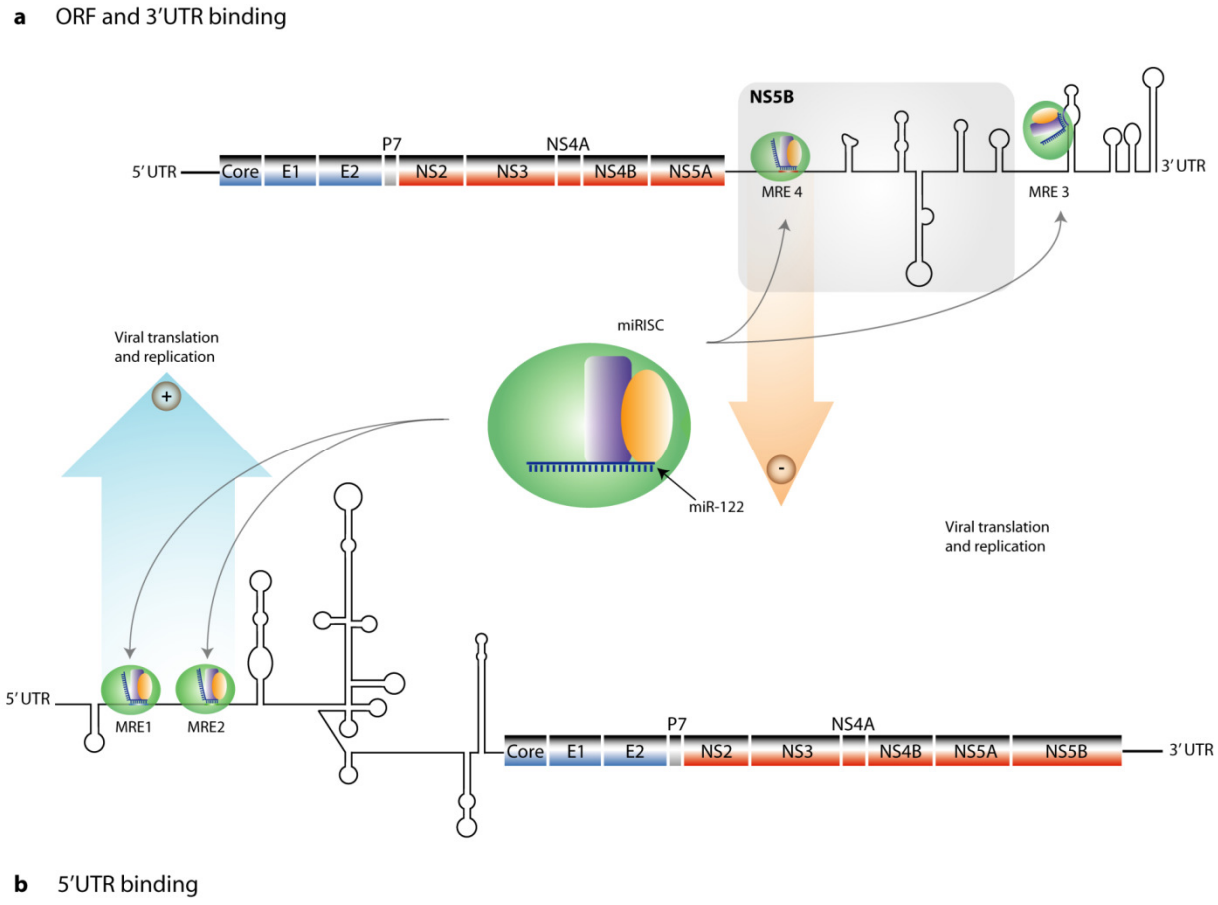

Figure 3-8. Competing roles of miR-122 seed sites in HCV RNA. Schematic depicting competing roles of microRNA binding sites in the 5′UTR (MREs 1 and 2) and those in the ORF and 3′UTR (MREs 2 and 3) in the HCV RNA genome. MicroRNA-122, upon association to the RNA induced silencing complex (RISC), will use its guide strand to bind these competing sites. This miRISC complex's association with the 5′UTR sites (b) will lead to an overall stimulatory effect on translation and replication. Conversely, binding with the ORF site (a) results in repression of these processes.

Chapter 4: Applying Activity-Based Protein Profiling to Investigate the Modulation of Fatty Acid Synthase Enzyme Activity during HCV Replication

Statement of Contributions

The content of this chapter has been published in the journal Chemistry and Biology (283) and permissions have been obtained for reusing the materials and figures in this thesis.

I helped to design all of the experiments in this chapter. I performed the majority of the experiments and analyzed the data along with my supervisor. I also wrote the drafts of the manuscript. Yanouchka Rouleau provided technical support and assistance for this project. The chimeric mice livers have been provided by Dr. Michael Joyce (University of Alberta), and Orlistat-based probe has been synthesized in the laboratory of Dr. Shao Yao (University of Singapore) (448).

4.1 Introduction

High-throughput genomic and proteomic profiling studies, along with other abundance-based approaches, have identified many host factors essential for HCV replication; however, more research is required to validate the biological and clinical relevance of these genes. Furthermore, these methods do not provide any information about the functional state, post-translational modifications, as well as association with co-factors and regulatory proteins that likely regulate the activity of host enzymes involved in the viral replication. Therefore, novel experimental approaches are required to interrogate the catalytic state of the host enzymes involved in viral infection, and provide an in-depth analysis of the dynamic and transient molecular interactions, which affect the enzymatic function of the host factors during HCV replication.

As mentioned previously, every step of HCV infection and replication is closely intertwined with host lipid metabolism (32, 55, 145, 183, 271, 316, 348). In this respect, HCV modulates the cellular lipid homeostasis in favour of excessive accumulation of triglycerides and other neutral

lipids (32, 270, 315, 363, 391). One of the key lipogenic enzymes whose expression is upregulated by HCV is fatty acid synthase (FASN; EC 2.3.1.85) (112, 388, 451). Importantly, HCV infection has been correlated with increased FASN levels in the serum of chronically infected patients (18, 181). FASN is a 270-kDa multifunctional enzyme that contains seven enzymatic domains and harbors the complete pathway required to synthesize palmitic acid *de novo* from acetyl and malonyl esters of coenzyme A (CoA) (423). Interestingly, while FASN activity appears to be essential for HCV replication, it does not seem to be required for adult tissue maintenance, as long as normal diet is maintained (61, 217, 359). Therefore FASN can be a target of anti-HCV drug development.

FASN enzyme activity has been shown to be essential in establishing infection of other RNA viruses through the creation of altered membrane structures. *De novo* lipid biosynthesis and incorporation of newly synthesized lipids at sites of viral replication has been shown to be necessary for the replication of other members of the *Flaviviridae* family including Dengue virus (DENV), yellow fever virus (YFV), Usutu virus (USUV), and West Nile virus (WNV). Inhibition of FASN by small molecule inhibitors such as Cerulenin, Orlistat and C75 leads to a drastic inhibition in replication of these viruses (140, 183, 256, 271, 314, 348, 388). Intriguingly, while the levels of FASN expression do not change significantly during DENV and WNV infection, its sub-cellular localization alters from the cytosol to being proximal to the sites of viral replication, so that nascent fatty acids can be utilized to establish or expand replication complexes (140, 256, 314). However, it is not known whether HCV modifies FASN localization and activity in a similar fashion. Transcriptional activation of lipogenic enzymes, such as FASN and acetyl-CoA carboxylase (ACC), has been demonstrated during HCV replication (430). To

date, however, it is not known whether these enzymes are catalytically active or if HCV recruits these enzymes to the vicinity of HCV replication complexes.

FASN enzyme activity requires post-translational activation, so that in order to be catalytically competent, the central acyl carrier domain (ACP) of FASN must be post-translationally modified by an intrinsic phosphopantetheine transferase (PPT) that covalently attaches the phosphopantetheine moiety of CoA onto a conserved serine residue of the ACP (174, 311, 358). Also, biotinylation is indispensible for the activity of ACC (302). Since traditional abundance-based approaches fail to report on the functional state of FASN and other enzymes, I used an ABP based on orlistat, an FDA approved drug (304), and known inhibitor of FASN (448-450), to investigate the HCV-induced alterations in the activity of FASN. Furthermore, I was interested in studying the localization of both total FASN and active FASN in the presence of HCV replicon using immunefluorescence and ABPP imaging. Lastly, I developed a quantitative ABPP method for relative quantification of FASN activity during HCV infection.

4.1.1 Lipid Biosynthesis Pathway

One of the major sources of hepatic lipids is *de novo* fatty acid biosynthesis, which occurs by transcriptional activation of lipogenic transcription factors such as sterol regulatory element-binding proteins (SREBPs) (151, 152) . Activation of SREBPs induces the expression of a series of lipogenic enzymes including FASN, stearoyl CoA desaturase (SCD), and acetyl CoA carboxylase (*ACC*). There are three isoforms of SREBP; SREBP-1a, SREBP-1c and SREBP-2. SREBP-1a activates all SREBP target genes, whereas SREBP-1c and SREBP-2 activate genes involved in fatty acid and cholesterol metabolism, respectively (151, 152). Activation of SREBPs in turn is induced by the liver X receptors (LXRs) as well as retinoid X receptor (RXR) α, which belong to a family of nuclear hormone receptors (336, 458) and are ultimately regulated

by insulin and glucagon (63, 78, 102, 300). Newly synthesized, inactive, SREBP is inserted into the ER membrane. When cells are depleted of sterols, SREBP is transferred to the Golgi, where it goes under proteolytic cleavages to release the nuclear domain (nSREBP) that is capable of activating the expression of sterol response element genes (SREs), which mediate the synthesis of cholesterol, fatty acids, and triglycerides (151, 152). Besides ACC and FASN that together produce palmitic acid (C16:0), fatty acid elongase complex, which converts palmitate to stearate (C18:0); SCD that converts stearate to oleate (C18:1); and glycerol-3-phosphate acyltransferase, which is involved in triglyceride and phospholipid synthesis, are among the main targets of SREBP1c (92, 151, 152, 275).

ACC is the rate-limiting enzyme in fatty acid biosynthesis that catalyzes the production of three-carbon intermediate, malonyl-coenzyme A (malonyl-CoA), from two two-carbon acetyl-coenzyme As (aceteyl-CoA) (194). FASN then catalyses the synthesis of palmitate using malonyl-CoA produced by ACC (377). Palmitate is the precursor of stearate and longer-chain saturated fatty acids, as well as the monounsaturated acids palmitoleate and oleate. The nascent fatty acids can then be incorporated into triglycerides and membrane phospholipids (337).

4.1.2 Fatty Acid Synthase (FASN)

Fatty acids are the main components of cellular membranes, energy storage, and signal transducer compounds, which are synthesized through multiple rounds of reactions by FASN, a proficient and multifunctional enzyme (423). The *de novo* synthesis of palmitic acid from glucose occurs through sequential extension of an alkanoic chain, two carbons at a time, by a series of decarboxylative condensation reactions that are summarized by this equation (378):

$$\text{Acetyl-CoA} + 7\ \text{Malonyl-CoA} + 14\ \text{NADPH} + 14\ H^{+} \rightarrow \text{Palmitic acid} + 7\ CO_2 + 8\ \text{CoA} + 14\ \text{NADP} + 6\ H_2O$$

Aside from its role in viral replication, human FASN is also an important diagnostic and prognostic marker for cancer, as FASN is expressed at abnormally elevated levels in many varieties of common human cancer (206, 264, 265). Moreover, FASN play a key role in obesity (47), therefore FASN is an attractive target for therapeutic interventions (62).

4.1.2.1 FASN Structure & Function

FASN is a complex homodimeric 552kDa (each subunit is about 273 kDa) enzyme containing 7 functional domains: malonyl/acetyl transferase (MAT), β-ketoacyl synthase (KS), dehydrase (DH), enoyl reductase (ER), β-ketoacyl reductase (KR), ACP and thioesterase (TE) (Figure 4-1) (234).

FASN catalyzes the synthesis of palmitic acid in three major steps: initiation, elongation, and termination. Initiation step involves the condensation of malonyl-CoA and acetyl-CoA catalyzed by MAT domain; elongation, which is a repeating cycle of reduction and dehydration to add 2 carbons in each cycle to the elongating fatty acid chain, is catalyzed by KS, KR, DH, and ER, respectively; and finally, termination step is catalyzed by TE and leads to releasing nascent fatty acid from ACP (378, 423).

Substrate loading in FASN occurs by MAT domain through translocation of acetyl and malonyl moieties, from CoA thioester to the phosphopantetheine thiol of the ACP domain. The catalytic active residue in the MAT domain is a nucleophilic serine (Ser581), plus an indispensible and highly conserved residue His683, that most likely increases the nucleophilicity of the Ser581 (268, 332). The overall condensation reaction is catalyzed by the KS domain in three steps: (1) transfer of the acyl moieties from acyl-ACP thioester to the active-site cysteine (Cys161) residue, (2) binding and decarboxylation of a malonyl-ACP thioester moiety to produce a reactive carbanion and (3) formation of a new carbon–carbon bond by nucleophilic attack of the

carbanion on the carbonyl carbon of the acyl moiety (179, 440). Interestingly, the catalytic activity of KS increases from C2 to C12 and decreases with increasing chain length beyond C12, reaching 0.05% for C18 (378). The catalytic residues of the β-processing domains i.e. DH, ER, and KR are His878, Gly1672, and Gly1888 respectively (378). The 16-carbon saturated palmitic acid is released from the phosphopantetheine thiol of the ACP domain by chain-terminating TE domain. The FASN TE is a serine active-site enzyme (Ser2308) in which nucleophilicity of the serine residue is supported by a conserved histidine residue (311). This domain has very limited activity toward substrates with less than 16 carbon atoms (378). This is particularly important because any ABP targeting this domain should have a fatty acid chain of 16 to 18 carbons.

Functional animal FASN exists as an antiparallel homodimer, in which the each ACP domain is involved in substrate loading and condensation reactions catalyzed by the MAT and KS domains of the opposite subunit. In contrast, the β-carbon processing reactions, together with the release of palmitate, are catalyzed by the cooperation of the ACP with catalytic domains of the same subunit (171, 378).

4.1.2.2 FASN Inhibitors

To date, several compounds are known to inhibit FASN. These include cerulenin, C75, orlistat, C93, and naturally occurring polyphenols (Figures 4-2 and 4-3) (244). Cerulenin, isolated from *Cephalosporium caerulens,* contains an epoxy group that react with and inhibit the KS domain (114). However, cerulenin is chemically unstable and cytotoxic (207); to overcome these drawbacks, C75 was developed based on the cerulenin mechanism of action (207). Nevertheless C75 is a weak, irreversible inhibitor of FASN and thus more potent analogs of C75 have been designed recently (428).

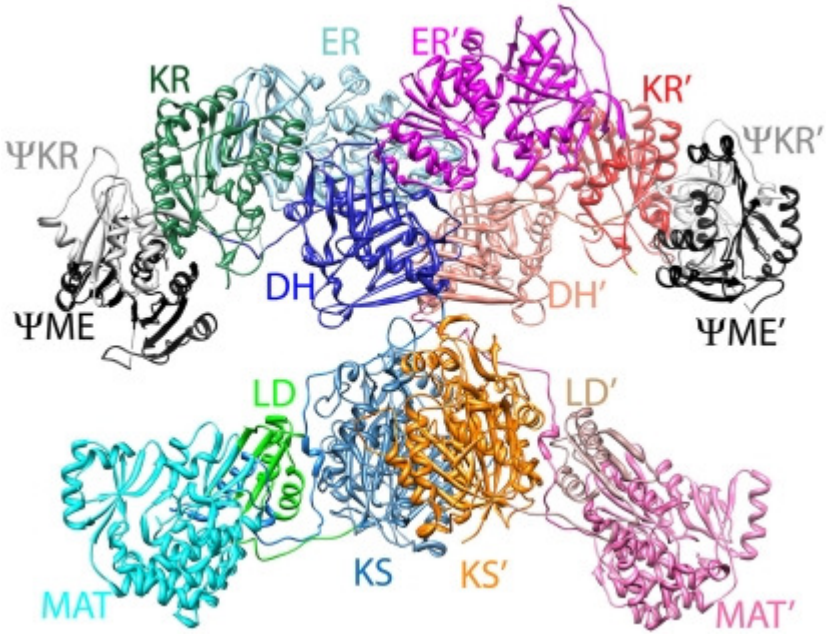

Figure 4-1. FASN forms an X-shaped homodimer and the two subunits are arranged in a fully extended head-to-tail organization (Figure adapted from (234)). malonyl/acetyl transferase (MAT), β-ketoacyl synthase (KS), dehydrase (DH), enoyl reductase (ER), β-ketoacyl reductase (KR), ACP and thioesterase (TE).

Natural products such as epigallocatechin gallate (EGCG), the principal polyphenol component of green tea, have also been demonstrated to inhibit the KR activity of FASN (221). The MAT domain of FASN is also extremely susceptible to inhibition by diethyl pyrocarbonate (378).

Lastly, orlistat, also known as tetrahydrolipstatin (THL), is a US FDA-approved FASN inhibitor, which was originally developed as an anti-obesity drug. The active moiety of orlistat is a β-lactone ring that undergoes a nucleophilic attack and forms a covalent adduct with the active serine (Ser2308) of FASN TE domain (311). Moreover, orlistat has been shown to have a modest anticancer activity in several *in vivo* models (409). Orlistat-like compounds have successfully been applied as activity-based probes to examine FASN activity in hepatocytes (448, 449).

4.2 Rationale

Conventional abundance-based proteomics approaches are labor-intensive, do not capture post-translational modifications, which regulate protein activity, and do not assign protein function. A general rationale for performing ABPP therefore is that it allows for the reporting of enzyme activity changes that may be independent of protein expression and to help assign function to proteins of unkown function. Activity-based probes can be used to investigate the HCV-induced alterations in the activity of hepatic enzymes in order to identify potential diagnostic and prognostic markers, and develop therapeutic interventions.

This chapter is concerned with the fact that HCV induces lipid biosynthesis in infected cell for its replication, and FASN is a key lipogenic enzyme that is likely involved. Orlistat is a specific inhibitor of the thioesterase domain of FASN, therefore an activity-based probe derived from

orlistat may represent an exciting tool to study the activity of FASN during HCV replication and report on any changes in enzyme activity.

4.3 Hypothesis

Orlistat-derived activity-based probe can be used to investigate the HCV-induced alterations in the activity and localization of FASN during HCV replication.

4.4 Results

4.4.1 Protein Profiling Using Orlistat-Based Probes

As mentioned previously, orlistat makes a covalent bond, through its β-lactone moiety (Figure 4-2A), to the nucleophilic serine (Ser2308) in the active site of the TE domain of FASN (311). Since orlistat is cell permeable (200), it makes a promising activity-based probe that can be applied both *in situ* and *in vitro* to report on the activity of its targets in subcellular environment and in homogenized cells or tissues, respectively. Moreover, minor structural modifications of orlistat, such as introducing an alkyne handle, can be performed without having a drastic effect on its biological activity (341, 448). As a result, conservative structural changes have been performed to the parental THL structure, to convert orlistat into a competent activity-based probe (341, 448). In addition, an alkyne handle has been introduced to the THL structure, which allows for conjugation of the protein/probe complex to reporter and affinity tags via bio-orthogonal click chemistry (Figure 4-3 B) (101, 448).

First, a library of seven orlistat-based probes (Figure 4-3B), which has already been applied to target FASN in HepG2 cells (448), was screened for its specificity against FASN in Huh7 cells. For this purpose, *in situ* (data not shown) and *in vitro* (Figure 4-3C) labeling was carried out and the reaction products were separated by SDS-PAGE and visualized in-gel using a flatbed

fluorescence scanner. As demonstrated, the orlistat analogue probes **1** to **5** all labeled FASN whereas analogues **6** and **7** did not label FASN appreciably. Probe **2** was chosen for further

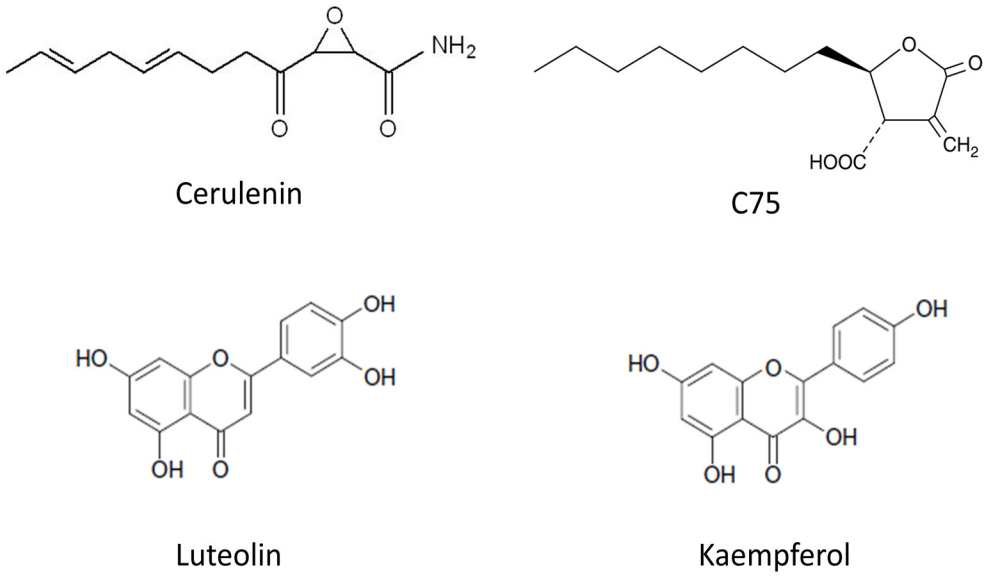

Figure 4-2. The structures of inhibitors of fatty acid synthase. Luteolin and Kaempferol are naturally occurring polyphenol inhibitors of this enzyme.

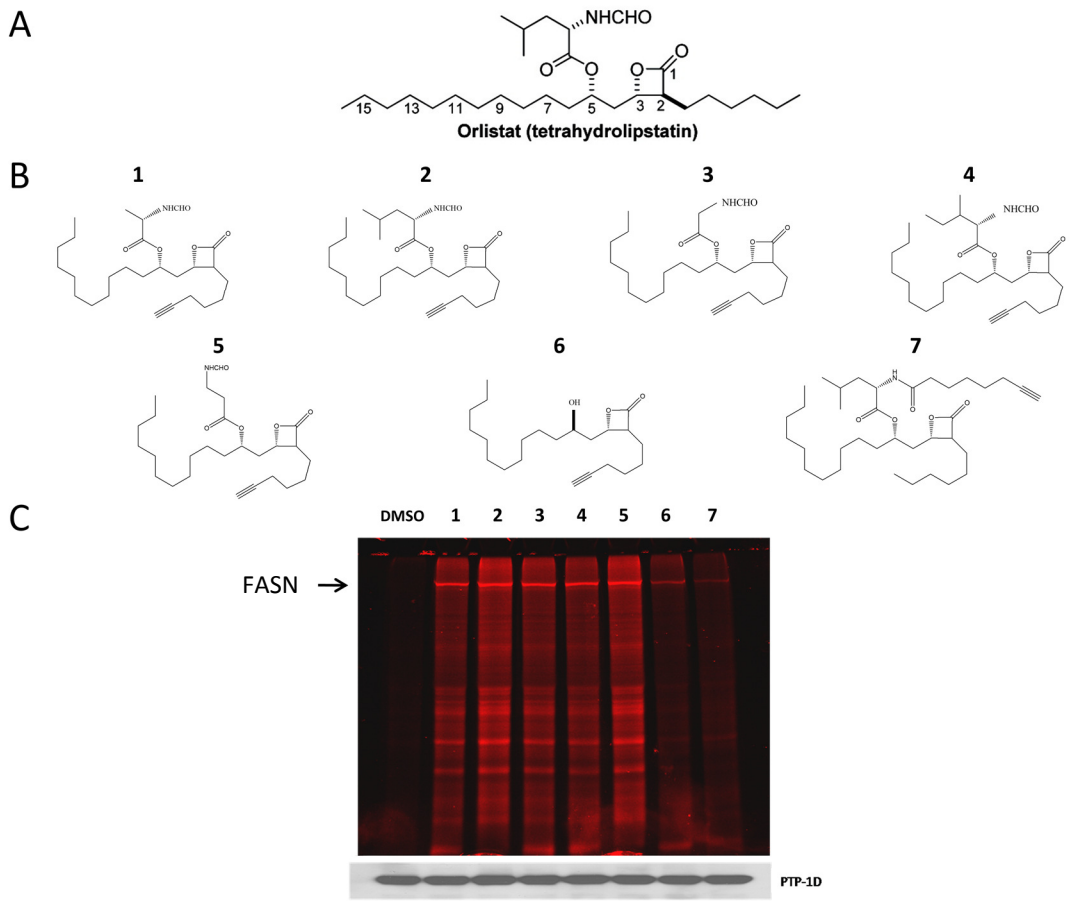

Figure 4-3. The structure and specificity of the orlistat-based probes. (A) The structure of orlistat. (B) Seven orlistat-derived probes were synthesized and screened in Huh7 cells for their ability to target FASN. (C) Huh7 cells were treated with orlistat-based probe for 4 hours, lysed and clicked with Rhodamine azide, A representative in-gel fluorescent scanning is shown. Black arrow points to the band corresponding to FASN. Click mix only (Rhodamine azide+CuSO4+TBTA+TCEP) produces no signal in the absence of orlistat-based probes (first lane, DMSO Control). Subsequent to in-gel fluorescent scanning, the gel was transferred to a PVDF membrane and probed with anti-PTP-1D, as the loading control to ensure equal loading**.**

experiments as it shows a strong specific activity-based labeling towards its FASN target. Overall, these results demonstrate that the orlistat-based probe can function as an activity-based probe in Huh7 human hepatoma cells to report on the activity of FASN.Next, the specificity of the orlistat-based probe **2** (Figure 4-4A) towards FASN was further evaluated by performing competitive ABPP, in which prior to labeling with the corresponding probe, the proteome is incubated with an excess of different inhibitors, some of which compete for the same active site that the probe targets (224). Thus, the proteome was preincubated with known FASN inhibitors, such as cerulenin and C75, which each irreversibly inactivate the β-ketoacyl-ACP synthase domain, but not the thioesterase domain of FASN (272, 305), as well as 5-(tetradecyloxy)-2-furoic acid (TOFA), an established inhibitor of ACC (133). As expected, in the presence of excessive amounts of orlistat inhibitor, the orlistat-based probe is out-competed and cannot label the thioesterase domain of FASN (Figure 4-4B, lane 3); however, neither C75, nor cerulenin abolishes the labeling of the orlistat-based probe towards FASN (4-4 B, lanes 4-5), which indicates that the labeling is both target- and domain-specific. This shows that the probe can also be used to distinguish between different domains of FASN. The percentage activity remaining was determined by measuring the integrated optical density (IOD) of the FASN band relative to a DMSO-only (no inhibitor) control (405), normalized to a loading control (PTP-1D) (Figure 4-4C). Moreover, the heat-denatured proteome (Δ; first lane) did not show any labeling with orlistat ABP, which further validates that the probe only targets the active proteome. Collectively, these data show that orlistat-based probe has high specificity towards the thioesterase domain of FASN and the attachment of the small alkyne handle does not change its preference in enzyme selectivity in Huh7 cells.

4.4.2 Expression and Activity of FASN Increases during HCV Infection

Previous reports have demonstrated that *de novo* fatty acid synthesis is required for HCV replication (183, 388), and HCV infection is associated with accumulation of lipid in hepatocytes (i.e., steatosis). To further confirm the role of FASN activity in HCV replication, I employed inhibitors of fatty acid synthesis to Huh7 cells that stably express a tricistronic HCV subgenomic replicon, with firefly luciferase reporter gene (Figure 1-1A). At 48h post-treatment the luciferase activity was examined as a measure of HCV replication. As shown in figure 4-5A, in the presence of orlisat, cerulenin and TOFA, HCV replication decreases by 50%, 70% and 65%, respectively, compared with DMSO treatment. This is consistent with the integral role of fatty acid synthesis in HCV replication.

Moreover, *in situ* studies have demonstrated that FASN expression increases during HCV replication (388, 451). To examine whether the activity of FASN is also elevated by HCV replication, I applied comparative ABPP (70), which compares the differential activity between naive and virus-infected host proteomes. Orlistat-based ABP (Figure 4-4A) was employed to profile the activity of FASN in Huh7.5 cells harbouring a full-length genotype 1b (Con1b) HCV genomic replicon (FGR) (Figure 1-1C). The activity was determined by measuring the integrated optical density (IOD) of the band corresponding to FASN in the fluorescent gel, normalized to IOD of the band corresponding to a loading control (PTP-1D) in the respective western blot. In both *in vitro* and *in situ* labeling experiments, FASN activity increased by approximately 75% in the presence of HCV replicon, while FASN expression, determined by IOD of the FASN band in the western blot normalized to the loading control, increased by 45% (Figure 4-5B and 4-5C).

A

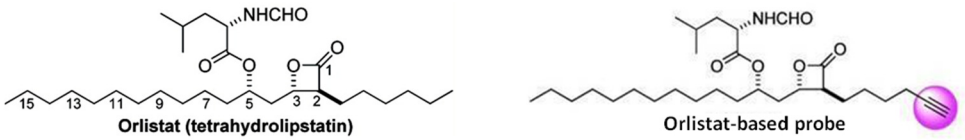

B

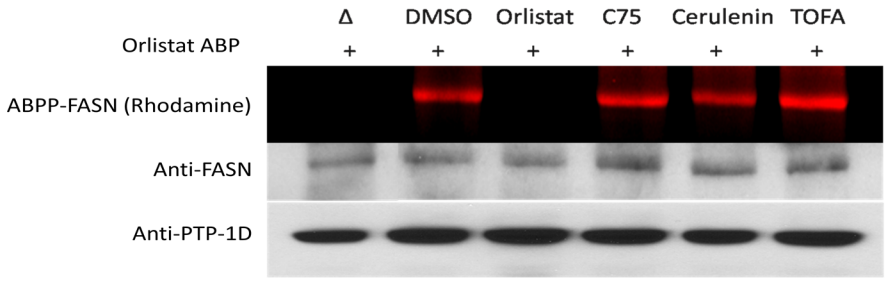

C

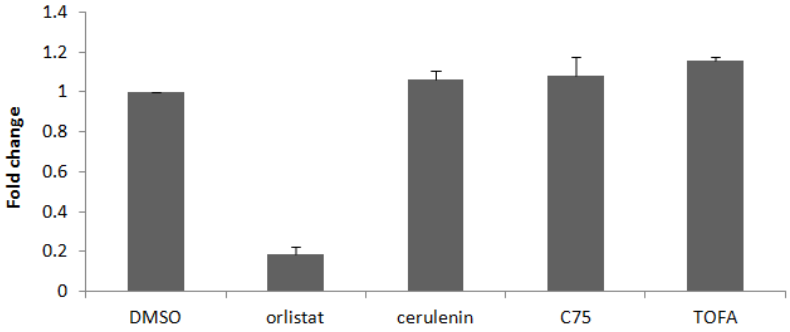

Figure 4-4. The orlistat-based probe is specific for the TE domain of FASN. (A) The structures of orlistat and the orlistat-based probe with alkyne moiety highlighted. (B) Fresh proteome isolated from Huh7 is incubated with 100 μM of inhibitors for 1h followed by labeling with 10μM of orlistat-based probe. Δ is the heat-denatured sample. (C) The percentage activity remaining was determined by measuring the integrated optical density (IOD) of the FASN band relative to a DMSO-only (no inhibitor) control normalized to a loading control (PTP-1D). The data represent the average of three independent gels. Error bars are standard deviation.

To further investigate the role of FASN in the HCV life cycle, an established mouse-model for HCV infection was employed, in which primary human hepatocytes are transplanted into SCID mice carrying a plasminogen activator transgene (*Alb-uPA*). This model has been shown to support HCV infection without inducing an adaptive immune response (266). In this *chimeric mouse*-model, HCV replication occurs at biologically relevant levels, and infectious viral particles are produced and released (266, 425). I conducted ABPP experiments in chimeric SCID/Alb-uPA mice infected with HCV genotype 1a, which is more common in North America (274). In these mice¸ clusters of human hepatocytes are easy to detect, as nodules of human cells are visible macroscopically (384). Furthermore the success of transplanation was determined by ELISA, detecting human albumin (hAlb) in serum (384). FASN activity was compared by applying orlistat-based ABP on liver samples obtained from four different nodules of three mock infected chimeric mice, as well as infected mice with HCV genotype 1a that maintained the HCV infection for 10 weeks with serum titers between 2×10^5 and 4×10^7 copies/mL (matched donors). As depicted in Figures 4-6A and 4-6B, HCV induces a 50% increase in the activity of FASN in the chimeric livers, with a *P*-value of 0.01calculated by two-tailed student t-test. Moreover, this increase in the activity of FASN in the liver of infected chimeric mice is in agreement with its total abundance (Figure 4-6C). These findings provide additional evidence that FASN activity is beneficial to HCV replication and therefore its expression and activity is increased by the virus.

A

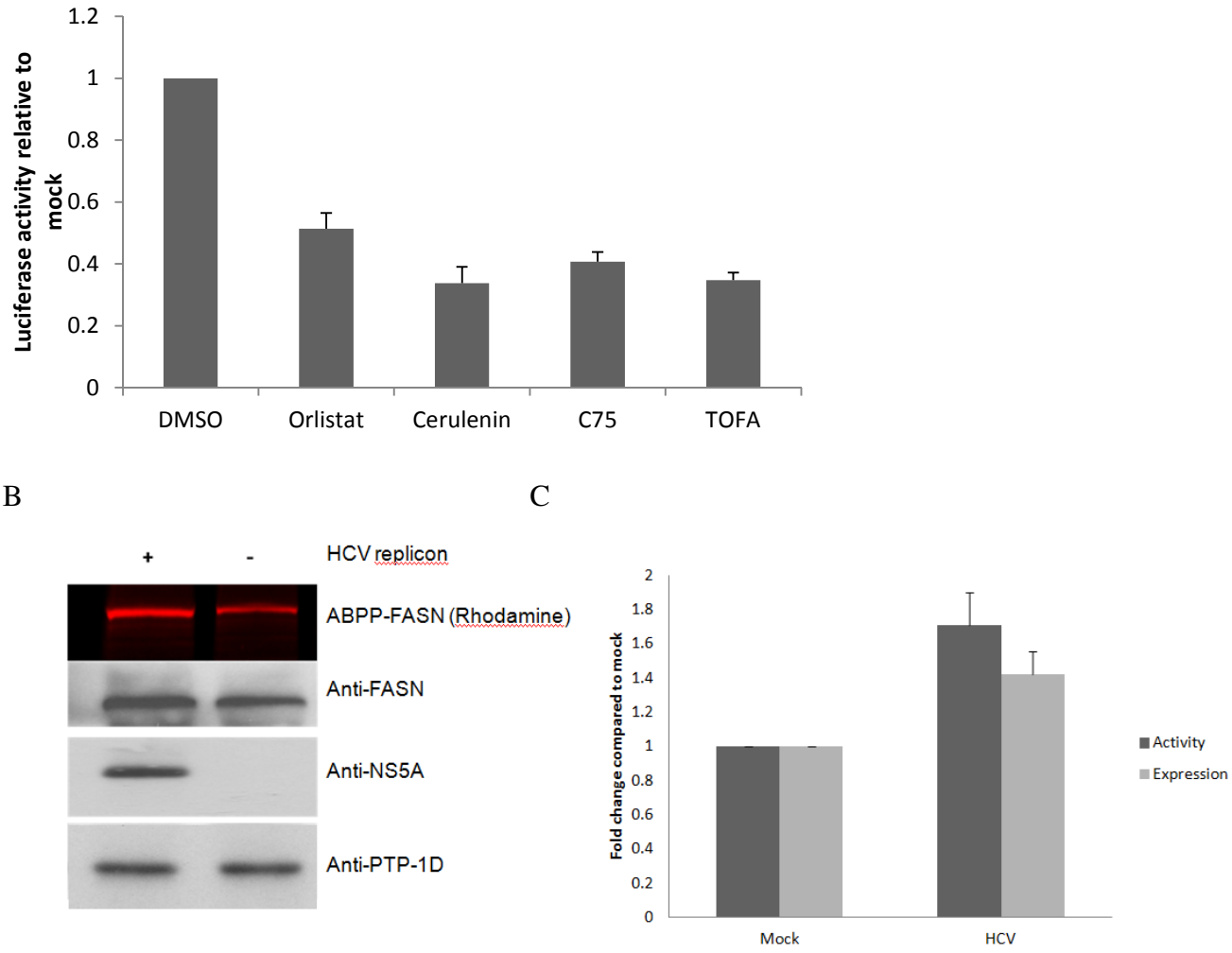

Figure 4-5. FASN activity increases during HCV replication. (A) Huh7 cells that stably express a tricistronic HCV replicon containing the firefly luciferase reporter gene were treated with the inhibitors of fatty acid synthesis at 10 µM for 48 h, and HCV replication was examined as a measure of luciferase activity compared to DMSO treatment. The results were normalized against total protein levels and are demonstrated as the average of three independent experiments and the error bars are standard deviation. (B) Huh7 cells expressing or not the Con1 full-length replicon (HCV), were lysed and probed against active FASN (ABPP-FASN), total FASN (anti-FASN), and PTP-1D (anti-PTP-1D). A representative gel is shown in which the activity and expression of FASN was examined in Huh7 cells harbouring full-length HCV replicon genotype 1b. (C) Comparison of the activity and expression of FASN in Huh7 cells harbouring the full-length HCV replicon with mock control. The data represent the average of four independent gels *P*-value= 0.005 and 0.008 for activity and expression respectively, calculated by two-tailed student t-test

A

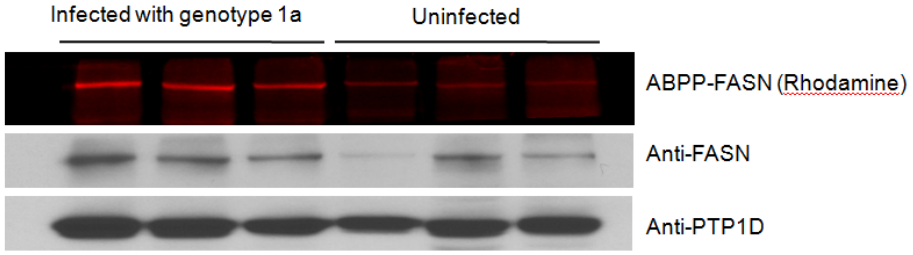

B

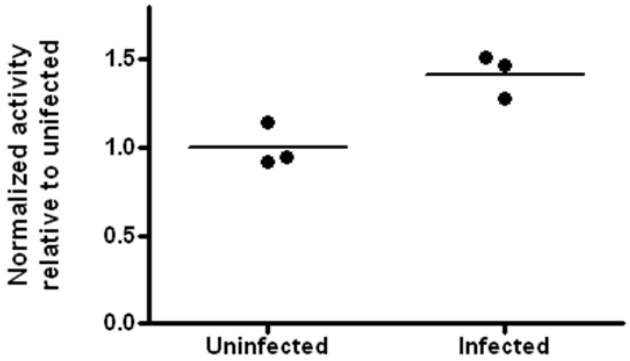

C

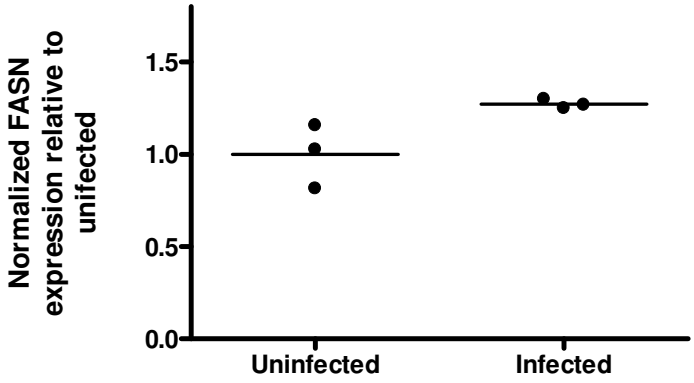

Figure 4-6. FASN activity increases during HCV infection. (A) Comparison of the activity and expression of FASN in chimeric mice infected with genotype 1a to uninfected control chimeric mice. A representative gel is shown (B) Quantification of signal intensity for the band corresponding to FASN was followed by background correction. (C) Quantification of FASN expression in the liver of chimeric mice infected or uninfected with HCV genotype 1a. Quantification of signal intensity for the band corresponding to FASN expression was performed by ImageJ and the results were normalized to PTP-1D expression as the loading control. The results are shown as normalized FASN activity of infected relative to uninfected chimeric mice. The data represent the average of four independent gels. *P*-value=0.01, calculated by two-tailed student t-test.

4.4.3 Modulation of the Activity and Expression of FASN by HCV-Encoded Proteins

As mentioned, FASN expression is primarily regulated at the transcriptional level by SREBP-1c (151) and some of the HCV structural and non-structural proteins, including core (165, 193), NS2 (295), NS4B (306), and NS5A (117, 443), have been demonstrated to activate SREBP-1c transcriptional pathway. Moreover, studies have shown that the HCV proteins core and NS5A can activate the phosophoinositide-3 kinase (PI3K)-AKT signalling cascade, which in turn leads to the activation of SREBP-1 pathway (166, 387). To study whether the activation of SREBP-1c pathway results in an increase in abundance of active FASN, I examined the alterations in the activity and expression of FASN in the presence of individual HCV proteins. For this purpose, the HCV proteins that have been shown to activate the SREBP-1c pathway in Huh7 cells, including E1/E2, core, NS2, NS4B, and NS5A were cloned and expressed. Forty-eight hours post-transfection, cell lysates from each transfection was first analyzed by western blotting to ensure transfection success (data not shown), and subsequently the activity and expression of FASN was examined as mentioned previously. The activity of FASN was significantly induced by NS4B, core, and NS5A, with 1.75, 1.5, and 1.4 fold increase compared to mock respectively; while E1/E2 and NS2 do not seem to have a drastic effect on the activity and expression of FASN (P-value>0.05) (Figure 4-7A and 4-7B). The increase in the activity of FASN in the activity of FASN is in accordance with an increase in the abundance of total FASN (Figure 4-7C).

A

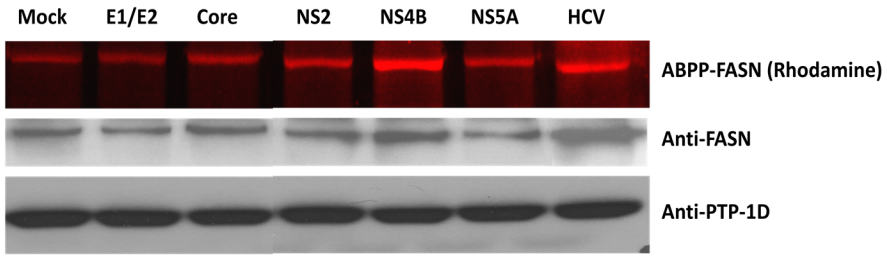

B

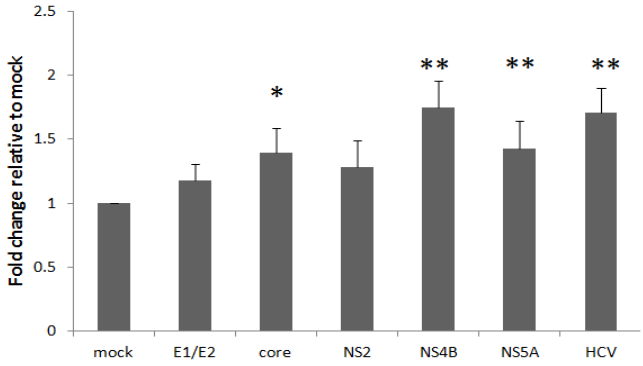

C

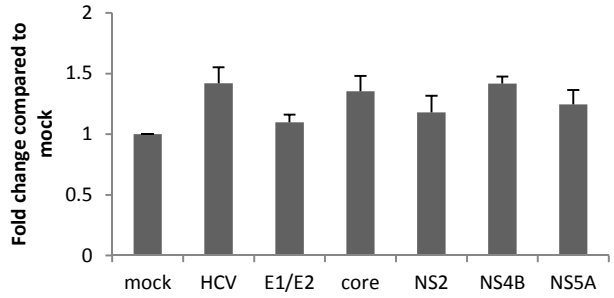

Figure 4-7. Investigating the effect of individual HCV proteins on FASN expression and activity. (A) Huh7 cells transfected with individual HCV genes, or expressing Con1 full-length replicon (HCV), were lysed and probed against active FASN (ABPP-FASN), total FASN (anti-FASN), and PTP-1D (anti-PTP-1D). A representative gel is shown demonstrating the alterations in the activity and expression of FASN in the presence of different HCV proteins. (B) Densitometry analysis of the bands corresponding to FASN on ABPP gels was performed by ImageJ, and the data were normalized to the loading control (PTP-1D) on corresponding western blots. (C) Quantification of FASN expression in the presence of HCV replicon or its individual proteins. Huh7 cells transfected with individual HCV genes, or expressing Con1 full-length replicon, were probed with antibodies against FASN, and PTP-1D. Densitometry analysis of the bands corresponding to FASN expression was performed and the results were normalized to the loading control (PTP-1D) on corresponding western blots. The results are demonstrated as fold changes compared to mock and represent the mean from 4 gels. The error bars represent standard deviation. *$p < 0.05$, **$p < 0.01$, calculated by two-tailed Student T-test.

4.4.4 Increased FASN Activity Reflects in the Cellular Triglyceride Levels

The main product of FASN is the 16-carbon saturated fatty acid palmitate, which can be processed to be incorporated into triglycerides (233). Therefore, to further study the changes in FASN activity induced by HCV and its proteins, I quantified the amount of cellular triglyceride (TG) levels as an indirect measurement of FASN activity. For this purpose, I analyzed cellular TG levels in Huh7 cells that stably express full-length HCV replicon (Huh7-FGR) or those transiently transfected with individual HCV proteins, or mock transfected Huh7 cells. As shown in figure 4-8, while NS4B, core, NS5A and the HCV replicon increased the total cellular TG content significantly, E1/E2 and NS2 did not cause a significant increase in cellular TG levels. Thus, it was concluded that increased activity of FASN in the presence of HCV replicon, core, NS5A and NS4B correlate with higher cellular TG levels.

4.4.5 The Localization of FASN Does Not Change during HCV Replication

Two of the HCV encoded proteins, core and NS4B, are palmitoylated at the cysteine residues of their C-terminal ends, and this palmitoylation is essential for the replication of the virus (252, 460). Palmitic acid produced by FASN, can be subsequently used by palmitoyltransferase (PAT) for palmitoylation of certain cysteine residues (86). It is possible that HCV requires FASN activity to palmitoylate core and NS4B. Furthermore, studies have shown that the distribution of FASN changes to colocalize with replication sites during infections with DENV, USUV, and WNV, which also belong to the *Flaviviridae* family, and require fatty acid synthesis for their replication (140, 314). Therefore I decided to investigate whether the subcellular localization of FASN similarly changes during HCV replication to the vicinity of replication complexes in membranous webs or lipid droplets, where NS4B and core also localize (27, 94).

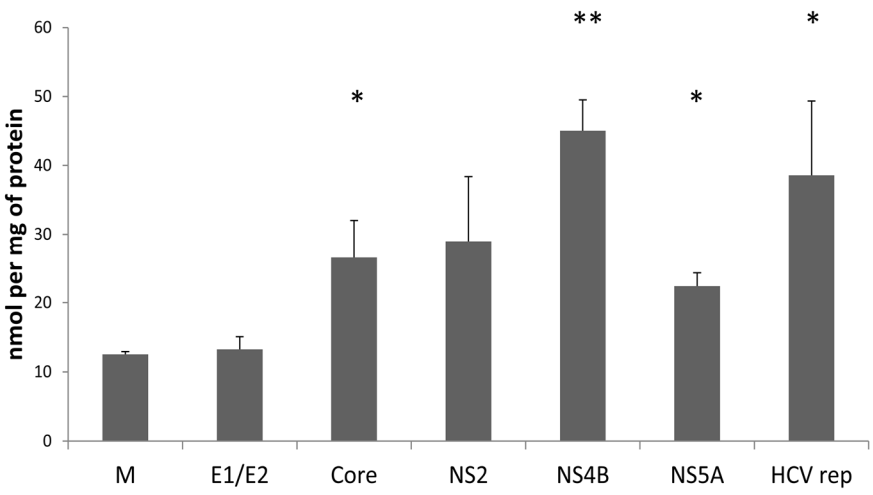

Figure 4-8. Total amount of cellular triglyceride in the presence of either the HCV replicon, or of individual HCV proteins. Huh7 cells transfected with individual HCV genes, or expressing Con1 full-length HCV replicon, were lysed and total amount of triglyceride was measured. The results of triglyceride assays were normalized to total protein content and demonstrated as nanomol per milligram of protein. The data represent the mean of three independent assays. The error bars are standard deviation.* $p < 0.05$, ** $p < 0.01$, calculated by two-tailed student t-test.

Huh7 cells expressing the HCV subgenomic replicon (SGR) (genotype 1b, Figure 1-1), as well as naïve Huh7 cells were immunostained with antibodies against FASN and HCV NS5A (Figure 4-9A), which associates with HCV replication complex (RC) (124), and dsRNA (Figure 4-9B), HCV replication intermediate. The negligible fluorescent signal observed for NS5A and dsRNA in naïve Huh7 cells was set as the background (Figure 4-11B) The cells were subsequently analyzed by fluorescence microscopy and the image analyses revealed that the distribution and localization of FASN, which is mainly perinuclear, does not change in the presence or absence of the HCV replicon (Figure 4-9A and 4-9B).

To investigate the possibility of colocalization between total FASN and NS5A, or dsRNA, I calculated the degree of colocalization by measuring Mander's coefficient (R) and Pearson correlation coefficient (Rr). Mander's coefficient indicates an actual overlap of the signals, and provides an estimation of the percentage of overlapped pixels. Its values vary from 0 to 1 (0=non-overlapping images and 1=colocalized images); importantly, it strictly measures co-occurrence independent of signal proportionality (91, 254). I also calculated the colocalization using the Pearson correlation coefficient, which measures the pixel-by-pixel covariance in the signal levels of two images, and describes the correlation of the intensity distribution between channels. The range for Pearson correlation coefficient is from -1 to 1 (-1 = total negative correlation, 0 = random correlation, and 1 = total positive correlation) (6, 465). The Mander's coefficient for overlapping signals between total FASN and NS5A, or dsRNA is 0.95 ± 0.03, and 0.93 ± 0.03, respectively. However, the Pearson correlation coefficient is only 0.53 ±0.11 and 0.42 ±0.09 for FASN and NS5A, or dsRNA, respectively. Therefore these data suggest that

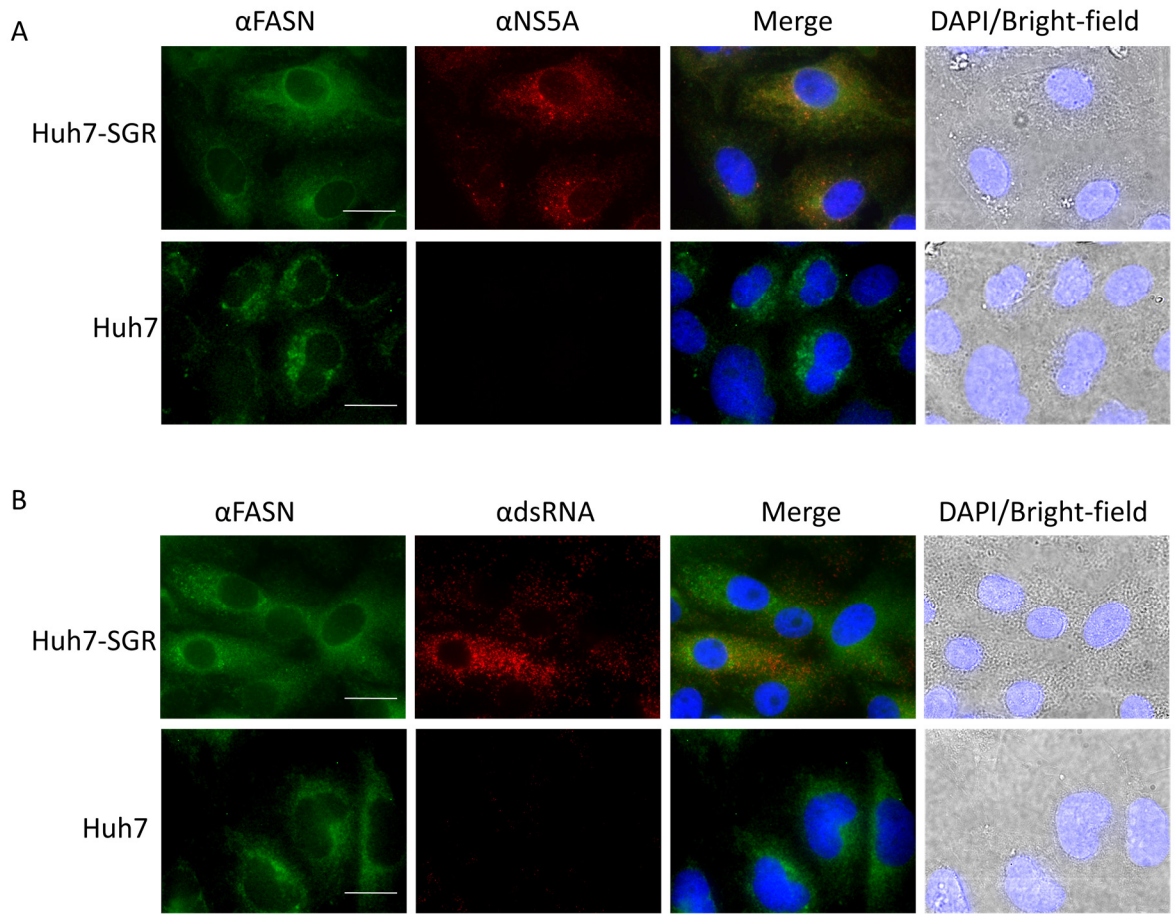

Figure 4-9. FASN does not colocalize with HCV replication complex. Huh7 cells and Huh7 cells harbouring subgenomic HCV replicon (Huh7-SGR) were fixed and probed against total FASN (α-FASN) and (A) HCV NS5A (α-NS5A) or (B) dsRNA (α-dsRNA), HCV replication intermediate, followed by DAPI staining. (Scale bar: 10 µm). The images are representative of 4 independent immunostaining experiments.

although there is some overlap between total FASN and NS5A, or dsRNA, there is a moderate or low correlation between their signal intensities, which could reflect that there is no direct molecular interaction between FASN and HCV replication complex

Next I set to examine the distribution of active FASN during HCV replication, by combining ABPP imaging with immunofluorescence microscopy. For this purpose, I first validated the specificity of the orlistat-based probe by treating Huh7 cells and Huh7-SGR cells with the orlisat-based probe, followed by conjugation to Rhodamine azide through click chemistry and immunostaining against total FASN. As shown in Figure 4-10A, ABPP-labeled FASN evidently colocalizes with total antibody-labeled FASN and shows a similar perinuclear pattern in both mock Huh7 cells and Huh7-SGR. The calculated Mander's and Pearson coefficients for the colocalization of total FASN and ABPP-FASN, in the presence of the HCV subgenomic replicon, are 0.97 ± 0.03, and 0.93 ±0.03, respectively, and in naïve Huh7 cells are 0.99 ± 0.01 and 0.94± 0.02, which indicate that active FASN highly colocalizes with total FASN in the presence or absence of the HCV subgenomic replicon. Importantly, minimal fluorescence was observed in Huh7 cells and Huh7-SGR cells treated with the click mix only in the absence of the orlistat probe (Figure 4-11A). There is also a considerable increase in the levels of active FASN detected in the presence of the HCV subgenomic replicon, which is consistent with previously shown data.

Subsequently, I examined the possible localization of active FASN to the proximity of HCV replication complexes, by probing against active FASN and NS5A (Figure 4-10B) or dsRNA (Figure 4-10C). As demonstrated, there is no apparent colocalization between active FASN and sites of active viral replication. Mander's and Pearson coefficients for ABPP FASN and NS5A

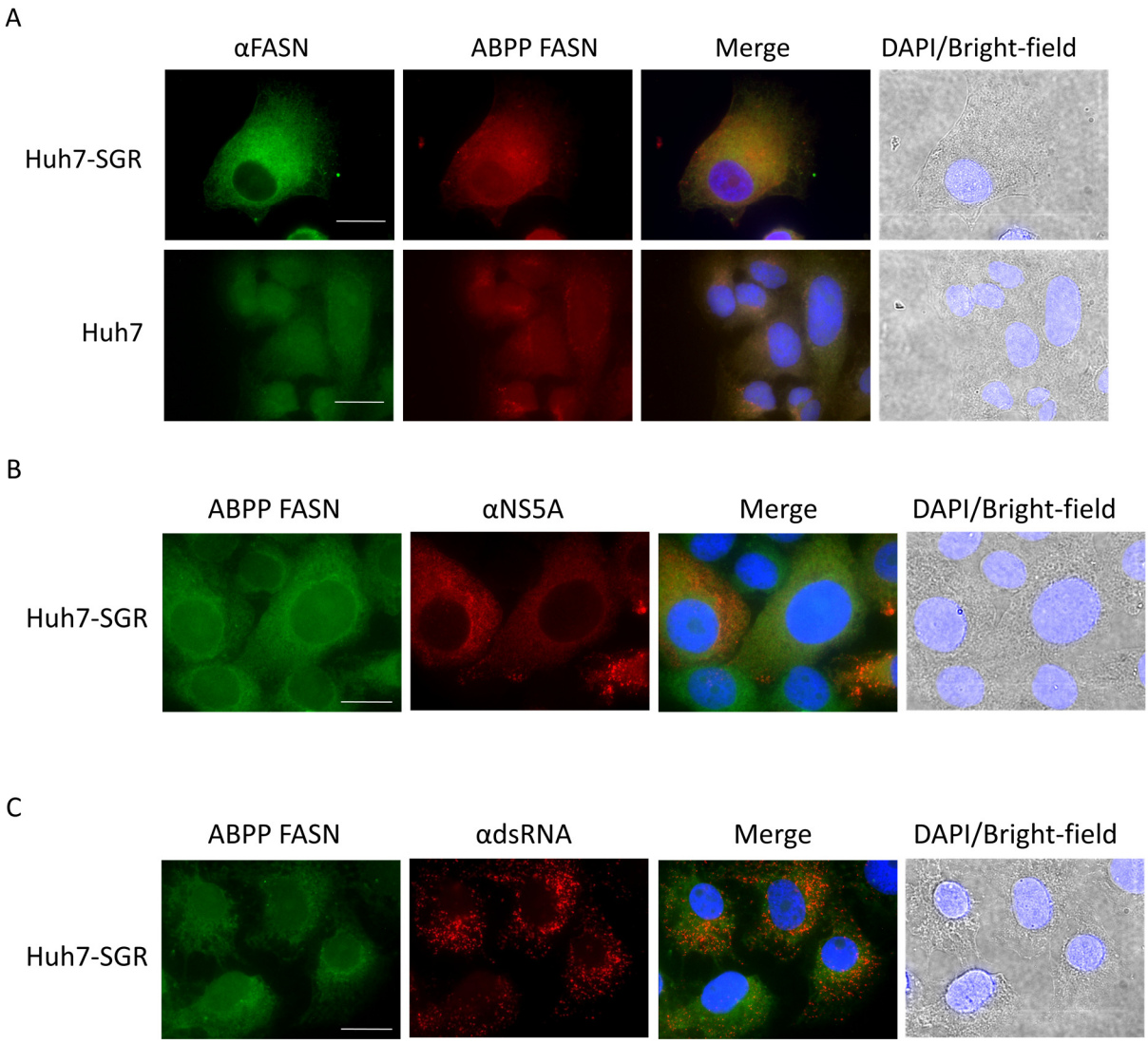

Figure 4-10. Active FASN is not recruited to sites of HCV replication. (A) Huh7 cells and Huh7 cells harbouring subgenomic HCV replicon (Huh7-SGR) were treated with Orlistat-based probe fixed and clicked with Rhodamine azide (ABPP FASN), followed by immunostaining against total FASN (α-FASN) (B) Huh7 cells harbouring subgenomic HCV replicon were probed against active FASN (ABPP FASN) and HCV NS5A (α-NS5A) or (C) dsRNA (α-dsRNA). The images are representative of 4 independent immunostaining experiments.

A

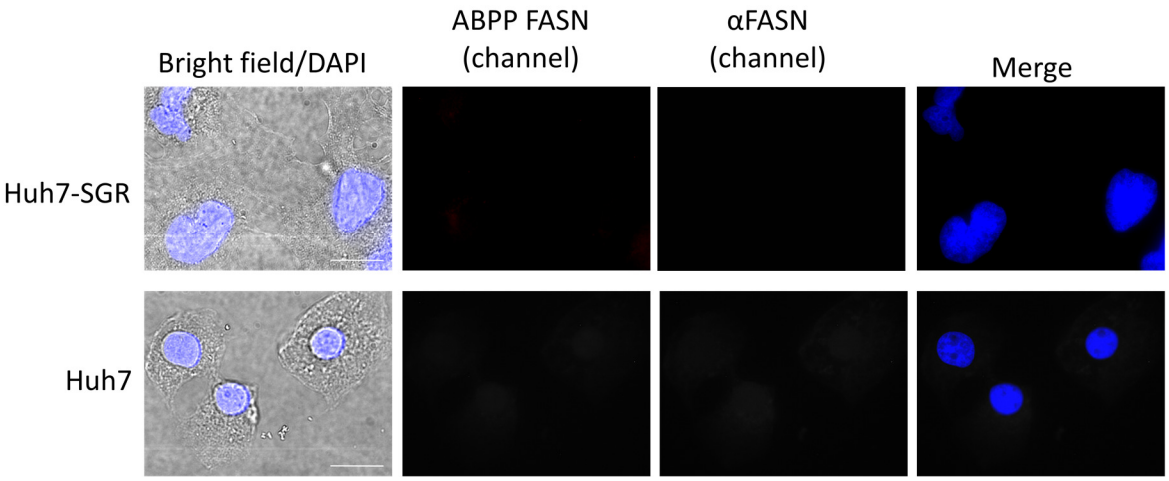

B

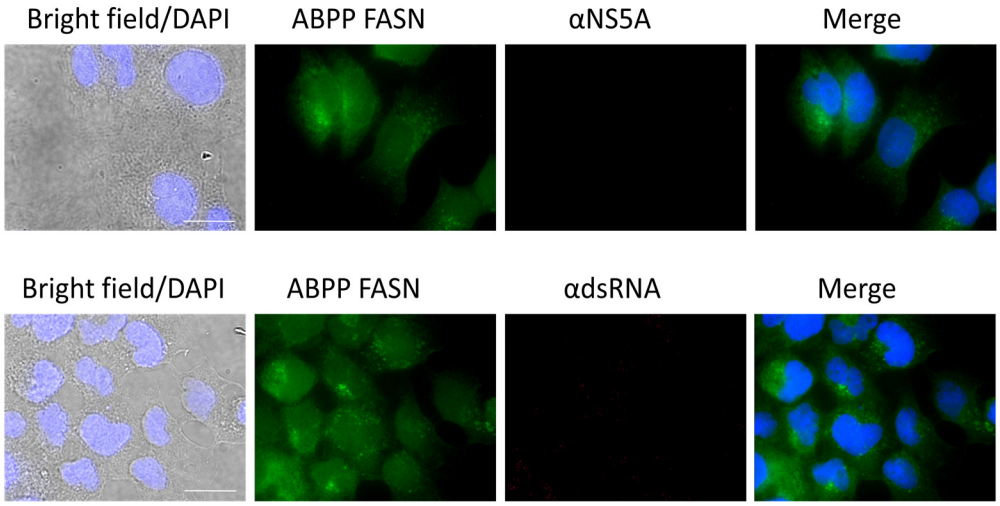

Figure 4-11. Fluorescent analyses of the background (A) Huh7 cells Huh7-SGR cells were fixed and treated with click mix only (no probe, no antibody) followed by washes and DAPI staining. The cells were then imaged by ABPP FASN channel (Rhodamine), and anti-FASN channel (Cy2). (B) Imaging active FASN, NS5A and dsRNA in Huh7 cells. (Scale bar: 10 µm). The images are representative of 4 independent immunostaining experiments.

are 0.97 ± 0.01 and 0.61 ± 0.18, respectively and for ABPP FASN and dsRNA are 0.97± 0.015 and 0.63 ± 0.08. These results indicate that the overlap between signals from active FASN and NS5A or dsRNA do not represent a true colocalization, and can be explained by the drastic increase in the levels of FASN throughout the cytoplasm during HCV replication, which leads to a coincidental overlap between HCV replication complexes that are also localize in the cytoplasm. Based on these results, we propose that the drastic increase in the activity and abundance of FASN during HCV replication leads to production of substantial amounts of fatty acids, and therefore HCV does not require the recruitment of FASN to the sites of active viral replication.

4.4.6 Developing a Quantitative ABPP Method; Combining Dimethyl Labeling with ABPPs

In order to accurately quantify the differential enzyme activity in various samples including clinical isolates, I developed a novel technique for quantitative ABPP, in which ABPP is combined with stable isotope dimethyl labeling (DML) that allows for introducing 'light', 'medium' and 'heavy' labels with stable isotope by reductive amination of primary amines at the N termini of every peptide as well as ε-position of lysine residues using formaldehyde (44). In this technique, the activity-labeled enzymes are captured through affinity purification, digested by trypsin and go under stable isotope dimethyl labeling, followed by mass spectrometry analyses. This method is efficient (all peptides are labeled), simple and potentially high-throughput, as there is no need for protein purification. Moreover, this technique is robust since it can be applied to virtually all types of protein specimens ranging from clinical samples to cell culture lysates, and provide insight into differential enzymatic activity during any pathological state, such as HCV infection.

In order to investigate HCV's influence on FASN activity in a more physiologically relevant model, I decided to examine the increase in the activity of FASN in human serum differentiated Huh7.5 cells (HS-Huh7.5) (385) infected with $JFH1_T$. It has already been demonstrated that treatment of Huh7.5 cells with media supplemented with 2% human serum (HS) over a period of 21 days leads to differentiation of Huh7.5 cells and dramatically promotes HCV infection (385). HS-Huh7.5 cells demonstrate growth arrest, contact inhibition, have a hepatocyte-like morphology, and express hepatocyte differentiation markers (385). Furthermore, these cells have increased lipid droplet content and are therefore more similar to primary hepatocytes (373, 385), without exhibiting the disadvantages of working with primary hepatocytes (25, 322). For this purpose, the proteome from infected and uninfected HS-Huh7.5 cells were labeled with the orlistat probe and clicked with biotin azide for subsequent affinity pull-down. To ensure the accuracy of the quantification, the experiment was performed in reciprocal sets; in one set the peptides from naïve HS-Huh7.5 cells were labeled with light formaldehyde and the JFH-1 infected HS-Huh7.5 peptides were labeled with medium formaldehyde; in the reverse set the peptides from naïve HS-Huh7.5 cells were labeled with medium formaldehyde and the JFH-1 infected HS-Huh7.5 peptides were labeled with light formaldehyde (Figure 4-12). The peptides were then mixed in 1:1 ratio and analyzed by LC-MS/MS. In this setting, the activity of FASN showed an increase of 90% in infected HS-Huh7.5 cells and this increase was consistent in both sets of the experiment. Interestingly, the FASN demonstrated higher activity during JFH-1 infection compared with Con1 replication (HCV-FGR) (90% versus 75%). This finding is in accordance with previous studies that cellular steatosis and FASN expression is higher during JFH-1 infection compared with Con1 replication (271, 451). To date, this is the first application of quantitative ABPP in virology.

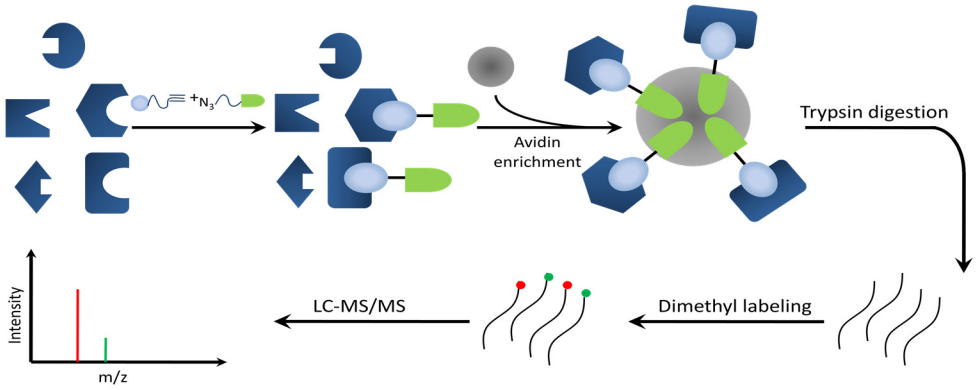

Figure 4-12. Quantitative ABPP by combining activity-based pull-down and dimethyl labeling. Subsequent to trypsin digestion, peptides are labeled with light, medium, or heavy formaldehyde. Peptides are then mixed in 1:1 ratio and analyzed my LC-MS/MS.

4.5 Discussion

FASN abundance and *de novo* fatty acid synthesis are frequently deregulated in a wide range of human cancers, metabolic diseases, and viral infections (264, 265, 288), indicating the importance of targeting this enzyme for therapeutic purposes. While previous studies have demonstrated that FASN is indispensible for HCV replication, and also that FASN abundance increases during HCV replication (113, 295, 388, 451), changes in FASN enzymatic activity and localization related to HCV propagation is not well understood. Herein I presented the first study of the changes in enzymatic activity of FASN during HCV replication, using activity-based protein profiling and activity-based imaging techniques.

Orlistat inhibits the activity of FASN by making an irreversible covalent bond to the active serine of the carboxy-terminal thioesterase domain of FASN (463). The TE domain is important because it determines the length of the fatty acyl chain by controlling its release from the enzyme complex (463). Therefore the TE domain plays a critical role in the terminal end of fatty acid biosynthesis, and using an ABPP probe to report on its catalytic activity would provide an insight into the overall activity of FASN. Consequently the orlistat-based probe was utilized to investigate the alterations in the activity of FASN during HCV replication.

Our results from ABPP studies both in cells expressing HCV proteins and in model systems for HCV propagation confirm the previous findings that HCV infection upregulates FASN expression at both transcriptional and proteins levels, and also demonstrate that the increase in FASN abundance during HCV replication, leads to an increase in the overall FASN catalytic activity (Figure 4-5B-C). Importantly, the effect of HCV replication on the expression and activity of FASN was observed in both cell models harboring genotype 1b replicon as well as chimeric SCID/Alb-uPA mice containing human hepatocytes infected with HCV genotype 1a, in

addition to JFH-1 (genotype 2a) infected HS-Huh7.5 cells. These observations demonstrate that the modulation of FASN by HCV occurs in different model systems and appears to occur with different subtypes of HCV. Moreover, these results show that elevated FASN activity during HCV replication leads to an increase in cellular TG content, although the FASN activity and cellular TG levels are more highly correlated in the case of core and NS4B as compared with NS5A. This inconsistency can be explained by the fact that other than becoming TG and being incorporated into lipid droplets, the nascent fatty acids synthesized by increased expression and activity of FASN can have different fates, such as incorporation into membranes and as substrates for enzymes that post-translationally lipidate (e.g. palmitoylate) protein targets. For example NS5A expression has been shown to activate phosophatydilinositol 3 kinase (PI3K) and PI4K (387, 410), which in turn induce the synthesis of phosphoinositide 3 and 4 phosphate, respectively. These phosphoinositides are essential for the formation and integrity of ER as well as the HCV-induced membranous web (386, 387, 410).

Previous reports have demonstrated that expression of NS4B alone induces the formation of membranous webs (125, 228), which are specific alterations in the ER membrane that harbor HCV replication complexes. Additionally, it has been shown that NS4B expression activates the SREBP1 pathway that can lead to increased transcription of FASN (24). We observed a robust increase in both FASN activity and TG levels in the presence of NS4B (Figures 4-7 and 4-8), which may reflect the need for lipid components for HCV to induce membrane rearrangements. The expression of core protein has also been associated with increased cellular lipid droplets and activation of the SREBP1 pathway. Consistent with this, these results demonstrated that core protein induces a significant increase in both FASN activity and TG levels. The involvement of NS4B and core in the induction of lipid biosynthesis and accumulation of lipid in hepatocytes

may also contribute to the pathogenesis of liver steatosis in patients with chronic hepatitis C (391). Importantly, I observed higher levels of activity compared to abundance of FASN in the presence of HCV. This could possibly be due to an influence of HCV on the post-translational modifications of FASN that ultimately regulate its conformation and enzymatic activity. Future works will be directed towards understanding the role of HCV replication, and its encoded proteins on post-translational modifications of FASN and other lipogenic enzymes in the liver.

Recent reports have shown that FASN activity is required for other members of *Flaviviridae*, including DENV, WNV, and USUV (140, 256, 314). Interestingly, during the replication of these viruses, the level of FASN abundance does not change, however, its distribution alters to co-localize with replication complexes. In fact, Randall and coworkers demonstrated that NS3 protein of DENV interacts with FASN and recruits it to the replication complexes (140). Therefore, I investigated the possible colocalization of FASN with HCV replication sites by fluorescence microscopy. The imaging results confirm the marked increase in FASN levels during HCV replication. However, in contrast to DENV, our imaging experiments show that FASN is not recruited to HCV replication complex, as its localization remains similar in the absence or presence of the HCV replicon. More in depth analysis of colocalization using image analysis methodologies helped us to address the question of HCV recruitment of FASN to replication sites.

The analysis of colocalization between FASN and NS5A or dsRNA, by calculating Mander's coefficient, revealed that there is some overlap between the signals, but since the Pearson coefficient, which is superior to Mander's coefficient in quantifying colocalization (6), is moderate for both sets of studies, it can be concluded that the overlap between FASN and NS5A or dsRNA is likely to be coincidental (Figures 4-9 and 4-10). Interestingly, a parallel study by

Huang and coworkers reported that HCV NS5B interacts with FASN, as deduced by immunoprecipitation, and this interaction appears to increase the RNA-dependent RNA polymerase (RdRp) activity (156). Herein I detected only a partial colocalization of FASN with HCV replication complex, which could still interact with NS5B, and enhance its RdRp activity. However, our study suggests that any interaction of NS5B (or other HCV proteins) with FASN is not sufficient to drastically alter FASN localization within the cell.

Next, I analyzed whether HCV alters the distribution of active FASN, using ABPP imaging to visualize the localization of active FASN during HCV replication. The results demonstrate that the ABPP-labeled FASN highly colocalizes with the antibody-labeled FASN, which confirms the specificity of ABPP imaging (Figure 4-10). Colocalization analyses based on Mander's coefficients (6) indicate that there is no significant colocalization between active FASN and either NS5A or dsRNA. Colocalization studies also confirm that active FASN is not recruited to the sites of HCV replication. However, the level of active FASN is considerably increased in Huh7-SGR cells and therefore there is some overlap between the signals from active FASN and NS5A or dsRNA, but these signals are not completely codependent. Consequently, we propose that the increases in FASN abundance and activity during HCV replication provides ample amounts of fatty acids and neutral lipids required for proper replication of the virus, and therefore there is no need for direct interaction and colocalization of FASN with the replication complex.

Lastly, I developed a quantitative method for examining the activity of FASN during HCV infection. This method combines activity-based pull-down with dimethyl labeling and because of its efficiency and simplicity; it can be applied for relative quantification of target enzymes in any protein sample. Consequently the qABPP platform facilitates quantitative comparison between

different biological states (e.g. virus infected versus uninfected) or treatments (e.g. various concentrations of an inhibitor or a drug). Importantly, the result of dimethyl labeling with orlistat probe is in accordance with former ABPP data that FASN activity increases dramatically during HCV infection, and is consistent between the reciprocal sets of the experiment.

In summary, this work demonstrated the application of ABPP to study the HCV-induced changes in the enzymatic activity of FASN. I showed that FASN expression is not only robustly induced during HCV replication, but this is commensurate with a significant increase in FASN catalytic activity. I also demonstrated that individual proteins such as core and NS4B are sufficient to induce FASN activity on their own and this increase in activity is correlated with increases in triglyceride neutral lipid products. Finally, fluorescence microscopy analyses show that colocalization of FASN with the replication complexes is not required for HCV propagation, unlike other flaviviruses. These results also highlight the potential for activity profiles of enzymes such as FASN to be considered as prognostic markers of HCV infection.

Chapter 5: Beta-Lactam-Derived Activity-Based Probes for Profiling Host Enzymatic Activity during HCV Replication

Statement of Contributions

The content of this chapter has been published in the journal Chembiochem (284) and permissions have been aquired for reusing the materials and figures in this thesis.

I helped to design all of the experiments in this chapter. I performed the majority of the experiments and analyzed the data along with my supervisor. I also wrote the drafts of the manuscript. β-Lactam probes have been synthesized by Dr. Craig McKay, and masspectrometry was carried out in the laboratory of Dr. Sue Twine.

5.1 Introduction

Due to both their biological activity and utility as therapeutic interventions, β-lactams represent one of the best known classes of biomolecular substrates.The β-lactam containing compounds, such as penicillin, are a commonly used class of antibiotics against bacterial infections. It has been demonstrated that β-lactams inhibit bacterial growth by targeting the penicillin binding proteins (PBPs), which are required for bacterial cell wall biosynthesis (247). The powerful antibiotic activities of β-lactams stem from their reaction with a catalytically active serine residue in bacterial trans-peptidases and carboxy-peptidases via a nucleophilic ring opening reaction of the β-lactam. β-lactam containing activity-based probes as well as other scaffolds have been used recently to study bacterial virulence and host responses (327). Elegant work by Sieber and Staub has shown that β-lactam analogues, both natural and synthetic, can be converted into activity-based probes and applied for comparative *in situ* profiling of prokaryotic proteomes to identify other enzymatic targets as well as determining bacterial sensitivity towards antibiotics. Interestingly, these studies demonstrated that in addition to PBPs, a broad range of bacterial enzymes, which contain a nucleophilic residue in their active pockets, can be targeted

by the electrophilic β-lactam ring (382, 383). Because β-lactam derived activity-based probes target divergent enzyme classes, they are considered as non-directed probes.

Since the former studies with β-lactam derived probes were only carried out on prokaryotic proteomes, the eukarotic targets of these reactive compounds remained unknown (71, 382, 383). This chapter describes the first identification of eukaryotic targets of β-lactam-containing compounds by activity-based protein profiling. Furthermore, I demonstrated that non-directed β-lactam-based activity probes can be applied to identify differentially active enzymes in different cell lines and during HCV replication.

5.1.1 Application of Non-directed Activity-Based Probes in Examination of Host-Pathogen Interactions

Non-directed probes have been applied to broaden the activity-based profiling of host enzymes families that could be involved in viral replication and infection. For example, a non-directed sulfonate ester probe has been employed to identify several differentially active proteins during viral replication that encompass many enzyme families (29, 372). These differential activities, which are likely attributed to post-translational modifications or cofactor/inhibitor association, would have been undetected by other conventional proteomic techniques. The identification of these non-directed ABPP targets suggests that both directed and non-directed ABPP methods can accelerate the discovery of protein activities associated with the pathogenic states of viral infections.

5.1.2 β-lactam Moiety for ABPP

Aside from potent antibiotic activity, β-lactams have other therapeutic applications, including inhibition of cholesterol absorption (389), inhibition of important viral proteases such as human

cytomegalovirus protease, as well as inhibition of bacterial β-lactamases (353), prostate-specific antigen (375), thrombin, chymases and elastases (8). Therefore, β-lactam activity-based probes originating from several known antibiotics as well as synthetic analogs have been employed to provide insight into the target preferences of these versatile scaffolds (382, 383, 464). For example Staub and Sieber employed a series of alkyne tagged β-lactam probes, including drug scaffolds as wells as synthetic monocyclic β-lactam probes to target several high and low molecular weight PBPs. Interestingly, the synthetic monocyclic β-lactam probes also had preference for other enzymes such as β-ketoacyl acyl carrier protein III (KAS III), β-lactamase, lipase acylhydrolase, alkyl hydroperoxide reductase, and the virulence-associated protein ClpP (383).

In a following study, Sieber and colleagues were able to identify five unique resistance associated enzymes by applying the monocyclic β-lactam probes to perform *in situ* comparative profiling of antibiotic-sensitive and multi-resistant *Staphylococcus aureus* strains (MRSA) (382). Therefore the synthetic β-lactam probes provided useful tools to not only monitor the activity of bacterial enzymes, but also to unravel the functions of yet uncharacterized MRSA specific enzymes with a potential for therapeutic intervention (382).

5.2 Rationale

Although many of the common antibiotics contain a β-lactam moiety, their eukaryotic targets are not known. It is expected however that they make enzyme adducts by reacting to the active residues of many enzyme families. Therefore they can be suitable non-directed activity probes to report on the activity of various enzyme classes and be applied in diverse comparative ABPP experiments.

5.3 Hypothesis

β-lactam derived activity-based probes can be utilized to profile the alterations in the activity of cellular enzymes during a disease state such as HCV infection.

5.4 Results

5.4.1 Design of Novel β-lactam Activity-Based Probes

To expand the scope of enzymes targeted by β-lactams, and to examine the role of hydrophobicity in directing β-lactam containing probes towards different enzyme classes, I employed novel monocyclic triaryl β-lactam probes that we call *cis*- and *trans*-monocyclic β-lactam alkyne probes (Scheme 5-1, **3a** and **3b**) and compare their target enzymes with a more traditional hydrophilic antibiotic, the bicyclic ampicillin-based alkyne probe AmpN, (Scheme 5-1, **4**). It was expected that the novel monocyclic probes can be accessed in hydrophobic microenvironments, such as intracellular membranes and organelles.

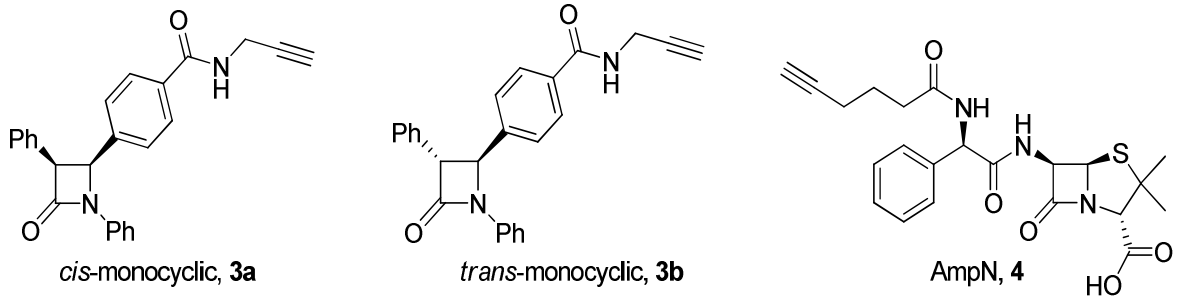

Scheme 5-1. Structures of monocyclic and bicyclic β-lactam probes.

5.4.2 Characterizing the Eukaryotic Targets of β-lactam Probes

Since β-lactam antibiotics are eventually taken up and metabolized by hepatocytes (406, 407), I decided to investigate their targets in human hepatoma cells (Huh7). For this purpose, freshly isolated Huh7 proteome was treated with β-lactam probes (**3a**, **3b**, and **4**) at various concentrations to identify the optimal labeling conditions and clicked with rhodamine azide, via copper(I)-catalyzed azide-alkyne cycloaddition (101). The optimal labeling condition for all the probes was observed to be 10 μM for 1 h at room temperature. Under these conditions, the heat denatured proteome revealed minimal non-specific reactivity, while displaying maximal specific proteome labeling as observed by in-gel fluorescence (Figure 5-1). Interestingly, the monocyclic and bicyclic β-lactam probes showed unique fluorescence labeling profile, when compared with each other and two other established activity-based probes, fluorophosphonate, known to target serine hydrolases (235), and an orlistat-based probe against fatty acid synthase and thioesterases (448) (Figure 5-1 and Figure 5-2).

To identify the enzymes labeled by the β-lactam probes, we adopted two approaches, which allowed for detection of maximum number of targets (Figure 5-3); first the combination of fluorescence 2D-gel electrophoresis (2D-GE) and tandem mass spectrometry was used (372), then target identification was further complemented by applying a gel-free method, which involves streptavidin-enrichment of the labeled Huh7 proteome samples, followed by on-bead trypsin digestion and analysis of the peptides by LC-MS/MS (380). In the first method, the fluorescently labeled proteins were separated by 2D-GE, scanned, silver stained (Figure 5-3 and 5-4 A, B), the fluorescent gel image was then aligned with the silver stained gel image to locate

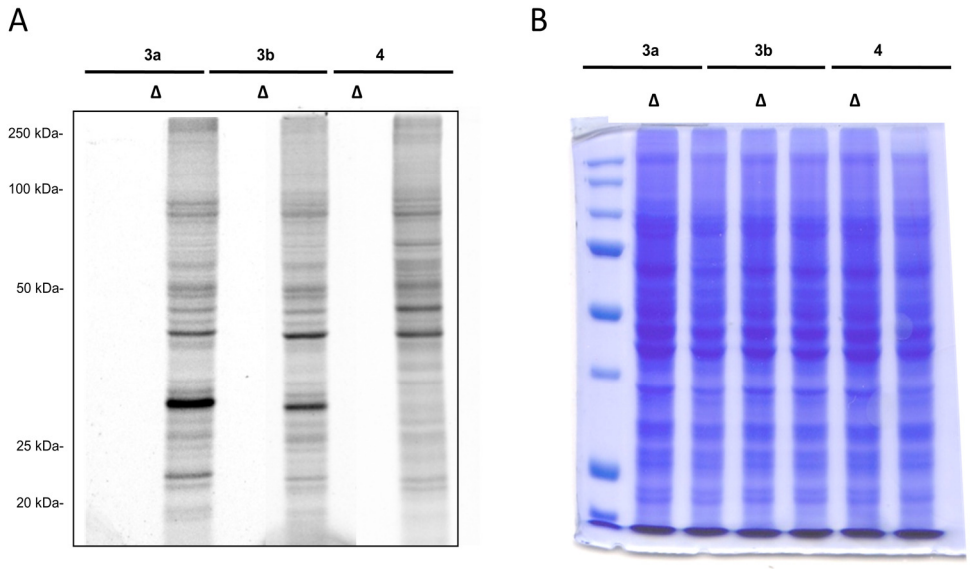

Figure 5-1. Active proteomes isolated from Huh7 cells were treated with the β-lactam probes with or without a denaturing preheating step (Δ = 95°C, 10 min), subjected to click chemistry with RhN_3, separated by SDS-PAGE electrophoresis. (A) In-gel fluorescence scanning (fluorescent gel is shown in gray scale). (B) Subsequently the gel was stained with coomassie blue to ensure equal loading.

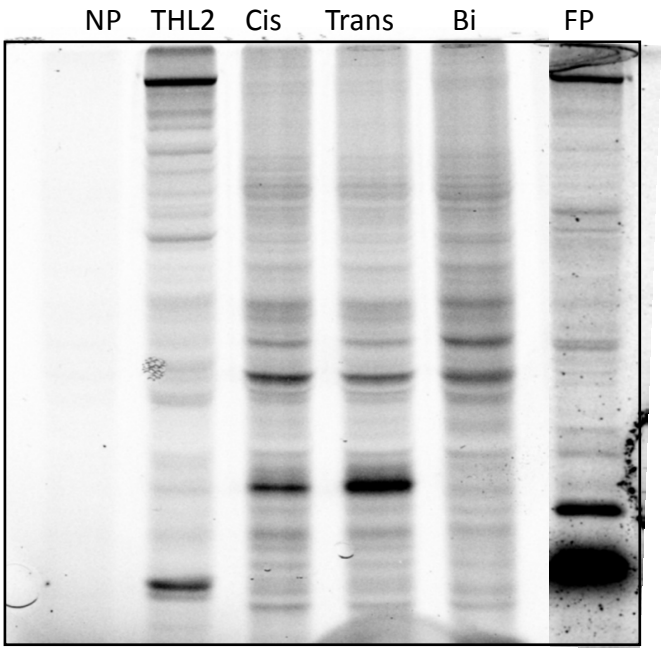

Figure 5-2. Active Huh7 proteome is mock labeled (NP) or labeled with the orlistat-based probes (THL2), β-lactam probes (monocyclic cis 3a, trans 3b, and bicyclic 4), followed by click chemistry with RhN3, also compared with labeling with fluorophosphonate (FP) azide which is conjugated to Alexa 488-alkyne through click chemistry.

the labeled protein spots that were subsequently subjected to in-gel trypsin digestion and protein identification using nano LC-MS/MS analyses. Proteins identified from heat-sensitive spots, which had Mascot scores higher than 30, and were reproducible in two independent experiments, were considered as candidates of the probe targets (Table 5-1). It is noteworthy that a number of enzymes, such as glutathione S-transferase, proteasome subunit β, and protein disulfide-isomerase, were targeted by all three probes, while there are several enzymes that were specifically labeled by only one probe.

Although a considerable fraction of the proteome can be analyzed with 2D-GE MS methods, many classes of proteins remain unidentified, including very large/small, highly basic/acidic, hydrophobic, membrane, and low abundance proteins. In an effort to further validate the MS results, and identify other protein targets of the probes, we performed a gel-free method, which involves streptavidin-enrichment of the labeled Huh7 proteome samples, followed by on-bead trypsin digestion (OBD) and analysis of the peptides by LC-MS/MS (Figure 5-3). Besides the enzymes identified by 2D-GE, many other less abundant target enzymes were detected by the gel-free method (Table 5-1). Analyses of the active sites of the identified enzymes showed that a broad range of enzymes, containing different amino acids in their active sites (serine, cysteine, glutamic acid, and lysine) were targeted by the β-lactam probes (all the 6 enzyme classes were labeled by these probes) (Table 5-1). This reveals the versatility of the β-lactam reactive group in labeling a variety of catalytic residues in mechanistically distinct enzymes. For example, protein disulfide isomerases possesses a catalytic cysteine residue (325) whereas glutathione S-transferase (GST) contains serine in its active pocket (362). Meanwhile, ATP synthase subunit beta possesses a catalytically active lysine (51). Importantly, several enzymes with unknown

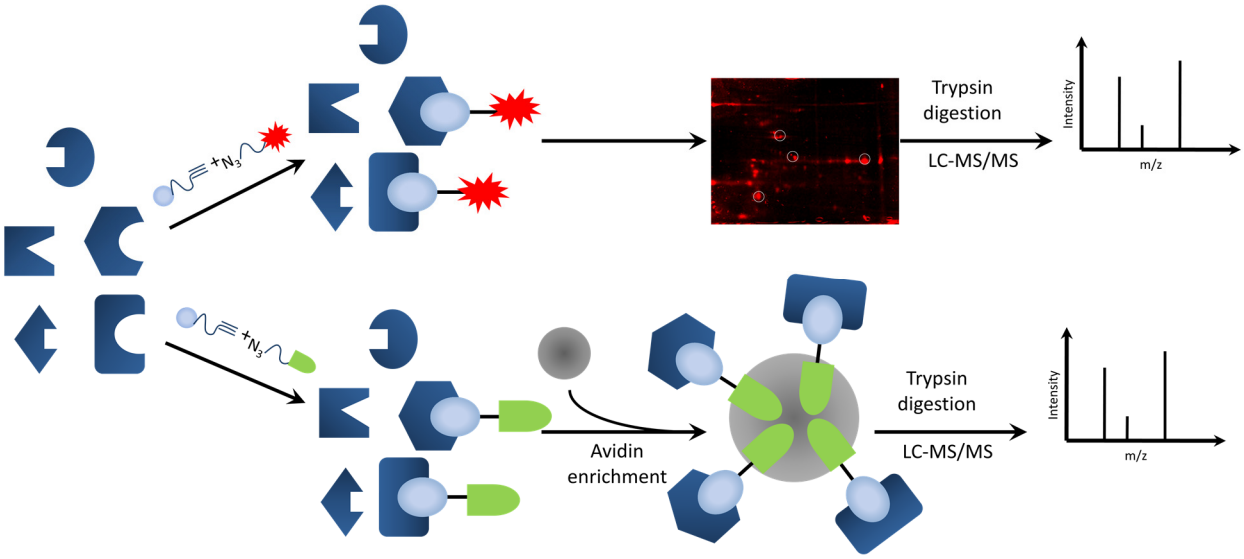

Figure 5-3. Schematic diagram of the methods used to identify the targets of β-lactam probes. In the first approach the proteome is separated by 2D gel and the labeled spots are analyzed by LC-MS/MS. In the gel-free method, the labeled proteome is caputred by avidin enrichment and analyzed by LC-MS/MS.

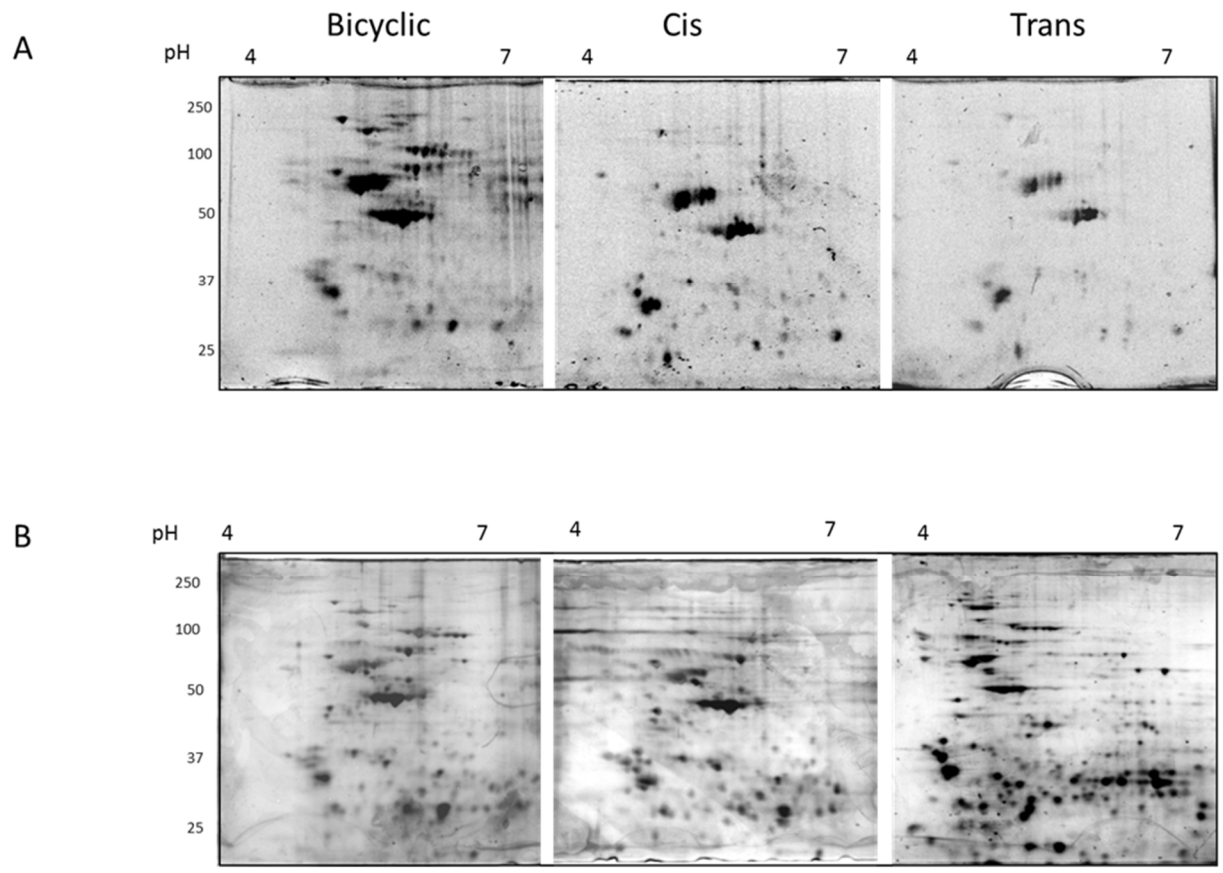

Figure 5-4. Identification of the eukaryotic targets of β-lactam probes. (A) Probe-labeled proteins were visualized by click chemistry conjugation to an azide-rhodamine tag, separated by 2D-GE, and in-gel fluorescence scanning (fluorescent gels are shown in gray scale). (B) Followed by in-gel fluorescent scanning, the 2D-GE gels were silver stained, and the fluorescent gel image was aligned with the silver stained gel image to locate the labeled protein spots.

functions (K1AA) were targeted by these probes, and further ABPP analysis will allow for assigning function to these enzymes. It is also noteworthy that the majority of the targeted enzymes belong to the enzyme classes 1, 2 and 3, therefore, it seems that there is a preference towards targeting, hydrolases, transferases and oxidoreductases, respectively (43). Moreover, as shown in Table 5-1, the number of enzymes targeted by the bicyclic β-lactam probe was higher compared with monocyclic probes. This can be explained by lower intrinsic reactivity of the monocyclic compounds compared with the constrained bicyclic compounds (383).

5.4.3 Application of β-lactam Probes in Comparative ABPP

5.4.3.1 Identification of Differentially Active Enzymes during HCV Replication Using β-lactam Probes

Due to the broad spectrum of targets, we hypothesized that β-lactam probes can be used as helpful tools for investigating the alterations in the cellular enzymes during a disease state, such as viral or bacterial infections and other physiological alterations. The strategy of using non-directed probes has been employed in a number of examples to study diverse patterns of protein reactivity, as well as profiling differentially active host enzymes during viral replication (3, 372). Therefore we decided to examine the applicability of the β-lactam probes in identification of differentially active enzymes, which can potentially be recognized as disease-associated biomarkers, during HCV replication.

For this purpose, I performed ABPP on naïve Huh7 cells and Huh7 cells harboring hepatitis C virus full-genomic replicon (HCV-FGR) (Figure 5-5). Moreover, in order to test the membrane

Table 5-1. Enzymes targeted by the β-lactam probes and identified by either 2D-gel electrophoresis (2D-GE), or on-bead digestion (OBD)

Target enzyme	Enzyme class [a]	Probe	Method [b]
Prostaglandin reductase 1	1.3.1.48	**3a**	OBD
Eukaryotic translation initiation factor 6	3.6.5.3	**3a**	2D-GE, OBD
Acetyl-CoA carboxylase 1	6.4.1.2	**3a**	OBD
Glucosidase II subunit beta	3.2.1.21	**3b**	2D-GE, OBD
NADH dehydrogenase flavoprotein 2	1.6.5.2	**3a-b**	2D-GE, OBD
Gamma-glutamylcyclotransferase	2.3.2.4	**3a-b**	2D-GE, OBD
Human 8-oxoguanine glycosylase	3.2.2.	**3a-b**	OBD
Cysteine protease ATG4A	3.4.22	**3a-b**	OBD
Inorganic pyrophosphatase	3.6.1.1	**3a-b**	2D-GE, OBD
ATP synthase subunit beta	3.6.3.14	**3a-b**	2D-GE, OBD
Inosine triphosphate pyrophosphatase	3.6.1.19	**3a-b**	2D-GE, OBD
Human glyoxalase I	4.4.1.5	**3a-b**	2D-GE, OBD
Methylcrotonoyl-CoA carboxylase subunit alpha, mitochondrial	6.4.1.4	**3a-b**	OBD
L-lactate dehydrogenase	1.1.1.27	**3a, 4**	OBD
Triosephosphate isomerase isoform 2	5.3.1.1	**3b, 4**	OBD
Retinal dehydrogenase 1	1.2.1.36	**3a-b, 4**	OBD
Thioredoxin-dependent peroxide reductase	1.11.1.15	**3a-b, 4**	2D-GE, OBD
Hydroxymethylglutaryl-CoA synthase	2.3.3.10	**3a-b, 4**	2D-GE, OBD
Glutathione S-transferase	2.5.1.18	**3a-b, 4**	2D-GE, OBD
Proteasome subunit beta type-4	3.4.25.1	**3a-b, 4**	2D-GE, OBD
Proteasome subunit alpha type-5	3.4.25.1	**3a-b, 4**	2D-GE, OBD
Ras-related protein Rab-1B	3.6.5.2	**3a-b, 4**	2D-GE, OBD
Protein disulfide-isomerase	5.3.4.1	**3a-b, 4**	2D-GE, OBD
Pyruvate carboxylase, mitochondrial	6.4.1.1	**3a-b, 4**	OBD
ADP-ribosylation GTPase-activating protein 1 (K1AA)		**3a-b, 4**	2D-GE, OBD
Isocitrate dehydrogenase [NADP] cytoplasmic	1.1.1.42	**4**	OBD
Phosphogluconate dehydrogenase, decarboxylating	1.1.1.44	**4**	OBD
D-3-phosphoglycerate dehydrogenase	1.1.1.95	**4**	OBD
Glyceraldehyde-3-phosphate dehydrogenase	1.2.1.12	**4**	OBD
Formyltetrahydrofolate dehydrogenase	1.5.1.6	**4**	OBD
Prolyl 3-hydroxylase 1	1.14.11.7	**4**	2D-GE, OBD
Phosphoserine aminotransferase	2.6.1.52	**4**	OBD
Pyruvate kinase	2.7.1.40	**4**	OBD
UMP-CMP kinase isoform a	2.7.4.14	**4**	2D-GE, OBD
Type I inositol-3,4-bisphosphate 4-phosphatase	3.1.3.66	**4**	OBD
Phosphodiesterase 1B	3.1.4.17	**4**	OBD
Ubiquitin carboxyl-terminal hydrolase isoform a	3.4.19.12	**4**	2D-GE, OBD
Fructose-bisphosphate aldolase A	4.1.2.13	**4**	OBD
Gamma-enolase	4.2.1.11	**4**	OBD
Alpha-enolase	4.2.1.11	**4**	2D-GE, OBD
Peptidyl-prolyl cis-trans isomerase	5.2.1.8	**4**	OBD
Ubiquitin-like modifier-activating enzyme 1	6.3.2.19	**4**	2D-GE, OBD

[a] Human proteome organization (HUPO) designation for enzyme class, [b] Two independent methods were used for the identification of the targeted enzymes

permeability of β-lactam probes, as well as identification of their targets in intact cells, *in situ* labeling experiments were carried out. For this purpose, the probes were added to the cell media and incubated for four hours, subsequent to cell lysis and proteome extraction for the click reaction. The labeled proteins were enriched and identified by OBD method (Figure 5-4). Table 5-2 summarizes the list of enzymes that were uniquely targeted in the absence or presence of HCV replication. Some enzymes that were only identified in HCV-FGR cells have been previously shown to play important roles in HCV replication cycle, such as, protein phosphatase 1B (PPM1B) that is capable of binding and dephosphorylating IFNAR1(IFN-α/β receptor chain 1), which leads to a decrease in the stability of this receptor. IFN-α/β signalling is essential for limiting HCV replication in hepatocytes (116). Therefore, the potential use of PPM1B inhibitors as antiviral drugs have been suggested (58). Moreover, acetyl-CoA carboxylase 2 (ACACB) was only targeted in HCV-FGR cells; there are numerous studies that have shown this lipogenic enzyme plays an essential role in HCV replication, and its expression is increased during HCV infection (217). Finally, Phosphatidylinositol 4-kinase type 2-alpha (PI4K2A) was detected in HCV-FGR cells, and several lines of evidence demonstrate the sites of HCV replication are enriched with phophoinositide 4 phosphate, which is the product of PI4K2A (40).

On the other hand, some enzymes were only identified in naïve Huh7 and not in HCV-FGR cells, interestingly; these enzymes are shown to be down-regulated by the HCV proteins. For example, cyclin-dependent kinase 2 (CDK2), was only targeted in Huh7 cells. It has been reported that HCV core protein reduces the activity of CDK2, which leads to a decrease in the percentage of cells in S-phase along with an accumulation of cells in the G(0)/G(1) phase of the cell cycle (286). Moreover, fructose-bisphosphate aldolase A (ALDOA), was also identified in Huh7 and not in HCV-FGR cells, the expression of this enzyme has already been reported to decrease

during HCV infection (457). Furthermore, tyrosine-protein kinase HCK, which was uniquely detected in Huh7 cells, has been reported to interact with HCV NS5A, and this interaction leads to a decrease in its activity (246). Lastly, down-regulation of denosylhomocysteinase (AHCY) has been associated with liver steatosis, a major complication of HCV infection (60). According to our results, this enzyme has only been detected in the absence of HCV replication, which leads to the assumption that HCV replication reduces the expression and activity of AHCY.

Since we obtained good data for the protein entries as evidenced by Mascot scores and the number of unique peptides matched per protein, we decided to examine the relative quantification of some of the targets that were detected in the presence and absence of the HCV replicon, while there are previous studies to show that their activity or abundance changes during HCV replication. We hypothesized that although the levels of these enzymes alter between the two cell lines, they remain within the detection threshold of nano LC-MS/MS. For this purpose, we applied a label-free approach, based on exponentially modified protein abundance index (emPAI) (163). In this method, protein abundance is measured from the total number of spectral evidences contributing to a given protein identification, and allows for semi-quantitative comparison of the protein abundance.

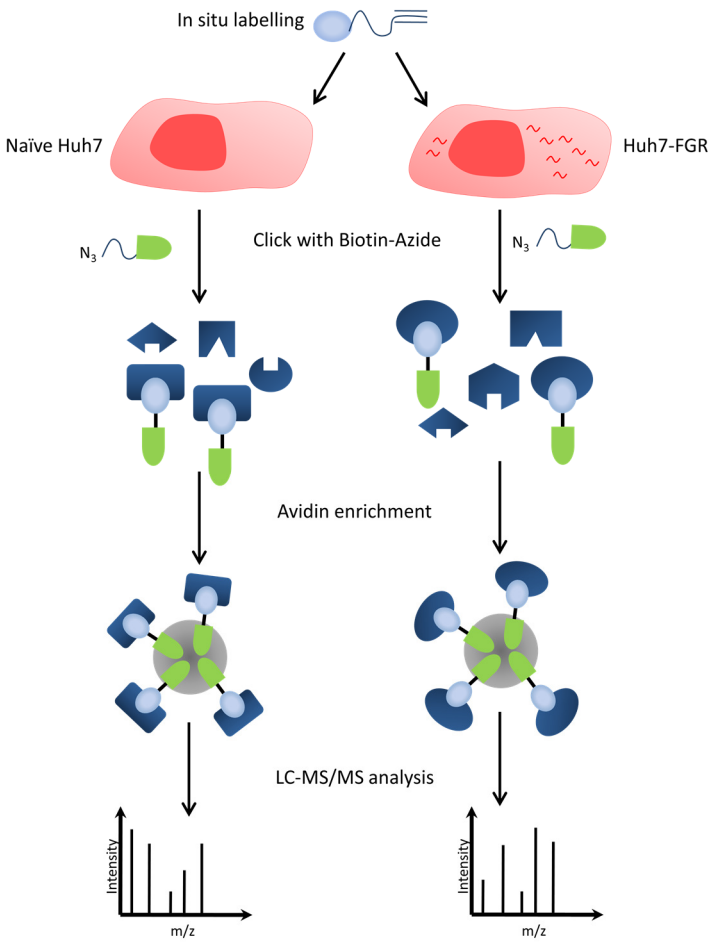

Figure 5-5. Schematic diagram of situ β-lactam labeling for comparative ABPP to identify differentially active enzymes during HCV replication. Labeled enzymes are identified by OBD method and are compared between naive Huh7 and Huh7 cells expressing full-genomic replicon (HCV-FGR).

Table 5-2. Enzymes that are differentially labeled in situ by the β-lactam probes in the presence or absence of HCV replicon and were identified by OBD followed by tandem mass spectrometry

Target enzyme	Enzyme class[a]	Probe	Cell line[b]
Allantoicase	3.5.3.4	**3a**	HCV-FGR
Serine/threonine phosphatase 6	3.1.3.16	**3a**	Huh7
Serine protease 45	3.4.21	**3a**	Huh7
Tyrosine phosphatase F	3.1.3.48	**3a,4**	Huh7
Aspartyl aminopeptidase	3.4.11.21	**3b**	HCV-FGR
Methionine synthase reductase	2.1.1.13	**3b**	Huh7
Protein phosphatase 1B	3.1.3.16	**3b**	HCV-FGR
Phosphotidylinositol 4-kinase type 2α	2.7.1.67	**3a. 3b, 4**	HCV-FGR
Acetyl-CoA caboxylase 2	6.4.1.2	**4**	HCV-FGR
Adenosylhomocysteinase	3.3.1.1	**4**	Huh7
Fructose-4phosphate adolase A	4.1.2.13	**4**	Huh7
Cyclin-dependent kinase 2	2.7.11.22	**4**	Huh7
Tyrosine-protein Kinase HCK	2.7.10.2	**4**	Huh7
Phosphomannomutase 2	5.4.2.8	**4**	Huh7
Triosephosphate isomerase	5.3.1.1	**4**	Huh7

[a] Human proteome organization (HUPO) designation for enzyme class, [b] Huh7: Human hepatoma cells, HCV-FGR: Huh7 cells harbouring HCV full length genomic replicon

Analyses of Mascot and emPAI scores for FASN, alpha-enolase (ENO1) and hydroxymethylglutaryl-CoA synthase (HMGCS1) three of the well-known HCV host factors that were targeted by all three probes in both naïve Huh7 and HCV-FGR cells, revealed that the expression and activity of these enzymes is increased in HCV-FGR cells (Table 5-3). The activity and expression of FASN, the key enzyme in lipogenesis, has been demonstrated to increase during HCV infection (283). Alpha enolase, which is a crucial enzyme in the glycolytic pathway, has been shown to over-express during HCV infection and also its expression is significantly higher in HCV associated hepatocellular carcinoma (396). The expression of HMGCS1 that is involved in both cholesterol synthesis and lipid metabolism pathways is highly activated by HCV replication (183, 328). Consequently, our spectral counting data are consistent with previous findings, and demonstrate that β-lactam probes can also be used for relative quantification of differentially active enzymes during viral replication.

5.3.3.2 Identification of Differentially Active Enzymes in Cells with Different Origins

To further ensure the specificity of the β-lactam probes in targeting the enzymes that are differentially active in different tissues and cell lines, we also performed in situ labeling on human embryonic kidney cells (HEK293), which have a completely different origin from Huh7 cells (Table 5-4). Interestingly, there are a number of enzymes such as alcohol dehydrogenase 7(ADH7), helicase-like transcription factor (HLTF), methionyl aminopeptidase 1(METAP1) and ST3 beta-galactoside alpha-2,3-sialyltransferase 5 (ST3GAL5) that are only targeted in HEK293 cells, and were not detected in Huh7 proteome. According to gene expression profiling databases, these enzymes are expressed at significantly higher levels in HEK293 cells compared with Huh7 cells (442). On the other hand, enzymes such as aldehyde dehydrogenase (ALDH1A),

Table 5-3. Relative quantification of some of the target enzymes that are differentially expressed in the presence of HCV replicon

Target enzyme	Enzyme class	Huh7		HCV-FGR	
		Mascot	emPAI	Mascot	emPAI
Fatty acid Synthase	2.3.1.85	56	0.1	75	0.2
Hydroxy methylglutaryl-Coenzyme A synthase	2.3.3.10	32	0	64	0.2
Alpha enolase	4.2.1.11	170	0.2	184	0.3

FASN, GSTP1, HMGCS1, isocitrate dehydrogenase 1 (IDH1), 8-oxoguanine glycosylase (OGG1), and 6-phosphogluconate (PGD), were only identified in Huh7 (Table 5-4). Gene expression analyses also confirm that these enzymes are expressed at drastically higher levels in Huh7 cells compared with HEK293 cells (442). The expression levels of other enzymes that were detected in both Huh7 and HEK293 cells is at comparable levels between the two cell lines (Table 5-4).

Notably, some of the protein targets were specifically labeled by the novel hydrophobic probes such as NADH dehydrogenase flavoprotein 2, which is a mitochondrial membrane protein involved in the transfer of electrons from NADH to the respiratory chain, human 8-oxoguanine glycosylase that mainly localizes in the nucleus and mitochondria and plays a role in DNA repair (20), as well as formimidoyltransferase-cyclodeaminase that primarily localizes in the Golgi (132). These findings suggest that the hydrophobic β-lactam probes are more membrane permeable compared with the AmpN-based probe, and access the enzymes within cell organelles more efficiently.

5.4 Discussion

In this chapter, I demonstrated the application of non-directed β-lactam derived probes to selectively target a broad range of enzyme families that show differential activity in different cell lines and during HCV replication. Herein, three β-lactam probes were examined that can be used for global and comparative profiling of the eukaryotic enzyme activity both *in vitro* and *in situ*. This work characterizes the eukaryotic targets of simple β-lactam probes of different structure and hydrophobicity. These results also demonstrated that while gel-based profiling identified a number of eukaryotic targets for the probes, the gel-free method allowed for identification of less abundant enzymes from diverse enzyme families. Differential labeling further confirms the

utility of these chemotypes in targeting different subsets of the proteome, with active site specificity and coverage of different enzyme classes. I have also demonstrated that the non-directed β-lactam probes can be applied to identify the differentially active enzymes in different cell lines and during HCV replication that can be associated with disease progression, with potential diagnostic and prognostic significance.

The β-lactam probes were also able to target a number of cysteine, serine, and threonine hydrolases that have been shown to be targeted by the β-lactone moiety as well. This finding demonstrates that β-lactones and β-lactams share similar preference for the nucleophilic residues of these enzyme categories.

In conclusion, side-chain-modified β-lactams represent promising structures for the design of novel activity-based probes, which can be utilized for screening enzyme activity of different eukaryotic and prokaryotic proteomes. I was able to identify a variety of mechanistically distinct target enzymes that show sensitive labeling by each of these probe molecules, and demonstrated that this approach is applicable for the identification of differentially active enzymes during various biological processes or disease states.

Table 5-4. Enzymes labeled in situ by the β-lactam probes in Huh7 and HEK293 cells, and were identified by OBD followed by tandem mass spectrometry

Target enzyme	Enzyme class[a]	Probe	Cell line[b]
Alcohol dehydrogenase class 4 mu/sigma chain	1.1.1.1	**3b**	HEK293
Plasma membrane calcium-transporting ATPase 1	3.6.3.8	**4**	HEK293
Helicase-like transcription factor	3.6.4	**4**	HEK293
E3 u4quitin-protein ligase RNF144B	6.3.2	**4**	HEK293
Lactosylceramide alpha-2,3-sialyltransferase	2.4.99.9	**4**	HEK293
Aldehyde oxidase	1.2.3.1	**3b**	HEK293
Beta-1,3-galactosyltransferase 1	2.4.1	**4**	HEK293
Formimidoyltransferase-cyclodeaminase	4.3.1.4	**3a**	HEK293
Methionine aminopeptidase 1	3.4.11.18	**3b**	HEK293
Adenosylhomocysteinase	3.3.1.1	**4**	Huh7
Retinal dehydrogenase 1	1.2.1.36	**3a, 3b, 4**	Huh7
Fructose-4sphosphate aldolase A	4.1.2.13	**4**	Huh7
Fatty acid synthase	2.3.1.85	**3a, 3b, 4**	Huh7
Glutathione S-transferase P	2.5.1.18	**3a, 3b, 4**	Huh7
Tyrosine-protein kinase HCK	2.7.10.2	**4**	Huh7
Hydroxymethylglutaryl-CoA synthase	2.3.3.10	**3a, 3b, 4**	Huh7
Isocitrate dehydrogenase [NADP]	1.1.1.42	**4, 3a**	Huh7
8-Oxoguanine glycosylase	3.2.2	**3b**	Huh7
6-phosphogluconate dehydrogenase, decarboxylating	1.1.1.44	**3a, 3b, 4**	Huh7
Phosphomannomutase 2	5.4.2.8	**4**	Huh7
Serine/threonine-protein phosphatase 6	3.1.3.16	**3a**	Huh7
Serine protease 45	3.4.21	**3a**	Huh7
Receptor-type tyrosine-protein phosphatase F	3.1.3.48	**4, 3a**	Huh7
Transitional endoplasmic reticulum ATPase	3.6.4.6	**3a, 3b, 4**	Huh7
Cyclin-dependent kinase 2	2.7.11.22	**4**	Huh7
Chymotrypsin-like elastase family member 1	3.4.21.36	**3b**	Huh7
Alpha-enolase	4.2.1.11	**3a, 3b, 4**	Huh7
Glyceraldehyde-3-phosphate dehydrogenase	1.21.12	**3a, 3b, 4**	Huh7
Methionine synthase	2.1.1.13	**3b**	Huh7
Protein disulfide-isomerase A6	5.3.4.1	**4**	Huh7
1-phosphatidylinositol-3-phosphate 5-kinase	2.7.1.150	**4**	Huh7
Pyruvate kinase isozymes M1/M2	2.7.1.40	**3a, 3b, 4**	Huh7
Triosephosphate isomerase	5.3.1.1	**4**	Huh7
Caspase 3	3.4.22.56	**3a, 3b**	Huh7, HEK293
L-lactate dehydrogenase A chain	1.1.1.27	**3a, 3b, 4**	Huh7, HEK293
Methylcrotonoyl-CoA carboxylase subunit alpha	6.4.1.4	**3a, 3b, 4**	Huh7, HEK293
Pyruvate carboxylase	6.4.1.1	**3a, 3b, 4**	Huh7, HEK293
Propionyl-CoA carboxylase alpha	6.4.1.3	**3a, 3b, 4**	Huh7, HEK293
Proteasome subunit alpha type-4	3.4.25.1	**4, 3b**	Huh7, HEK293

[a] Human proteome organization (HUPO) designation for enzyme class, [b] HEK293: Human embryonic Kidney cells (HEK 293)

Chapter 6: Activity-Based Profiling of Lipid Kinases during HCV Replication

Statement of Contributions

The content of this chapter has been published in the journal Chembiochem (284) and permissions have been aquired for reusing the materials and figures in this thesis.

I helped to design all of the experiments in this chapter, except for the chemical synthesis, which were designed by Dr. Craig McKay. I performed the majority of the experiments and analyzed the data along with my supervisor. I also wrote the drafts of the manuscript. PIK-BPyne has been synthesized by Dr. Craig McKay, and its specificity has been characterized by Dr. Allison Sherratt. Mass spectrometry was carried out in the laboratory of Dr. Daniel Figeys.

6.1 Introduction

RNA viruses that replicate in the cytoplasm have been shown to induce reorganization of the host intracellular membranes to establish sites of replication and assembly (23, 410). The resulting structures provide scaffolds for anchorage of the viral replicase complex, increase local concentration of essential host factors, and shield the virus from the cellular innate immune response (23, 334, 335, 410). Therefore, besides modulation of the host lipid metabolism, HCV causes cellular membrane remodeling to form its replication complexes, and organize its secretion process (140, 141).

Although HCV NS4B protein clearly contributes to the creation of the membrane structures where the replication occurs, there is increasing evidence for the roles of host factors, involved in lipid signaling, in formation of the viral replication complex (RC) (23, 34, 35, 49, 334, 335, 394, 410). These reports have led to a model in which the modulation of these lipid signaling molecules directs cellular membrane trafficking to generate the HCV RC, and coordinates viral secretion (141, 175).

In this chapter, the process of modulation of the activity of phosphoinositide kinases, the key lipid signaling enzymes, by HCV will be discussed. Herein, it will be demonstrated that activity-based protein profiling is a suitable tool to capture the viral-induced alteration in the activity of major lipid signaling enzymes. Importantly, the findings of this chapter aids in understanding the early stages of the viral particle secretion.

6.1.1 Phosphoinositides & Phosphoinositide Kinases

Phosphoinositides (PIs) are membrane phospholipids derived from mono-, di- and tri-phosphorylation of phosphatidylinositol, and regulate essential cellular and intercellular processes (reviewed in (83)). Therefore the spatio-temporal regulation of these molecules, which occurs through phosphorylation/dephosphorylation of the inositol ring, is critical for vital physiological processes including cell proliferation, death, motility, cytoskeletal regulation, intracellular vesicle trafficking and cell metabolism (403). Phosphatidylinositol kinases (PIKs) are responsible for inositol ring phosphorylation and their highly-regulated activities lead to the generation of seven PIs that are concentrated in different subcellular localizations (83). Due to their integral roles in cellular function, PIKs have emerged as important drug targets in therapeutic areas such as cancer, inflammatory disorders, and even host-pathogen interactions (11, 40, 354, 432).

6.1.2 The Role of Phosphoinositide Kinases during HCV Replication

As formerly mentioned, HCV induces the rearrangement of intracellular membranes to form viral replication complexes, called membranous web (MW) (276). These structures are enriched with PI4P; moreover, studies applying genome wide siRNA screens have identified the PI4P pathway to be critical for HCV replication (34, 335, 394, 395). It has been suggested that PI4P may contribute to the curvature or integrity of the MW (10, 93). Also PI4P has been shown to

interact with HCV replicase proteins to stimulate their function and keep them anchored in the MW (335). Alternatively, PI4P may bind to essential host factors through their pleckstrin homology (PH) domains and therefore recruit these factors to the sites of active HCV replication and assembly. In fact several crucial host factors such as oxysterol binding protein (OSBP), ceramide transfer protein (CERT), four-phosphate adaptor proteins 1 and 2 (FAPP1 and FAPP2), and Golgi phosphoprotein 3 (GOLPH3) are thought to be recruited through PI4P binding (40, 427).

Four different PI4Ks that localize to distinct membrane compartments catalyze the production of PI4P from PIs (23, 259).The involvement of PI4KIIIα and PI4KIIIβ in the HCV life cycle has been shown by several studies, however, PI4KIIα and PI4KIIβ are not essential host factors for HCV replication (35, 410). While several studies demonstrated that ER-localized PI4KIIIα provides the PI4P supply for the MW and activates the RdRp of HCV due to its interaction with NS5A(18, 49, 334, 335), there are controversial reports regarding the role of the Golgi-localized PI4KIIIβ in the HCV lifecycle. In fact the role of the Golgi in HCV replication cycle is not clear, although, it is generally believed that the Golgi is involved in particle assembly and packaging. Also, there are several lines of evidence that suggest a genotype-specific dependence for PI4KIIIβ in viral replication (215, 335, 404), whereas others indicate a separate role in viral secretion (summarized in (79)). Moreover, the activity of PI3K has been shown to be essential for HCV replication (40), as HCV infection leads to activation of the PI3K/Akt pathway by various mechanisms (138, 166, 248, 319). PI3K/AKT signalling pathway regulates critical cellular processes such as apoptosis and metabolism, hence its activation leads to increased cell survival, and lipid biosynthesis (99). Consequently activation of this pathway provides a hospitable environment for HCV replication within hepatocytes.

6.1.3 Activity-Based Probes to Profile the Activity of Phosphoinositide Kinases

One method to characterize PIK activity is activity-based protein profiling (ABPP), which involves converting selective small molecule inhibitors into activity-based probes (ABPs), to interrogate the functional state of these kinases. However, the majority of kinase inhibitors bind to the highly conserved kinase ATP-binding site (73, 199), and thus identification of kinase inhibitors that are both potent and selective is a challenging task. Nevertheless ABPP probes based on wortmannin or acyl-ATP/ADP analogues that have a large number of targets have been shown to successfully label PIK enzymes (236, 307, 454). Wortmannin, which is a fungal metabolite derived from *Penicillium wortmannii*, is a strong inhibitor of PI3K and PI3K-related kinases (19, 452), as it can react irreversibly with the critical lysine residue in the active pocket of these enzymes. Wortmannin-based ABP has been shown to be able to dynamically profile the activity changes of a limited set of kinases within the cellular proteome (236, 454). Moreover, wortmannin-based probe has been used to monitor differences in the activation state of its targets under various physiological states, such as drug treatments (454).

Acyl phosphate probes are based on acyl phosphates of ATP or ADP that irreversibly react with protein kinases on conserved lysine residues in the ATP binding pocket. These probes have been successfully applied to profile the activity of at least 75% of the known human protein kinases (307). Moreover, adenosine has been replaced by guanosine to report on the functional states of GTP-dependent proteins (307). Similarly other nuscleosides can replace adenosine to produce a variety of probes that provide insight into the activity of nucleotide binding proteome. However, major drawback of ADP/ATP-based probes is the presence of highly abundant ATP binding proteins such as actin and heat shock proteins that could interfere with kinase detection.

In this chapter, I demonstrate the application of a novel, and more selective probe against lipid kinases, based on PIK-93 inhibitor, to study the activity of PIKs during HCV replication. This probe proved to be a powerful tool for examining the biological activity of selective PIKs and other lipid kinases within their native environment.

6.2 Rationale

PI4KIIIβ is hypothesized as a host factor for HCV infection; however, its role in the HCV life cycle is unclear. Also, the PI3K-AKT pathway is activated by several HCV non-structural proteins. PIK-93 is a reversible lipid kinase inhibitor that specifically reacts with PI4KIIIβ and PI3K. Therefore an activity-based probe based on PIK-93 may provide insight into the alterations in the activity of these enzymes during HCV replication.

6.3 Hypothesis

Activity-based protein profiling may allow for the investigation of the alterations in the activity of phosphoinositide kinases during HCV replication.

6.4 Results

6.4.1 Design of a Novel Activity-based Probe for Profiling the Activity of Lipid Kinases

In order to examine the changes in the activity of lipid kinases during HCV replication, a probe based on the PIK-93 inhibitor was designed and synthesized in our laboratory by Dr. Allison Sherratt and Dr. Craig McKay (199). PIK-93 is a reversible lipid kinase inhibitor that competes for ATP binding interactions (Figure 6-1A) (199). The PIK-93 based probe, PIK-BPyne, (Figure 6-1B) was prepared by adding a photo-crosslinkable group, benzophenone (BP), to a core structure similar to PIK-93 (Figure 6-1 B) (364). Introduction of BP moiety enables covalent modification of the target enzymes (Figure 6-1C). Photo-activatable groups have previously been

exploited in the synthesis of activity-based probes (182, 205, 227, 352, 398) (350, 351). Moreover, the biologically inert alkyne handle was added to facilitate the conjugation of bulky reporter or affinity tags through click chemistry.

To ensure that the PIK-BPyne probe successfully targets PI4K isoforms, as well as PI3K, the specific targets were profiled by performing western blot analysis on the affinity pull-down of the labeled proteomes (Figure 6-2A and 6-2B). For this purpose, human breast cancer (MDA-MB-468), cervical cancer (HeLa), hepatoma (Huh-7), and embryonic kidney (HEK 293T) proteomes were labeled with PIK-BPyne, streptavidin-enriched, then probed for PI3K (catalytic subunit, i.e. 110 KDa) and PI4K (types: IIα, IIIα, IIIβ) to determine differences in kinase activities compared to relative abundances (Figure 6-2B). Most lipid kinases probed using this activity pull-down method revealed differential activity compared to kinase abundance for the cell lines tested (Figure 6-2B). This is evident for the equally abundant PI4K-IIIβ, which appears highly active in HeLa and HEK 293T proteomes, and less active in MDA-MB-468 and Huh7 proteomes, based on PIK-BPyne's ability to compete for ATP binding interactions of this kinase. Furthermore, our group has demonstrated the competitive inhibition of PIK-BPyne labeling with wortmannin (364), suggesting similar targets between PIK-93 and wortmannin. While parallel *in situ* labeling experiments using WM-alkyne, failed to pull-down active PI4K-IIIβ (364), highlighting the specificity of PIK-BPyne toward this lipid kinase.

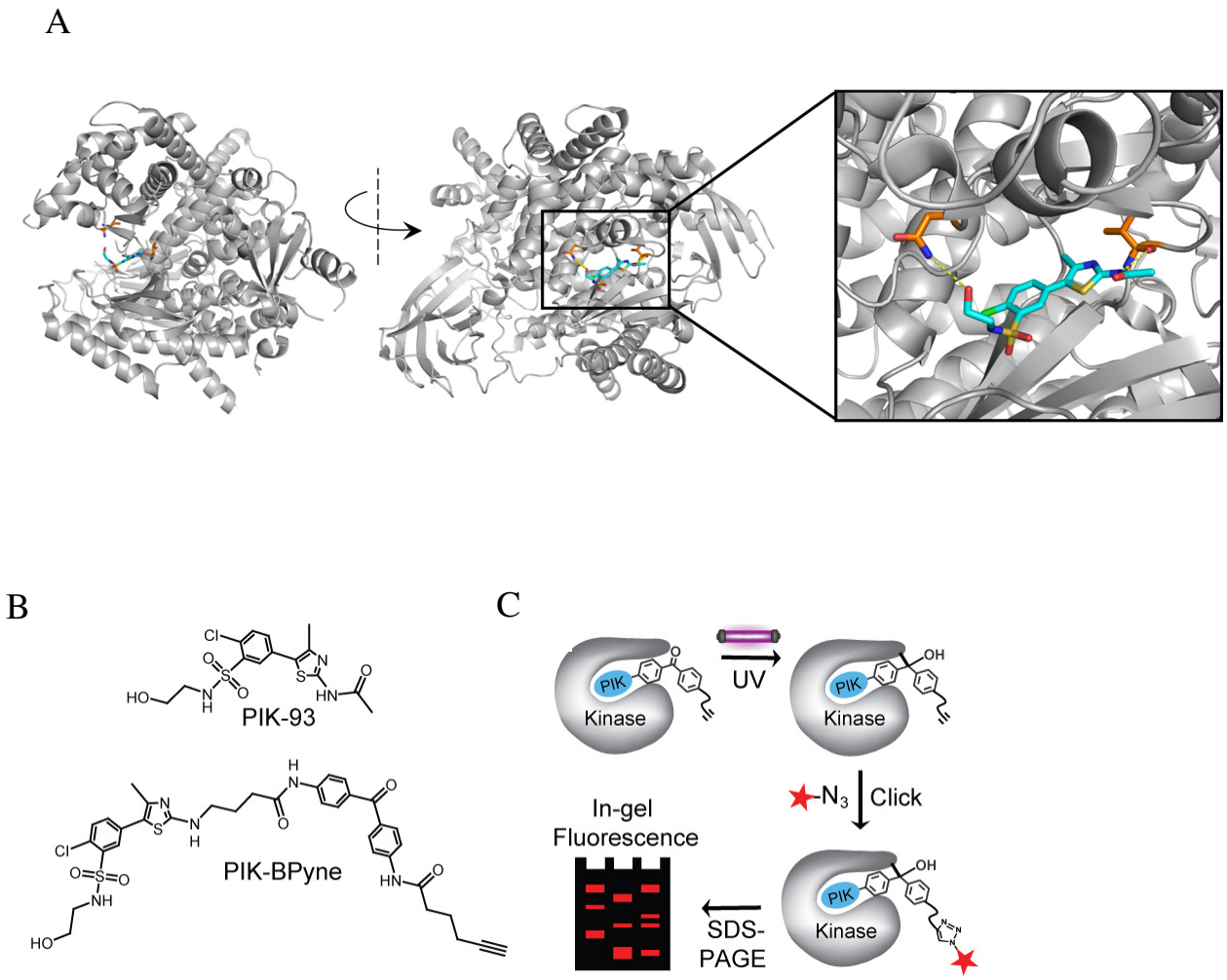

Figure 6-1. Interaction of novel PIK-BPyne probe to the activie site of lipid kinases. A) Crystal structures and model of PIK-93 inhibitor bound to p110 subunit of PI3K (Figure adapted from (198) B) Structures of lipid kinase inhibitor PIK-93 and PIK-BPyne ABP. C) Schematic representation of ABPP with PIK-BPyne. The BP group of PIK-BPyne is photo-activated by irradiation with UV light (365nm) to crosslink with associated protein. An azide-functionalized reporter tag (red star: rhodamine-azide) is then reacted with the alkyne handle of PIK-BPyne by click chemistry to fluorescently identify labeled protein in gel. Click chemistry with an alternate reporter tag, such as biotin-azide, allows for streptavidin-enrichment and analysis of labeled protein.

6.4.2 Investigation of Phosphoinositide4 Kinase III β (PI4K-IIIβ) Expression and Activity during HCV Replication

Having established PIK-BPyne as a useful probe for lipid kinase activity in living cells, I investigated whether this probe could provide insight into the role of PI4KIIIβ in the HCV lifecycle. For this reason, I performed *in situ* PIK-BPyne labeling followed by activity pull-down analysis on naïve Huh7.5 cells versus Huh 7.5 cells stably expressing the non-infectious HCV full-genomic replicon of genotype 1b (FGR, Con1), as well as Huh7.5 cells infected with the HCV infectious model (JFH-1, genotype 2a, 4 days post infection). This set-up allowed me to compare the PI4KIIIβ activity in both genotypes, since siRNA knockdown studies have implicated genotype dependency for PI4KIIIβ (49, 404). As shown in Figure 6-3A, and 6-3B, presence of HCV-FGR induced a 2.7 fold increase in PI4KIIIβ activity, while expression remained unchanged. Importantly, we observed a 2.3 fold increase in the PI4KIIIβ activity during HCV infection, even though the abundance remained unaltered (Figure 6-3). These findings clearly demonstrate that the activity of PI4KIIIβ is not correlated with its expression, and emphasize on the role of post-translational modifications in regulating the activity of this enzyme.

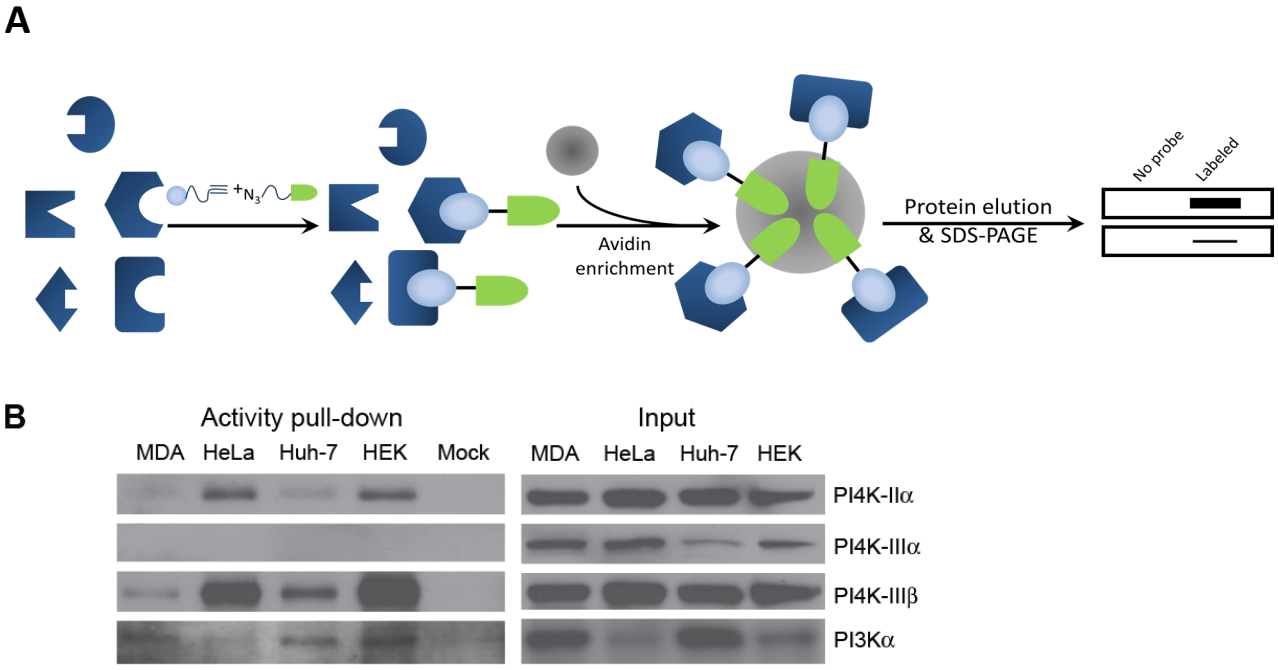

Figure 6-2. Profiling the specific targets of PIK-BPyne probe. A) The labeled enzymes are enriched by streptavidin-coated beads and analyzed by western blot. B) Relative activity and abundance of PI3K and PI4K isoforms in various cell proteomes. Proteome samples (1 mg) of MDA-MB-468 (MDA), HeLa, Huh7 and HEK 293T (HEK) cell lines were labeled with PIK-BPyne, streptavidin-enriched and probed for various isoforms of PI4K and PI3K by western analysis.

.

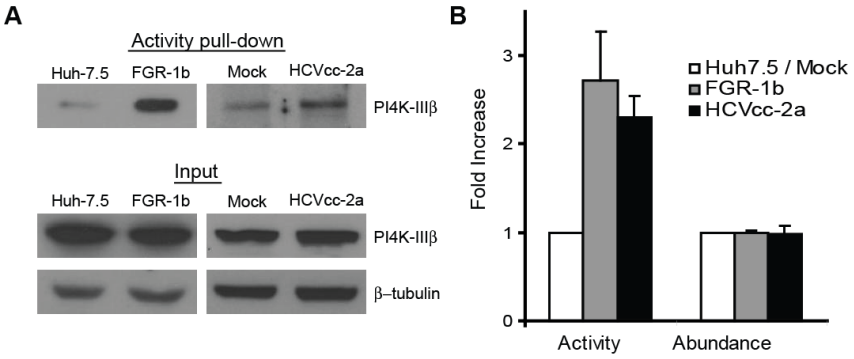

Figure 6-3. Effect of HCV replication on PI4KIIIβ activity and abundance. A) Relative activity and abundance ("Input") of PI4KIIIβ in Huh7.5 versus Huh-7.5 cells stably expressing genotype 1b(FGR-1b; left) ; and mock-infected Huh7.5 cells versus Huh7.5 cells infected with HCV genotype 2a (JFH-1; right), labeled in situ with PIK-BPyne. B) Densitometric analysis of PI4KIIIβ activity and abundance relative to naive Huh7.5 or mock-infected controls, normalized to β-tubulin loading control (n=3, error bars: SD).

6.4.3 Differential Activity of Phosphoinositide3 Kinase (PI3K) during HCV Replication, Examined by Quantitative ABPP

Having successfully employed PIK-BPyne to examine the activity of PI4KIIIβ, I decided to apply this probe to investigate the functional state of other lipid kinases whose activities may be modulated by HCV replication. In order to accurately quantify the potential differences in enzyme activity, I performed quantitative ABPP. Following the *in situ* labeling of naïve Huh7.5 and HCV-FGR expressing Huh7.5 cells, activity pull-down was performed, and captured peptides underwent dimethyl labeling (44). To ensure the accuracy of quantification, the experiment was carried out in reciprocal sets; in one set the peptides from naïve Huh7.5 cells were labeled with light formaldehyde and the HCV-FGR peptides were labeled with medium formaldehyde; in the reverse set the peptides from Huh7.5 cells were labeled with medium formaldehyde and the HCV-FGR peptides were labeled with light formaldehyde (Figure 6-4). The peptides were then mixed in 1:1 ratio and analyzed by LC-MS/MS.

The results of dimethyl labeling were filtered so that the targets with H/L ratios (fold change in HCV-FGR) smaller than 0.8 and bigger than 1.5 ($R<0.8$ and $R>1.5$) were selected. Table 6-1 shows the relative quantification of selected targets of PIK-BPyne that have already been shown to be involved in HCV replication. As demonstrated in the list, the H/L ratios are rather consistent between the two sets, which demonstrate the accuracy of quantification. I also did pathway analysis for the protein targets that their activities altered by more than 50% in the presence of HCV replication, using ToppGene Suite program (64). Interestingly, the lipid metabolism pathway was identified by the software with P-value= 8.544E. Importantly, hydroxymethylglutaryl-CoA synthase (HMG-CoA), as well as acetyl-CoA carboxylase (ACC) and fatty acid synthase (FASN) are labeled by the PIK-BPyne probe and showed 80% to 90%

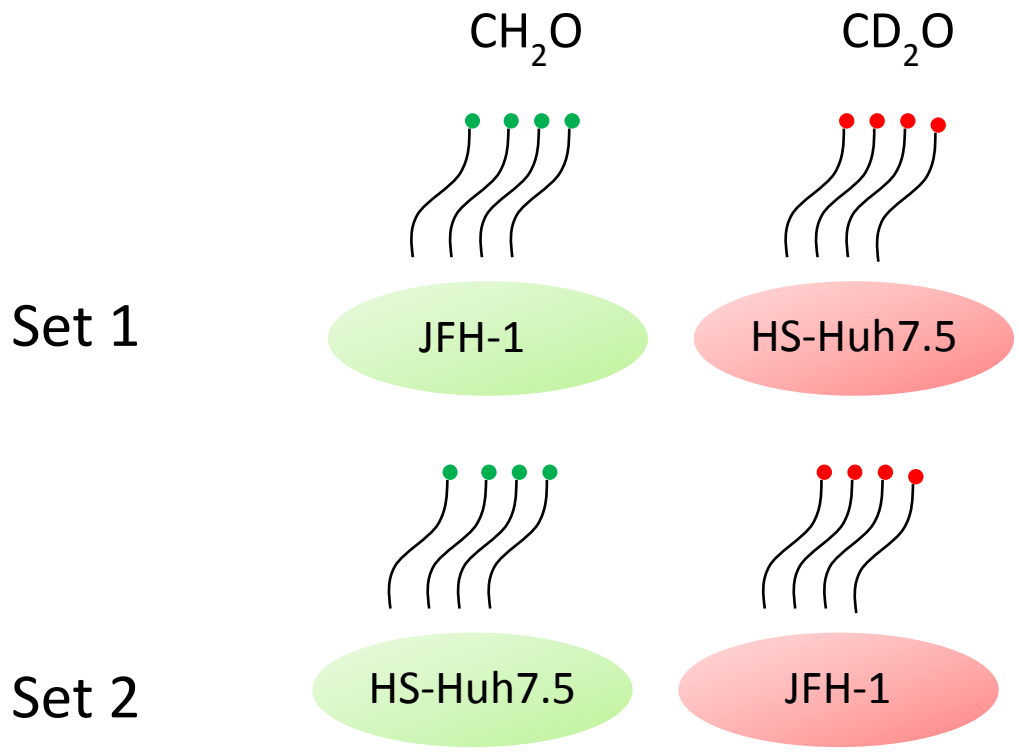

Figure 6-4. The quantitative ABPP experiment was set up in two sets; cells were equally labeled with PIK-BPyne probe clicked with biotin azide, affinity purified, and labeled with light or medium formaldehyde subsequent to trypsinization.

increase in the activity in HCV-FGR cells respectively (Table 6-1). This is also in accordance with our previous findings (283, 328) that the expression and activity of these lipogenic enzymes significantly increase during HCV replication. However, it is unknown at this time whether these proteins are labeled through their active sites.

In order to improve the chance of identifying low abundance enzymes such as the lipid kinases, I repeated the quantitative ABPP with higher concentration of PIK-BPyne probe, and longer MS running time. This time the catalytic subunit of PI3K was identified among the targets and showed nearly a 3 fold (2.95 fold) increase in HCV-FGR expressing cells compared to naïve Huh7.5 cells. As mentioned previously, PI3K/AKT pathway has been shown to be activated during HCV replication; however, this finding is particularly important as in this technique the activity of PI3K was directly examined, instead of monitoring the phosphorylation status of AKT, as an indirect measure of PI3K activation (57).

6.5 Discussion

Phosphoinositides function as fundamental signaling molecules, which regulate various cellular processes. They also play crucial roles in different aspects of the HCV life cycle, including the formation of vital intracellular organelles for HCV replication and assembly such as MW and lipid droplets. While accumulating evidence implicate PI4KIIIα and PI4KIIIβ as critical host factors of HCV replication, and their inhibitors consistently showed potent anti-HCV effects (35, 49, 394); at least two independent reports have shown that the activity of PI4KIIα and PI4KIIβ are dispensable for HCV replication (35, 410).

Table 6-1. Relative quantification of selected targets of PIK-Bpyne probe, which have a role in HCV replication

Set 1		**Set 2**	
Protein name	**H/L ratio**	**Protein name**	**H/L ratio**
Aldehyde dehydrogenase	6.1545	Aldehyde dehydrogenase (ALDH)	0.31808
Carnitine O-palmitoyltransferase 2	2.5833	Carnitine O-palmitoyltransferase 2	0.48586
Hydroxysteroid dehydrogenase	2.5029	Hydroxysteroid dehydrogenase	0.56508
NADP-isocitrate dehydrogenase	2.2494	NADP-isocitrate dehydrogenase	0.62435
Glutathione S-transferase	2.1383	Glutathione S-transferase	0.4632
Hydroxymethylglutaryl-CoA synthase	1.9178	Hydroxymethylglutaryl-CoA synthase	0.58189
Fatty acid synthase	1.8899	Fatty acid synthase	0.55853
Acetyl-CoA carboxylase	1.7806	Acetyl-CoA carboxylase	0.56986
Elongation factor 1-alpha	0.76592	Elongation factor 1-alpha	1.5829
Pyruvate kinase	0.58459	Pyruvate kinase	1.6408

H/L ratio: Heavy over light ratio. Representing the fold change in HCV-FGR cells

Several studies have focused on deciphering the role of PI4KIIIα in formation and integrity of MW as well as activation of the HCV replicase complex; however, participation of PI4KIIIβ in HCV replication cycle remained largely unknown. PI4KIIIβ is normally involved in regulation of transportation to and from the trans-Golgi network, as well as budding and cleavage of Golgi-derived vesicles (121, 215). PI4KIIIβ generates PI4P, the precursor of important regulatory PIs as well as an eminent regulatory molecule in its own right (23, 259). It has been shown that PI4Ps generally exert their regulatory roles by recruiting their binding proteins to certain intracellular sites such as trans-Golgi network. Moreover, recent reports indicate that knockdown of OSBP or GOLPH3, major PI4P-binding proteins in Golgi, leads to a significant decrease in HCV secretion (13, 40), indicating these PI4P effectors are crucial for infectious HCV particle production. Therefore, it can be speculated that these PI4P binding effectors in may modulate the transition from HCV genome replication to virus particle production (189). In this study a novel PIK-BPyne probe was applied to profile the alteration in the activity PI4KIIIβ during HCV replication and for the first time it was demonstrated that despite the abundance of this enzyme remaining unchanged, its activity increases by 2.7 and 2.3 fold during the replication of HCV genotype 1b, and 2a respectively (Figure 6-3). This discrepancy in the activity of PI4KIIIβ during the replication of different HCV genotypes is in accordance with other studies that suggest a genotype-specific dependence for PI4KIIIβ activity during HCV replication (215, 335, 404). Interestingly, increased activity of PI4KIIIβ over its abundance was also observed in HeLa and HEK 293T cells compared with MDA-MB-468 and Huh7 cells (Figure 6-2). These findings are ground-breaking as they establish the fact that enzyme abundance does not necessarily correlate with its activity, and therefore conventional abundance-based proteomic techniques would fail in detecting these differential activities, which are likely attributed to post-

translational modifications or cofactor/inhibitor association. Importantly, the activity of PI4KIIIβ is post-translationally regulated by protein kinase D (PKD) through phosphorylation of Ser268 (137), consequently further experiments are needed to examine whether HCV infection leads to Ser268 phosphorylation, or the functional status of PI4KIIIβ is further regulated through other mechanisms.

Aside from HCV, PI4KIIIβ is an essential host factor for the replication of several major human pathogens such as Dengue virus, Polio virus, human Rhinovirus type C, Coxsakievirus, and SARS (140, 154, 263, 402, 411, 447). Therefore ABPP with PIK-BPyne not only provides insight into the functional state of this enzyme during viral replication, but also allows for identification of novel inhibitors that can act against multiple classes of dangerous human viruses.

I also employed quantitative ABPP to directly examine the activity of PI3K during HCV replication and observed a three-fold increase in its activity in the presence of HCV-FGR. The activity of PI3K is also post-translationally regulated by a variety of growth factors and receptors (82, 111, 184), therefore in spite of its expression level, its functional status is controlled by an array of cellular and intercellular factors. The PI3K pathway is implicated in many human diseases including diabetes, cancer, autoimmune diseases, as well as infectious diseases (18, 98, 279, 296, 379). Importantly more than 100 proteins are known to be regulated by PI3K. Therefore monitoring the activity of this enzyme is the key to understanding the molecular aspects of many human diseases.

To summarize, in this chapter it was demonstrated that ABPP with PIK-BPyne probe allows for detection and isolation of multiple classes of PIKs as well as other targets within live cells.

Therefore this functional proteomic approach can be applied to decipher the role of these enzymes in various physiological and pathological states, such as HCV replication.

Chapter 7: Conclusions & Future Directions

7.1 Developing Tools for Studying RNA Silencing

Current therapeutic regimens against HCV only partially achieve sustained virological response in infected patients (201), hence, there is an urgent need for the design of novel therapies, such as those that are directed against the essential host factors or target the viral genomic RNA (283, 285). However, designing therapeutic agents that target HCV's genome remains challenging, as the HCV genomic RNA is large and highly structured with long-range genome-scale ordered RNA structures, which have strong impact on siRNA and miRNA seed site accessibility (347). Therefore target site accessibility remains a significant barrier to the design of effective therapeutics such as small interfering RNAs against different strains of HCV. In this thesis, a method that interrogates the folding of HCV RNA was developed that employs HCV RNA-coated magnetic beads (VRB) to determine target site accessibility for RNA silencing against the HCV genome. This method predicted the relative affinity of small RNAs towards HCV genomic RNA that are not easily predicted by informatic means. For that reason, VRB assays could be an attractive tool for the examination of target site accessibility for both siRNAs and miRNAs.

MicroRNA-122 is one of the essential host factors for HCV replication. Direct interaction of miR-122 with the two of its MREs in the 5'UTR is required for viral replication and protein translation (168, 169, 177, 178, 374). In chapter three, the relative affinity of miR-122 to these sites was investigated using the VRB assay, along with applying mutagenesis and probes to disrupt interactions of miR-122 at specific sites. Also cooperativity in binding between the closely spaced MREs within the 5'UTR *in vitro* was demonstrated, and a well conserved fourth site in the coding region with high affinity towards miR-122 was identified. Site-directed mutagenesis of the MREs revealed competing roles of the stimulatory MREs in the 5'UTR and

inhibitory role of an MRE in the open reading frame. These data have important implications in elucidating the mechanism of interaction between miR-122 and HCV RNA.

The VRB assay can also be adapted to highthroughput systems such as microfluidic platforms that enable the miniaturization, integration, and automation of biochemical experiments (255). In an unpublished work, we have successfully implemented the VRB assay on an electrowetting platform in which magnetic beads that serve as solid nucleic acid binding phase, are controlled by a built-in magnet (253). In this setting, all the procedures including hybridization and washes are performed on a single chip, which allows for a rapid and sensitive examination of target site accessibility.

The application of VRBs can be further extended to miRNA sensing assays (282). In this approach, RNA probes complimentary to various miRNA sequences are immobilized on the surface of magnetic beads, and used to capture miRNA in different biological preparations such as cell extracts. Captured miRNAs are sensed by p19, a tombusvirus-encoded suppressor of RNA interference that demonstrates sequence-independent and size-selective affinity toward 19-bp RNA duplexes (72, 413, 453). Signal amplification occurs through specific binding of p19 to the miRNA–probe duplex as part of an amplified enzyme immunoassay (EIA). This method allows for sensitive detection of miRNAs, with the detection limit of 1fmol and a linear dynamic range from 1pmol to 1fmol (282).

Consequently, VRB-based assays can be employed to determine the target site accessibility of long and structured RNAs, such as viral genomes, as well as miRNA profiling. miRNA expression profiling has helped to identify miRNAs that regulate a range of processes, including tissue differentiation and maintenance, as well as human diseases such as cancer, heart disease, diabetes, and neurodegenerative disorders (56, 142, 161, 323, 324, 412, 420). Therefore,

miRNAs are being investigated as therapeutic reagents, and are being considered as biomarkers for diagnosis and prognosis of different stages of various human diseases.

7.2 Applying Activity-Based Protein Profiling to Investigate Host-Virus Interactions

Activity-based protein profiling (ABPP) is a powerful strategy for dissecting the function of a myriad of enzymes relevant to human physiology and pathology. Besides protein function annotation, activity-based chemical probes (ABPs) have been employed to unravel protein localization, and regulatory dynamics, as well as to discover novel inhibitors with therapeutic potentials (70). ABPP encompasses the application of a broad collection of probe motifs that vary in both protein reactivity and mode of binding in diverse biological systems (41, 42). In this thesis, diverse and mechanistically distinct ABPs have been applied *in situ* and *in vitro*, combined with gel electrophoresis, fluorescence microscopy, and/or mass spectrometry, to provide insights into the host-HCV interactions, and introduce novel cellular factors that can be regarded as potential therapeutic and diagnostic targets.

7.2.1 Modulation of Fatty Acid Synthase Enzyme Activity by HCV

Every steps of the HCV life cycle depends on elements of the cellular lipid metabolism pathway (355). Fatty acid synthase (FASN) is a multi-domain enzyme that plays a key role in the biosynthesis of fatty acids and its expression is upregulated during HCV infection (234, 451). In chapter 4 of this thesis, ABPP was applied to study the alterations in activity of FASN during HCV replication. For this purpose, I used an activity-based probe based on the FASN inhibitor orlistat, and observed an increase in the activity of FASN in the presence of a subgenomic and a genomic HCV replicon as well as in chimeric SCID/Alb-uPA mice infected with HCV genotype 1a. To study the molecular basis for this increase in FASN activity, individual HCV proteins were expressed in Huh7 cells and it was observed that the presence of core and NS4B proteins

increased the expression and activity of FASN, as measured by western blots and ABPP, respectively. Triglyceride levels were also elevated in accordance with FASN expression and activity. Lastly, immunofluorescence and ABPP imaging analyses demonstrated that while the abundance and activity of FASN increases significantly in the presence of HCV, its localization does not change. Together these data suggest that the HCV-induced production of fatty acids and neutral lipids is provided by an increase in FASN abundance and activity that is sufficient to allow HCV propagation without transporting FASN to the replication complexes.

Moreover, I have developed a quantitative ABPP method for relative quantification of FASN activity during HCV infection. In this novel technique, comparative ABPP is combined with stable isotope dimethyl labeling (DML), to efficiently report on the relative activity of the target enzymes in any protein sample. For this purpose, JFH-1 virus, the infectious model of HCV was used and the result of dimethyl labeling with orlistat probe was in accordance with former ABPP data that FASN activity increases dramatically during HCV infection, and is consistent between the reciprocal sets of the experiment.

7.2.2 β-lactam-Derived Activity-Based Probes for Global Profiling of Host Enzymatic Activity during HCV Replication

β-lactams are generally known as powerful antibiotics against bacterial infections, however, because the β-lactam moiety is a potent electrophile, it can react with the active residues of enzymes from different classes (382, 383). Therefore β-lactam derived ABPs allows for functional examination of diverse enzyme families.

In chapter 5, the eukaryotic targets of β-lactam-containing compounds were identified by employing activity-based protein profiling. I demonstrated that β-lactam-based activity probes can target mechanistically diverse groups of enzymes and thus can be applied to identify

differentially active enzymes in different cell lines and during a pathological state, such as viral or bacterial infections.

Subsequently, β-lactam probes were employed for global profiling of the alterations in the activity of cellular enzymes during HCV replication. For this purpose, comparative ABPP was performed on naïve Huh7 cells and Huh7 cells harboring HCV full-genomic replicon (HCV-FGR). We were able to identify a variety of mechanistically distinct enzymes that demonstrate differential activity during HCV replication. Some of these enzymes have been previously reported to play important roles in HCV replication cycle, such as protein phosphatase 1B that is involved in interferon signalling, acetyl-CoA carboxylase, the rate-limiting enzyme in lipogenesis as well as cyclin-dependent kinase 2, which is the key enzyme in cell-cycle regulation. Importantly, we identified several other host enzymes whose activities dramatically changed during HCV infection, but their role in the viral life cycle is yet unclear. These enzymes can potentially be recognized as disease-associated biomarkers, with diagnostic and therapeutic significance.

In conclusion, we successfully applied ampicilin-based as well as novel β-lactam derived ABPs for functional screening of enzyme activity in intact cells, and were able to identify a variety of mechanistically distinct target enzymes that show differential activity during HCV replication. These results will accelerate the discovery of protein activities associated with the pathogenic states of HCV infection, and therefore facilitate the discovery of new biomarkers as well as potential targets for therapeutic interventions. As such, β-lactam probes may represent valuable tools in cell biology, and microbiology studies.

7.2.3 Examining the Activity of Lipid Kinsaes during HCV Replication Using PIK-BPyne Probe

Phosphatidylinositol kinases (PIKs) are key enzymatic regulators of membrane phospholipids and membrane environments that control many aspects of cellular function, from signal transduction to secretion, through the Golgi apparatus. Importantly, the activity of PI3K and PI4K has been shown to be essential for HCV replication (40). Therefore, in chapter 6, I explained the application of a novel probe based on the PIK-93 inhibitor (198) to investigate alterations in the activity of these enzymes during HCV replication.

The PIK-BPyne probe was prepared by adding a photo-crosslinkable group, benzophenone (BP), to a core structure similar to PIK-93 to enable covalent modification of the target enzymes. As shown, this probe successfully targets several PI4K isoforms, as well as PI3K (364). Due to controversial reports regarding the role of PI4KIIIβ in HCV replication, I set to investigate the possible modulation of the activity of this enzyme by HCV replication. For this reason, I performed western blot analyses on the enriched PIK-BPyne-labeled proteome from naïve Huh7 and Huh7 HCV-FGR (genotype 1b) cells , as well as Huh7 cells infected with the infectious model of HCV, JFH1, (genotype 2a). I observed 2.7 fold, and 2.3 fold increase in the activity, but not expression, of PI4KIIIβ, in HCV-FGR cells and JFH-1 infected cells respectively.

Since PI4KIIIβ is responsible for establishing the Golgi PI4P, which in turn is required for the localization of a number of Golgi-specific host factors that are involved in viral secretion (40), it can be hypothesized that PI4KIIIβ is also involved in HCV particle packaging and secretion. Further experiments are required to clarify the potential role of PI4KIIIβ in the HCV life cycle.

Additionally, I performed quantitative ABPP using PIK-BPyne probe and discovered that the activity of PI3K increased by nearly 3 folds during HCV replication. Several reports have

indicated the activation of PI3K/Akt pathway in HCV infection (306, 386, 387); however this is the first time that changes in the activity of PI3K during viral replication, was directly monitored and reported. These results establish the utility of PIK-BPyne for activity-based protein profiling studies of PIK function in native biological systems, including microbial infections.

Bibliography

1. A user's guide to the encyclopedia of DNA elements (ENCODE). PLoS Biol **9:**e1001046.
2. **Abecasis, G. R., D. Altshuler, A. Auton, L. D. Brooks, R. M. Durbin, R. A. Gibbs, M. E. Hurles, and G. A. McVean.** A map of human genome variation from population-scale sequencing. Nature **467:**1061-73.
3. **Adam, G. C., B. F. Cravatt, and E. J. Sorensen*.** 2001. Profiling the specific reactivity of the proteome with non-directed activity-based probes. Chemistry & Biology **8:**81-95.
4. **Adam, G. C., E. J. Sorensen, and B. F. Cravatt.** 2002. Proteomic profiling of mechanistically distinct enzyme classes using a common chemotype. Nat Biotechnol **20:**805-9.
5. **Adinolfi, L. E., M. Gambardella, A. Andreana, M. F. Tripodi, R. Utili, and G. Ruggiero.** 2001. Steatosis accelerates the progression of liver damage of chronic hepatitis C patients and correlates with specific HCV genotype and visceral obesity. Hepatology **33:**1358-64.
6. **Adler, J., and I. Parmryd.** 2010. Quantifying colocalization by correlation: The Pearson correlation coefficient is superior to the Mander's overlap coefficient. Cytometry Part A **77A:**733-742.
7. **Agrawal, N., P. V. Dasaradhi, A. Mohmmed, P. Malhotra, R. K. Bhatnagar, and S. K. Mukherjee.** 2003. RNA interference: biology, mechanism, and applications. Microbiol Mol Biol Rev **67:**657-85.
8. **Alcaide, B., and P. Almendros.** 2004. Beta-lactams as versatile synthetic intermediates for the preparation of heterocycles of biological interest. Curr Med Chem **11:**1921-49.
9. **Ali, S., C. Pellerin, D. Lamarre, and G. Kukolj.** 2004. Hepatitis C virus subgenomic replicons in the human embryonic kidney 293 cell line. J Virol **78:**491-501.
10. **Aligo, J., S. Jia, D. Manna, and K. V. Konan.** 2009. Formation and function of hepatitis C virus replication complexes require residues in the carboxy-terminal domain of NS4B protein. Virology **393:**68-83.
11. **Altan-Bonnet, N., and T. Balla.** Phosphatidylinositol 4-kinases: hostages harnessed to build panviral replication platforms. Trends Biochem Sci **37:**293-302.
12. **Altun, M., H. B. Kramer, L. I. Willems, J. L. McDermott, C. A. Leach, S. J. Goldenberg, K. G. Kumar, R. Konietzny, R. Fischer, E. Kogan, M. M. Mackeen, J. McGouran, S. V. Khoronenkova, J. L. Parsons, G. L. Dianov, B. Nicholson, and B. M. Kessler.** 2011. Activity-based chemical proteomics accelerates inhibitor development for deubiquitylating enzymes. Chem Biol **18:**1401-12.
13. **Amako, Y., A. Sarkeshik, H. Hotta, J. Yates, 3rd, and A. Siddiqui.** 2009. Role of oxysterol binding protein in hepatitis C virus infection. J Virol **83:**9237-46.
14. **Amako, Y., G. H. Syed, and A. Siddiqui.** Protein kinase D negatively regulates hepatitis C virus secretion through phosphorylation of oxysterol-binding protein and ceramide transfer protein. J Biol Chem **286:**11265-74.
15. **Amiel, J., L. de Pontual, and A. Henrion-Caude.** 2012. miRNA, development and disease. Adv Genet **80:**1-36.
16. **Andre, P., G. Perlemuter, A. Budkowska, C. Brechot, and V. Lotteau.** 2005. Hepatitis C virus particles and lipoprotein metabolism. Semin Liver Dis **25:**93-104.
17. **Appel, N., T. Schaller, F. Penin, and R. Bartenschlager.** 2006. From structure to function: new insights into hepatitis C virus RNA replication. J Biol Chem **281:**9833-6.
18. **Aragones, G., C. Alonso-Villaverde, C. Oliveras-Ferraros, R. Beltran-Debon, A. Rull, F. Rodriguez-Sanabria, J. Camps, A. V. Martin, J. A. Menendez, and J. Joven.** 2010. Infection with HIV and HCV enhances the release of fatty acid synthase into circulation: evidence for a novel indicator of viral infection. BMC Gastroenterol **10:**92.
19. **Arcaro, A., and M. P. Wymann.** 1993. Wortmannin is a potent phosphatidylinositol 3-kinase inhibitor: the role of phosphatidylinositol 3,4,5-trisphosphate in neutrophil responses. Biochem J **296 (Pt 2):**297-301.
20. **Ashburner, M., C. A. Ball, J. A. Blake, D. Botstein, H. Butler, J. M. Cherry, A. P. Davis, K. Dolinski, S. S. Dwight, J. T. Eppig, M. A. Harris, D. P. Hill, L. Issel-Tarver, A. Kasarskis, S.**

Lewis, J. C. Matese, J. E. Richardson, M. Ringwald, G. M. Rubin, and G. Sherlock. 2000. Gene ontology: tool for the unification of biology. The Gene Ontology Consortium. Nat Genet **25:**25-9.

21. **Bachovchin, D. A., S. J. Brown, H. Rosen, and B. F. Cravatt.** 2009. Identification of selective inhibitors of uncharacterized enzymes by high-throughput screening with fluorescent activity-based probes. Nat Biotechnol **27:**387-94.
22. **Bai, S., M. W. Nasser, B. Wang, S. H. Hsu, J. Datta, H. Kutay, A. Yadav, G. Nuovo, P. Kumar, and K. Ghoshal.** 2009. MicroRNA-122 inhibits tumorigenic properties of hepatocellular carcinoma cells and sensitizes these cells to sorafenib. J Biol Chem **284:**32015-27.
23. **Balla, A., and T. Balla.** 2006. Phosphatidylinositol 4-kinases: old enzymes with emerging functions. Trends Cell Biol **16:**351-61.
24. **Ballinger, A., and S. R. Peikin.** 2002. Orlistat: its current status as an anti-obesity drug. Eur J Pharmacol **440:**109-17.
25. **Banaudha, K., J. M. Orenstein, T. Korolnek, G. C. St Laurent, 3rd, T. Wakita, and A. Kumar.** Primary hepatocyte culture supports hepatitis C virus replication: a model for infection-associated hepatocarcinogenesis. Hepatology **51:**1922-32.
26. **Bantounas, I., L. A. Phylactou, and J. B. Uney.** 2004. RNA interference and the use of small interfering RNA to study gene function in mammalian systems. J Mol Endocrinol **33:**545-57.
27. **Barba, G., F. Harper, T. Harada, M. Kohara, S. Goulinet, Y. Matsuura, G. Eder, Z. Schaff, M. J. Chapman, T. Miyamura, and C. Brechot.** 1997. Hepatitis C virus core protein shows a cytoplasmic localization and associates to cellular lipid storage droplets. Proc Natl Acad Sci U S A **94:**1200-5.
28. **Barglow, K. T., and B. F. Cravatt.** 2007. Activity-based protein profiling for the functional annotation of enzymes. Nat Methods **4:**822-7.
29. **Barglow, K. T., and B. F. Cravatt.** 2004. Discovering disease-associated enzymes by proteome reactivity profiling. Chem Biol **11:**1523-31.
30. **Bartel, D. P.** 2009. MicroRNAs: target recognition and regulatory functions. Cell **136:**215-33.
31. **Barth, H.** Hepatitis C virus: Is it time to say goodbye yet? Perspectives and challenges for the next decade. World J Hepatol **7:**725-37.
32. **Bassendine, M. F., D. A. Sheridan, D. J. Felmlee, S. H. Bridge, G. L. Toms, and R. D. Neely.** 2011. HCV and the hepatic lipid pathway as a potential treatment target. J Hepatol **55:**1428-40.
33. **Beck, M., A. Schmidt, J. Malmstroem, M. Claassen, A. Ori, A. Szymborska, F. Herzog, O. Rinner, J. Ellenberg, and R. Aebersold.** The quantitative proteome of a human cell line. Mol Syst Biol **7:**549.
34. **Berger, K. L., S. M. Kelly, T. X. Jordan, M. A. Tartell, and G. Randall.** 2011. Hepatitis C virus stimulates the phosphatidylinositol 4-kinase III alpha-dependent phosphatidylinositol 4-phosphate production that is essential for its replication. J Virol **85:**8870-83.
35. **Berger, K. L., and G. Randall.** 2009. Potential roles for cellular cofactors in hepatitis C virus replication complex formation. Commun Integr Biol **2:**471-3.
36. **Bernhard, O. K., R. J. Diefenbach, and A. L. Cunningham.** 2005. New insights into viral structure and virus-cell interactions through proteomics. Expert Rev Proteomics **2:**577-88.
37. **Betel, D., M. Wilson, A. Gabow, D. S. Marks, and C. Sander.** 2008. The microRNA.org resource: targets and expression. Nucleic Acids Res **36:**D149-53.
38. **Bianco, A., V. Reghellin, L. Donnici, S. Fenu, R. Alvarez, C. Baruffa, F. Peri, M. Pagani, S. Abrignani, P. Neddermann, and R. De Francesco.** 2012. Metabolism of phosphatidylinositol 4-kinase IIIalpha-dependent PI4P Is subverted by HCV and is targeted by a 4-anilino quinazoline with antiviral activity. PLoS Pathog **8:**e1002576.
39. **Birmingham, A., E. Anderson, K. Sullivan, A. Reynolds, Q. Boese, D. Leake, J. Karpilow, and A. Khvorova.** 2007. A protocol for designing siRNAs with high functionality and specificity. Nat Protoc **2:**2068-78.

40. **Bishe, B., G. Syed, and A. Siddiqui.** 2012. Phosphoinositides in the hepatitis C virus life cycle. Viruses **4:**2340-58.
41. **Blais, D. R., R. K. Lyn, M. A. Joyce, Y. Rouleau, R. Steenbergen, N. Barsby, L. F. Zhu, A. F. Pegoraro, A. Stolow, D. L. Tyrrell, and J. P. Pezacki.** 2010. Activity-based protein profiling identifies a host enzyme, carboxylesterase 1, which is differentially active during hepatitis C virus replication. J Biol Chem **285:**25602-12.
42. **Blais, D. R., N. Nasheri, C. S. McKay, M. C. Legault, and J. P. Pezacki.** 2012. Activity-based protein profiling of host-virus interactions. Trends Biotechnol **30:**89-99.
43. **Boeckmann, B., A. Bairoch, R. Apweiler, M. C. Blatter, A. Estreicher, E. Gasteiger, M. J. Martin, K. Michoud, C. O'Donovan, I. Phan, S. Pilbout, and M. Schneider.** 2003. The SWISS-PROT protein knowledgebase and its supplement TrEMBL in 2003. Nucleic Acids Res **31:**365-70.
44. **Boersema, P. J., R. Raijmakers, S. Lemeer, S. Mohammed, and A. J. Heck.** 2009. Multiplex peptide stable isotope dimethyl labeling for quantitative proteomics. Nat Protoc **4:**484-94.
45. **Bohula, E. A., M. P. Playford, and V. M. Macaulay.** 2003. Targeting the type 1 insulin-like growth factor receptor as anti-cancer treatment. Anticancer Drugs **14:**669-82.
46. **Bohula, E. A., A. J. Salisbury, M. Sohail, M. P. Playford, J. Riedemann, E. M. Southern, and V. M. Macaulay.** 2003. The efficacy of small interfering RNAs targeted to the type 1 insulin-like growth factor receptor (IGF1R) is influenced by secondary structure in the IGF1R transcript. J Biol Chem **278:**15991-7.
47. **Boizard, M., X. Le Liepvre, P. Lemarchand, F. Foufelle, P. Ferre, and I. Dugail.** 1998. Obesity-related overexpression of fatty-acid synthase gene in adipose tissue involves sterol regulatory element-binding protein transcription factors. J Biol Chem **273:**29164-71.
48. **Boja, E. S., and H. Rodriguez.** Proteogenomic convergence for understanding cancer pathways and networks. Clin Proteomics **11:**22.
49. **Borawski, J., P. Troke, X. Puyang, V. Gibaja, S. Zhao, C. Mickanin, J. Leighton-Davies, C. J. Wilson, V. Myer, I. Cornellataracido, J. Baryza, J. Tallarico, G. Joberty, M. Bantscheff, M. Schirle, T. Bouwmeester, J. E. Mathy, K. Lin, T. Compton, M. Labow, B. Wiedmann, and L. A. Gaither.** 2009. Class III phosphatidylinositol 4-kinase alpha and beta are novel host factor regulators of hepatitis C virus replication. J Virol **83:**10058-74.
50. **Boulant, S., P. Targett-Adams, and J. McLauchlan.** 2007. Disrupting the association of hepatitis C virus core protein with lipid droplets correlates with a loss in production of infectious virus. J Gen Virol **88:**2204-13.
51. **Boyer, P. D.** 1997. The ATP synthase--a splendid molecular machine. Annu Rev Biochem **66:**717-49.
52. **Brennecke, J., A. Stark, R. B. Russell, and S. M. Cohen.** 2005. Principles of microRNA-target recognition. PLoS Biol **3:**e85.
53. **Brodersen, P., and O. Voinnet.** 2009. Revisiting the principles of microRNA target recognition and mode of action. Nat Rev Mol Cell Biol **10:**141-8.
54. **Brown, K. M., C. Y. Chu, and T. M. Rana.** 2005. Target accessibility dictates the potency of human RISC. Nat Struct Mol Biol **12:**469-70.
55. **Bugianesi, E., F. Salamone, and F. Negro.** 2012. The interaction of metabolic factors with HCV infection: does it matter? J Hepatol **56 Suppl 1:**S56-65.
56. **Calin, G. A., and C. M. Croce.** 2006. MicroRNA signatures in human cancers. Nat Rev Cancer **6:**857-66.
57. **Cantley, L. C.** 2002. The phosphoinositide 3-kinase pathway. Science **296:**1655-7.
58. **Carbone, C. J., H. Zheng, S. Bhattacharya, J. R. Lewis, A. M. Reiter, P. Henthorn, Z. Y. Zhang, D. P. Baker, R. Ukkiramapandian, K. K. Bence, and S. Y. Fuchs.** 2012. Protein tyrosine phosphatase 1B is a key regulator of IFNAR1 endocytosis and a target for antiviral therapies. Proc Natl Acad Sci U S A **109:**19226-31.

59. **Carthew, R. W., and E. J. Sontheimer.** 2009. Origins and Mechanisms of miRNAs and siRNAs. Cell **136:**642-55.
60. **Castaldo, G., G. Calcagno, R. Sibillo, R. Cuomo, G. Nardone, L. Castellano, C. Del Vecchio Blanco, G. Budillon, and F. Salvatore.** 2000. Quantitative analysis of aldolase A mRNA in liver discriminates between hepatocellular carcinoma and cirrhosis. Clin Chem **46:**901-6.
61. **Chakravarthy, M. V., Z. Pan, Y. Zhu, K. Tordjman, J. G. Schneider, T. Coleman, J. Turk, and C. F. Semenkovich.** 2005. "New" hepatic fat activates PPARalpha to maintain glucose, lipid, and cholesterol homeostasis. Cell Metab **1:**309-22.
62. **Chakravarty, B., Z. Gu, S. S. Chirala, S. J. Wakil, and F. A. Quiocho.** 2004. Human fatty acid synthase: structure and substrate selectivity of the thioesterase domain. Proc Natl Acad Sci U S A **101:**15567-72.
63. **Chen, G., G. Liang, J. Ou, J. L. Goldstein, and M. S. Brown.** 2004. Central role for liver X receptor in insulin-mediated activation of Srebp-1c transcription and stimulation of fatty acid synthesis in liver. Proc Natl Acad Sci U S A **101:**11245-50.
64. **Chen, J., E. E. Bardes, B. J. Aronow, and A. G. Jegga.** 2009. ToppGene Suite for gene list enrichment analysis and candidate gene prioritization. Nucleic Acids Res **37:**W305-11.
65. **Chen, R., G. I. Mias, J. Li-Pook-Than, L. Jiang, H. Y. Lam, E. Miriami, K. J. Karczewski, M. Hariharan, F. E. Dewey, Y. Cheng, M. J. Clark, H. Im, L. Habegger, S. Balasubramanian, M. O'Huallachain, J. T. Dudley, S. Hillenmeyer, R. Haraksingh, D. Sharon, G. Euskirchen, P. Lacroute, K. Bettinger, A. P. Boyle, M. Kasowski, F. Grubert, S. Seki, M. Garcia, M. Whirl-Carrillo, M. Gallardo, M. A. Blasco, P. L. Greenberg, P. Snyder, T. E. Klein, R. B. Altman, A. J. Butte, E. A. Ashley, M. Gerstein, K. C. Nadeau, H. Tang, and M. Snyder.** Personal omics profiling reveals dynamic molecular and medical phenotypes. Cell **148:**1293-307.
66. **Cheng, Y., S. Dharancy, M. Malapel, and P. Desreumaux.** 2005. Hepatitis C virus infection down-regulates the expression of peroxisome proliferator-activated receptor alpha and carnitine palmitoyl acyl-CoA transferase 1A. World J Gastroenterol **11:**7591-6.
67. **Choi, M., S. Lee, T. Choi, and C. Lee.** A hepatitis C virus NS4B inhibitor suppresses viral genome replication by disrupting NS4B's dimerization/multimerization as well as its interaction with NS5A. Virus Genes **47:**395-407.
68. **Coller, K. E., N. S. Heaton, K. L. Berger, J. D. Cooper, J. L. Saunders, and G. Randall.** Molecular determinants and dynamics of hepatitis C virus secretion. PLoS Pathog **8:**e1002466.
69. **Coller, K. E., N. S. Heaton, K. L. Berger, J. D. Cooper, J. L. Saunders, and G. Randall.** 2012. Molecular determinants and dynamics of hepatitis C virus secretion. PLoS Pathog **8:**e1002466.
70. **Cravatt, B. F., A. T. Wright, and J. W. Kozarich.** 2008. Activity-based protein profiling: from enzyme chemistry to proteomic chemistry. Annu Rev Biochem **77:**383-414.
71. **Czaika, V. A., J. Siebenbrock, F. Czekalla, T. Zuberbier, and M. A. Sieber.** Reactive oxygen species and the bacteriostatic and bactericidal effects of isoconazole nitrate. Mycoses **56 Suppl 1:**16-22.
72. **Danielson, D. C., and J. P. Pezacki.** Studying the RNA silencing pathway with the p19 protein. FEBS Lett **587:**1198-205.
73. **Dar, A. C., and K. M. Shokat.** The evolution of protein kinase inhibitors from antagonists to agonists of cellular signaling. Annu Rev Biochem **80:**769-95.
74. **Date, T., T. Kato, M. Miyamoto, Z. Zhao, K. Yasui, M. Mizokami, and T. Wakita.** 2004. Genotype 2a hepatitis C virus subgenomic replicon can replicate in HepG2 and IMY-N9 cells. J Biol Chem **279:**22371-6.
75. **Davis, M., S. M. Sagan, J. P. Pezacki, D. J. Evans, and P. Simmonds.** 2008. Bioinformatic and physical characterizations of genome-scale ordered RNA structure in mammalian RNA viruses. J Virol **82:**11824-36.

76. **de Faria, I. J., R. P. Olmo, E. G. Silva, and J. T. Marques.** dsRNA sensing during viral infection: lessons from plants, worms, insects, and mammals. J Interferon Cytokine Res **33:**239-53.
77. **de Gottardi, A., V. Pazienza, P. Pugnale, F. Bruttin, L. Rubbia-Brandt, C. E. Juge-Aubry, C. A. Meier, A. Hadengue, and F. Negro.** 2006. Peroxisome proliferator-activated receptor-alpha and -gamma mRNA levels are reduced in chronic hepatitis C with steatosis and genotype 3 infection. Aliment Pharmacol Ther **23:**107-14.
78. **DeBose-Boyd, R. A., J. Ou, J. L. Goldstein, and M. S. Brown.** 2001. Expression of sterol regulatory element-binding protein 1c (SREBP-1c) mRNA in rat hepatoma cells requires endogenous LXR ligands. Proc Natl Acad Sci U S A **98:**1477-82.
79. **Delang, L., J. Paeshuyse, and J. Neyts.** 2012. The role of phosphatidylinositol 4-kinases and phosphatidylinositol 4-phosphate during viral replication. Biochem Pharmacol **84:**1400-8.
80. **Delgrange, D., A. Pillez, S. Castelain, L. Cocquerel, Y. Rouille, J. Dubuisson, T. Wakita, G. Duverlie, and C. Wychowski.** 2007. Robust production of infectious viral particles in Huh-7 cells by introducing mutations in hepatitis C virus structural proteins. J Gen Virol **88:**2495-503.
81. **DeVincenzo, J., J. E. Cehelsky, R. Alvarez, S. Elbashir, J. Harborth, I. Toudjarska, L. Nechev, V. Murugaiah, A. Van Vliet, A. K. Vaishnaw, and R. Meyers.** 2008. Evaluation of the safety, tolerability and pharmacokinetics of ALN-RSV01, a novel RNAi antiviral therapeutic directed against respiratory syncytial virus (RSV). Antiviral Res **77:**225-31.
82. **Dhand, R., I. Hiles, G. Panayotou, S. Roche, M. J. Fry, I. Gout, N. F. Totty, O. Truong, P. Vicendo, K. Yonezawa, and et al.** 1994. PI 3-kinase is a dual specificity enzyme: autoregulation by an intrinsic protein-serine kinase activity. EMBO J **13:**522-33.
83. **Di Paolo, G., and P. De Camilli.** 2006. Phosphoinositides in cell regulation and membrane dynamics. Nature **443:**651-7.
84. **Diaz-Toledano, R., A. Ariza-Mateos, A. Birk, B. Martinez-Garcia, and J. Gomez.** 2009. In vitro characterization of a miR-122-sensitive double-helical switch element in the 5' region of hepatitis C virus RNA. Nucleic Acids Res **37:**5498-510.
85. **Didiano, D., and O. Hobert.** 2006. Perfect seed pairing is not a generally reliable predictor for miRNA-target interactions. Nat Struct Mol Biol **13:**849-51.
86. **Dietrich, L. E., and C. Ungermann.** 2004. On the mechanism of protein palmitoylation. EMBO Rep **5:**1053-7.
87. **Diviney, S., A. Tuplin, M. Struthers, V. Armstrong, R. M. Elliott, P. Simmonds, and D. J. Evans.** 2008. A hepatitis C virus cis-acting replication element forms a long-range RNA-RNA interaction with upstream RNA sequences in NS5B. J Virol **82:**9008-22.
88. **Dorner, M., J. A. Horwitz, B. M. Donovan, R. N. Labitt, W. C. Budell, T. Friling, A. Vogt, M. T. Catanese, T. Satoh, T. Kawai, S. Akira, M. Law, C. M. Rice, and A. Ploss.** 2013. Completion of the entire hepatitis C virus life cycle in genetically humanized mice. Nature **501:**237-41.
89. **Dorner, M., J. A. Horwitz, J. B. Robbins, W. T. Barry, Q. Feng, K. Mu, C. T. Jones, J. W. Schoggins, M. T. Catanese, D. R. Burton, M. Law, C. M. Rice, and A. Ploss.** 2011. A genetically humanized mouse model for hepatitis C virus infection. Nature **474:**208-11.
90. **Dubuisson, J., F. Penin, and D. Moradpour.** 2002. Interaction of hepatitis C virus proteins with host cell membranes and lipids. Trends Cell Biol **12:**517-23.
91. **Dunn, K. W., M. M. Kamocka, and J. H. McDonald.** 2011. A practical guide to evaluating colocalization in biological microscopy. Am J Physiol Cell Physiol **300:**C723-42.
92. **Edwards, P. A., D. Tabor, H. R. Kast, and A. Venkateswaran.** 2000. Regulation of gene expression by SREBP and SCAP. Biochim Biophys Acta **1529:**103-13.
93. **Egger, D., B. Wolk, R. Gosert, L. Bianchi, H. E. Blum, D. Moradpour, and K. Bienz.** 2002. Expression of hepatitis C virus proteins induces distinct membrane alterations including a candidate viral replication complex. J Virol **76:**5974-84.

94. **Elazar, M., P. Liu, C. M. Rice, and J. S. Glenn.** 2004. An N-terminal amphipathic helix in hepatitis C virus (HCV) NS4B mediates membrane association, correct localization of replication complex proteins, and HCV RNA replication. J Virol **78:**11393-400.
95. **Elbashir, S. M., J. Harborth, W. Lendeckel, A. Yalcin, K. Weber, and T. Tuschl.** 2001. Duplexes of 21-nucleotide RNAs mediate RNA interference in cultured mammalian cells. Nature **411:**494-8.
96. **Elbashir, S. M., J. Harborth, K. Weber, and T. Tuschl.** 2002. Analysis of gene function in somatic mammalian cells using small interfering RNAs. Methods **26:**199-213.
97. **Elmen, J., M. Lindow, A. Silahtaroglu, M. Bak, M. Christensen, A. Lind-Thomsen, M. Hedtjarn, J. B. Hansen, H. F. Hansen, E. M. Straarup, K. McCullagh, P. Kearney, and S. Kauppinen.** 2008. Antagonism of microRNA-122 in mice by systemically administered LNA-antimiR leads to up-regulation of a large set of predicted target mRNAs in the liver. Nucleic Acids Res **36:**1153-62.
98. **Engelman, J. A.** 2009. Targeting PI3K signalling in cancer: opportunities, challenges and limitations. Nat Rev Cancer **9:**550-62.
99. **Engelman, J. A., J. Luo, and L. C. Cantley.** 2006. The evolution of phosphatidylinositol 3-kinases as regulators of growth and metabolism. Nat Rev Genet **7:**606-19.
100. **Esau, C., S. Davis, S. F. Murray, X. X. Yu, S. K. Pandey, M. Pear, L. Watts, S. L. Booten, M. Graham, R. McKay, A. Subramaniam, S. Propp, B. A. Lollo, S. Freier, C. F. Bennett, S. Bhanot, and B. P. Monia.** 2006. miR-122 regulation of lipid metabolism revealed by in vivo antisense targeting. Cell Metab **3:**87-98.
101. **Evans, M. J., and B. F. Cravatt.** 2006. Mechanism-based profiling of enzyme families. Chem Rev **106:**3279-301.
102. **Evans, R. M., and D. J. Mangelsdorf.** Nuclear Receptors, RXR, and the Big Bang. Cell **157:**255-66.
103. **Farci, P.** New insights into the HCV quasispecies and compartmentalization. Semin Liver Dis **31:**356-74.
104. **Farci, P., and R. H. Purcell.** 2000. Clinical significance of hepatitis C virus genotypes and quasispecies. Semin Liver Dis **20:**103-26.
105. **Farh, K. K., A. Grimson, C. Jan, B. P. Lewis, W. K. Johnston, L. P. Lim, C. B. Burge, and D. P. Bartel.** 2005. The widespread impact of mammalian MicroRNAs on mRNA repression and evolution. Science **310:**1817-21.
106. **Felmlee, D. J., M. L. Hafirassou, M. Lefevre, T. F. Baumert, and C. Schuster.** Hepatitis C virus, cholesterol and lipoproteins--impact for the viral life cycle and pathogenesis of liver disease. Viruses **5:**1292-324.
107. **Flynn, R. A., L. Martin, R. C. Spitale, B. T. Do, S. M. Sagan, B. Zarnegar, K. Qu, P. A. Khavari, S. R. Quake, P. Sarnow, and H. Y. Chang.** Dissecting noncoding and pathogen RNA-protein interactomes. RNA **21:**135-43.
108. **Fornari, F., L. Gramantieri, C. Giovannini, A. Veronese, M. Ferracin, S. Sabbioni, G. A. Calin, G. L. Grazi, C. M. Croce, S. Tavolari, P. Chieco, M. Negrini, and L. Bolondi.** 2009. MiR-122/cyclin G1 interaction modulates p53 activity and affects doxorubicin sensitivity of human hepatocarcinoma cells. Cancer Res **69:**5761-7.
109. **Friebe, P., and R. Bartenschlager.** 2009. Role of RNA structures in genome terminal sequences of the hepatitis C virus for replication and assembly. J Virol **83:**11989-95.
110. **Friebe, P., V. Lohmann, N. Krieger, and R. Bartenschlager.** 2001. Sequences in the 5' nontranslated region of hepatitis C virus required for RNA replication. J Virol **75:**12047-57.
111. **Fry, M. J.** 1994. Structure, regulation and function of phosphoinositide 3-kinases. Biochim Biophys Acta **1226:**237-68.
112. **Fujino, T., M. Nakamuta, R. Yada, Y. Aoyagi, K. Yasutake, M. Kohjima, K. Fukuizumi, T. Yoshimoto, N. Harada, M. Yada, M. Kato, K. Kotoh, A. Taketomi, Y. Maehara, M.**

Nakashima, and M. Enjoji. 2010. Expression profile of lipid metabolism-associated genes in hepatitis C virus-infected human liver. Hepatol Res **40:**923-9.
113. **Fukasawa, M., Y. Tanaka, S. Sato, Y. Ono, Y. Nitahara-Kasahara, T. Suzuki, T. Miyamura, K. Hanada, and M. Nishijima.** 2006. Enhancement of de novo fatty acid biosynthesis in hepatic cell line Huh7 expressing hepatitis C virus core protein. Biol Pharm Bull **29:**1958-61.
114. **Funabashi, H., A. Kawaguchi, H. Tomoda, S. Omura, S. Okuda, and S. Iwasaki.** 1989. Binding site of cerulenin in fatty acid synthetase. J Biochem **105:**751-5.
115. **Gantier, M. P.** Processing of double-stranded RNA in Mammalian cells: a direct antiviral role? J Interferon Cytokine Res **34:**469-77.
116. **Gao, B., F. Hong, and S. Radaeva.** 2004. Host factors and failure of interferon-alpha treatment in hepatitis C virus. Hepatology **39:**880-90.
117. **Garcia-Mediavilla, M. V., S. Pisonero-Vaquero, E. Lima-Cabello, I. Benedicto, P. L. Majano, F. Jorquera, J. Gonzalez-Gallego, and S. Sanchez-Campos.** 2012. Liver X receptor [alpha]-mediated regulation of lipogenesis by core and NS5A proteins contributes to HCV-induced liver steatosis and HCV replication. Lab Invest **92:**11.
118. **Ge, Q., M. T. McManus, T. Nguyen, C. H. Shen, P. A. Sharp, H. N. Eisen, and J. Chen.** 2003. RNA interference of influenza virus production by directly targeting mRNA for degradation and indirectly inhibiting all viral RNA transcription. Proc Natl Acad Sci U S A **100:**2718-23.
119. **Gebert, L. F., M. A. Rebhan, S. E. Crivelli, R. Denzler, M. Stoffel, and J. Hall.** Miravirsen (SPC3649) can inhibit the biogenesis of miR-122. Nucleic Acids Res **42:**609-21.
120. **Geiger, T., A. Wehner, C. Schaab, J. Cox, and M. Mann.** Comparative proteomic analysis of eleven common cell lines reveals ubiquitous but varying expression of most proteins. Mol Cell Proteomics **11:**M111 014050.
121. **Godi, A., P. Pertile, R. Meyers, P. Marra, G. Di Tullio, C. Iurisci, A. Luini, D. Corda, and M. A. De Matteis.** 1999. ARF mediates recruitment of PtdIns-4-OH kinase-beta and stimulates synthesis of PtdIns(4,5)P2 on the Golgi complex. Nat Cell Biol **1:**280-7.
122. **Goffard, A., N. Callens, B. Bartosch, C. Wychowski, F. L. Cosset, C. Montpellier, and J. Dubuisson.** 2005. Role of N-linked glycans in the functions of hepatitis C virus envelope glycoproteins. J Virol **79:**8400-9.
123. **Gogela, N. A., M. V. Lin, J. L. Wisocky, and R. T. Chung.** Enhancing our understanding of current therapies for hepatitis C virus (HCV). Curr HIV/AIDS Rep **12:**68-78.
124. **Gosert, R., D. Egger, V. Lohmann, R. Bartenschlager, H. E. Blum, K. Bienz, and D. Moradpour.** 2003. Identification of the hepatitis C virus RNA replication complex in Huh-7 cells harboring subgenomic replicons. J Virol **77:**5487-92.
125. **Gouttenoire, J., F. Penin, and D. Moradpour.** Hepatitis C virus nonstructural protein 4B: a journey into unexplored territory. Rev Med Virol **20:**117-29.
126. **Graham, T. R., and C. G. Burd.** 2011. Coordination of Golgi functions by phosphatidylinositol 4-kinases. Trends in cell biology **21:**113-121.
127. **Grimson, A., K. K. Farh, W. K. Johnston, P. Garrett-Engele, L. P. Lim, and D. P. Bartel.** 2007. MicroRNA targeting specificity in mammals: determinants beyond seed pairing. Mol Cell **27:**91-105.
128. **Group, G. B. O. H. C. W.** 2004. Global burden of disease (GBD) for hepatitis C. J Clin Pharmacol **44:**20-29.
129. **Gu, S., L. Jin, F. Zhang, P. Sarnow, and M. A. Kay.** 2009. Biological basis for restriction of microRNA targets to the 3' untranslated region in mammalian mRNAs. Nat Struct Mol Biol **16:**144-50.
130. **Guo, H., N. T. Ingolia, J. S. Weissman, and D. P. Bartel.** 2010. Mammalian microRNAs predominantly act to decrease target mRNA levels. Nature **466:**835-40.
131. **Guo, J. T., V. V. Bichko, and C. Seeger.** 2001. Effect of alpha interferon on the hepatitis C virus replicon. J Virol **75:**8516-23.

132. **Hagiwara, H., Y. Tajika, T. Matsuzaki, T. Suzuki, T. Aoki, and K. Takata.** 2006. Localization of Golgi 58K protein (formiminotransferase cyclodeaminase) to the centrosome. Histochem Cell Biol **126:**251-9.
133. **Halvorson, D. L., and S. A. McCune.** 1984. Inhibition of fatty acid synthesis in isolated adipocytes by 5-(tetradecyloxy)-2-furoic acid. Lipids **19:**851-6.
134. **Hamilton, A., O. Voinnet, L. Chappell, and D. Baulcombe.** 2002. Two classes of short interfering RNA in RNA silencing. EMBO J **21:**4671-9.
135. **Harrington, M.** 2012. State of the (research) chimp. Lab Anim (NY) **41:**31.
136. **Harrow, J., A. Frankish, J. M. Gonzalez, E. Tapanari, M. Diekhans, F. Kokocinski, B. L. Aken, D. Barrell, A. Zadissa, S. Searle, I. Barnes, A. Bignell, V. Boychenko, T. Hunt, M. Kay, G. Mukherjee, J. Rajan, G. Despacio-Reyes, G. Saunders, C. Steward, R. Harte, M. Lin, C. Howald, A. Tanzer, T. Derrien, J. Chrast, N. Walters, S. Balasubramanian, B. Pei, M. Tress, J. M. Rodriguez, I. Ezkurdia, J. van Baren, M. Brent, D. Haussler, M. Kellis, A. Valencia, A. Reymond, M. Gerstein, R. Guigo, and T. J. Hubbard.** GENCODE: the reference human genome annotation for The ENCODE Project. Genome Res **22:**1760-74.
137. **Hausser, A., P. Storz, S. Martens, G. Link, A. Toker, and K. Pfizenmaier.** 2005. Protein kinase D regulates vesicular transport by phosphorylating and activating phosphatidylinositol-4 kinase IIIbeta at the Golgi complex. Nat Cell Biol **7:**880-6.
138. **He, Y., H. Nakao, S. L. Tan, S. J. Polyak, P. Neddermann, S. Vijaysri, B. L. Jacobs, and M. G. Katze.** 2002. Subversion of cell signaling pathways by hepatitis C virus nonstructural 5A protein via interaction with Grb2 and P85 phosphatidylinositol 3-kinase. J Virol **76:**9207-17.
139. **Heale, B. S., H. S. Soifer, C. Bowers, and J. J. Rossi.** 2005. siRNA target site secondary structure predictions using local stable substructures. Nucleic Acids Res **33:**e30.
140. **Heaton, N. S., R. Perera, K. L. Berger, S. Khadka, D. J. LaCount, R. J. Kuhn, and G. Randall.** 2010. Dengue virus nonstructural protein 3 redistributes fatty acid synthase to sites of viral replication and increases cellular fatty acid synthesis. Proceedings of the National Academy of Sciences **107:**17345-17350.
141. **Heaton, N. S., and G. Randall.** Multifaceted roles for lipids in viral infection. Trends Microbiol **19:**368-75.
142. **Hebert, S. S., and B. De Strooper.** 2009. Alterations of the microRNA network cause neurodegenerative disease. Trends Neurosci **32:**199-206.
143. **Helenius, A.** 2013. p. 87-104. *In* D. H. Knipe, PM. (ed.), Fields Virology, 6th ed, vol. 1. Lippincott Williams & Wilkins, Philadelphia.
144. **Henke, J. I., D. Goergen, J. Zheng, Y. Song, C. G. Schuttler, C. Fehr, C. Junemann, and M. Niepmann.** 2008. microRNA-122 stimulates translation of hepatitis C virus RNA. EMBO J **27:**3300-10.
145. **Herker, E., and M. Ott.** 2011. Unique ties between hepatitis C virus replication and intracellular lipids. Trends Endocrinol Metab **22:**241-8.
146. **Hijikata, M., H. Mizushima, T. Akagi, S. Mori, N. Kakiuchi, N. Kato, T. Tanaka, K. Kimura, and K. Shimotohno.** 1993. Two distinct proteinase activities required for the processing of a putative nonstructural precursor protein of hepatitis C virus. J Virol **67:**4665-75.
147. **Hijikata, M., H. Mizushima, Y. Tanji, Y. Komoda, Y. Hirowatari, T. Akagi, N. Kato, K. Kimura, and K. Shimotohno.** 1993. Proteolytic processing and membrane association of putative nonstructural proteins of hepatitis C virus. Proc Natl Acad Sci U S A **90:**10773-7.
148. **Holen, T., M. Amarzguioui, M. T. Wiiger, E. Babaie, and H. Prydz.** 2002. Positional effects of short interfering RNAs targeting the human coagulation trigger Tissue Factor. Nucleic Acids Res **30:**1757-66.
149. **Holz, C. L., E. Albina, C. Minet, R. Lancelot, O. Kwiatek, G. Libeau, and R. Servan de Almeida.** RNA interference against animal viruses: how morbilliviruses generate extended diversity to escape small interfering RNA control. J Virol **86:**786-95.

150. **Hope, R. G., D. J. Murphy, and J. McLauchlan.** 2002. The domains required to direct core proteins of hepatitis C virus and GB virus-B to lipid droplets share common features with plant oleosin proteins. J Biol Chem **277:**4261-70.
151. **Horton, J. D., J. L. Goldstein, and M. S. Brown.** 2002. SREBPs: activators of the complete program of cholesterol and fatty acid synthesis in the liver. J Clin Invest **109:**1125-31.
152. **Horton, J. D., J. L. Goldstein, and M. S. Brown.** 2002. SREBPs: transcriptional mediators of lipid homeostasis. Cold Spring Harb Symp Quant Biol **67:**491-8.
153. **Houghton, M.** 2011. Prospects for prophylactic and therapeutic vaccines against the hepatitis C viruses. Immunol Rev **239:**99-108.
154. **Hsu, N. Y., O. Ilnytska, G. Belov, M. Santiana, Y. H. Chen, P. M. Takvorian, C. Pau, H. van der Schaar, N. Kaushik-Basu, T. Balla, C. E. Cameron, E. Ehrenfeld, F. J. van Kuppeveld, and N. Altan-Bonnet.** 2010. Viral reorganization of the secretory pathway generates distinct organelles for RNA replication. Cell **141:**799-811.
155. **Hsu, P. W., L. Z. Lin, S. D. Hsu, J. B. Hsu, and H. D. Huang.** 2007. ViTa: prediction of host microRNAs targets on viruses. Nucleic Acids Res **35:**D381-5.
156. **Huang, J. T., C. P. Tseng, M. H. Liao, S. C. Lu, W. Z. Yeh, N. Sakamoto, C. M. Chen, and J. C. Cheng.** Hepatitis C virus replication is modulated by the interaction of non-structural protein NS5B and fatty acid synthase. J Virol.
157. **Hutvagner, G.** 2005. Small RNA asymmetry in RNAi: function in RISC assembly and gene regulation. FEBS Lett **579:**5850-7.
158. **Hutvagner, G., and P. D. Zamore.** 2002. A microRNA in a multiple-turnover RNAi enzyme complex. Science **297:**2056-60.
159. **Idrees, S., U. A. Ashfaq, and S. Khaliq.** 2013. RNAi: antiviral therapy against dengue virus. Asian Pac J Trop Biomed **3:**232-6.
160. **Ikeda, M., M. Yi, K. Li, and S. M. Lemon.** 2002. Selectable subgenomic and genome-length dicistronic RNAs derived from an infectious molecular clone of the HCV-N strain of hepatitis C virus replicate efficiently in cultured Huh7 cells. J Virol **76:**2997-3006.
161. **Ikeda, S., S. W. Kong, J. Lu, E. Bisping, H. Zhang, P. D. Allen, T. R. Golub, B. Pieske, and W. T. Pu.** 2007. Altered microRNA expression in human heart disease. Physiol Genomics **31:**367-73.
162. **Ipsaro, J. J., and L. Joshua-Tor.** From guide to target: molecular insights into eukaryotic RNA-interference machinery. Nat Struct Mol Biol **22:**20-28.
163. **Ishihama, Y., Y. Oda, T. Tabata, T. Sato, T. Nagasu, J. Rappsilber, and M. Mann.** 2005. Exponentially modified protein abundance index (emPAI) for estimation of absolute protein amount in proteomics by the number of sequenced peptides per protein. Mol Cell Proteomics **4:**1265-72.
164. **Ivashkina, N., B. Wolk, V. Lohmann, R. Bartenschlager, H. E. Blum, F. Penin, and D. Moradpour.** 2002. The hepatitis C virus RNA-dependent RNA polymerase membrane insertion sequence is a transmembrane segment. J Virol **76:**13088-93.
165. **Jackel-Cram, C., L. A. Babiuk, and Q. Liu.** 2007. Up-regulation of fatty acid synthase promoter by hepatitis C virus core protein: Genotype-3a core has a stronger effect than genotype-1b core. Journal of Hepatology **46:**999-1008.
166. **Jackel-Cram, C., L. Qiao, Z. Xiang, R. Brownlie, Y. Zhou, L. Babiuk, and Q. Liu.** 2010. Hepatitis C virus genotype-3a core protein enhances sterol regulatory element-binding protein-1 activity through the phosphoinositide 3-kinase-Akt-2 pathway. J Gen Virol **91:**1388-95.
167. **Jacobsen, A., J. Wen, D. S. Marks, and A. Krogh.** Signatures of RNA binding proteins globally coupled to effective microRNA target sites. Genome Res **20:**1010-9.
168. **Jangra, R. K., M. Yi, and S. M. Lemon.** 2010. miR-122 Regulation of Hepatitis C Virus Translation and Infectious Virus Production. J Virol.
169. **Jangra, R. K., M. Yi, and S. M. Lemon.** 2010. Regulation of hepatitis C virus translation and infectious virus production by the microRNA miR-122. J Virol **84:**6615-25.

170. **Janssen, H. L., H. W. Reesink, E. J. Lawitz, S. Zeuzem, M. Rodriguez-Torres, K. Patel, A. J. van der Meer, A. K. Patick, A. Chen, Y. Zhou, R. Persson, B. D. King, S. Kauppinen, A. A. Levin, and M. R. Hodges.** 2013. Treatment of HCV infection by targeting microRNA. N Engl J Med **368:**1685-94.
171. **Jayakumar, A., S. S. Chirala, and S. J. Wakil.** 1997. Human fatty acid synthase: assembling recombinant halves of the fatty acid synthase subunit protein reconstitutes enzyme activity. Proc Natl Acad Sci U S A **94:**12326-30.
172. **Jessani, N., and B. F. Cravatt.** 2004. The development and application of methods for activity-based protein profiling. Curr Opin Chem Biol **8:**54-9.
173. **Jiang, M., and J. Milner.** 2002. Selective silencing of viral gene expression in HPV-positive human cervical carcinoma cells treated with siRNA, a primer of RNA interference. Oncogene **21:**6041-8.
174. **Johansson, P., B. Mulinacci, C. Koestler, R. Vollrath, D. Oesterhelt, and M. Grininger.** 2009. Multimeric options for the auto-activation of the Saccharomyces cerevisiae FAS type I megasynthase. Structure **17:**1063-74.
175. **Jones, D. M., and J. McLauchlan.** Hepatitis C virus: assembly and release of virus particles. J Biol Chem **285:**22733-9.
176. **Jopling, C.** Liver-specific microRNA-122: Biogenesis and function. RNA Biol **9:**137-42.
177. **Jopling, C. L., S. Schutz, and P. Sarnow.** 2008. Position-dependent function for a tandem microRNA miR-122-binding site located in the hepatitis C virus RNA genome. Cell Host Microbe **4:**77-85.
178. **Jopling, C. L., M. Yi, A. M. Lancaster, S. M. Lemon, and P. Sarnow.** 2005. Modulation of hepatitis C virus RNA abundance by a liver-specific MicroRNA. Science **309:**1577-81.
179. **Joshi, A. K., A. Witkowski, and S. Smith.** 1997. Mapping of functional interactions between domains of the animal fatty acid synthase by mutant complementation in vitro. Biochemistry **36:**2316-22.
180. **Joshi, D., M. Pinzani, I. Carey, and K. Agarwal.** 2014. Recurrent HCV after liver transplantation-mechanisms, assessment and therapy. Nat Rev Gastroenterol Hepatol.
181. **Joven, J., E. Espinel, A. Rull, R. Beltran-Debon, G. Aragones, E. Rodriguez-Gallego, J. Camps, J. Pedro-Botet, T. Sans, J. A. Menendez, and C. Alonso-Villaverde.** 2011. Serum fatty acid synthase concentration is increased in patients with hepatitis viral infection and may assist in the prediction of liver steatosis. J Clin Virol **51:**199-201.
182. **Kalesh, K. A., D. S. Sim, J. Wang, K. Liu, Q. Lin, and S. Q. Yao.** Small molecule probes that target Abl kinase. Chem Commun (Camb) **46:**1118-20.
183. **Kapadia, S. B., and F. V. Chisari.** 2005. Hepatitis C virus RNA replication is regulated by host geranylgeranylation and fatty acids. Proc Natl Acad Sci U S A **102:**2561-6.
184. **Kaplan, D. R., M. Whitman, B. Schaffhausen, D. C. Pallas, M. White, L. Cantley, and T. M. Roberts.** 1987. Common elements in growth factor stimulation and oncogenic transformation: 85 kd phosphoprotein and phosphatidylinositol kinase activity. Cell **50:**1021-9.
185. **Karlikow, M., B. Goic, and M. C. Saleh.** RNAi and antiviral defense in Drosophila: setting up a systemic immune response. Dev Comp Immunol **42:**85-92.
186. **Kato, T., T. Date, M. Miyamoto, Z. Zhao, M. Mizokami, and T. Wakita.** 2005. Nonhepatic cell lines HeLa and 293 support efficient replication of the hepatitis C virus genotype 2a subgenomic replicon. J Virol **79:**592-6.
187. **Kedde, M., M. J. Strasser, B. Boldajipour, J. A. Oude Vrielink, K. Slanchev, C. le Sage, R. Nagel, P. M. Voorhoeve, J. van Duijse, U. A. Orom, A. H. Lund, A. Perrakis, E. Raz, and R. Agami.** 2007. RNA-binding protein Dnd1 inhibits microRNA access to target mRNA. Cell **131:**1273-86.
188. **Kertesz, M., N. Iovino, U. Unnerstall, U. Gaul, and E. Segal.** 2007. The role of site accessibility in microRNA target recognition. Nat Genet **39:**1278-84.

189. **Khan, I., D. S. Katikaneni, Q. Han, L. Sanchez-Felipe, K. Hanada, R. L. Ambrose, J. M. Mackenzie, and K. V. Konan.** Modulation of hepatitis C virus genome replication by glycosphingolipids and four-phosphate adaptor protein 2. J Virol **88:**12276-95.
190. **Khattab, M. A.** 2009. Targeting host factors: a novel rationale for the management of hepatitis C virus. World J Gastroenterol **15:**3472-9.
191. **Khvorova, A., A. Reynolds, and S. D. Jayasena.** 2003. Functional siRNAs and miRNAs exhibit strand bias. Cell **115:**209-16.
192. **Kieffer, T. L., and S. George.** Resistance to hepatitis C virus protease inhibitors. Curr Opin Virol **8C:**16-21.
193. **Kim, K. H., S. P. Hong, K. Kim, M. J. Park, K. J. Kim, and J. Cheong.** 2007. HCV core protein induces hepatic lipid accumulation by activating SREBP1 and PPARgamma. Biochem Biophys Res Commun **355:**883-8.
194. **Kim, K. H., F. Lopez-Casillas, D. H. Bai, X. Luo, and M. E. Pape.** 1989. Role of reversible phosphorylation of acetyl-CoA carboxylase in long-chain fatty acid synthesis. FASEB J **3:**2250-6.
195. **Kim, M. S., S. M. Pinto, D. Getnet, R. S. Nirujogi, S. S. Manda, R. Chaerkady, A. K. Madugundu, D. S. Kelkar, R. Isserlin, S. Jain, J. K. Thomas, B. Muthusamy, P. Leal-Rojas, P. Kumar, N. A. Sahasrabuddhe, L. Balakrishnan, J. Advani, B. George, S. Renuse, L. D. Selvan, A. H. Patil, V. Nanjappa, A. Radhakrishnan, S. Prasad, T. Subbannayya, R. Raju, M. Kumar, S. K. Sreenivasamurthy, A. Marimuthu, G. J. Sathe, S. Chavan, K. K. Datta, Y. Subbannayya, A. Sahu, S. D. Yelamanchi, S. Jayaram, P. Rajagopalan, J. Sharma, K. R. Murthy, N. Syed, R. Goel, A. A. Khan, S. Ahmad, G. Dey, K. Mudgal, A. Chatterjee, T. C. Huang, J. Zhong, X. Wu, P. G. Shaw, D. Freed, M. S. Zahari, K. K. Mukherjee, S. Shankar, A. Mahadevan, H. Lam, C. J. Mitchell, S. K. Shankar, P. Satishchandra, J. T. Schroeder, R. Sirdeshmukh, A. Maitra, S. D. Leach, C. G. Drake, M. K. Halushka, T. S. Prasad, R. H. Hruban, C. L. Kerr, G. D. Bader, C. A. Iacobuzio-Donahue, H. Gowda, and A. Pandey.** A draft map of the human proteome. Nature **509:**575-81.
196. **Kim, Y. K., C. S. Kim, S. H. Lee, and S. K. Jang.** 2002. Domains I and II in the 5' nontranslated region of the HCV genome are required for RNA replication. Biochem Biophys Res Commun **290:**105-12.
197. **Kim, Y. K., S. H. Lee, C. S. Kim, S. K. Seol, and S. K. Jang.** 2003. Long-range RNA-RNA interaction between the 5' nontranslated region and the core-coding sequences of hepatitis C virus modulates the IRES-dependent translation. RNA **9:**599-606.
198. **Knight, Z. A., B. Gonzalez, M. E. Feldman, E. R. Zunder, D. D. Goldenberg, O. Williams, R. Loewith, D. Stokoe, A. Balla, B. Toth, T. Balla, W. A. Weiss, R. L. Williams, and K. M. Shokat.** 2006. A pharmacological map of the PI3-K family defines a role for p110alpha in insulin signaling. Cell **125:**733-47.
199. **Knight, Z. A., and K. M. Shokat.** 2005. Features of selective kinase inhibitors. Chem Biol **12:**621-37.
200. **Knowles, L. M., F. Axelrod, C. D. Browne, and J. W. Smith.** 2004. A fatty acid synthase blockade induces tumor cell-cycle arrest by down-regulating Skp2. J Biol Chem **279:**30540-5.
201. **Kohli, A., A. Shaffer, A. Sherman, and S. Kottilil.** Treatment of hepatitis C: a systematic review. JAMA **312:**631-40.
202. **Kolb, H. C., M. G. Finn, and K. B. Sharpless.** 2001. Click Chemistry: Diverse Chemical Function from a Few Good Reactions. Angew Chem Int Ed Engl **40:**2004-2021.
203. **Kretschmer-Kazemi Far, R., and G. Sczakiel.** 2003. The activity of siRNA in mammalian cells is related to structural target accessibility: a comparison with antisense oligonucleotides. Nucleic Acids Res **31:**4417-24.
204. **Krieger, N., V. Lohmann, and R. Bartenschlager.** 2001. Enhancement of hepatitis C virus RNA replication by cell culture-adaptive mutations. J Virol **75:**4614-24.

205. **Krishnamurty, R., J. L. Brigham, S. E. Leonard, P. Ranjitkar, E. T. Larson, E. J. Dale, E. A. Merritt, and D. J. Maly.** Active site profiling reveals coupling between domains in SRC-family kinases. Nat Chem Biol **9:**43-50.
206. **Kuhajda, F. P.** 2006. Fatty acid synthase and cancer: new application of an old pathway. Cancer Res **66:**5977-80.
207. **Kuhajda, F. P., E. S. Pizer, J. N. Li, N. S. Mani, G. L. Frehywot, and C. A. Townsend.** 2000. Synthesis and antitumor activity of an inhibitor of fatty acid synthase. Proc Natl Acad Sci U S A **97:**3450-4.
208. **Kuiken, C., C. Combet, J. Bukh, I. T. Shin, G. Deleage, M. Mizokami, R. Richardson, E. Sablon, K. Yusim, J. M. Pawlotsky, and P. Simmonds.** 2006. A comprehensive system for consistent numbering of HCV sequences, proteins and epitopes. Hepatology **44:**1355-61.
209. **Kumar, D., G. C. Farrell, J. Kench, and J. George.** 2005. Hepatic steatosis and the risk of hepatocellular carcinoma in chronic hepatitis C. J Gastroenterol Hepatol **20:**1395-400.
210. **Kwon, H. J., W. Xing, K. Chan, A. Niedziela-Majka, K. M. Brendza, T. Kirschberg, D. Kato, J. O. Link, G. Cheng, X. Liu, and R. Sakowicz.** Direct binding of ledipasvir to HCV NS5A: mechanism of resistance to an HCV antiviral agent. PLoS One **10:**e0122844.
211. **Lanford, R. E., C. Bigger, S. Bassett, and G. Klimpel.** 2001. The chimpanzee model of hepatitis C virus infections. ILAR J **42:**117-26.
212. **Lanford, R. E., E. S. Hildebrandt-Eriksen, A. Petri, R. Persson, M. Lindow, M. E. Munk, S. Kauppinen, and H. Orum.** 2010. Therapeutic silencing of microRNA-122 in primates with chronic hepatitis C virus infection. Science **327:**198-201.
213. **Lavanchy, D.** 2009. The global burden of hepatitis C. Liver Int **29 Suppl 1:**74-81.
214. **Lecellier, C. H., P. Dunoyer, K. Arar, J. Lehmann-Che, S. Eyquem, C. Himber, A. Saib, and O. Voinnet.** 2005. A cellular microRNA mediates antiviral defense in human cells. Science **308:**557-60.
215. **Lee, C.** Roles of phosphoinositides and phosphoinositides kinases in hepatitis C virus RNA replication. Arch Pharm Res **35:**1701-11.
216. **Lee, H., H. Shin, E. Wimmer, and A. V. Paul.** 2004. cis-acting RNA signals in the NS5B C-terminal coding sequence of the hepatitis C virus genome. J Virol **78:**10865-77.
217. **Lerat, H., H. L. Kammoun, I. Hainault, E. Merour, M. R. Higgs, C. Callens, S. M. Lemon, F. Foufelle, and J. M. Pawlotsky.** 2009. Hepatitis C virus proteins induce lipogenesis and defective triglyceride secretion in transgenic mice. J Biol Chem **284:**33466-74.
218. **Lewis, A. P., and C. L. Jopling.** 2010. Regulation and biological function of the liver-specific miR-122. Biochem Soc Trans **38:**1553-7.
219. **Lewis, B. P., C. B. Burge, and D. P. Bartel.** 2005. Conserved seed pairing, often flanked by adenosines, indicates that thousands of human genes are microRNA targets. Cell **120:**15-20.
220. **Lewis, B. P., I. H. Shih, M. W. Jones-Rhoades, D. P. Bartel, and C. B. Burge.** 2003. Prediction of mammalian microRNA targets. Cell **115:**787-98.
221. **Li, B. H., X. F. Ma, Y. Wang, and W. X. Tian.** 2005. Structure-activity relationship of polyphenols that inhibit fatty acid synthase. J Biochem **138:**679-85.
222. **Li, Q., A. L. Brass, A. Ng, Z. Hu, R. J. Xavier, T. J. Liang, and S. J. Elledge.** 2009. A genome-wide genetic screen for host factors required for hepatitis C virus propagation. Proc Natl Acad Sci U S A **106:**16410-5.
223. **Li, S., M. S. Brown, and J. L. Goldstein.** Bifurcation of insulin signaling pathway in rat liver: mTORC1 required for stimulation of lipogenesis, but not inhibition of gluconeogenesis. Proc Natl Acad Sci U S A **107:**3441-6.
224. **Li, W., J. L. Blankman, and B. F. Cravatt.** 2007. A functional proteomic strategy to discover inhibitors for uncharacterized hydrolases. J Am Chem Soc **129:**9594-5.
225. **Li, Y., T. Masaki, and S. M. Lemon.** miR-122 and the Hepatitis C RNA genome: more than just stability. RNA Biol **10:**919-23.

226. **Li, Y., T. Masaki, D. Yamane, D. R. McGivern, and S. M. Lemon.** Competing and noncompeting activities of miR-122 and the 5' exonuclease Xrn1 in regulation of hepatitis C virus replication. Proc Natl Acad Sci U S A **110:**1881-6.
227. **Li, Y. M., M. Xu, M. T. Lai, Q. Huang, J. L. Castro, J. DiMuzio-Mower, T. Harrison, C. Lellis, A. Nadin, J. G. Neduvelil, R. B. Register, M. K. Sardana, M. S. Shearman, A. L. Smith, X. P. Shi, K. C. Yin, J. A. Shafer, and S. J. Gardell.** 2000. Photoactivated gamma-secretase inhibitors directed to the active site covalently label presenilin 1. Nature **405:**689-94.
228. **Liefhebber, J. M., B. W. Brandt, R. Broer, W. J. Spaan, and H. C. van Leeuwen.** 2009. Hepatitis C virus NS4B carboxy terminal domain is a membrane binding domain. Virol J **6:**62.
229. **Lindenbach, B. D.** 2013. Virion assembly and release. Curr Top Microbiol Immunol **369:**199-218.
230. **Lindenbach, B. D., and C. M. Rice.** 2013. Flaviviridae, p. 712–746. *In* Knipe DM and H. PM (ed.), Fields Virology, 6th ed, vol. 1. Lippincott Williams & Wilkins, Philadelphia.
231. **Lindenbach, B. D., and C. M. Rice.** 2013. The ins and outs of hepatitis C virus entry and assembly. Nat Rev Microbiol **11:**688-700.
232. **Lindenbach, B. D., and C. M. Rice.** 2005. Unravelling hepatitis C virus replication from genome to function. Nature **436:**933-8.
233. **Listenberger, L. L., X. Han, S. E. Lewis, S. Cases, R. V. Farese, Jr., D. S. Ory, and J. E. Schaffer.** 2003. Triglyceride accumulation protects against fatty acid-induced lipotoxicity. Proc Natl Acad Sci U S A **100:**3077-82.
234. **Liu, H., J. Y. Liu, X. Wu, and J. T. Zhang.** Biochemistry, molecular biology, and pharmacology of fatty acid synthase, an emerging therapeutic target and diagnosis/prognosis marker. Int J Biochem Mol Biol **1:**69-89.
235. **Liu, Y., M. P. Patricelli, and B. F. Cravatt.** 1999. Activity-based protein profiling: the serine hydrolases. Proc Natl Acad Sci U S A **96:**14694-9.
236. **Liu, Y., K. R. Shreder, W. Gai, S. Corral, D. K. Ferris, and J. S. Rosenblum.** 2005. Wortmannin, a widely used phosphoinositide 3-kinase inhibitor, also potently inhibits mammalian polo-like kinase. Chem Biol **12:**99-107.
237. **Livak, K. J., and T. D. Schmittgen.** 2001. Analysis of relative gene expression data using real-time quantitative PCR and the 2(-Delta Delta C(T)) Method. Methods **25:**402-8.
238. **Lohmann, V., and R. Bartenschlager.** 2014. On the history of hepatitis C virus cell culture systems. J Med Chem **57:**1627-42.
239. **Lohmann, V., F. Korner, A. Dobierzewska, and R. Bartenschlager.** 2001. Mutations in hepatitis C virus RNAs conferring cell culture adaptation. J Virol **75:**1437-49.
240. **Lohmann, V., F. Korner, J. Koch, U. Herian, L. Theilmann, and R. Bartenschlager.** 1999. Replication of subgenomic hepatitis C virus RNAs in a hepatoma cell line. Science **285:**110-3.
241. **Long, D., R. Lee, P. Williams, C. Y. Chan, V. Ambros, and Y. Ding.** 2007. Potent effect of target structure on microRNA function. Nat Struct Mol Biol **14:**287-94.
242. **Love, T. M., H. F. Moffett, and C. D. Novina.** 2008. Not miR-ly small RNAs: big potential for microRNAs in therapy. J Allergy Clin Immunol **121:**309-19.
243. **Luna, J. M., T. K. Scheel, T. Danino, K. S. Shaw, A. Mele, J. J. Fak, E. Nishiuchi, C. N. Takacs, M. T. Catanese, Y. P. de Jong, I. M. Jacobson, C. M. Rice, and R. B. Darnell.** Hepatitis C virus RNA functionally sequesters miR-122. Cell **160:**1099-110.
244. **Lupu, R., and J. A. Menendez.** 2006. Pharmacological inhibitors of Fatty Acid Synthase (FASN)--catalyzed endogenous fatty acid biogenesis: a new family of anti-cancer agents? Curr Pharm Biotechnol **7:**483-93.
245. **Lyn, R. K., D. C. Kennedy, A. Stolow, A. Ridsdale, and J. P. Pezacki.** 2010. Dynamics of lipid droplets induced by the hepatitis C virus core protein. Biochem Biophys Res Commun **399:**518-24.

246. **Macdonald, A., K. Crowder, A. Street, C. McCormick, and M. Harris.** 2004. The hepatitis C virus NS5A protein binds to members of the Src family of tyrosine kinases and regulates kinase activity. J Gen Virol **85:**721-9.
247. **Macheboeuf, P., C. Contreras-Martel, V. Job, O. Dideberg, and A. Dessen.** 2006. Penicillin binding proteins: key players in bacterial cell cycle and drug resistance processes. FEMS Microbiol Rev **30:**673-91.
248. **Maehama, T., M. Fukasawa, T. Date, T. Wakita, and K. Hanada.** A class II phosphoinositide 3-kinase plays an indispensable role in hepatitis C virus replication. Biochem Biophys Res Commun **440:**150-6.
249. **Mahajan, V. S., A. Drake, and J. Chen.** 2009. Virus-specific host miRNAs: antiviral defenses or promoters of persistent infection? Trends Immunol **30:**1-7.
250. **Maheshwari, A., S. Ray, and P. J. Thuluvath.** 2008. Acute hepatitis C. Lancet **372:**321-32.
251. **Mailly, L., E. Robinet, P. Meuleman, T. F. Baumert, and M. B. Zeisel.** 2013. Hepatitis C virus infection and related liver disease: the quest for the best animal model. Front Microbiol **4:**213.
252. **Majeau, N., R. Fromentin, C. Savard, M. Duval, M. J. Tremblay, and D. Leclerc.** 2009. Palmitoylation of hepatitis C virus core protein is important for virion production. J Biol Chem **284:**33915-25.
253. **Malic, L., T. Veres, and M. Tabrizian.** 2009. Biochip functionalization using electrowetting-on-dielectric digital microfluidics for surface plasmon resonance imaging detection of DNA hybridization. Biosens Bioelectron **24:**2218-24.
254. **Manders, E. M. M., F. J. Verbeek, and J. A. Aten.** 1993. Measurement of co-localization of objects in dual-colour confocal images. Journal of Microscopy **169:**375-382.
255. **Mark, D., S. Haeberle, G. Roth, F. von Stetten, and R. Zengerle.** Microfluidic lab-on-a-chip platforms: requirements, characteristics and applications. Chem Soc Rev **39:**1153-82.
256. **MartÃn-Acebes, M. A., A.-B. n. BlÃ¡zquez, N. JimÃ©nez de Oya, E. Escribano-Romero, and J.-C. Saiz.** 2011. West Nile Virus Replication Requires Fatty Acid Synthesis but Is Independent on Phosphatidylinositol-4-Phosphate Lipids. PLoS One **6:**e24970.
257. **Martin, B. R., C. Wang, A. Adibekian, S. E. Tully, and B. F. Cravatt.** 2011. Global profiling of dynamic protein palmitoylation. Nat Methods **9:**84-9.
258. **Matranga, C., Y. Tomari, C. Shin, D. P. Bartel, and P. D. Zamore.** 2005. Passenger-strand cleavage facilitates assembly of siRNA into Ago2-containing RNAi enzyme complexes. Cell **123:**607-20.
259. **McCrea, H. J., and P. De Camilli.** 2009. Mutations in phosphoinositide metabolizing enzymes and human disease. Physiology (Bethesda) **24:**8-16.
260. **McLauchlan, J., M. K. Lemberg, G. Hope, and B. Martoglio.** 2002. Intramembrane proteolysis promotes trafficking of hepatitis C virus core protein to lipid droplets. EMBO J **21:**3980-8.
261. **McMullan, L. K., A. Grakoui, M. J. Evans, K. Mihalik, M. Puig, A. D. Branch, S. M. Feinstone, and C. M. Rice.** 2007. Evidence for a functional RNA element in the hepatitis C virus core gene. Proc Natl Acad Sci U S A **104:**2879-84.
262. **Meister, G., and T. Tuschl.** 2004. Mechanisms of gene silencing by double-stranded RNA. Nature **431:**343-9.
263. **Mello, C., E. Aguayo, M. Rodriguez, G. Lee, R. Jordan, T. Cihlar, and G. Birkus.** Multiple classes of antiviral agents exhibit in vitro activity against human rhinovirus type C. Antimicrob Agents Chemother **58:**1546-55.
264. **Menendez, J. A., and R. Lupu.** 2007. Fatty acid synthase and the lipogenic phenotype in cancer pathogenesis. Nat Rev Cancer **7:**763-77.
265. **Menendez, J. A., A. Vazquez-Martin, F. J. Ortega, and J. M. Fernandez-Real.** 2009. Fatty acid synthase: association with insulin resistance, type 2 diabetes, and cancer. Clin Chem **55:**425-38.

266. **Mercer, D. F., D. E. Schiller, J. F. Elliott, D. N. Douglas, C. Hao, A. Rinfret, W. R. Addison, K. P. Fischer, T. A. Churchill, J. R. Lakey, D. L. Tyrrell, and N. M. Kneteman.** 2001. Hepatitis C virus replication in mice with chimeric human livers. Nat Med **7:**927-33.
267. **Merz, A., G. Long, M. S. Hiet, B. Brugger, P. Chlanda, P. Andre, F. Wieland, J. Krijnse-Locker, and R. Bartenschlager.** 2011. Biochemical and morphological properties of hepatitis C virus particles and determination of their lipidome. J Biol Chem **286:**3018-32.
268. **Mikkelsen, J., P. Hojrup, M. M. Rasmussen, P. Roepstorff, and J. Knudsen.** 1985. Amino acid sequence around the active-site serine residue in the acyltransferase domain of goat mammary fatty acid synthetase. Biochem J **227:**21-7.
269. **Miranda, K. C., T. Huynh, Y. Tay, Y. S. Ang, W. L. Tam, A. M. Thomson, B. Lim, and I. Rigoutsos.** 2006. A pattern-based method for the identification of MicroRNA binding sites and their corresponding heteroduplexes. Cell **126:**1203-17.
270. **Mirandola, S., S. Realdon, J. Iqbal, M. Gerotto, F. Dal Pero, G. Bortoletto, M. Marcolongo, A. Vario, C. Datz, M. M. Hussain, and A. Alberti.** 2006. Liver microsomal triglyceride transfer protein is involved in hepatitis C liver steatosis. Gastroenterology **130:**1661-9.
271. **Miyanari, Y., K. Atsuzawa, N. Usuda, K. Watashi, T. Hishiki, M. Zayas, R. Bartenschlager, T. Wakita, M. Hijikata, and K. Shimotohno.** 2007. The lipid droplet is an important organelle for hepatitis C virus production. Nat Cell Biol **9:**1089-97.
272. **Moche, M., G. Schneider, P. Edwards, K. Dehesh, and Y. Lindqvist.** 1999. Structure of the Complex between the Antibiotic Cerulenin and Its Target, Î²-Ketoacyl-Acyl Carrier Protein Synthase. Journal of Biological Chemistry **274:**6031-6034.
273. **Moghaddas Gholami, A., H. Hahne, Z. Wu, F. J. Auer, C. Meng, M. Wilhelm, and B. Kuster.** Global proteome analysis of the NCI-60 cell line panel. Cell Rep **4:**609-20.
274. **Mohd Hanafiah, K., J. Groeger, A. D. Flaxman, and S. T. Wiersma.** Global epidemiology of hepatitis C virus infection: new estimates of age-specific antibody to HCV seroprevalence. Hepatology **57:**1333-42.
275. **Moon, Y. A., N. A. Shah, S. Mohapatra, J. A. Warrington, and J. D. Horton.** 2001. Identification of a mammalian long chain fatty acyl elongase regulated by sterol regulatory element-binding proteins. J Biol Chem **276:**45358-66.
276. **Moradpour, D., F. Penin, and C. M. Rice.** 2007. Replication of hepatitis C virus. Nat Rev Microbiol **5:**453-63.
277. **Mortimer, S. A., and J. A. Doudna.** Unconventional miR-122 binding stabilizes the HCV genome by forming a trimolecular RNA structure. Nucleic Acids Res **41:**4230-40.
278. **Munoz, J., and A. J. Heck.** From the human genome to the human proteome. Angew Chem Int Ed Engl **53:**10864-6.
279. **Muoio, D. M., and C. B. Newgard.** 2008. Mechanisms of disease: molecular and metabolic mechanisms of insulin resistance and beta-cell failure in type 2 diabetes. Nat Rev Mol Cell Biol **9:**193-205.
280. **Murayama, A., T. Kato, D. Akazawa, N. Sugiyama, T. Date, T. Masaki, S. Nakamoto, Y. Tanaka, M. Mizokami, O. Yokosuka, A. Nomoto, and T. Wakita.** Production of infectious chimeric hepatitis C virus genotype 2b harboring minimal regions of JFH-1. J Virol **86:**2143-52.
281. **Nagaraj, N., J. R. Wisniewski, T. Geiger, J. Cox, M. Kircher, J. Kelso, S. Paabo, and M. Mann.** Deep proteome and transcriptome mapping of a human cancer cell line. Mol Syst Biol **7:**548.
282. **Nasheri, N., J. Cheng, R. Singaravelu, P. Wu, M. T. McDermott, and J. P. Pezacki.** 2011. An enzyme-linked assay for the rapid quantification of microRNAs based on the viral suppressor of RNA silencing protein p19. Anal Biochem **412:**165-72.
283. **Nasheri, N., M. Joyce, Y. Rouleau, P. Yang, S. Yao, D. L. Tyrrell, and J. P. Pezacki.** 2013. Modulation of fatty acid synthase enzyme activity and expression during hepatitis C virus replication. Chem Biol **20:**570-82.

284. **Nasheri, N., C. S. McKay, K. Fulton, S. Twine, M. H. Powdrill, A. R. Sherratt, and J. P. Pezacki.** 2014. Hydrophobic triaryl-substituted beta-lactams as activity-based probes for profiling eukaryotic enzymes and host-pathogen interactions. Chembiochem **15:**2195-200.
285. **Nasheri, N., R. Singaravelu, M. Goodmurphy, R. K. Lyn, and J. P. Pezacki.** 2011. Competing roles of microRNA-122 recognition elements in hepatitis C virus RNA. Virology **410:**336-44.
286. **Nguyen, H., M. Mudryj, M. Guadalupe, and S. Dandekar.** 2003. Hepatitis C virus core protein expression leads to biphasic regulation of the p21 cdk inhibitor and modulation of hepatocyte cell cycle. Virology **312:**245-53.
287. **Nguyen, L. T., E. Gray, J. Dean, M. Carr, J. Connell, C. De Gascun, L. A. Nguyen, A. O'Leary, C. Bergin, W. Hall, and S. Norris.** Baseline prevalence and emergence of protease inhibitor resistance mutations following treatment in chronic HCV genotype 1-infected individuals. Antivir Ther.
288. **Nguyen, P. L., J. Ma, J. E. Chavarro, M. L. Freedman, R. Lis, G. Fedele, C. Fiore, W. Qiu, M. Fiorentino, S. Finn, K. L. Penney, A. Eisenstein, F. R. Schumacher, L. A. Mucci, M. J. Stampfer, E. Giovannucci, and M. Loda.** 2010. Fatty acid synthase polymorphisms, tumor expression, body mass index, prostate cancer risk, and survival. J Clin Oncol **28:**3958-64.
289. **Nielsen, S. U., M. F. Bassendine, A. D. Burt, C. Martin, W. Pumeechockchai, and G. L. Toms.** 2006. Association between hepatitis C virus and very-low-density lipoprotein (VLDL)/LDL analyzed in iodixanol density gradients. J Virol **80:**2418-28.
290. **Niphakis, M. J., and B. F. Cravatt.** 2014. Enzyme inhibitor discovery by activity-based protein profiling. Annu Rev Biochem **83:**341-77.
291. **Nomura, D. K., M. M. Dix, and B. F. Cravatt.** 2010. Activity-based protein profiling for biochemical pathway discovery in cancer. Nat Rev Cancer **10:**630-8.
292. **Nookathota, M., and S. Mukherjee.** 2014. Antiviral therapy for chronic hepatitis C in 2014. Expert Rev Clin Pharmacol **7:**499-505.
293. **Novina, C. D., M. F. Murray, D. M. Dykxhoorn, P. J. Beresford, J. Riess, S. K. Lee, R. G. Collman, J. Lieberman, P. Shankar, and P. A. Sharp.** 2002. siRNA-directed inhibition of HIV-1 infection. Nat Med **8:**681-6.
294. **Obernosterer, G., H. Tafer, and J. Martinez.** 2008. Target site effects in the RNA interference and microRNA pathways. Biochem Soc Trans **36:**1216-9.
295. **Oem, J.-K., C. Jackel-Cram, Y.-P. Li, Y. Zhou, J. Zhong, H. Shimano, L. A. Babiuk, and Q. Liu.** 2008. Activation of sterol regulatory element-binding protein 1c and fatty acid synthase transcription by hepatitis C virus non-structural protein 2. Journal of General Virology **89:**1225-1230.
296. **Ohashi, P. S.** 2002. T-cell signalling and autoimmunity: molecular mechanisms of disease. Nat Rev Immunol **2:**427-38.
297. **Ohata, K., K. Hamasaki, K. Toriyama, K. Matsumoto, A. Saeki, K. Yanagi, S. Abiru, Y. Nakagawa, M. Shigeno, S. Miyazoe, T. Ichikawa, H. Ishikawa, K. Nakao, and K. Eguchi.** 2003. Hepatic steatosis is a risk factor for hepatocellular carcinoma in patients with chronic hepatitis C virus infection. Cancer **97:**3036-43.
298. **Orban, T. I., and E. Izaurralde.** 2005. Decay of mRNAs targeted by RISC requires XRN1, the Ski complex, and the exosome. RNA **11:**459-69.
299. **Otto, G. A., and J. D. Puglisi.** 2004. The pathway of HCV IRES-mediated translation initiation. Cell **119:**369-80.
300. **Ou, J., H. Tu, B. Shan, A. Luk, R. A. DeBose-Boyd, Y. Bashmakov, J. L. Goldstein, and M. S. Brown.** 2001. Unsaturated fatty acids inhibit transcription of the sterol regulatory element-binding protein-1c (SREBP-1c) gene by antagonizing ligand-dependent activation of the LXR. Proc Natl Acad Sci U S A **98:**6027-32.

301. **Ovaa, H., B. M. Kessler, U. Rolen, P. J. Galardy, H. L. Ploegh, and M. G. Masucci.** 2004. Activity-based ubiquitin-specific protease (USP) profiling of virus-infected and malignant human cells. Proc Natl Acad Sci U S A **101:**2253-8.
302. **Pacheco-Alvarez, D., R. S. Solorzano-Vargas, R. A. Gravel, R. Cervantes-Roldan, A. Velazquez, and A. Leon-Del-Rio.** 2004. Paradoxical regulation of biotin utilization in brain and liver and implications for inherited multiple carboxylase deficiency. J Biol Chem **279:**52312-8.
303. **Padmore, L., G. K. Radda, and K. A. Knox.** 1996. Wortmannin-mediated inhibition of phosphatidylinositol 3-kinase activity triggers apoptosis in normal and neoplastic B lymphocytes which are in cell cycle. Int Immunol **8:**585-94.
304. **Padwal, R. S., and S. R. Majumdar.** 2007. Drug treatments for obesity: orlistat, sibutramine, and rimonabant. Lancet **369:**71-7.
305. **Pappenberger, G. n., J. r. Benz, B. Gsell, M. Hennig, A. Ruf, M. Stihle, R. Thoma, and M. G. Rudolph.** 2010. Structure of the Human Fatty Acid Synthase KSâ€"MAT Didomain as a Framework for Inhibitor Design. Journal of Molecular Biology **397:**508-519.
306. **Park, C.-Y., H.-J. Jun, T. Wakita, J. H. Cheong, and S. B. Hwang.** 2009. Hepatitis C Virus Nonstructural 4B Protein Modulates Sterol Regulatory Element-binding Protein Signaling via the AKT Pathway. Journal of Biological Chemistry **284:**9237-9246.
307. **Patricelli, M. P., A. K. Szardenings, M. Liyanage, T. K. Nomanbhoy, M. Wu, H. Weissig, A. Aban, D. Chun, S. Tanner, and J. W. Kozarich.** 2007. Functional interrogation of the kinome using nucleotide acyl phosphates. Biochemistry **46:**350-8.
308. **Pauley, K. M., and S. Cha.** RNAi Therapeutics in Autoimmune Disease. Pharmaceuticals (Basel) **6:**287-94.
309. **Pedersen, I. M., G. Cheng, S. Wieland, S. Volinia, C. M. Croce, F. V. Chisari, and M. David.** 2007. Interferon modulation of cellular microRNAs as an antiviral mechanism. Nature **449:**919-22.
310. **Pekow, J. R., A. K. Bhan, H. Zheng, and R. T. Chung.** 2007. Hepatic steatosis is associated with increased frequency of hepatocellular carcinoma in patients with hepatitis C-related cirrhosis. Cancer **109:**2490-6.
311. **Pemble, C. W. t., L. C. Johnson, S. J. Kridel, and W. T. Lowther.** 2007. Crystal structure of the thioesterase domain of human fatty acid synthase inhibited by Orlistat. Nat Struct Mol Biol **14:**704-9.
312. **Penin, F., J. Dubuisson, F. A. Rey, D. Moradpour, and J. M. Pawlotsky.** 2004. Structural biology of hepatitis C virus. Hepatology **39:**5-19.
313. **Pereira, D. M., P. M. Rodrigues, P. M. Borralho, and C. M. Rodrigues.** 2013. Delivering the promise of miRNA cancer therapeutics. Drug Discov Today **18:**282-9.
314. **Perera, R., C. Riley, G. Isaac, A. S. Hopf-Jannasch, R. J. Moore, K. W. Weitz, L. Pasa-Tolic, T. O. Metz, J. Adamec, and R. J. Kuhn.** 2012. Dengue virus infection perturbs lipid homeostasis in infected mosquito cells. PLoS Pathog **8:**e1002584.
315. **Perlemuter, G., A. Sabile, P. Letteron, G. Vona, A. Topilco, Y. Chretien, K. Koike, D. Pessayre, J. Chapman, G. Barba, and C. Brechot.** 2002. Hepatitis C virus core protein inhibits microsomal triglyceride transfer protein activity and very low density lipoprotein secretion: a model of viral-related steatosis. FASEB J **16:**185-94.
316. **Pezacki, J. P., R. Singaravelu, and R. K. Lyn.** 2010. Host-virus interactions during hepatitis C virus infection: a complex and dynamic molecular biosystem. Mol Biosyst **6:**1131-42.
317. **Pietschmann, T., A. Kaul, G. Koutsoudakis, A. Shavinskaya, S. Kallis, E. Steinmann, K. Abid, F. Negro, M. Dreux, F. L. Cosset, and R. Bartenschlager.** 2006. Construction and characterization of infectious intragenotypic and intergenotypic hepatitis C virus chimeras. Proc Natl Acad Sci U S A **103:**7408-13.
318. **Pietschmann, T., V. Lohmann, A. Kaul, N. Krieger, G. Rinck, G. Rutter, D. Strand, and R. Bartenschlager.** 2002. Persistent and transient replication of full-length hepatitis C virus genomes in cell culture. J Virol **76:**4008-21.

319. **Pisonero-Vaquero, S., M. V. Garcia-Mediavilla, F. Jorquera, P. L. Majano, M. Benet, R. Jover, J. Gonzalez-Gallego, and S. Sanchez-Campos.** Modulation of PI3K-LXRalpha-dependent lipogenesis mediated by oxidative/nitrosative stress contributes to inhibition of HCV replication by quercetin. Lab Invest **94:**262-74.
320. **Plasterk, R. H.** 2002. RNA silencing: the genome's immune system. Science **296:**1263-5.
321. **Ploss, A., M. J. Evans, V. A. Gaysinskaya, M. Panis, H. You, Y. P. de Jong, and C. M. Rice.** 2009. Human occludin is a hepatitis C virus entry factor required for infection of mouse cells. Nature **457:**882-6.
322. **Ploss, A., S. R. Khetani, C. T. Jones, A. J. Syder, K. Trehan, V. A. Gaysinskaya, K. Mu, K. Ritola, C. M. Rice, and S. N. Bhatia.** 2010. Persistent hepatitis C virus infection in microscale primary human hepatocyte cultures. Proc Natl Acad Sci U S A **107:**3141-5.
323. **Poy, M. N., L. Eliasson, J. Krutzfeldt, S. Kuwajima, X. Ma, P. E. Macdonald, S. Pfeffer, T. Tuschl, N. Rajewsky, P. Rorsman, and M. Stoffel.** 2004. A pancreatic islet-specific microRNA regulates insulin secretion. Nature **432:**226-30.
324. **Pritchard, C. C., H. H. Cheng, and M. Tewari.** MicroRNA profiling: approaches and considerations. Nat Rev Genet **13:**358-69.
325. **Puig, A., M. M. Lyles, R. Noiva, and H. F. Gilbert.** 1994. The role of the thiol/disulfide centers and peptide binding site in the chaperone and anti-chaperone activities of protein disulfide isomerase. J Biol Chem **269:**19128-35.
326. **Pumplin, N., and O. Voinnet.** 2014. RNA silencing suppression by plant pathogens: defence, counter-defence and counter-counter-defence. Nat Rev Microbiol **11:**745-60.
327. **Puri, A. W., and M. Bogyo.** 2013. Applications of Small Molecule Probes in Dissecting Mechanisms of Bacterial Virulence and Host Responses. Biochemistry.
328. **Rakic, B., S. M. Sagan, M. Noestheden, S. Belanger, X. Nan, C. L. Evans, X. S. Xie, and J. P. Pezacki.** 2006. Peroxisome proliferator-activated receptor alpha antagonism inhibits hepatitis C virus replication. Chem Biol **13:**23-30.
329. **Rana, T. M.** 2007. Illuminating the silence: understanding the structure and function of small RNAs. Nat Rev Mol Cell Biol **8:**23-36.
330. **Rand, T. A., S. Petersen, F. Du, and X. Wang.** 2005. Argonaute2 cleaves the anti-guide strand of siRNA during RISC activation. Cell **123:**621-9.
331. **Randall, G., A. Grakoui, and C. M. Rice.** 2003. Clearance of replicating hepatitis C virus replicon RNAs in cell culture by small interfering RNAs. Proc Natl Acad Sci U S A **100:**235-40.
332. **Rangan, V. S., and S. Smith.** 1997. Alteration of the substrate specificity of the malonyl-CoA/acetyl-CoA:acyl carrier protein S-acyltransferase domain of the multifunctional fatty acid synthase by mutation of a single arginine residue. J Biol Chem **272:**11975-8.
333. **Reed, K. E., J. Xu, and C. M. Rice.** 1997. Phosphorylation of the hepatitis C virus NS5A protein in vitro and in vivo: properties of the NS5A-associated kinase. J Virol **71:**7187-97.
334. **Reiss, S., C. Harak, I. Romero-Brey, D. Radujkovic, R. Klein, A. Ruggieri, I. Rebhan, R. Bartenschlager, and V. Lohmann.** 2013. The lipid kinase phosphatidylinositol-4 kinase III alpha regulates the phosphorylation status of hepatitis C virus NS5A. PLoS Pathog **9:**e1003359.
335. **Reiss, S., I. Rebhan, P. Backes, I. Romero-Brey, H. Erfle, P. Matula, L. Kaderali, M. Poenisch, H. Blankenburg, M. S. Hiet, T. Longerich, S. Diehl, F. Ramirez, T. Balla, K. Rohr, A. Kaul, S. Buhler, R. Pepperkok, T. Lengauer, M. Albrecht, R. Eils, P. Schirmacher, V. Lohmann, and R. Bartenschlager.** 2011. Recruitment and activation of a lipid kinase by hepatitis C virus NS5A is essential for integrity of the membranous replication compartment. Cell Host Microbe **9:**32-45.
336. **Repa, J. J., G. Liang, J. Ou, Y. Bashmakov, J. M. Lobaccaro, I. Shimomura, B. Shan, M. S. Brown, J. L. Goldstein, and D. J. Mangelsdorf.** 2000. Regulation of mouse sterol regulatory element-binding protein-1c gene (SREBP-1c) by oxysterol receptors, LXRalpha and LXRbeta. Genes Dev **14:**2819-30.

337. **Reshef, L., Y. Olswang, H. Cassuto, B. Blum, C. M. Croniger, S. C. Kalhan, S. M. Tilghman, and R. W. Hanson.** 2003. Glyceroneogenesis and the triglyceride/fatty acid cycle. J Biol Chem **278:**30413-6.
338. **Restivo, L., R. Zampino, B. Guerrera, L. Ruggiero, and L. E. Adinolfi.** 2012. Steatosis is the predictor of relapse in HCV genotype 3- but not 2-infected patients treated with 12 weeks of pegylated interferon-alpha-2a plus ribavirin and RVR. J Viral Hepat **19:**346-52.
339. **Reynolds, A., D. Leake, Q. Boese, S. Scaringe, W. S. Marshall, and A. Khvorova.** 2004. Rational siRNA design for RNA interference. Nat Biotechnol **22:**326-30.
340. **Richards, A. L., A. E. Merrill, and J. J. Coon.** 2015. Proteome sequencing goes deep. Curr Opin Chem Biol **24C:**11-17.
341. **Richardson, R. D., G. Ma, Y. Oyola, M. Zancanella, L. M. Knowles, P. Cieplak, D. Romo, and J. W. Smith.** 2008. Synthesis of novel beta-lactone inhibitors of fatty acid synthase. J Med Chem **51:**5285-96.
342. **Robins, H., Y. Li, and R. W. Padgett.** 2005. Incorporating structure to predict microRNA targets. Proc Natl Acad Sci U S A **102:**4006-9.
343. **Rodriguez-Torres, M., S. Govindarajan, M. Diago, T. Morgan, B. Anand, K. Barange, F. Suter, A. Lin, G. Hooper, and M. Shiffman.** 2009. Hepatic steatosis in patients with chronic hepatitis C virus genotype 2 or 3 does not affect viral response in patients treated with peginterferon alpha-2a (40KD) (PEGASYS) plus ribavirin (COPEGUS) for 16 or 24 weeks. Liver Int **29:**237-41.
344. **Rolen, U., V. Kobzeva, N. Gasparjan, H. Ovaa, G. Winberg, F. Kisseljov, and M. G. Masucci.** 2006. Activity profiling of deubiquitinating enzymes in cervical carcinoma biopsies and cell lines. Mol Carcinog **45:**260-9.
345. **Russell, R. S., J. C. Meunier, S. Takikawa, K. Faulk, R. E. Engle, J. Bukh, R. H. Purcell, and S. U. Emerson.** 2008. Advantages of a single-cycle production assay to study cell culture-adaptive mutations of hepatitis C virus. Proc Natl Acad Sci U S A **105:**4370-5.
346. **Saetrom, P., B. S. Heale, O. Snove, Jr., L. Aagaard, J. Alluin, and J. J. Rossi.** 2007. Distance constraints between microRNA target sites dictate efficacy and cooperativity. Nucleic Acids Res **35:**2333-42.
347. **Sagan, S. M., N. Nasheri, C. Luebbert, and J. P. Pezacki.** 2010. The efficacy of siRNAs against hepatitis C virus is strongly influenced by structure and target site accessibility. Chem Biol **17:**515-27.
348. **Sagan, S. M., Y. Rouleau, C. Leggiadro, L. Supekova, P. G. Schultz, A. I. Su, and J. P. Pezacki.** 2006. The influence of cholesterol and lipid metabolism on host cell structure and hepatitis C virus replication. Biochem Cell Biol **84:**67-79.
349. **Sagan, S. M., and P. Sarnow.** Molecular biology. RNAi, Antiviral after all. Science **342:**207-8.
350. **Saghatelian, A., N. Jessani, A. Joseph, M. Humphrey, and B. F. Cravatt.** 2004. Activity-based probes for the proteomic profiling of metalloproteases. Proc Natl Acad Sci U S A **101:**10000-5.
351. **Salisbury, C. M., and B. F. Cravatt.** 2007. Activity-based probes for proteomic profiling of histone deacetylase complexes. Proceedings of the National Academy of Sciences **104:**1171-1176.
352. **Salisbury, C. M., and B. F. Cravatt.** 2008. Optimization of activity-based probes for proteomic profiling of histone deacetylase complexes. J Am Chem Soc **130:**2184-94.
353. **Sandanayaka, V. P., and A. S. Prashad.** 2002. Resistance to beta-lactam antibiotics: structure and mechanism based design of beta-lactamase inhibitors. Curr Med Chem **9:**1145-65.
354. **Sasaki, T., S. Takasuga, J. Sasaki, S. Kofuji, S. Eguchi, M. Yamazaki, and A. Suzuki.** 2009. Mammalian phosphoinositide kinases and phosphatases. Prog Lipid Res **48:**307-43.
355. **Schaefer, E. A., and R. T. Chung.** 2014. HCV and host lipids: an intimate connection. Semin Liver Dis **33:**358-68.

356. **Schmid-Antomarchi, H., M. Benkirane, V. Breittmayer, H. Husson, M. Ticchioni, C. Devaux, and B. Rossi.** 1996. HIV induces activation of phosphatidylinositol 4-kinase and mitogen-activated protein kinase by interacting with T cell CD4 surface molecules. Eur J Immunol **26:**717-20.
357. **Schwarz, D. S., G. Hutvagner, T. Du, Z. Xu, N. Aronin, and P. D. Zamore.** 2003. Asymmetry in the assembly of the RNAi enzyme complex. Cell **115:**199-208.
358. **Schweizer, E., and J. Hofmann.** 2004. Microbial type I fatty acid synthases (FAS): major players in a network of cellular FAS systems. Microbiol Mol Biol Rev **68:**501-17.
359. **Semenkovich, C. F.** 1997. Regulation of fatty acid synthase (FAS). Prog Lipid Res **36:**43-53.
360. **Shah, P. P., T. Wang, R. L. Kaletsky, M. C. Myers, J. E. Purvis, H. Jing, D. M. Huryn, D. C. Greenbaum, A. B. Smith, 3rd, P. Bates, and S. L. Diamond.** 2010. A small-molecule oxocarbazate inhibitor of human cathepsin L blocks severe acute respiratory syndrome and ebola pseudotype virus infection into human embryonic kidney 293T cells. Mol Pharmacol **78:**319-24.
361. **Shah, S. R., K. Patel, P. Marcellin, G. R. Foster, M. Manns, S. Kottilil, L. Healey, E. Pulkstenis, G. M. Subramanian, J. G. McHutchison, M. S. Sulkowski, S. Zeuzem, and D. R. Nelson.** 2011. Steatosis is an independent predictor of relapse following rapid virologic response in patients with HCV genotype 3. Clin Gastroenterol Hepatol **9:**688-93.
362. **Sheehan, D., G. Meade, V. M. Foley, and C. A. Dowd.** 2001. Structure, function and evolution of glutathione transferases: implications for classification of non-mammalian members of an ancient enzyme superfamily. Biochem J **360:**1-16.
363. **Sheikh, M. Y., J. Choi, I. Qadri, J. E. Friedman, and A. J. Sanyal.** 2008. Hepatitis C virus infection: molecular pathways to metabolic syndrome. Hepatology **47:**2127-33.
364. **Sherratt, A. R., N. Nasheri, C. S. McKay, S. O'Hara, A. Hunt, Z. Ning, D. Figeys, N. K. Goto, and J. P. Pezacki.** 2014. A new chemical probe for phosphatidylinositol kinase activity. Chembiochem **15:**1253-6.
365. **Shiffman, M. L.** 2014. Hepatitis C virus therapy in the direct acting antiviral era. Curr Opin Gastroenterol **30:**217-22.
366. **Shimakami, T., D. Yamane, R. K. Jangra, B. J. Kempf, C. Spaniel, D. J. Barton, and S. M. Lemon.** 2012. Stabilization of hepatitis C virus RNA by an Ago2-miR-122 complex. Proc Natl Acad Sci U S A **109:**941-6.
367. **Shinozaki-Ushiku, A., A. Kunita, and M. Fukayama.** 2015. Update on Epstein-Barr virus and gastric cancer (Review). Int J Oncol.
368. **Shreder, K. R., Y. Liu, T. Nomanhboy, S. R. Fuller, M. S. Wong, W. Z. Gai, J. Wu, P. S. Leventhal, J. R. Lill, and S. Corral.** 2004. Design and synthesis of AX7574: a microcystin-derived, fluorescent probe for serine/threonine phosphatases. Bioconjug Chem **15:**790-8.
369. **Simmonds, P., J. Bukh, C. Combet, G. Deleage, N. Enomoto, S. Feinstone, P. Halfon, G. Inchauspe, C. Kuiken, G. Maertens, M. Mizokami, D. G. Murphy, H. Okamoto, J. M. Pawlotsky, F. Penin, E. Sablon, I. T. Shin, L. J. Stuyver, H. J. Thiel, S. Viazov, A. J. Weiner, and A. Widell.** 2005. Consensus proposals for a unified system of nomenclature of hepatitis C virus genotypes. Hepatology **42:**962-73.
370. **Simmonds, P., D. B. Smith, F. McOmish, P. L. Yap, J. Kolberg, M. S. Urdea, and E. C. Holmes.** 1994. Identification of genotypes of hepatitis C virus by sequence comparisons in the core, E1 and NS-5 regions. J Gen Virol **75 (Pt 5):**1053-61.
371. **Simmonds, P., A. Tuplin, and D. J. Evans.** 2004. Detection of genome-scale ordered RNA structure (GORS) in genomes of positive-stranded RNA viruses: Implications for virus evolution and host persistence. RNA **10:**1337-51.
372. **Singaravelu, R., D. R. Blais, C. S. McKay, and J. P. Pezacki.** 2010. Activity-based protein profiling of the hepatitis C virus replication in Huh-7 hepatoma cells using a non-directed active site probe. Proteome Sci **8:**5.

373. **Singaravelu, R., R. K. Lyn, P. Srinivasan, J. Delcorde, R. H. Steenbergen, D. L. Tyrrell, and J. P. Pezacki.** 2014. Human serum activates CIDEB-mediated lipid droplet enlargement in hepatoma cells. Biochem Biophys Res Commun **441:**447-52.
374. **Singaravelu, R., R. S. Russell, D. L. Tyrrell, and J. P. Pezacki.** Hepatitis C virus and microRNAs: miRed in a host of possibilities. Curr Opin Virol **7C:**1-10.
375. **Singh, P., S. A. Williams, M. H. Shah, T. Lectka, G. J. Pritchard, J. T. Isaacs, and S. R. Denmeade.** 2008. Mechanistic insights into the inhibition of prostate specific antigen by beta-lactam class compounds. Proteins **70:**1416-28.
376. **Smith, D. B., S. Pathirana, F. Davidson, E. Lawlor, J. Power, P. L. Yap, and P. Simmonds.** 1997. The origin of hepatitis C virus genotypes. J Gen Virol **78 (Pt 2):**321-8.
377. **Smith, S.** 1994. The animal fatty acid synthase: one gene, one polypeptide, seven enzymes. FASEB J **8:**1248-59.
378. **Smith, S., A. Witkowski, and A. K. Joshi.** 2003. Structural and functional organization of the animal fatty acid synthase. Prog Lipid Res **42:**289-317.
379. **Sodhi, A., S. Montaner, and J. S. Gutkind.** 2004. Viral hijacking of G-protein-coupled-receptor signalling networks. Nat Rev Mol Cell Biol **5:**998-1012.
380. **Speers, A. E., and B. F. Cravatt.** 2009. Activity-Based Protein Profiling (ABPP) and Click Chemistry (CC)-ABPP by MudPIT Mass Spectrometry. Curr Protoc Chem Biol **1:**29-41.
381. **Speers, A. E., and B. F. Cravatt.** 2004. Profiling enzyme activities in vivo using click chemistry methods. Chem Biol **11:**535-46.
382. **Staub, I., and S. A. Sieber.** 2009. Beta-lactam probes as selective chemical-proteomic tools for the identification and functional characterization of resistance associated enzymes in MRSA. J Am Chem Soc **131:**6271-6.
383. **Staub, I., and S. A. Sieber.** 2008. Beta-lactams as selective chemical probes for the in vivo labeling of bacterial enzymes involved in cell wall biosynthesis, antibiotic resistance, and virulence. J Am Chem Soc **130:**13400-9.
384. **Steenbergen, R. H., M. A. Joyce, G. Lund, J. Lewis, R. Chen, N. Barsby, D. Douglas, L. F. Zhu, D. L. Tyrrell, and N. M. Kneteman.** Lipoprotein profiles in SCID/uPA mice transplanted with human hepatocytes become human-like and correlate with HCV infection success. Am J Physiol Gastrointest Liver Physiol **299:**G844-54.
385. **Steenbergen, R. H., M. A. Joyce, B. S. Thomas, D. Jones, J. Law, R. Russell, M. Houghton, and D. L. Tyrrell.** 2013. Human serum leads to differentiation of human hepatoma cells, restoration of VLDL secretion and a 1000-fold increase in HCV JFH-1 titers. Hepatology.
386. **Street, A., A. Macdonald, K. Crowder, and M. Harris.** 2004. The Hepatitis C virus NS5A protein activates a phosphoinositide 3-kinase-dependent survival signaling cascade. J Biol Chem **279:**12232-41.
387. **Street, A., A. Macdonald, C. McCormick, and M. Harris.** 2005. Hepatitis C virus NS5A-mediated activation of phosphoinositide 3-kinase results in stabilization of cellular beta-catenin and stimulation of beta-catenin-responsive transcription. J Virol **79:**5006-16.
388. **Su, A. I., J. P. Pezacki, L. Wodicka, A. D. Brideau, L. Supekova, R. Thimme, S. Wieland, J. Bukh, R. H. Purcell, P. G. Schultz, and F. V. Chisari.** 2002. Genomic analysis of the host response to hepatitis C virus infection. Proceedings of the National Academy of Sciences **99:**15669-15674.
389. **Sun, L., H. Qian, and W. Huang.** 2014. Virtual Screening for Cholesterol Absorption Inhibitors. Med Chem.
390. **Swaminathan, G., S. Navas-Martin, and J. Martin-Garcia.** 2014. MicroRNAs and HIV-1 infection: antiviral activities and beyond. J Mol Biol **426:**1178-97.
391. **Syed, G. H., Y. Amako, and A. Siddiqui.** 2010. Hepatitis C virus hijacks host lipid metabolism. Trends in Endocrinology & Metabolism **21:**33-40.
392. **Szittya, G., and J. Burgyan.** 2013. RNA interference-mediated intrinsic antiviral immunity in plants. Curr Top Microbiol Immunol **371:**153-81.

393. **Tafer, H., S. L. Ameres, G. Obernosterer, C. A. Gebeshuber, R. Schroeder, J. Martinez, and I. L. Hofacker.** 2008. The impact of target site accessibility on the design of effective siRNAs. Nat Biotechnol **26:**578-83.
394. **Tai, A. W., Y. Benita, L. F. Peng, S. S. Kim, N. Sakamoto, R. J. Xavier, and R. T. Chung.** 2009. A functional genomic screen identifies cellular cofactors of hepatitis C virus replication. Cell Host Microbe **5:**298-307.
395. **Tai, A. W., and S. Salloum.** 2011. The role of the phosphatidylinositol 4-kinase PI4KA in hepatitis C virus-induced host membrane rearrangement. PLoS One **6:**e26300.
396. **Takashima, M., Y. Kuramitsu, Y. Yokoyama, N. Iizuka, M. Fujimoto, T. Nishisaka, K. Okita, M. Oka, and K. Nakamura.** 2005. Overexpression of alpha enolase in hepatitis C virus-related hepatocellular carcinoma: association with tumor progression as determined by proteomic analysis. Proteomics **5:**1686-92.
397. **Tang, S., M. Bosch-Marce, A. Patel, T. P. Margolis, and P. R. Krause.** 2015. Characterization of HSV-2 primary miRNA transcript regulation. J Virol.
398. **Tantama, M., W. C. Lin, and S. Licht.** 2008. An activity-based protein profiling probe for the nicotinic acetylcholine receptor. J Am Chem Soc **130:**15766-7.
399. **Tateno, C., Y. Yoshizane, N. Saito, M. Kataoka, R. Utoh, C. Yamasaki, A. Tachibana, Y. Soeno, K. Asahina, H. Hino, T. Asahara, T. Yokoi, T. Furukawa, and K. Yoshizato.** 2004. Near completely humanized liver in mice shows human-type metabolic responses to drugs. Am J Pathol **165:**901-12.
400. **Tellinghuisen, T. L., K. L. Foss, and J. Treadaway.** 2008. Regulation of hepatitis C virion production via phosphorylation of the NS5A protein. PLoS Pathog **4:**e1000032.
401. **tenOever, B. R.** RNA viruses and the host microRNA machinery. Nat Rev Microbiol **11:**169-80.
402. **Teterina, N. L., Y. Pinto, J. D. Weaver, K. S. Jensen, and E. Ehrenfeld.** Analysis of poliovirus protein 3A interactions with viral and cellular proteins in infected cells. J Virol **85:**4284-96.
403. **Toker, A.** 2002. Phosphoinositides and signal transduction. Cell Mol Life Sci **59:**761-79.
404. **Trotard, M., C. Lepere-Douard, M. Regeard, C. Piquet-Pellorce, D. Lavillette, F. L. Cosset, P. Gripon, and J. Le Seyec.** 2009. Kinases required in hepatitis C virus entry and replication highlighted by small interference RNA screening. FASEB J **23:**3780-9.
405. **Tsuboi, K., D. A. Bachovchin, A. E. Speers, S. J. Brown, T. Spicer, V. Fernandez-Vega, J. Ferguson, B. F. Cravatt, P. Hodder, and H. Rosen.** 2010. Optimization and Characterization of an Inhibitor for Glutathione S-Tranferase Omega 1 (GSTO1).
406. **Tsuji, A., T. Terasaki, I. Tamai, and K. Takeda.** 1990. In vivo evidence for carrier-mediated uptake of beta-lactam antibiotics through organic anion transport systems in rat kidney and liver. J Pharmacol Exp Ther **253:**315-20.
407. **Tsuji, A., T. Yoshikawa, K. Nishide, H. Minami, M. Kimura, E. Nakashima, T. Terasaki, E. Miyamoto, C. H. Nightingale, and T. Yamana.** 1983. Physiologically based pharmacokinetic model for beta-lactam antibiotics I: Tissue distribution and elimination in rats. J Pharm Sci **72:**1239-52.
408. **Tuplin, A., D. J. Evans, and P. Simmonds.** 2004. Detailed mapping of RNA secondary structures in core and NS5B-encoding region sequences of hepatitis C virus by RNase cleavage and novel bioinformatic prediction methods. J Gen Virol **85:**3037-47.
409. **Turrado, C., T. Puig, J. Garcia-Carceles, M. Artola, B. Benhamu, S. Ortega-Gutierrez, J. Relat, G. Oliveras, A. Blancafort, D. Haro, P. F. Marrero, R. Colomer, and M. L. Lopez-Rodriguez.** New synthetic inhibitors of fatty acid synthase with anticancer activity. J Med Chem **55:**5013-23.
410. **Vaillancourt, F. H., M. Brault, L. Pilote, N. Uyttersprot, E. T. Gaillard, J. H. Stoltz, B. L. Knight, L. Pantages, M. McFarland, S. Breitfelder, T. T. Chiu, L. Mahrouche, A. M. Faucher, M. Cartier, M. G. Cordingley, R. C. Bethell, H. Jiang, P. W. White, and G.**

Kukolj. 2012. Evaluation of Phosphatidylinositol-4-Kinase IIIalpha as a Hepatitis C Virus Drug Target. J Virol **86:**11595-607.

411. **van der Schaar, H. M., L. van der Linden, K. H. Lanke, J. R. Strating, G. Purstinger, E. de Vries, C. A. de Haan, J. Neyts, and F. J. van Kuppeveld.** 2012. Coxsackievirus mutants that can bypass host factor PI4KIIIbeta and the need for high levels of PI4P lipids for replication. Cell Res **22:**1576-92.
412. **van Rooij, E., and E. N. Olson.** 2007. MicroRNAs: powerful new regulators of heart disease and provocative therapeutic targets. J Clin Invest **117:**2369-76.
413. **Vargason, J. M., G. Szittya, J. Burgyan, and T. M. Hall.** 2003. Size selective recognition of siRNA by an RNA silencing suppressor. Cell **115:**799-811.
414. **Vespasiani-Gentilucci, U., P. Gallo, A. De Vincentis, G. Galati, and A. Picardi.** 2014. Hepatitis C virus and metabolic disorder interactions towards liver damage and atherosclerosis. World J Gastroenterol **20:**2825-38.
415. **Vickers, T. A., S. Koo, C. F. Bennett, S. T. Crooke, N. M. Dean, and B. F. Baker.** 2003. Efficient reduction of target RNAs by small interfering RNA and RNase H-dependent antisense agents. A comparative analysis. J Biol Chem **278:**7108-18.
416. **Vieyres, G., J. Dubuisson, and T. Pietschmann.** Incorporation of hepatitis C virus E1 and E2 glycoproteins: the keystones on a peculiar virion. Viruses **6:**1149-87.
417. **Vieyres, G., X. Thomas, V. Descamps, G. Duverlie, A. H. Patel, and J. Dubuisson.** 2010. Characterization of the envelope glycoproteins associated with infectious hepatitis C virus. J Virol **84:**10159-68.
418. **Vocadlo, D. J., and C. R. Bertozzi.** 2004. A strategy for functional proteomic analysis of glycosidase activity from cell lysates. Angew Chem Int Ed Engl **43:**5338-42.
419. **Voinnet, O.** 2005. Induction and suppression of RNA silencing: insights from viral infections. Nat Rev Genet **6:**206-20.
420. **Volinia, S., G. A. Calin, C. G. Liu, S. Ambs, A. Cimmino, F. Petrocca, R. Visone, M. Iorio, C. Roldo, M. Ferracin, R. L. Prueitt, N. Yanaihara, G. Lanza, A. Scarpa, A. Vecchione, M. Negrini, C. C. Harris, and C. M. Croce.** 2006. A microRNA expression signature of human solid tumors defines cancer gene targets. Proc Natl Acad Sci U S A **103:**2257-61.
421. **von Eije, K. J., O. ter Brake, and B. Berkhout.** 2008. Human immunodeficiency virus type 1 escape is restricted when conserved genome sequences are targeted by RNA interference. J Virol **82:**2895-903.
422. **von Schaewen, M., and A. Ploss.** 2014. Murine models of hepatitis C: what can we look forward to? Antiviral Res **104:**15-22.
423. **Wakil, S. J.** 1989. Fatty acid synthase, a proficient multifunctional enzyme. Biochemistry **28:**4523-30.
424. **Wakita, T., T. Pietschmann, T. Kato, T. Date, M. Miyamoto, Z. Zhao, K. Murthy, A. Habermann, H. G. Krausslich, M. Mizokami, R. Bartenschlager, and T. J. Liang.** 2005. Production of infectious hepatitis C virus in tissue culture from a cloned viral genome. Nat Med **11:**791-6.
425. **Walters, K. A., M. A. Joyce, J. C. Thompson, M. W. Smith, M. M. Yeh, S. Proll, L. F. Zhu, T. J. Gao, N. M. Kneteman, D. L. Tyrrell, and M. G. Katze.** 2006. Host-specific response to HCV infection in the chimeric SCID-beige/Alb-uPA mouse model: role of the innate antiviral immune response. PLoS Pathog **2:**e59.
426. **Wang, C., M. Gale, Jr., B. C. Keller, H. Huang, M. S. Brown, J. L. Goldstein, and J. Ye.** 2005. Identification of FBL2 as a geranylgeranylated cellular protein required for hepatitis C virus RNA replication. Mol Cell **18:**425-34.
427. **Wang, H., J. W. Perry, A. S. Lauring, P. Neddermann, R. De Francesco, and A. W. Tai.** 2014. Oxysterol-binding protein is a phosphatidylinositol 4-kinase effector required for HCV replication membrane integrity and cholesterol trafficking. Gastroenterology **146:**1373-85 e1-11.

428. **Wang, X., J. Lin, Y. Chen, W. Zhong, G. Zhao, H. Liu, S. Li, and L. Wang.** 2009. Novel fatty acid synthase (FAS) inhibitors: design, synthesis, biological evaluation, and molecular docking studies. Bioorg Med Chem **17:**1898-904.
429. **Wang, X. H., R. Aliyari, W. X. Li, H. W. Li, K. Kim, R. Carthew, P. Atkinson, and S. W. Ding.** 2006. RNA interference directs innate immunity against viruses in adult Drosophila. Science **312:**452-4.
430. **Waris, G., D. J. Felmlee, F. Negro, and A. Siddiqui.** 2007. Hepatitis C virus induces proteolytic cleavage of sterol regulatory element binding proteins and stimulates their phosphorylation via oxidative stress. J Virol **81:**8122-30.
431. **Watts, J. M., K. K. Dang, R. J. Gorelick, C. W. Leonard, J. W. Bess, Jr., R. Swanstrom, C. L. Burch, and K. M. Weeks.** 2009. Architecture and secondary structure of an entire HIV-1 RNA genome. Nature **460:**711-6.
432. **Waugh, M. G.** 2012. Phosphatidylinositol 4-kinases, phosphatidylinositol 4-phosphate and cancer. Cancer Lett **325:**125-31.
433. **Wilhelm, M., J. Schlegl, H. Hahne, A. Moghaddas Gholami, M. Lieberenz, M. M. Savitski, E. Ziegler, L. Butzmann, S. Gessulat, H. Marx, T. Mathieson, S. Lemeer, K. Schnatbaum, U. Reimer, H. Wenschuh, M. Mollenhauer, J. Slotta-Huspenina, J. H. Boese, M. Bantscheff, A. Gerstmair, F. Faerber, and B. Kuster.** 2014. Mass-spectrometry-based draft of the human proteome. Nature **509:**582-7.
434. **Wilson, J. A., and A. Huys.** miR-122 promotion of the hepatitis C virus life cycle: sound in the silence. Wiley Interdiscip Rev RNA **4:**665-76.
435. **Wilson, J. A., S. Jayasena, A. Khvorova, S. Sabatinos, I. G. Rodrigue-Gervais, S. Arya, F. Sarangi, M. Harris-Brandts, S. Beaulieu, and C. D. Richardson.** 2003. RNA interference blocks gene expression and RNA synthesis from hepatitis C replicons propagated in human liver cells. Proc Natl Acad Sci U S A **100:**2783-8.
436. **Wilson, J. A., and C. D. Richardson.** 2005. Hepatitis C virus replicons escape RNA interference induced by a short interfering RNA directed against the NS5b coding region. J Virol **79:**7050-8.
437. **Wilson, J. A., and S. M. Sagan.** 2014. Hepatitis C virus and human miR-122: insights from the bench to the clinic. Curr Opin Virol **7C:**11-18.
438. **Wilson, J. A., C. Zhang, A. Huys, and C. D. Richardson.** Human Ago2 is required for efficient microRNA 122 regulation of hepatitis C virus RNA accumulation and translation. J Virol **85:**2342-50.
439. **Winter, J., S. Jung, S. Keller, R. I. Gregory, and S. Diederichs.** 2009. Many roads to maturity: microRNA biogenesis pathways and their regulation. Nat Cell Biol **11:**228-34.
440. **Witkowski, A., A. K. Joshi, and S. Smith.** 1997. Characterization of the interthiol acyltransferase reaction catalyzed by the beta-ketoacyl synthase domain of the animal fatty acid synthase. Biochemistry **36:**16338-44.
441. **Wolters, D. A., M. P. Washburn, and J. R. Yates, 3rd.** 2001. An automated multidimensional protein identification technology for shotgun proteomics. Anal Chem **73:**5683-90.
442. **Wu, C., I. Macleod, and A. I. Su.** 2013. BioGPS and MyGene.info: organizing online, gene-centric information. Nucleic Acids Res **41:**D561-5.
443. **Xiang, Z., L. Qiao, Y. Zhou, L. A. Babiuk, and Q. Liu.** 2010. Hepatitis C virus nonstructural protein-5A activates sterol regulatory element-binding protein-1c through transcription factor Sp1. Biochemical and Biophysical Research Communications **402:**549-553.
444. **Xu, Z., J. Choi, T. S. Yen, W. Lu, A. Strohecker, S. Govindarajan, D. Chien, M. J. Selby, and J. Ou.** 2001. Synthesis of a novel hepatitis C virus protein by ribosomal frameshift. EMBO J **20:**3840-8.
445. **Yaginuma, R., K. Ikejima, K. Okumura, K. Kon, S. Suzuki, Y. Takei, and N. Sato.** 2006. Hepatic steatosis is a predictor of poor response to interferon alpha-2b and ribavirin combination therapy in Japanese patients with chronic hepatitis C. Hepatol Res **35:**19-25.

446. **Yang, J. S., and E. C. Lai.** 2011. Alternative miRNA biogenesis pathways and the interpretation of core miRNA pathway mutants. Mol Cell **43:**892-903.
447. **Yang, N., P. Ma, J. Lang, Y. Zhang, J. Deng, X. Ju, G. Zhang, and C. Jiang.** 2012. Phosphatidylinositol 4-kinase IIIbeta is required for severe acute respiratory syndrome coronavirus spike-mediated cell entry. J Biol Chem **287:**8457-67.
448. **Yang, P. Y., K. Liu, M. H. Ngai, M. J. Lear, M. R. Wenk, and S. Q. Yao.** 2010. Activity-based proteome profiling of potential cellular targets of Orlistat--an FDA-approved drug with anti-tumor activities. J Am Chem Soc **132:**656-66.
449. **Yang, P. Y., K. Liu, C. Zhang, G. Y. Chen, Y. Shen, M. H. Ngai, M. J. Lear, and S. Q. Yao.** 2011. Chemical modification and organelle-specific localization of orlistat-like natural-product-based probes. Chem Asian J **6:**2762-75.
450. **Yang, P. Y., M. Wang, K. Liu, M. H. Ngai, O. Sheriff, M. J. Lear, S. K. Sze, C. Y. He, and S. Q. Yao.** 2012. Parasite-based screening and proteome profiling reveal orlistat, an FDA-approved drug, as a potential anti Trypanosoma brucei agent. Chemistry **18:**8403-13.
451. **Yang, W., B. L. Hood, S. L. Chadwick, S. Liu, S. C. Watkins, G. Luo, T. P. Conrads, and T. Wang.** 2008. Fatty acid synthase is up-regulated during hepatitis C virus infection and regulates hepatitis C virus entry and production. Hepatology **48:**1396-1403.
452. **Yano, H., S. Nakanishi, K. Kimura, N. Hanai, Y. Saitoh, Y. Fukui, Y. Nonomura, and Y. Matsuda.** 1993. Inhibition of histamine secretion by wortmannin through the blockade of phosphatidylinositol 3-kinase in RBL-2H3 cells. J Biol Chem **268:**25846-56.
453. **Ye, K., L. Malinina, and D. J. Patel.** 2003. Recognition of small interfering RNA by a viral suppressor of RNA silencing. Nature **426:**874-8.
454. **Yee, M. C., S. C. Fas, M. M. Stohlmeyer, T. J. Wandless, and K. A. Cimprich.** 2005. A cell-permeable, activity-based probe for protein and lipid kinases. J Biol Chem **280:**29053-9.
455. **Yehia, B. R., A. J. Schranz, C. A. Umscheid, and V. Lo Re, 3rd.** 2014. The treatment cascade for chronic hepatitis C virus infection in the United States: a systematic review and meta-analysis. PLoS One **9:**e101554.
456. **Yi, M., and S. M. Lemon.** 2003. 3' nontranslated RNA signals required for replication of hepatitis C virus RNA. J Virol **77:**3557-68.
457. **Yokoyama, Y., Y. Kuramitsu, M. Takashima, N. Iizuka, T. Toda, S. Terai, I. Sakaida, M. Oka, K. Nakamura, and K. Okita.** 2004. Proteomic profiling of proteins decreased in hepatocellular carcinoma from patients infected with hepatitis C virus. Proteomics **4:**2111-6.
458. **Yoshikawa, T., H. Shimano, M. Amemiya-Kudo, N. Yahagi, A. H. Hasty, T. Matsuzaka, H. Okazaki, Y. Tamura, Y. Iizuka, K. Ohashi, J. Osuga, K. Harada, T. Gotoda, S. Kimura, S. Ishibashi, and N. Yamada.** 2001. Identification of liver X receptor-retinoid X receptor as an activator of the sterol regulatory element-binding protein 1c gene promoter. Mol Cell Biol **21:**2991-3000.
459. **You, S., and C. M. Rice.** 2008. 3' RNA elements in hepatitis C virus replication: kissing partners and long poly(U). J Virol **82:**184-95.
460. **Yu, G. Y., K. J. Lee, L. Gao, and M. M. Lai.** 2006. Palmitoylation and polymerization of hepatitis C virus NS4B protein. J Virol **80:**6013-23.
461. **Zamore, P. D., and B. Haley.** 2005. Ribo-gnome: the big world of small RNAs. Science **309:**1519-24.
462. **Zein, N. N.** 2000. Clinical significance of hepatitis C virus genotypes. Clin Microbiol Rev **13:**223-35.
463. **Zhang, W., B. Chakravarty, F. Zheng, Z. Gu, H. Wu, J. Mao, S. J. Wakil, and F. A. Quiocho.** 2011. Crystal structure of FAS thioesterase domain with polyunsaturated fatty acyl adduct and inhibition by dihomo-gamma-linolenic acid. Proc Natl Acad Sci U S A **108:**15757-62.
464. **Zhang, W., R. D. Richardson, S. Chamni, J. W. Smith, and D. Romo.** 2008. Beta-lactam congeners of orlistat as inhibitors of fatty acid synthase. Bioorg Med Chem Lett **18:**2491-4.

465. **Zinchuk, V., and O. Grossenbacher-Zinchuk.** 2011. Quantitative Colocalization Analysis of Confocal Fluorescence Microscopy Images, Current Protocols in Cell Biology. John Wiley & Sons, Inc.
466. **Zubarev, R. A.** 2013. The challenge of the proteome dynamic range and its implications for in-depth proteomics. Proteomics **13:**723-6.